

Thesis for the degree of Doctor of Philosophy

*Development and Characterisation of
Selective Ion or Molecular Receptors*

Rachel F. Wall B.Sc.

Dublin City University
School of Chemical Sciences



June 2003

Supervisors: Prof. Dermot Diamond and Dr. Kieran Nolan

I hereby certify that this material, which I now submit for assessment on the programme of study leading to the award of Doctor of Philosophy is entirely my own work and has not been taken from the work of others save and to the extent that such work has been cited and acknowledged within the text of my work

Signed Rachel Wall
Rachel Wall

ID No 95677917

Date 20-08-03

Table of Contents

Declaration	II
Table of Contents	III
Acknowledgements	VIII
Abstract	XI
1 Calixarenes Derivatives and their Applications as Ion and Molecular Receptors	1
1 1 Calixarenes	2
1 1 1 <i>Historical Aspects</i>	2
1 1 2 <i>Nomenclature and Representation</i>	3
1 1 3 <i>Synthesis of Calixarenes</i>	6
1 1 3 1 One-Pot Synthesis	6
1 1 3 2 Multistep Synthesis	8
1 1 4 <i>Functionalisation of Calixarenes</i>	10
1 1 4 1 Complete Functionalisation	11
1 1 4 2 Selective Functionalisation	19
1 1 5 <i>Applications of Calixarenes</i>	29
1 2 Molecular Receptors for Guest Species [Cationic, Anionic & Neutral Species]	30
1 2 1 <i>Historical Aspects</i>	30
1 2 2 <i>Characteristics of Guest Species</i>	31
1 2 3 <i>Binding and Recognition of Guest Species</i>	33
1 2 3 1 Complexations of Cations	33
1 2 3 2 Complexation of Anions	37
1 2 3 3 Complexation of Neutral Species	46
1 3 Molecular Host-Guest Complexation	48
1 3 1 <i>Concept of Molecular Host-Guest Chemistry</i>	48
1 3 2 <i>Application of Calixarenes as Molecular Receptors</i>	49
1 3 2 1 Calixarene-based Cation Receptors	49
1 3 2 2 Calixarene-based Anion Receptors	52
1 3 2 3 Calixarene-based Neutral Receptors	53

1 3 3	<i>Design of a Molecular Host</i>	54
1 3 4	<i>Design of a Molecular Host for Complexation of a Tetrahedrally Shaped Guest</i>	56
2	LC-MS Optimisation of the Synthesis of a Disubstituted Calix[4]arene Derivative	58
2 1	<i>Introduction</i>	59
2 2	<i>Liquid Chromatography Mass Spectrometry(LC-MS) and Liquid Chromatography Diode Array Detection (LC-DAD)</i>	60
2 3	<i>Results and Discussion</i>	66
2 3 1	Synthesis of 5,11,17,23-Tetra- <i>t</i> -Butyl-25,27-bis (ethoxycarbonyl methoxy)-26,28-dihydroxycalix[4]arene	66
2 3 2	Reaction Stoichiometry	68
2 3 3	Reaction Time	68
2 3 4	LC, DI-MS and LC-MS Monitoring of Reaction C	70
2 3 5	Development of an Alternative Route to Partially Functionalised Calixarene Derivatives	73
2 3 6	Formation of 1,3- Vs 1,2-diester isomers	74
2 3 7	Effects of Reaction Conditions	76
	2 3 7 1 <i>Influence of Solvent Polarity on S_n2 Reactions</i>	77
	2 3 7 2 <i>Influence of Base</i>	80
	2 3 7 3 A ' <i>Metal Template</i> ' Effect	81
2 3 8	Characterisation of Partially Substituted Calix[4]arene Derivatives	83
2 4	<i>Conclusion</i>	86
2 5	<i>Experimental</i>	87
2 5 1	Reagents and Chemicals	87
2 5 2	LC-MS Analysis	87
	2 5 2 1 <i>LC Method 1</i>	87
	2 5 2 2 <i>LC Method 2</i>	87
	2 5 2 3 <i>MS Method</i>	87
2 5 3	Direct Infusion Mass Spectral Analysis	88
2 5 4	LC-DAD Analysis	88
2 5 5	Synthetic Procedures	88
2 5 6	Molecular Modelling	90

3	Synthesis and Characterisation of Partially Substituted Calix[4]arene Derivatives	91
3 1	<i>Introduction</i>	92
3 2	<i>Results and Discussion</i>	93
3 2 1	Characterisation of Partially Substituted Calix[4]arene Derivatives	93
3 2 1 1	<i>Disubstituted Calix[4]arene Derivatives</i>	93
3 2 1 2	<i>Monosubstituted Calix[4]arene Derivatives</i>	101
3 2 2	Investigation of the Conformational Mobility of the Disubstituted Calix[4]arenes by Temperature NMR Studies	103
3 3	<i>Conclusion</i>	110
3 4	<i>Experimental</i>	111
3 4 1	General	111
3 4 2	Synthetic Procedures	111
3 4 2 1	<i>Synthetic Procedure 1</i>	111
3 4 2 2	<i>Synthetic Procedure 2</i>	111
3 4 3	Direct Infusion Mass Spectral Analysis	113
3 4 4	LC-DAD Analysis	113
4	'Host-Guest Chemistry' of Partially Functionalised Calix[4]arene Derivatives	115
4 1	<i>Introduction</i>	116
4 2	<i>Results and Discussion</i>	117
4 2 1	Determination of Host-Guest Complexation by Ion Selective Analysis	117
4 2 1 1	<i>ISE Analysis of 70 and 140</i>	120
4 2 1 2	<i>ISE Analysis of 147 and 148</i>	124
4 2 1 3	<i>ISE Analysis of 145</i>	125
4 2 2	Determination of Host-Guest Complexation by NMR Titration	126
4 2 2 1	<i>¹H NMR Coordination Studies of 147</i>	127
4 2 2 2	<i>¹H NMR Coordination Studies of 148</i>	132
4 2 2 3	<i>¹H and ¹³C NMR Coordination Studies of 70</i>	134

4 2 2 4	¹³ C NMR Coordination Studies of	145
4 2 3	Determination of Host-Guest Complexation (Potentiometry Vs NMR Spectroscopy)	137
4 3	Conclusion	139
4 4	Expenmental	140
4 4 1	General	140
4 4 2	Direct Infusion Mass Spectal Analysis	140
4 4 3	Molecular Modelling	140
4 4 4	NMR Titration Expenments	140
4 4 5	Preparation of Electrodes	140
5	Synthesis of a Calix[4]arene Derivative possessing a 'Tetrahedral' Binding Site	142
5 1	Introduction	143
5 2	Results and Discussion	146
5 2 1	Use of a Metal Carbonate Base	148
5 2 2	Use of an Organic Base	154
5 2 3	Use of a Hindered Base	155
5 2 4	Use of the Michael Addition Reaction	156
5 2 5	Use of NaH as Base	158
5 2 6	Isolation and Charactensation of a Novel Tetrahedrally Shaped Calix[4]arene	162
5 2 7	Optimisation Studies of the Reaction of <i>p</i> -tetra- <i>t</i> - butylcalix[4]arene-(1,3)-diethyl ester and Ethyl 3- bromopropionate	165
5 2 7 1	The Influence of Stoichiometry and Time	167
5 2 7 2	The Influence of the Mode of Addition of NaH	169
5 2 8	Rationalisation of Product Formation	174
5 2 8 1	'A Hydrolysis Phenomenon'	174
5 2 8 2	'A Cleavage Phenomenon'	175
5 3	Conclusion	181
5 4	Expenmental	182
5 4 1	General	182
5 4 2	Synthesis of a Differentially 1,3 and 2,4- Substituted <i>p</i> -tetra- <i>t</i> -butylcalix[4]arene	182

5 4 3	Exhaustive Alkylation of 70 using NaH as base	183
5 4 4	Direct Infusion Mass Spectral Analysis	185
5 4 5	LC-DAD Analysis	185
 Conclusion		186
 Bibliography		190
 Appendix		201

Acknowledgements

Now that this mammoth task is finally over, there are a number of people that deserve an enormous amount of thanks and gratitude.

Firstly, I would like to thank Prof. Dermot Diamond and Dr. Kieran Nolan, my esteemed supervisors for their help, advice, direction and constant support. I was extremely fortunate to have two supervisors who exhibited enthusiasm and offered guidance when it was vital to my thesis and to my sanity!

My appreciation is also extended to Dr. Gillian Mc Mahon whose knowledge and experience was fundamental to this thesis. I am extremely grateful to both Gillian and Dr. Kim Lau for all those words of wisdom and encouragement.

A sincere thank you to all in the chemistry department, staff members and postgrads over the past few years who have made working there easier, by their generous help and good humour. Thank you to Dr. Paraic James for his help and support throughout my time in DCU. To the technicians, Mick, Maurice, Damien, Veronica, Ann, John, Vinny and Ambrose for their willingness to help and teach the postgrads with such good humour and patience. I greatly appreciate all the help and knowledge given by you over the last few years. Gratitude also to all the staff of the NCSR.

Cheers to the members of the DD-RG, past and present, Paddy, Darren, Fran, Brendan, Aogan, Karl, Karen, Liam, Michaela, Susan, Valerie, Ben and Sarah and those of the KN-RG, Shane, John, Andrea, Ian, Yang, Nameer and Steven who were great people to work with and the best of luck for the future. A special word of thanks to my 'partner in crime' in the calixarene underworld, Carol, whose constant support and encouragement was greatly needed and appreciated. Thank you to all the chemistry postgrads in DCU who understand the process and support one another.

Thank you Steph for your calming influence and reassuring words and to Susan for supporting me during this time, for all the words of (drunken) wisdom, encouragement and for being a great friend. I'm forever indebted to you!

To my brother Niall for always being there in a crisis with computers, printers or life. Both you and Brona can relax, safe in the knowledge that the thesis is finally printed, computer hasn't died and I'm reasonably sane! Thank you for everything. To Georgia, my wee angel who always made me smile.

Finally to my parents Ray and Bridie, for their never-ending support, financial and otherwise. No amount of thanks or praise can express my gratitude for what you've given me, you've always supported and encouraged me in whatever I chose to do and for that I will always be grateful.

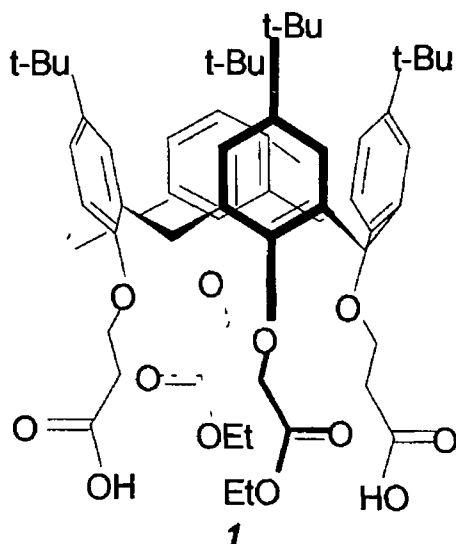
Abstract

The research entailed the Synthesis and Characterisation of a range of Molecular Receptors. The target receptor was a calix[4]arene derivative, possessing a tetrahedral 'pocket' at the lower rim defined by four pendant ligating groups, with opposing groups differing in length. To achieve this, the spacer units in the 1,3 positions of the calixarene must differ in length than the spacer units in the 2,4 positions by a single methylene spacer, thus generating a selective 3-dimensional binding site.

LC-UV-MS analysis of the products of the derivatisation of p-t-butyl calix[4]arene with ethyl bromoacetate has been carried out in order to optimise the synthesis of the 1,3-disubstituted product. LC-DAD and LC-UV-MS methods have been developed to successfully identify and characterise the compounds being formed in these complex reactions. Obtaining reliable routes to partially substituted calixarene derivatives is of growing interest as they provide a template for generating complex derivatives with mixed functionality and/or greater diversity.

The synthesis has led to the generation of a series of partially substituted calix[4]arene derivatives, as well as derivatives of the tetrahedrally arranged target receptor.

The various receptors have been assessed for ion-complexation properties by a number of methods, principally NMR spectroscopy, and ion-selective electrode studies. In the electrode measurements, the receptors are dispersed in a plasticised PVC membrane, and the ion-selectivity of the device is assessed.



Patterns related to the selectivity of Group I, II ions and a diverse group of anions have been determined. The 1,3-diester produces a sensor that exhibits a Nernstian Response with a number of ions, but does not reproduce the well-known selectivity of the calix[4]arene tetraesters. Functionalisation at the 2,4 position with ethyl 3-bromopropionate realises a calix[4]arene derivative with differing spatial arrangements of differing binding sites, a novel diacid, diester calix[4]arene derivative (fig 1). This will provide a unique platform for building a new series of calix[4]arene receptors with tetrahedral rather than an octahedral arrangement of binding sites.

Figure 1 p-tetra-t-butylcalix[4]arene-
(1,3)-diethyl ester-(2,4)-dipropyl acid

***1. Calixarene Derivatives & their
Application as Ion or Molecular
Receptors***

1 1 Calixarenes

1 1 1 Historical aspects

The founding father of phenol-formaldehyde chemistry was Adolph von Baeyer, who discovered that a "very complex product" resulted, following condensation of formaldehyde with phenol, in the presence of a mineral acid. The vast analytical tools available today were non-existent to Baeyer who could not perform characterisable investigations on these polymeric substances.

In 1902, Leo Hendrik Baekeland initiated an amazing investigation of the reaction between phenol and formaldehyde, which eventually led to modern synthetic plastics. Baekeland proved that by using a controlled amount of base, a hard cement-like substance, bakelite resulted, a potential plastic material.

Both scientists proposed a structure where a methylene ($-\text{CH}_2$) or methoxy methyl ether ($-\text{CH}_2\text{OCH}_2$) linkage exists between a pair of aromatic rings in the formaldehyde-phenol condensation product as shown in Figure 1 1. Possible structural units in this bakelite material are

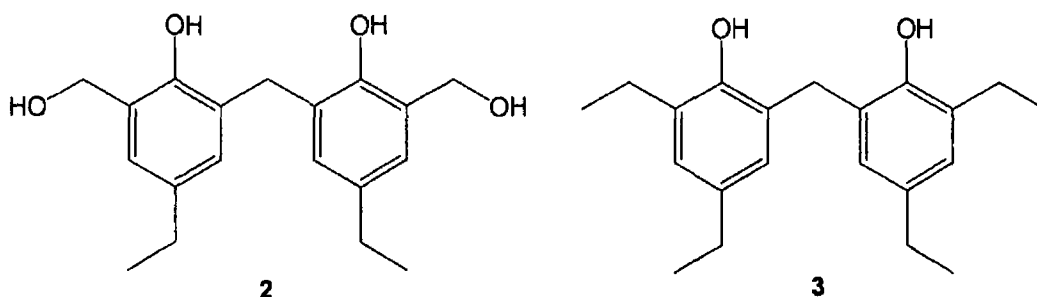


Figure 1 1 "Resoles" and "Novolacs"

Base induced condensation of phenol with formaldehyde yielded a complex product, due to the reactive *ortho*- and *para*-positions, thus forming a highly crosslinked polymer.

In 1942, Alois Zinke and Erich Ziegler simplified this problem by experimenting with a *para*-alkyl phenol. Crosslinking was minimised as only two *ortho*- positions are available to react. A linear polymer was hypothesised as the preferable product but Zinke later clarified that the cyclic tetramer was the actual product. He isolated the acetate, prepared from *p*-(1,1,3,3-tetramethylbutyl) phenol and formaldehyde. This had a cryoscopic molecular weight of 876, which compared favourably with the calculated molecular weight of 873.

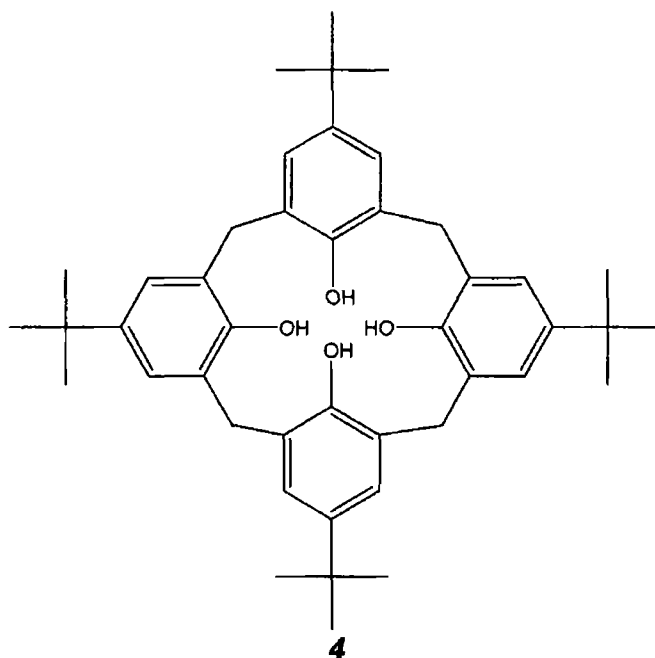


Figure 1 2 *p*-tetra-*t*-butylcalix[4]arene (**4**)

During the 1970's, David Gutsche began to explore the potential use of Zinke's cyclic tetramer (**4**) (Fig 1 2) as a foundation for building more complex molecular baskets and enzyme mimics. He proposed that by functionalising **4** with ligating groups, it may complex with a substrate molecule and thus act as a receptor for a suitable guest. On observing a similarity in shape between a molecular model of the cyclic tetramer and a greek vase "calix crater", he christened the cyclic tetramer 'calix[4]arene', derived from 'calix' meaning vase and 'arene' due to the aryl groups [1,2]. It was this research that has given rise to the tremendous amount of basic and applied investigations into calixarene derivatives since then.

1 1 2 Nomenclature and Representation

Calixarenes are cyclic molecules composed of phenol units linked by methylene groups. Calixarenes are usually composed of 4-8 phenol units, with the number involved denoted in brackets e.g. calix[8]arene.

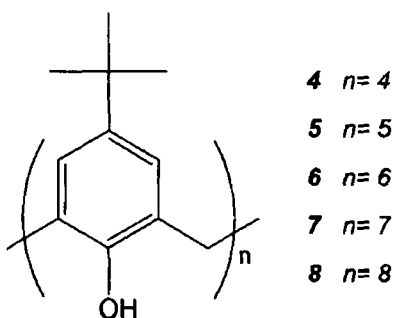


Figure 1 3 Parent Calix[*n*]arene

Figure 1 4 is a schematic diagram of a calixarene, comprising of two sections, an 'upper nm', the para-position of the phenols and a 'lower nm', the phenolic hydroxy groups

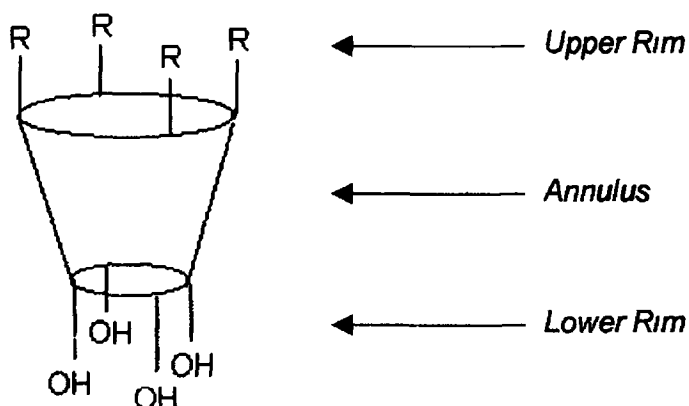


Figure 1 4 Designation of the faces of calix[n]arenes

To indicate the arrangement of substituents on both the lower and upper nm, each phenol unit is labelled alphabetically. Thus, a disubstituted calix[4]arene may be designated as 'A,B' or 'A,C'-disubstituted calix[4]arene (Fig 1 5) [2]

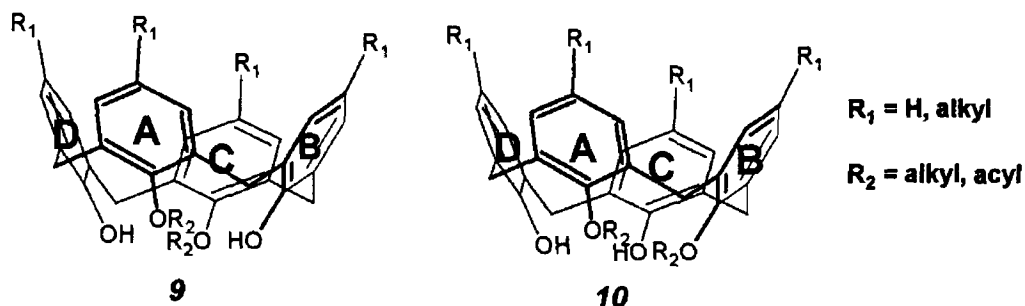


Figure 1 5 (A,C) & (A,B) disubstitution of calix[4]arene

Their size and shape imparts flexibility, which may lead to ring inversion. Two pathways are available to a calixarene for conformational inversion: 'Upper Rim through the Annulus' and 'Lower Rim through the Annulus' (Fig 1 6). To freeze a calixarene in a particular conformation, it is convenient to functionalize the lower rim with groups that are too bulky to rotate through the annulus.

upper rim through
the annulus pathway

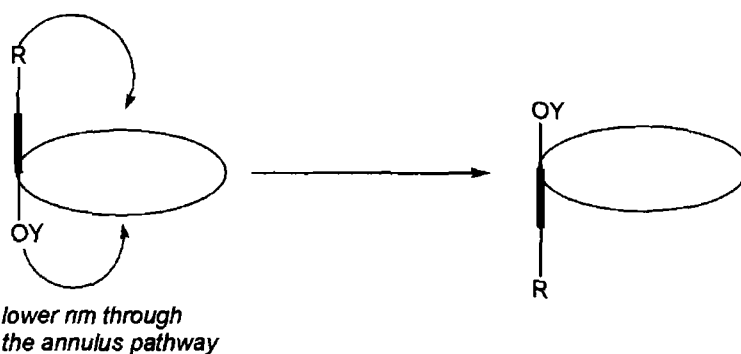


Figure 1 6 Pathways for conformational isomerism of calix[n]arenes

Cornforth first recognised that calix[4]arenes were capable of assuming four conformations, with various numbers of aryl groups projecting upward ("u") or downward ("d") relative to a plane defined by the bridge methylene groups. Gutsche later named these conformations as 'cone' (u,u,u,u), 'partial cone' (u,u,u,d), '1,2-alternate' (u,u,d,d) and '1,3-alternate' (u,d,u,d), (Fig 1 7) [2,3]

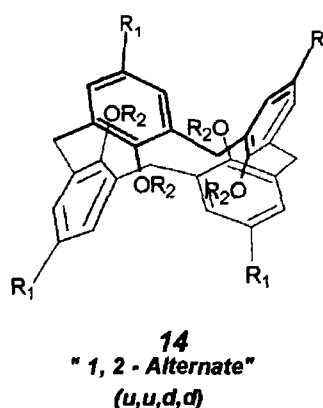
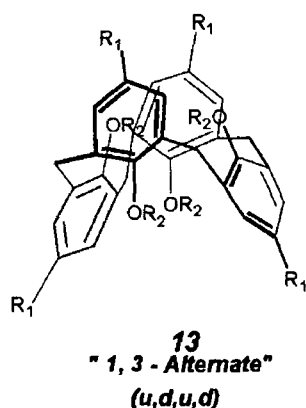
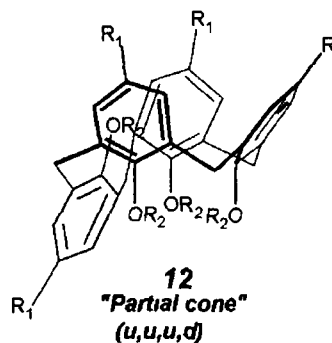
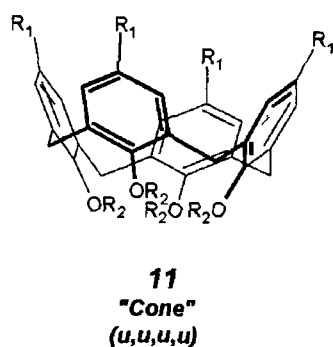


Figure 1 7 Four conformations of calix[4]arene

1 1 3 Synthesis of Calixarenes

Calixarenes can be synthesised by two general procedures 'One-pot' and 'multistep' synthesis

1 1 3 1 One-pot Synthesis

One-pot synthesis of calixarenes can be accomplished using acid or base reaction conditions

Base induced condensation of *p*-*t*-butylphenol and formaldehyde using an alkali hydroxide yielded the tetra-, hexa- and octamer in good yield [1] *Figure 1 8* details the reaction mechanism for the formation of calix[*n*]arenes

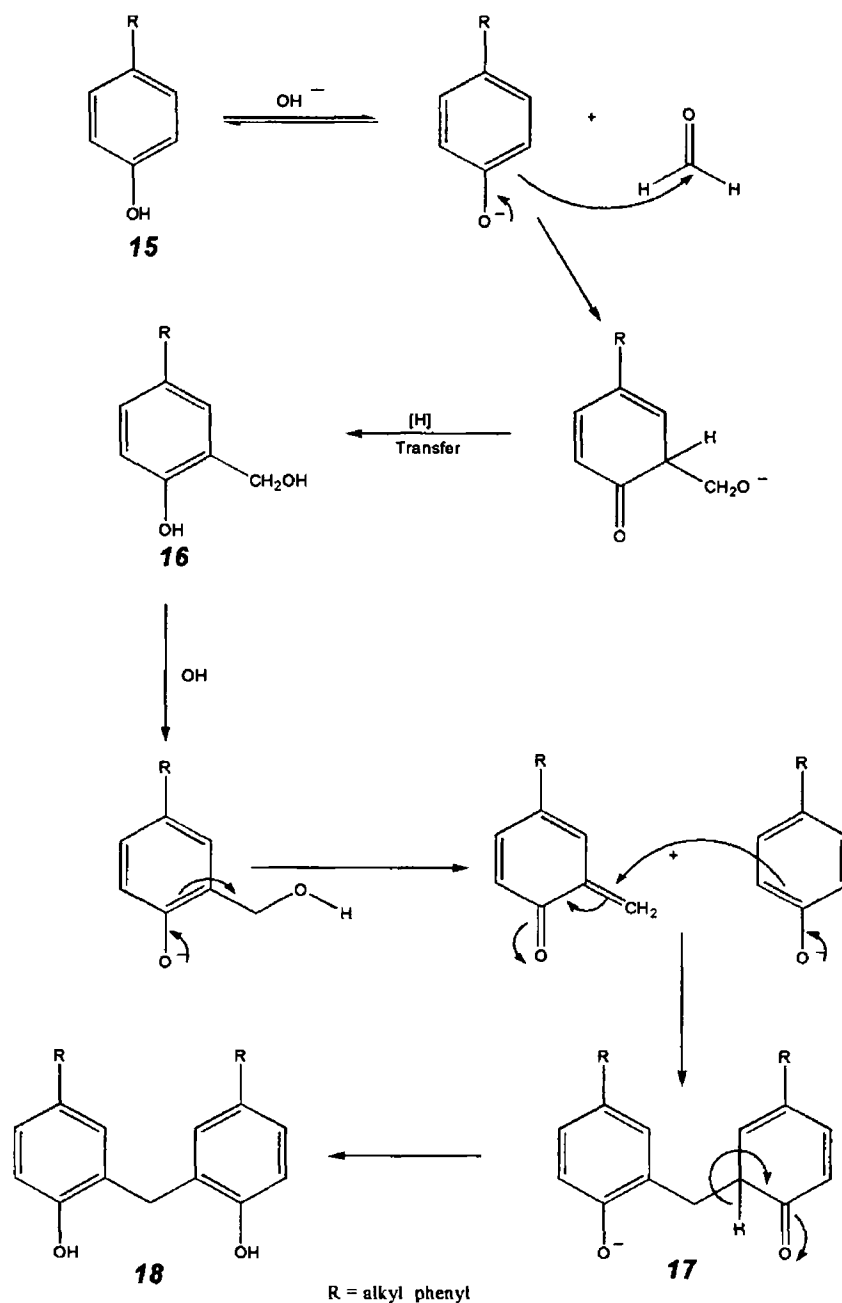


Figure 1 8 Reaction pathway for base induced formation of calix[*n*]arenes

The base abstracts the phenoxy proton, generating the phenoxide ion, an effective nucleophile which subsequently attacks the electropositive carbon of the carbonyl group of formaldehyde. This unstable intermediate transforms to the resonance stabilized, hydroxymethyl phenol via proton transfer.

This reaction proceeds further to give diaryl methyl compounds via quinonemethide intermediates. Ensuing reactions occur to give a linear oligomer which undergoes cyclization to form calix[n]arenes [2].

There are three general procedures for the base induced preparation of calix[n]arenes. The modified Zincke-Cornforth and Petrolite procedures entail heating a mixture of *p*-*t*-butylphenol, formaldehyde and base for two to four hours. The modified Zincke-Cornforth gave a 30-35% yield of cyclic tetramer whilst the modified Petrolite procedure yielded ~75% cyclic hexamer. The final process, the Standard Petrolite procedure is a general procedure for the preparation of the cyclic octamer in 60 – 65% yield, employing *p*-*t*-butylphenol, paraformaldehyde and base.

It was concluded that the reaction conditions exert a controlling influence on the type of calixarenes synthesised. The general observation was that higher reaction temperatures favour calix[4]arene formation. The cyclic hexamer and octamer are converted to the cyclic tetramer at higher temperatures and under basic conditions. Larger amounts of base (specifically potassium hydroxide and rubidium hydroxide) are necessary for the formation of calix[6]arene (Fig 1.9).

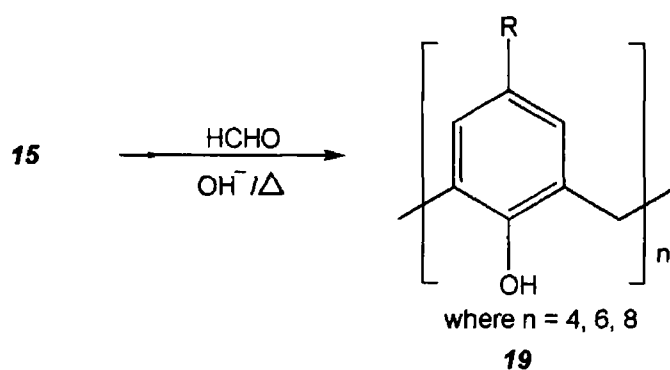


Figure 1.9 General reaction scheme for the synthesis of calix[n]arene

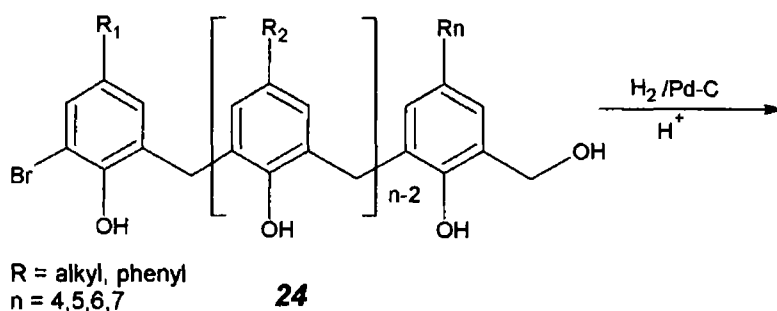
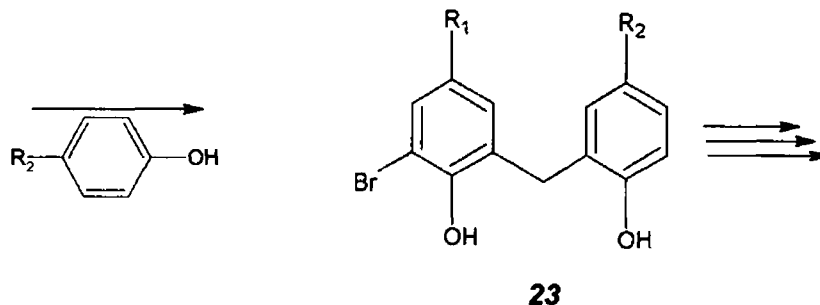
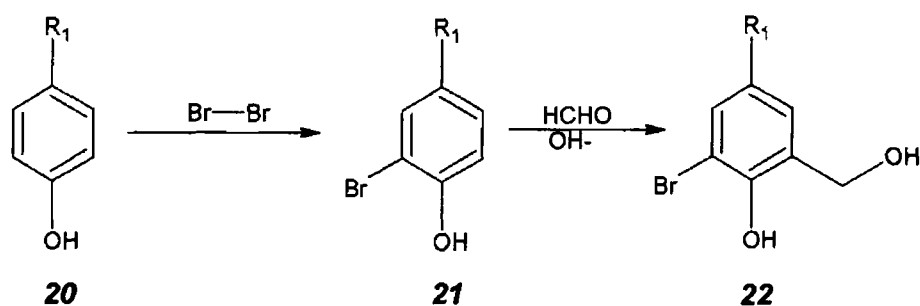
These two procedures yield 4, 6, and 8 in multigram quantities. 5 or 7 may be prepared by the same procedures but in much smaller quantities (5-10%). It was generally conceived that the acid catalysed reaction of *p*-alkylphenol and formaldehyde produced the linear oligomers but in fact under certain conditions, this reaction produced calixarenes in almost quantitative yield [3,4,5,136].

1 1 3 2 Multistep Synthesis

The synthetic alternative to the 'One-pot synthesis' is that of the 'multistep synthesis' proposed by Hayes, Hunter and Kammerer-Hagel, that provides an effectual route to asymmetrically substituted calix[n]arenes. The principle synthetic strategies are outlined below

1 1.3 2.1 'Non-convergent stepwise synthesis'

The principle attributes of this synthesis are the protection of the ortho position of the phenol by bromination, subsequent hydroxymethylation of this *o*-bromo-*p*-alkylphenol and arylation by acid catalysis, furnishing a linear oligomer that cyclizes under dilute acid conditions



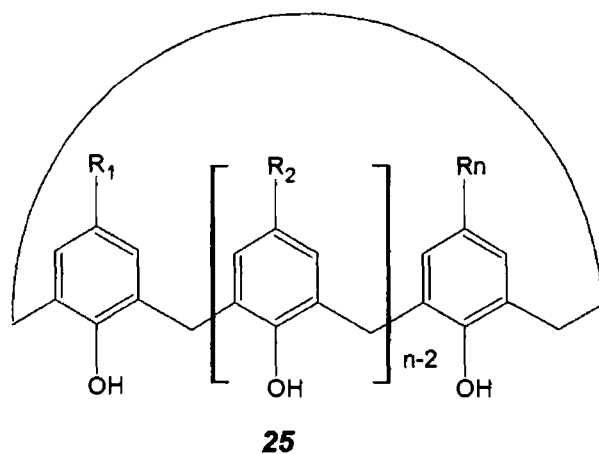


Figure 1 10 Stepwise synthesis of calix[n]arenes

The synthesis is tedious, complicated, affording low yields typically less than 10% due to the large number of steps in this synthesis [5,6]

1 1 3 2 2 'Convergent stepwise synthesis' (fragment condensation)

Condensing two or more calixarene fragments and subsequent cyclization, afforded asymmetrically substituted calixarenes in larger quantities, typically 30-40% *Figure 1 11* demonstrates the synthesis of a cyclic tetramer by two different routes, '3 + 1' and '2 + 2' fragment condensation [2,5,9]

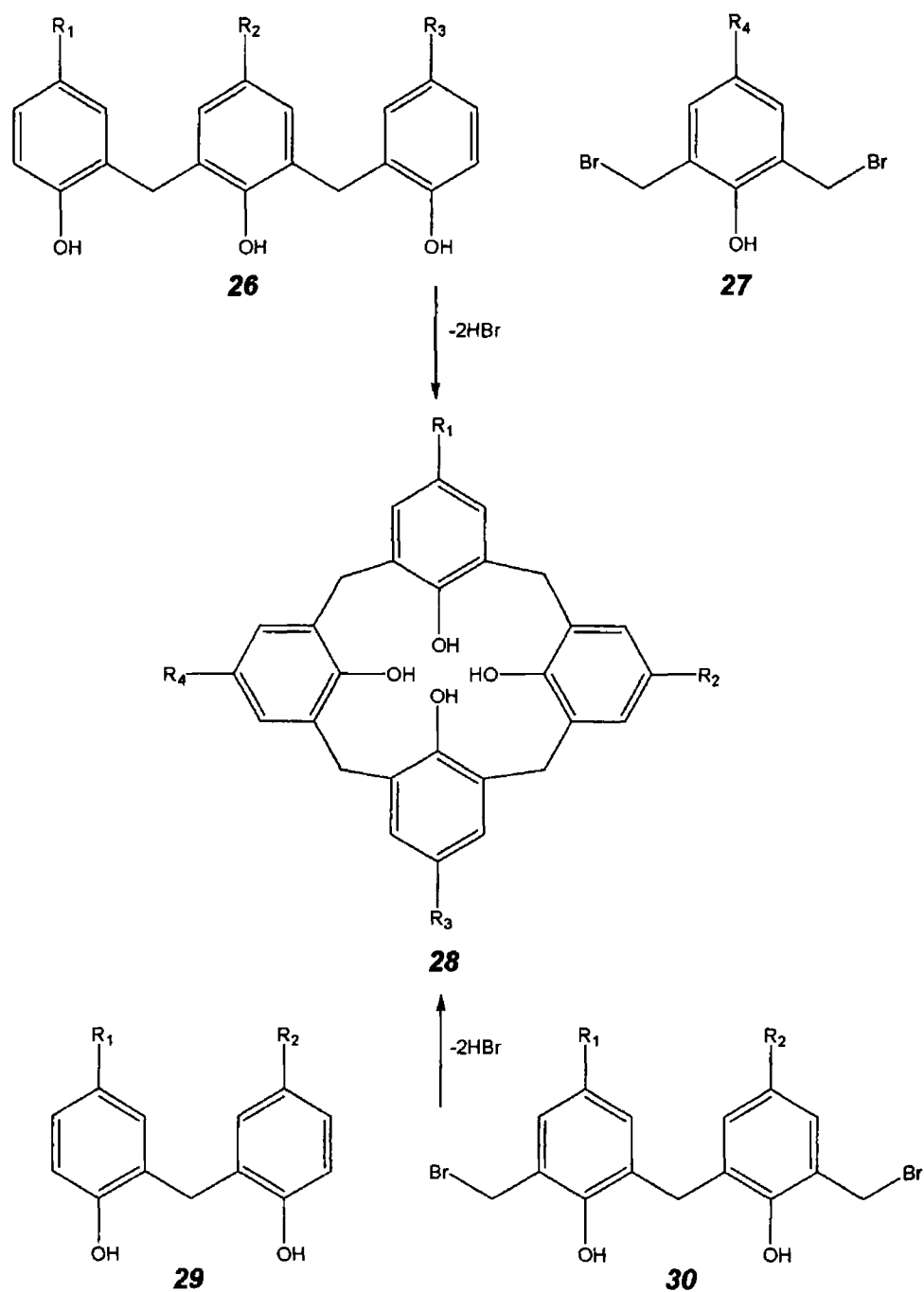


Figure 1 11 “3+1” & “2+2” convergent stepwise synthesis of calix[4]arene

1 1 4 Functionalisation of Calixarenes

The parent calixarenes (*Fig 1 3*) demonstrated limited practical use whereas calixarene dervatives continue to exhibit numerous applications. It is fortuitous that calixarenes possess a unique structure, readily functionalised at the upper and lower rim.

Modification of the calixarene is possible by functionalising the phenolic hydroxy groups (*lower rim*) or electrophilic substitution at the position *para* to the phenolic hydroxy group (*upper rim*).

1 1 4 1 Complete Functionalisation

1 1 4 1 1 The phenolic hydroxy groups (Lower rim)

Functionalisation at the lower rim of the calixarene has been achieved by two procedures

Etherification

Complete alkylation of the hydroxide groups with simple alkyl halides has been attempted successfully by utilising a large excess of alkylating agent. A range of tetra-alkyl ethers e.g. methyl, ethyl, allyl and benzyl ethers were obtained by treatment of the calix[n]arene, $n = 4, 5, 6$ or 8 , with sodium hydride (**NaH**) followed by the alkyl halide in dimethyl formamide (**DMF**) / tetrahydrofuran (**THF**) (Fig 1 12) [1,2,5,12,16,22,26]

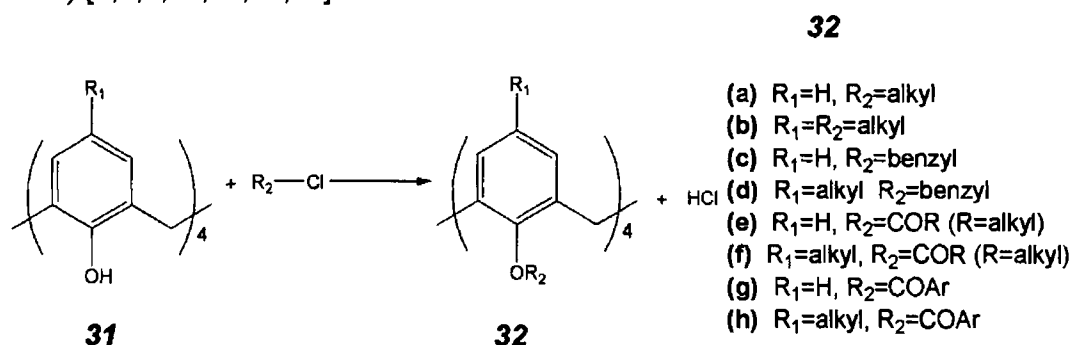


Figure 1.12 Etherification pathway of a calix[4]arene

Alkylating agents of the structure XCH_2Y (X is a leaving group, e.g. Br or tosyl, Y is a functional group), termed polyfunctional reagents have been used to introduce functionality onto the lower rim according to etherification procedures. Such functionalities include amide (**33**) [15-18,19], ester (**34**) [13,14,18, 23-25] and ketone groups (**35**) [13,14] amenable to further transformation by hydrolysis [22,37], transesterification [45] and reduction [27,38] (Fig 1 13)

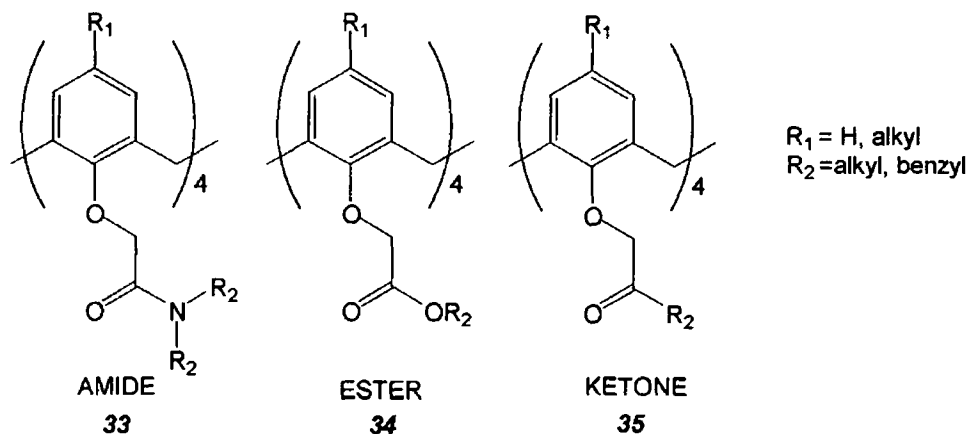


Figure 1 13 Various calixarene derivatives (using polyfunctional reagents)

A fixed degree of control of stereochemistry of these alkylation reactions has been accomplished. Simple alkylation of calix[n]arenes using NaH as base and DMF or THF/DMF as solvent results in the ether fixed into a cone conformation (n = 4, u,u,u,u). Modification of the reaction conditions for alkylation generates different conformers of the tetra-alkyl ether calix[n]arene derivatives. Tetraethers of calix[4]arenes e.g. tetramethyl and tetrapropyl are quite flexible and exist in variable conformations whilst tetraacetates and higher order esters of calix[4]arenes are conformationally inflexible [28,29,30,31].

The '1,3-alternate' conformation ("2 up and 2 down") predominates when acetonitrile (ACN) and caesium carbonate (Cs_2CO_3) are employed as solvent and base respectively [23,24,25]. The 'partial cone' structure ("3 up and 1 down") is mainly obtained by using potassium t-butoxide in benzene [28,29,30]. There has been little success in the development of a selective synthetic procedure of a tetra-alkyl ether calix[n]arene derivative fixed in a '1,2-alternate' conformation ("2 up and 2 down") [30,31].

To synthesise a tetra-O-propylated calix[4]arene derivative, a large excess ~ 10 fold of Cs_2CO_3 was employed which yielded a diverse conformer distribution of 24% **37**, 67% **38**, 9% **39** and no **36** [29].

The tert-butyl groups present in the para- position destabilise the cone and 1,2-alternate conformation as it is arduous to reduce the increased steric crowding by the conformational change. The partial cone structure alters significantly to alleviate the increased steric crowding caused by the t-butyl groups, thus stabilising this conformation. The t-butyl groups cause slight steric crowding of the 1,3-alternate conformation but to a lesser extent than observed for the 'cone' and '1,2-alternate' conformation. Thus, the 'partial cone' and '1,3-alternate' are the most stable conformers (*Fig 1 14*) [34,35,36].

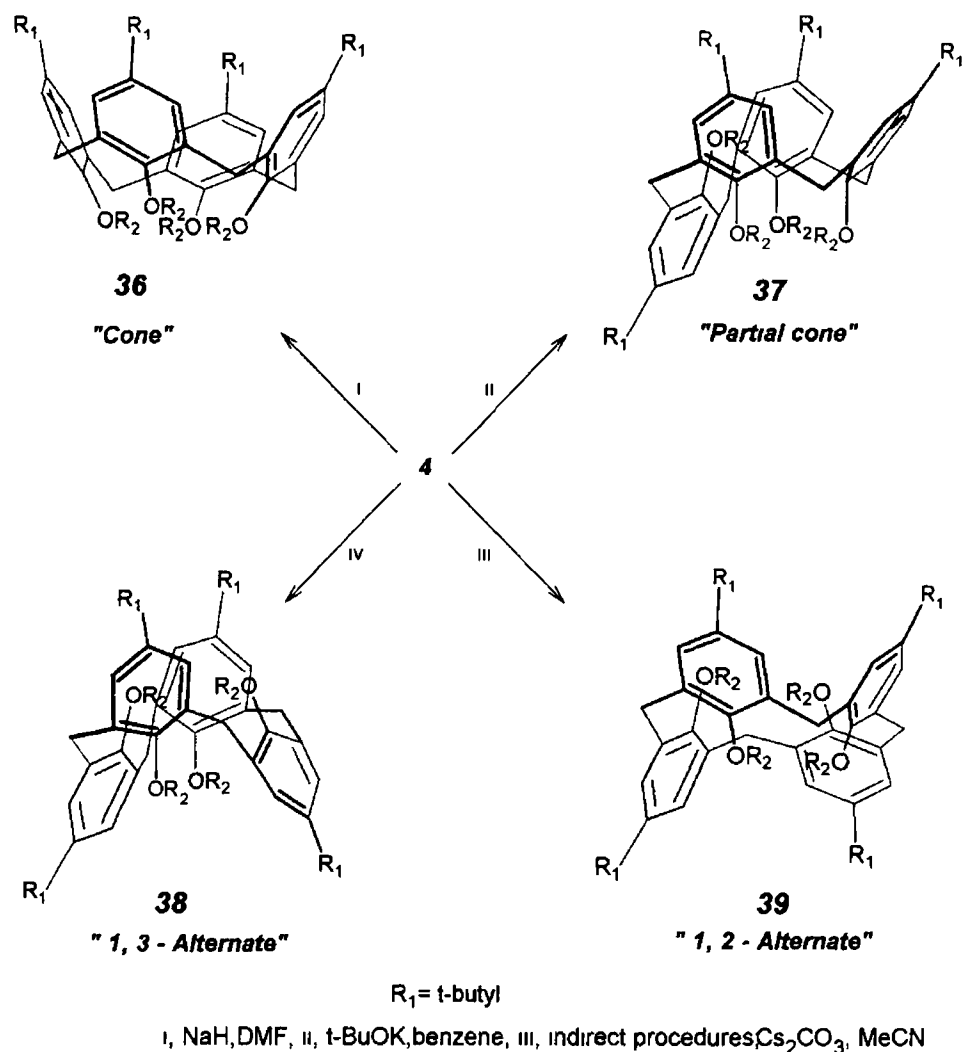


Figure 1.14 Various conformers of a tetrasubstituted calix[4]arene by four different pathways

Shinkai et al investigated the influence of solvent and base on the relative yield of conformers synthesised from the alkylation of calix[4]arenes[29] His results indicated that conformer distribution in O-alkylated calix[4]arenes was principally governed by metal template effects

Sodium, barium or calcium act as a template for 'cone' conformation whereas the 'partial cone' conformer dominates with caesium as this cannot act as a template Table 1.1 indicates a change in selectivity from 100% cone in the presence of sodium carbonate to 100% partial cone with caesium carbonate [25] Metal template effects on % conformer distribution are also evident in O-alkylation reactions using polyfunctional reagents

Solvent	Base	Cone (%)	Partial cone (%)
THF	NaH	100	0
DMF	Li ₂ CO ₃	100	0
DMF	Na ₂ CO ₃	88	12
DMF	K ₂ CO ₃	84	16
DMF	Cs ₂ CO ₃	27	73
Acetone	Na ₂ CO ₃	100	0
Acetone	K ₂ CO ₃	96	4

Table 1 1 Conformation distribution of tetra-alkylated dervative

Esterification.

Complete esterification of calix[n]arenes was achieved by utilising acid halides and NaH, acid halides and aluminium trichloride (AlCl₃) or acid anhydrides and sulphuric acid (H₂SO₄)

Acetylation, propionylation, benzoylation of **4** and **41** all yield the tetraacylates, by employing the aforementioned conditions. Penta-acetate, -benzoate, and -tosylate of **5** were prepared by using acid halide/NaH or anhydride/H₂SO₄. Complete acetylation of **6** was possible whilst arylation resulted in partial esterification. Compound **7** has remained largely unstudied while **8** may be readily converted to its octaacetate counterpart (*Fig 1 15*) [2,4,5]

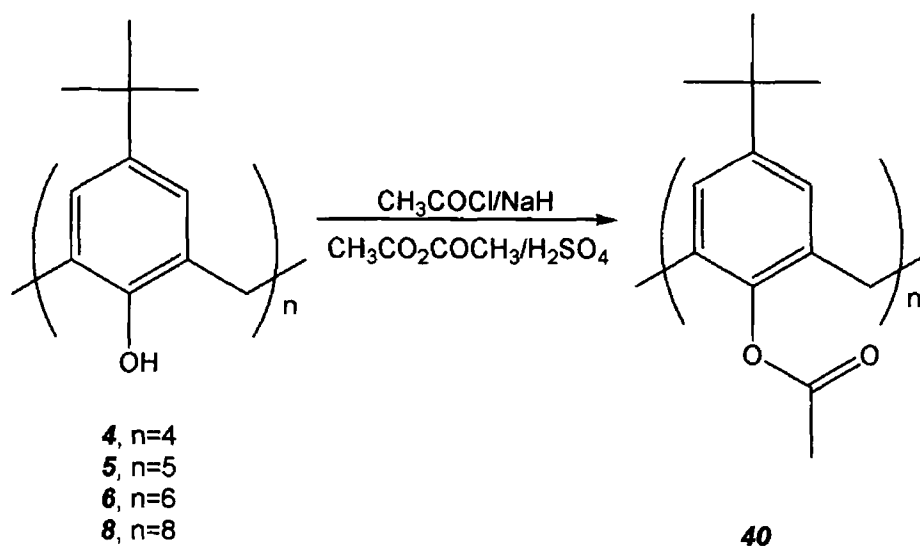


Figure 1 15 Esterification pathway of calixarenes

1 1 4 1 2 The aromatic nuclei (upper rim)

The *t*-butyl groups para to the phenolic hydroxy groups are easily removed via a reverse Friedel-Craft reaction [39,40]. The Lewis acid, AlCl_3 catalyses the transfer of the butyl groups from the calixarene to toluene, the solvent used [41,42]. Phenol is added to the reaction mixture to increase the rate of reaction. Typical yields for this reaction are 65% calix[4]arenes (**41**), 89% calix[6]arenes (**43**) and 93% calix[8]arene (**45**) (Fig 1 16) [43,44,46].

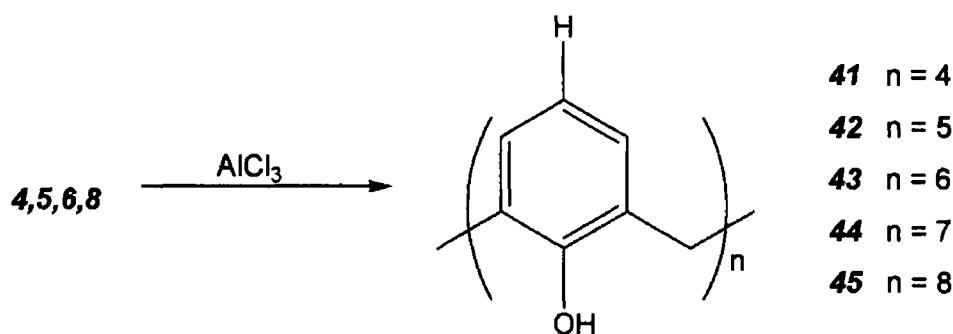


Figure 1 16 De-*tert*-butylation of calix[*n*]arenes

With the *para*-substituted position vacant, electrophilic aromatic substitution reactions, (EAS) prevail. EAS functionalisation reactions studied include halogenation, nitration and sulphonation (Fig 1 17).

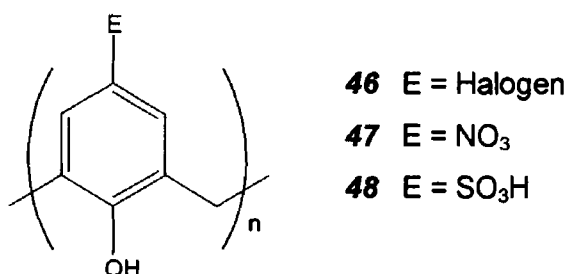


Figure 1 17 Electrophilic aromatic substitution of calix[*n*]arenes

Halogenation

Complete bromination of the *para*-position of calix[4]arene has been effected by reacting the tetra alkyl ethers with *N*-bromosuccinimide. There has been relatively little success in complete *para*-substitution with other halogens, including chlorine and fluorine [46,48].

Nitration and Sulphonation

Early attempts of direct nitration of calix[4]arene was difficult. In 1986, Dr No et al reported the synthesis of tetra-*p*-nitrocalix[4]arene, in 53% yield by treating calix[4]arene first with sodium hydroxide and sodium nitrate in water followed by

oxidation with dilute nitric acid. Direct nitration of calix[4]arene with nitric acid in an acetic acid-benzene solution gave an 87% yield of **54**, $n=4$. These nitrocalixarenes favour the introduction of different functional groups, for example reduction of **54** to **55** using hydrazine and Raney nickel or iron chloride as catalysts [49,51,52]. Conversion of these aminocalixarenes to amides or diazonium salts, generates many calixarene derivatives with potentially useful applications.

Electrophilic aromatic substitution results in *o*-, *m*-, *p*-substitution of C_6H_5Y but in theory there is a possibility of attack by an electrophile (E^+), occurring on the ring carbon atom to which the substituent, Y , is already attached. The process of displacement of Y^+ is referred to as *ipso*-substitution. *Ipso*-nitration of calixarenes has been studied whereby the *t*-butyl groups are directly replaced by nitro groups, obviating the necessity for their prior removal in a separate step. The procedure fails for **4** but is successful for its ether derivatives. Tetramethyl ether of **4** gave the tetra nitro derivative, **50** in 75% yield, following treatment with 20 equiv of 100% HNO_3 . *Ipso*-substitution of calix[6]arenes may also be effected, **49**, $n = 6$ was directly converted to **51** in 50% yield [2].

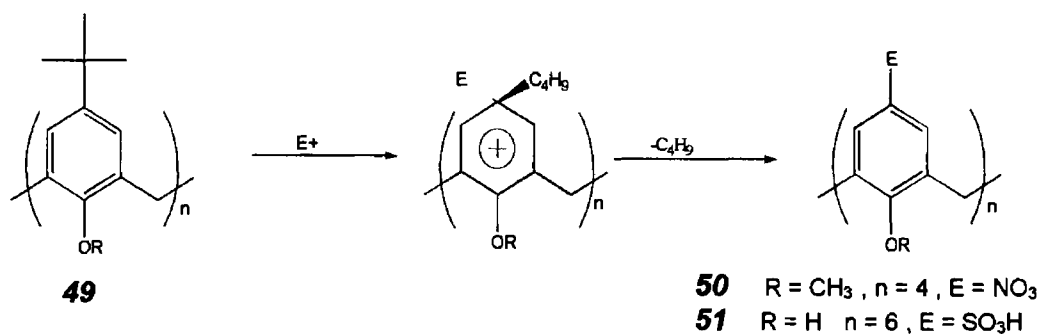


Figure 1.18 *Ipso*-Substitution of calix[n]arenes

Shinkai et al. successfully explored both nitration and sulphonation of the upper rim of calixarenes with varying ring sizes. The following trends were observed: (a) **54**, $n=8$, was synthesised in 27% yield by direct nitration [53], (b) successful sulphonation of **43**, **47** in 78-88% yield and 75% yield for **45** (Fig 1.18) [53,54,55]. The sulfonatocalixarenes provide a convenient route to further functionalisation, including the generation of sulfonamides and *N*-alkylsulfonamides [56,57]. The sulfonatocalixarenes are important, as they are water-soluble, a property that renders them useful as additives in CE and HPLC or as catalysts in ring opening hydrolysis. With appropriate functionalisation, they may also be potential ionophores in aqueous based sensors.

Hydroxycalix[n]arene *p*-sulfonate is selective for the uranyl ion (UO_2^{2+}) in aqueous solutions [126] These electrophilic aromatic substitutions may be summarized as shown (Fig 1 19)

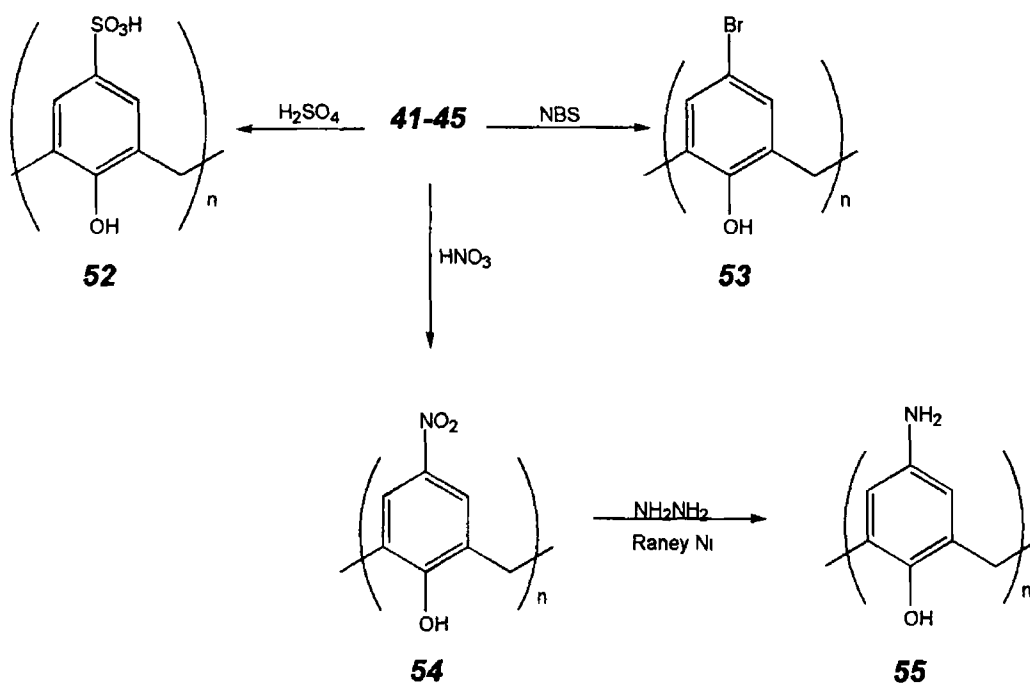


Figure 1 19 Electrophilic substitution reactions of calixarenes

Functionalisation via *para*-Claisen Rearrangement

The Claisen rearrangement is an intramolecular sigmatropic rearrangement which entails the migration of a sigma (σ) bond within a pi (π) electron framework. This rearrangement typically converts allyl phenyl ethers to *o*-alkylphenols via an enolisation intermediate [61]. As is the case with calix[n]arenes, the *ortho*-positions are unavailable due to the methylene groups. *Para*-enolisation may occur resulting in the more stable *p*-substituted phenol (Fig 1 20) [45]

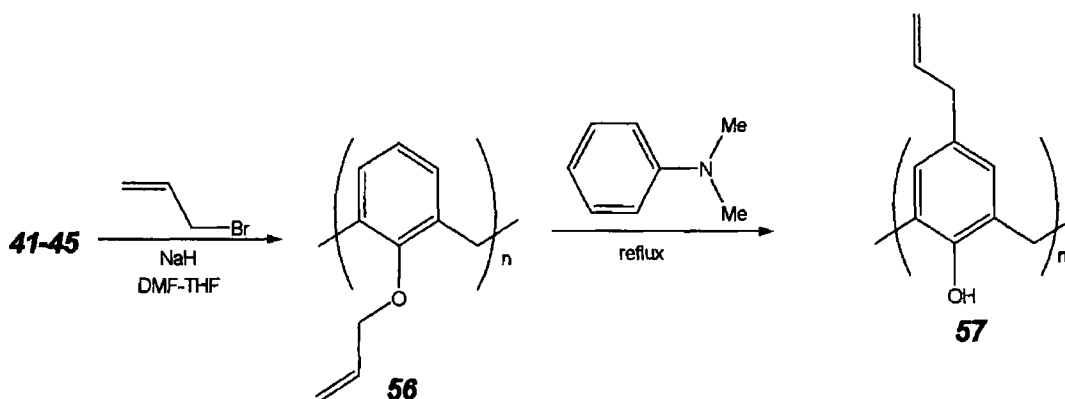


Figure 1 20 *para*-Claisen rearrangement route of calixarenes

The *p*-Claisen rearrangement of calix[n]arenes has been extensively explored resulting in a diverse range of calix[n]arenes with varying substituents appended onto the upper rim. Such substituents included an aldehyde functionality, which reduces to its alcoholic counterpart. The reactivity of this alcohol derivative was enhanced by modification to an alkyl halide facilitating conversion to an azide or amine derivative [62,63].

Functionalisation by the Friedel-Craft reaction:

Alkyl groups have been appended onto the upper rim of calix[n]arenes by the Friedel-Crafts reaction. The *p*-alkylated derivative of **41** was prepared in 63% yield, by treatment of **41** with *i*-propyl bromide and iron chloride (FeCl₃) in chloroform (CHCl₃) [72,73]. One of the most effective Friedel-Craft alkylation reactions is that of chloromethylation which was first applied to calix[n]arenes by Ungaro and his co-workers. A chloromethylene group was affixed to the *para*-position by treatment of **41** with octyl chloromethyl ether and tin chloride (Fig. 1.21).

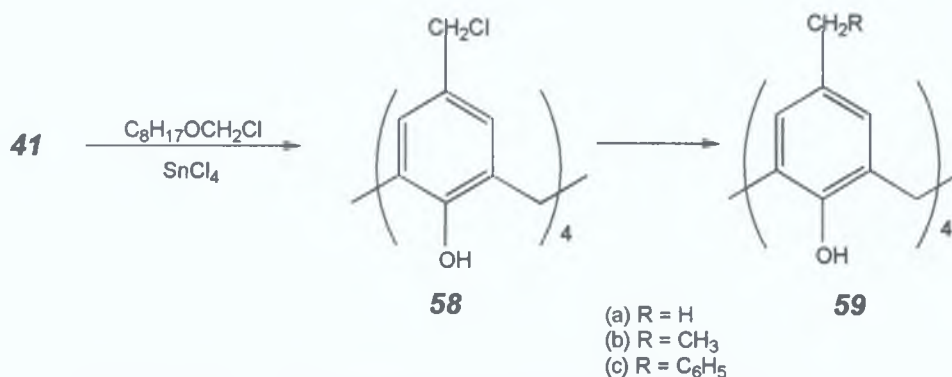


Figure 1.21 The *p*-chloromethylation of calixarenes

The chloromethylation was a useful reaction, facilitating conversion of **58** to **59a** and by reduction with lithium aluminium hydride, and to **59b** [65,74]. Tetra-*p*-benzylcalix[4]arene, **59c** was synthesised by treatment of **41** with benzene and boron trifluoride [74].

Functionalisation via the *p*-Quinonemethide route:

The *p*-quinonemethide procedure involves aminomethylation of **41**, with dimethylamine and formaldehyde. Quaternisation of this derivative with methyl iodide, **60**, and subsequent treatment of the quaternary salt with a nucleophile functionalises the upper rim [66,67].

The cyanomethylcalix[4]arene, **63**, $n=4$, obtained by the action of CN on the quaternary salt, **61**, is a valuable intermediate for the synthesis of other p -substituted calix[4]arenes, the corresponding carboxymethyl compound, **64a** ($n=4$) by hydrolysis, the aminoethyl compound, **64b** ($n=4$) by reduction [76]. Thus, the quinonemethide route is an effective method of functionalising the p -position of the upper rim with a variety of functional groups (Fig 1 22)

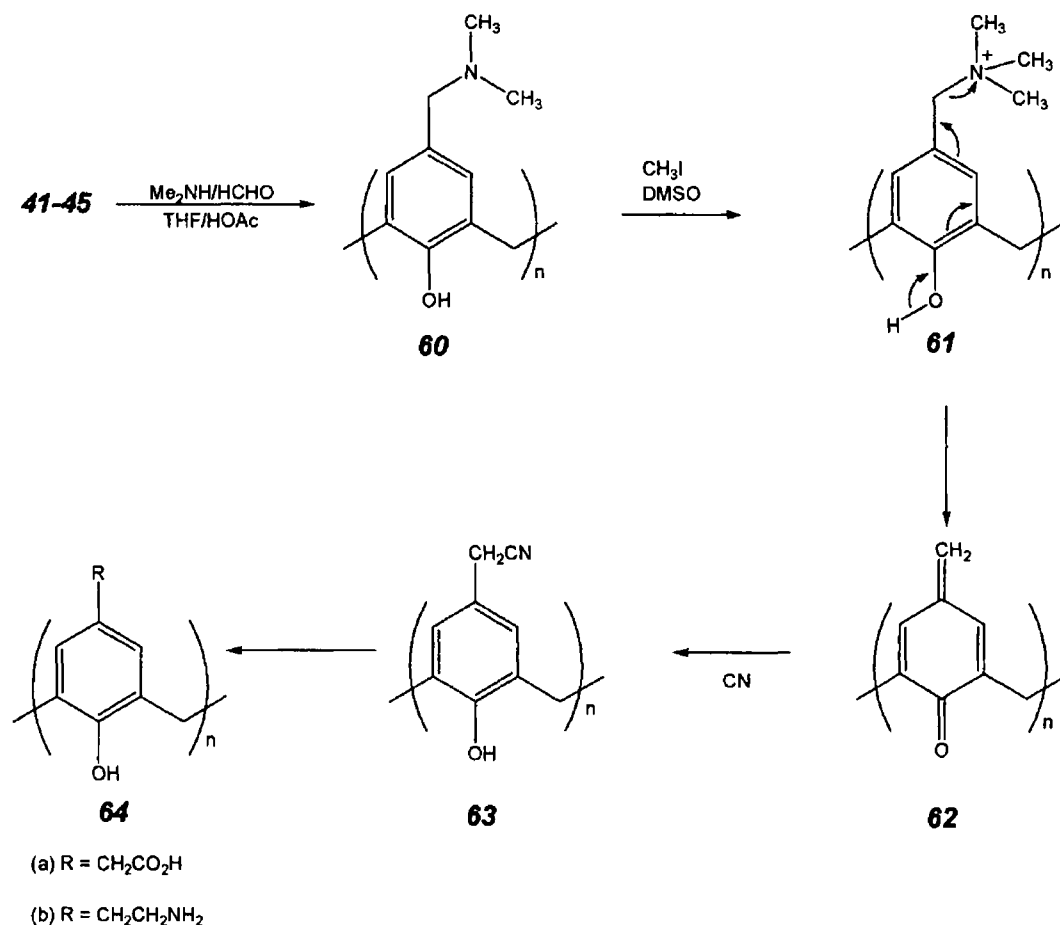


Figure 1 22 Functionalisation of calixarenes via the p -quinonemethide route

1 1.4.2 Selective Functionalisation

The selective functionalisation of the calix[n]arene at both the lower and upper rim has recently warranted much interest due to the potential application of these compounds as polyfunctional ion binders, molecular complexing agents and as enzyme mimics

1 1.4.2.1 Selective Reactions at the lower rim.

The functionalisation reactions of the lower rim described in the preceding section were modified in order to selectively functionalise one, two or three of the phenolic hydroxy groups of the lower rim. Figure 1 23 highlights the varying

reaction conditions required for mono-, di- or tri- substituted calixarene derivatives in varying conformers

Mono-O-alkylated or acylated tetra-*p*-*t*-butylcalix[4]arene can be synthesised by controlling the alkylating agent using caesium fluoride (CsF) as base and DMF as solvent or potassium carbonate (K_2CO_3) as base and ACN as solvent [77]

The distal (1,3)-disubstituted calix[4]arene (**65**) was obtained by using K_2CO_3/CH_3CN or Na_2CO_3 /Acetone Proximal (1,2)-disubstitution (**64**) of **4** was successfully synthesised using sodium hydride (NaH) and DMF [31,32] The trisubstituted calixarene derivative in the cone conformation was obtained using barium hydroxide ($Ba(OH)_2$) as base [32,33]

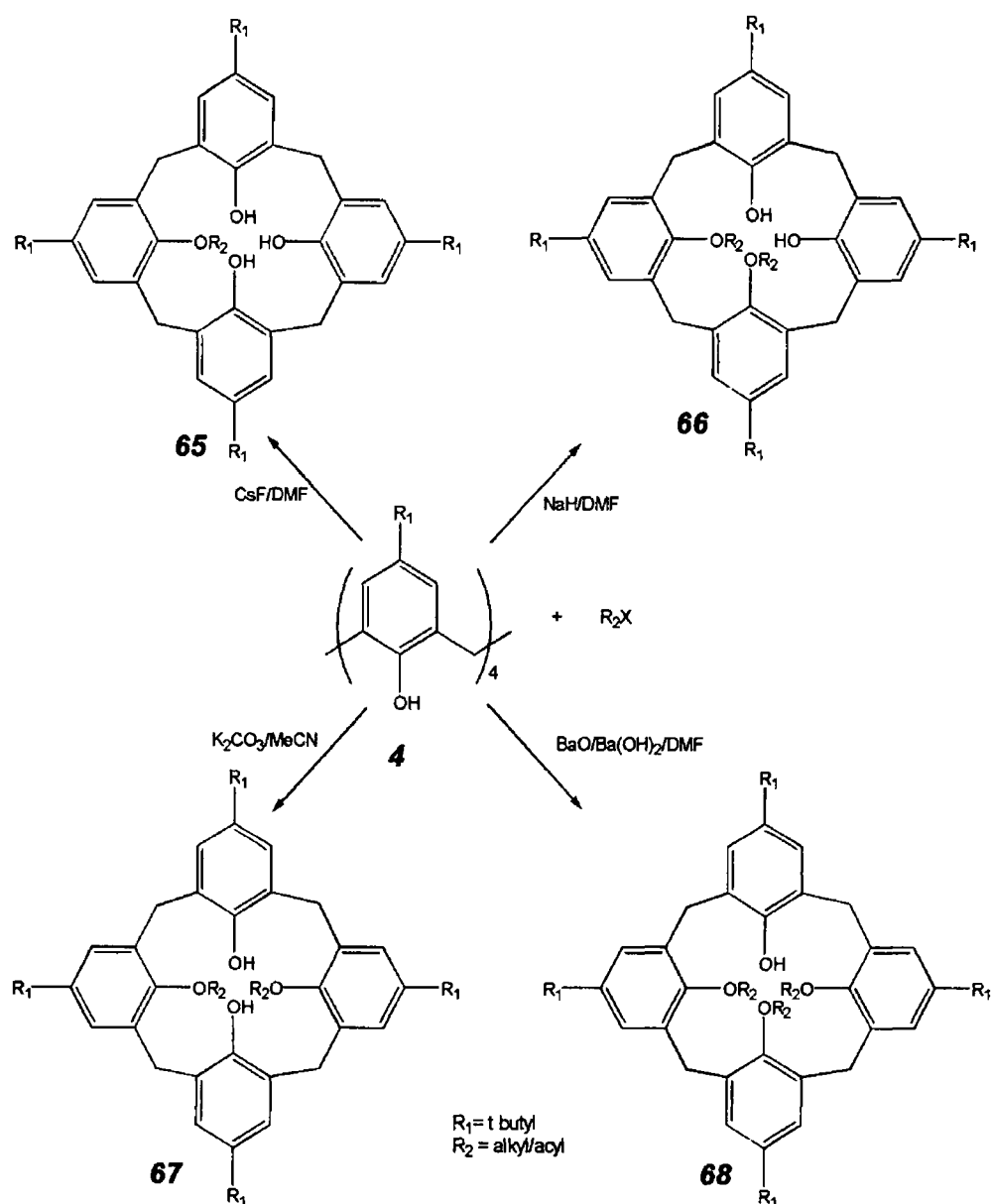


Figure 1.23 Selective functionalisation of calix[4]arene at the lower rim

Monoethers have been synthesized in moderate to good yields by direct alkylation using 1.2 equivalents of a K_2CO_3 in acetonitrile, CsF or $Ba(OH)_2$ in DMF or NaH in toluene. Other methods of preparation of mono-substituted calixarenes have evolved. One particular procedure by Casnati et al. was the dealkylation of calixarene ethers in the presence of ether cleavage reagents. Both calix[4]arene tetraether (**69**) and the diether derivative (**67**) were treated with a stoichiometric amount of iodotrimethylsilane to form the monoalkyl ether (**65**) in good yield (~40-50%) (Fig 1.24) [78].

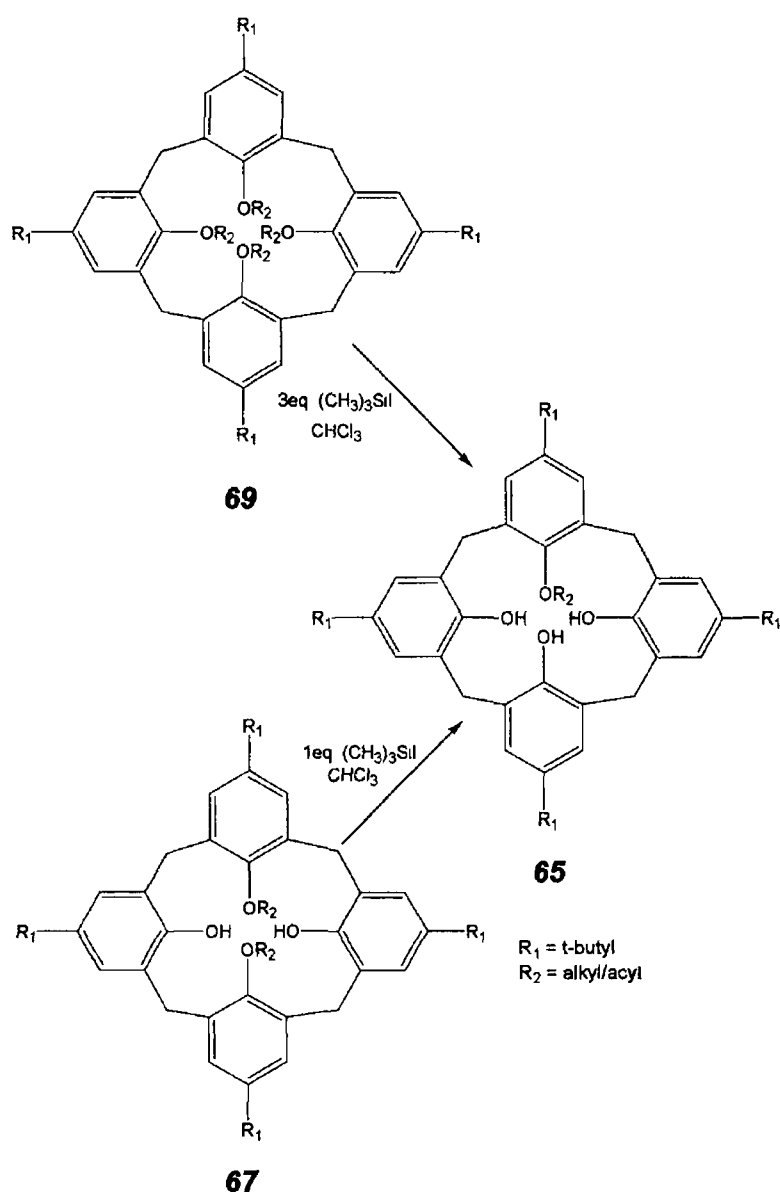


Figure 1.24 Synthesis of the mono-alkylether calix[4]arene derivative

1 1 4 2 1 A Proposed Mechanism for Partial Substitution

To achieve partial substitution, the choice of base and the stoichiometry of the reagents play an instrumental role. Base removes a proton, generating a mono-anion that may be stabilised by hydrogen bonding by the two flanking hydroxide groups, which in turn are stabilised by hydrogen bonding with the remaining hydroxide group. Nucleophilic attack of O on either the ester or the ether molecule generates a mono-substituted derivative.

From *Figure 1 5*, there are two types of disubstitution, distal (1,3) or A,C-disubstitution, **11**, and proximal (1,2) or A,B-disubstitution, **12**.

Realistically, diametrical substitution is favoured to proximal substitution. Regio- and conformational selectivity governs this former substitution. The proton abstracted from the hydroxide group is opposite the mono-substituted moiety. The negative charge of the anion is primarily located on the oxygen atom, diametrically opposite the mono-substituted group, as this is the most stabilised structure due to hydrogen bonding and steric effects. These factors predominate the substitution of the mono-substituted species at the less hindered site i.e. distal (1,3) and not proximal (1,2) disubstitution [81,83].

(1,3)-distal selective-O-functionalisation of calix[4]arenes was reported by McKervey et al. by the reaction of two equivalents of alkylating agent to one equivalent of **4** and one equivalent of K_2CO_3 in ~ 80% yield (**70**). **71** can be prepared in 98% yield by treatment of **4** with an excess of benzyl bromide, K_2CO_3 in acetone [31,32].

It is essential that weak bases be used if **70** and **71** are required. Reinholdt et al. proposed that the reaction ceases at this point even in excess alkylating or acylating agent, as other hydroxide groups no longer flank the remaining hydroxide group so there is no hydrogen bonding available to stabilise the anion. Thus, distal (1,3)-disubstituted calix[4]arenes may be obtained in good yields [28,29,30].

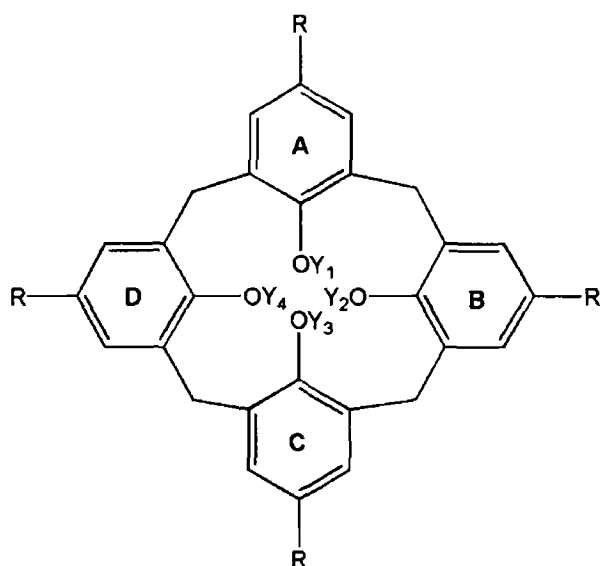


Figure 1 25
(1,3)-distal disubstituted
calix[4]arene

- 70** R = t-butyl
Y₁=Y₃=H
Y₂=Y₄=CH₂CO₂Et
- 71** R = t-butyl
Y₁=Y₃=CH₂C₆H₅
Y₂=Y₄=H

Employing a strong base and a limiting amount of alkylating or acylating agent in DMF produces **66**. Reinhoudt et al treated **4** with six equivalents of NaH and then with 5 equivalents of bromoethyl ether in DMF at 80°C to afford the tetraalkylated cone conformer and the syn-1,2-bis(ethoxyethyl) derivative, of which the latter derivative was postulated to be an intermediate in the NaH/DMF tetraalkylation reaction.

Consequently, they investigated this reaction by treating **4** with 2.2 equivalents of ethyl iodide whilst varying reaction conditions. Conclusions from this investigation were that the reaction conditions govern the intermediate and final conformation of the reaction.

Utilising 2.2 equivalents of ethyl iodide, with NaH and DMF/ACN gave a mixture of products, **65**, **66** while the cone conformer of **69** was synthesised by treatment with excess ethyl iodide. Using 2.2 equivalents of ethyl iodide with potassium hydride (KH) and DMF, yielded **65**, **66**, **67**, and **69**. Reaction with excess ethyl iodide gave 2% **36**, 64% **37**, 17% **38**, 17% **39** (Fig 1 23).

The tetra-anion of a calix[4]arene exists in the cone conformation with Li⁺ or Na⁺ as the counter ions. The tetra-anion can conformationally interconvert at temperatures greater than 140°C for Li⁺, 80°C for Na⁺ and 20°C for K⁺. Due to the strong metal template effect, one or more Na⁺ or Li⁺ cations affix the four negatively charged oxygen atoms into a cone conformation whereas the K⁺ cation gave differing conformers possibly due to rapid interconversion of the

tetra-anion at 20°C. At 20°C, flipping between the different conformers occurs quite readily due to low energy barrier between these states [28,29,30,85,86]

Previous attempts at tri-O-substitution involved NaH and THF-DMF. HPLC analysis of the reaction products of **4** and n-propyl bromide gave a disubstituted intermediate and very little trisubstituted *p*-*t*-butylcalix[4]arene. Instead, attention focussed on the use of Ba(OH)₂ for the preparation of the cone conformer of the trisubstituted *p*-*t*-butylcalix[4]arene derivative. This selectivity was rationalized in terms of the strong banum (Ba²⁺) - phenoxide interactions. In the cone conformation, there are four negatively charged oxygen atoms that are stabilised by Ba²⁺. These Ba²⁺ interactions are stronger than the Na⁺-phenoxide interactions. Thus, **68** may be synthesised in 100% selectivity using Ba(OH)₂ as base [32,33,87,88]

As mentioned in the preceding section (*pp* 19), the base used in tetra-alkylation plays an important role in the conformer distribution of the tetra-substituted calixarene due to a metal template effect [89-91]. Shinkai et al. reported that tetra-O-propylation of **4** in the presence of NaH yielded **36** and **37** in equal ratio. However, the aforementioned reaction in the presence of CsF gave a mixture of **37** (34%), **38** (57%), **39** (9%). The Cs²⁺-phenoxide ion-pair is weak, thus the caesium cannot retain the cone conformation thus, enhancing phenol inversion to yield a mixture of conformers [28-30,33]

1.1.4.2.1 B. Unsymmetrical Calixarene Derivatives

Chiral calixarene derivatives can be synthesised by regio- and stereoselective functionalisation at the lower rim i.e. molecular asymmetry at the lower rim [92]. An unsymmetrical calix[4]arene bearing four different substituents at the lower rim was synthesised following a six step reaction sequence devised by Chung et al. This was quite a novel, unique derivative as prior to this only mono-, di-, tri- or tetra- substitution reactions had been performed, in which the substituents were identical.

The first alkyl group, R₁ = Ph-CH₂- was introduced using R₁Br and sodium methoxide (CH₃ONa). This was treated with propyl chloride to yield a difunctionalised calixarene (**75**) in the 1 & 3 positions. The strategy of the trisubstitution step was of protection of one of the remaining hydroxy groups using benzoyl chloride. The third alkyl group R₃X = CH₂=CH-CH₂-Br was appended onto the lower rim of the calixarene using NaH as a base. The hydroxy

group was deprotected and subsequently alkylated using butyl chloride, to form **77**. By virtue of differing substituents on the lower rim the calixarene was rendered inherently chiral (*Fig 1 26*) [93]

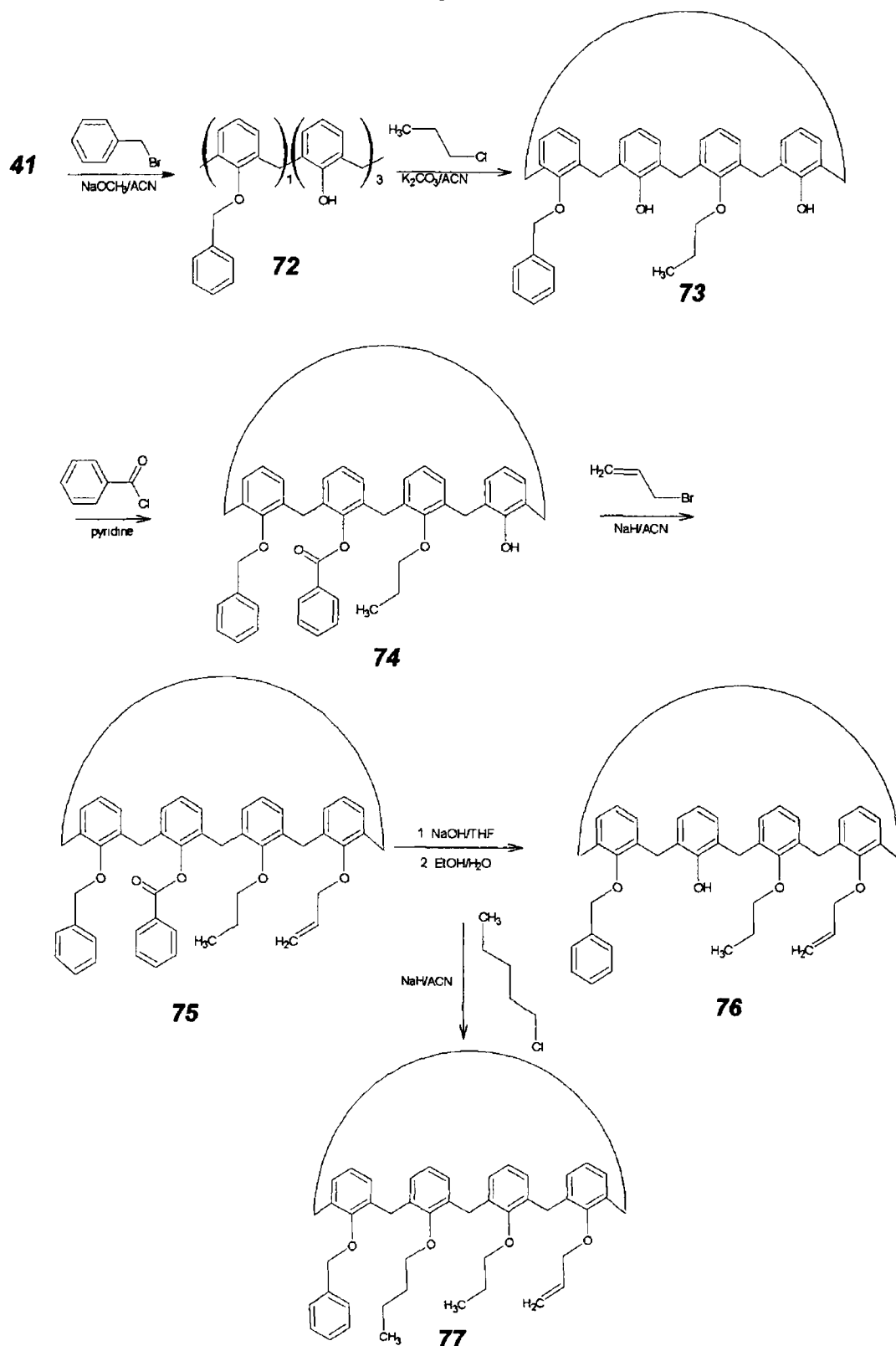


Figure 1 26 Generation of an inherently chiral calix[4]arene

1 1 4 2 2 Selective Reactions at the upper rim.

To selectively functionalise the *p*-position of calixarenes, three synthetic strategies have been applied (1) the functionalisation of the upper rim of a calixarene that has previously been selectively functionalised at the lower rim, (2) the selective de-*t*-butylation of partially O-alkylated or O-acylated calixarenes under controlled conditions, followed by functionalisation on the now vacant para positions and (3) selective Claisen rearrangement on the upper rim [82,94,95]

The first strategy involves selective functionalisation at the upper rim without blocking any of the *para* positions. Reinhoudt et al., demonstrated that bromination of 26,28-dimethoxycalix[4]arene (**78**) in CHCl_3 at room temperature gave 11,23-dibromo-26,28-dimethoxycalix[4]arene (**79**) in 82% yield. Nitration was performed on **78**, with 2 equivalents of nitric acid in a dichloromethane/acetic acid mixture, to give 11,23-dinitro-26,28-dimethoxycalix[4]arene (**80**) (Fig 1 28)

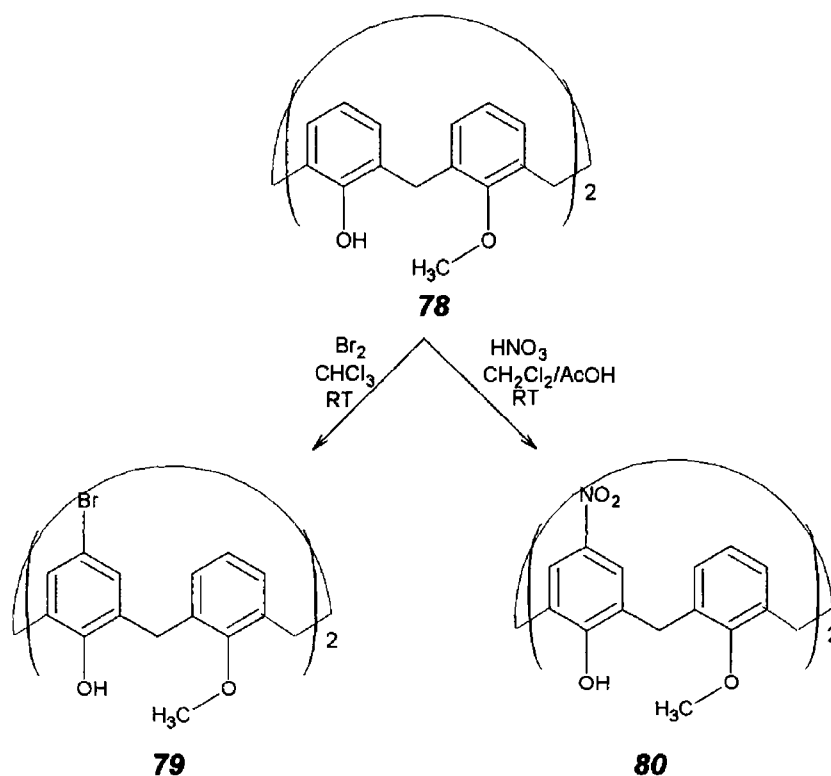


Figure 1 27 Selective functionalisation of the upper rim of calix[4]arene

Selective functionalisation of the upper rim, as shown above, manipulates the different reactivity between phenol and the phenol ether or ester units. The lower electronic activation of the phenol ether or ester units lowers their reactivity to electrophilic attack [95]

Strategy two involves the selective removal of the *t*-butyl group from the

phenolic nuclei and subsequent functionalisation 26,28-Diethoxy-*p*-tetra-*t*-butylcalix [4]arene (**81**) was treated with two equivalents of AlCl_3 in toluene. Two *t*-butyl groups were removed thus rendering the para positions of two phenol rings available for substitution (Fig 1 28) [94,95]

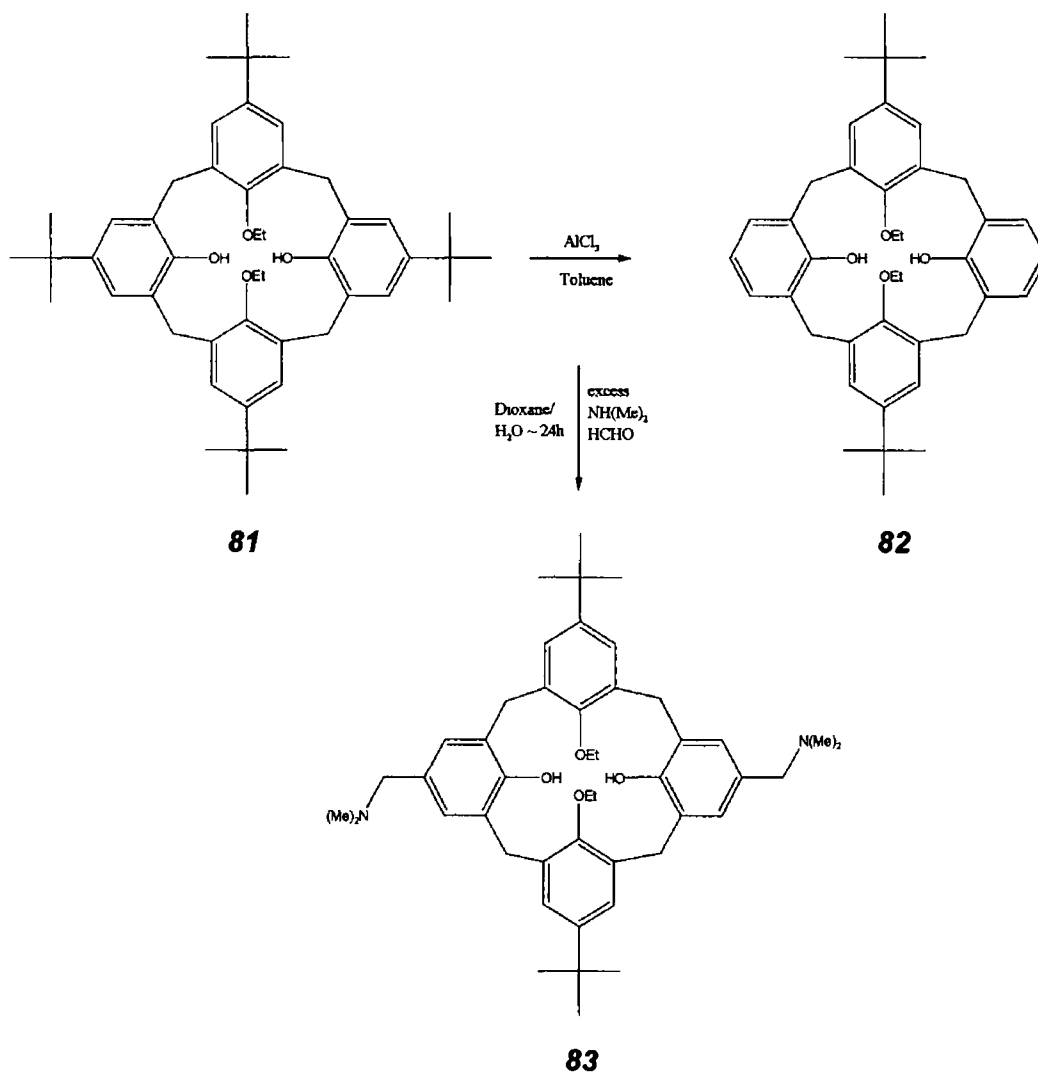


Figure 1 28 Selective functionalisation of the upper rim of calix[4]arene

Strategy three relies on the Claisen rearrangement reaction. The transfer of the functionality from the lower to the upper rim has achieved selective functionalisation of the upper rim. This procedure was described successfully for both mono- and (1,3)-diallylethers of calix[4]arenes. Compound **78** was treated with allyl bromide to yield **84**. Claisen rearrangement of this product gave a *p*-disubstituted structure. The *p*-allyl group is susceptible to conversion to a variety of functional groups, ozonolysis produces the aldehyde (*p*- CH_2CHO) derivative from which the alcohol, amine and alkyl bromide may be synthesised (Fig 1 29) [45,82,95,98]

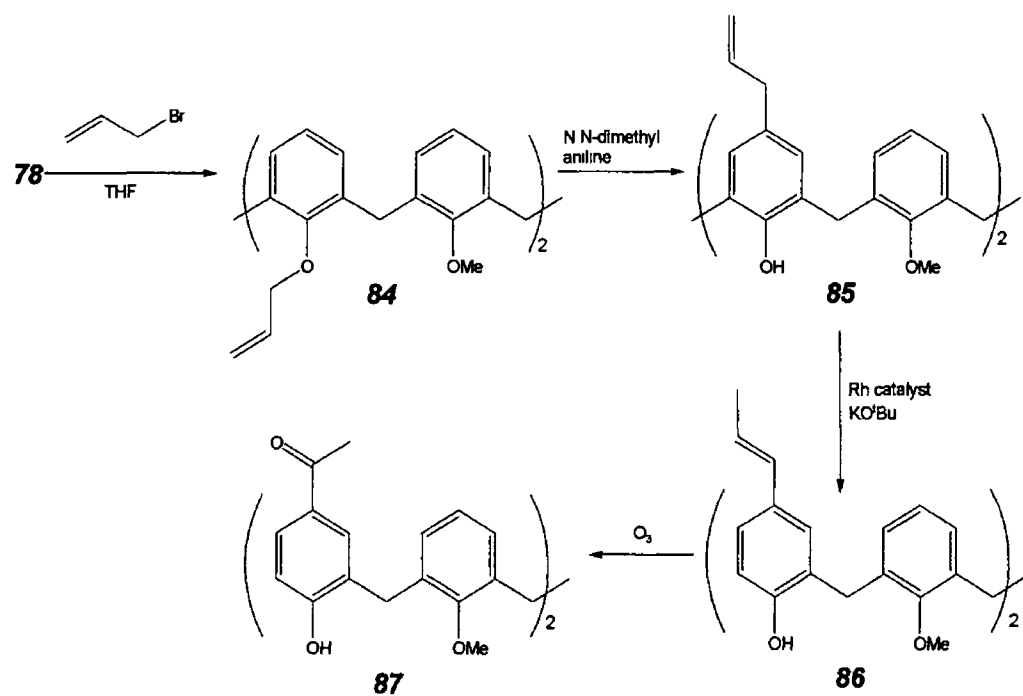


Figure 1 29 Selective functionalisation of the upper nm (Claisen rearrangement)

1 1 5 Applications of Calixarenes

Calixarenes are attractive molecular receptors, as they possess rigid structures with binding sites on their pendant arms, preorganised to form a cavity. Even though calix[n]arenes have low solubility in organic solvents, they present many advantages to their potential use as molecular receptors, for example

- easy and cheap syntheses
- availability in differing ring sizes
- ease of chemical modification of the upper and lower rim
- large variety of potential derivatives

Calixarene-catalysed processes remain the least developed facets of calixarene chemistry. An example of a calixarene catalysed addition reaction is that of the hydration of 1-benzyl-1,4-dihydronicotinamide by **51**. Other calixarene-based catalysts have been employed in hydrolysis reactions including the hydrolysis of 2,4-dinitrophenyl phosphate, which is catalysed, by a calixarene carrying p-trimethylammonium groups [1].

Calixarenes have also been used as stationary phases in chromatographic columns for the analysis of compounds such as barbiturates, xanthine derivatives, estradiol epimers, nitroanilines, peptides and uracil derivatives [2].

Thus, calix[n]arenes provide a route to well defined cavities with both polar and non-polar properties at the lower and upper rim respectively. Calix[n]arenes and their derivatives are employed as selective ionophoric agents, for example, calix[4]arene derivatives for such cations as sodium [26,110], calcium [126], silver [110] and calix[6]arenes for mercury in ion selective electrodes.

The breadth of application of calixarenes is documented in several books by C D Gutsche [1,2] and V Bohmer [3].

1 2 Molecular Receptors for Guest Species [Cationic, Anionic & Neutral Species]

1 2 1 Historical Aspects

In April and November of 1967, two manuscripts were submitted for publication to the Journal of the American Chemical Society by C J Pedersen and by C H Park and H E Simmons. Pedersen's historical paper dealt with the first series of crown ethers. The second manuscript reported the first synthetic organic ligands of the bicyclic diammonium type, displaying halide complexation (*Fig 1 30*) [137,113]

In terms of chemical archaeology, it was interesting that synthetic molecules capable of binding cations and anions were discovered at the same time. Whereas the coordination chemistry of cations has been extensively studied, anion coordination has been studied to a lesser extent.

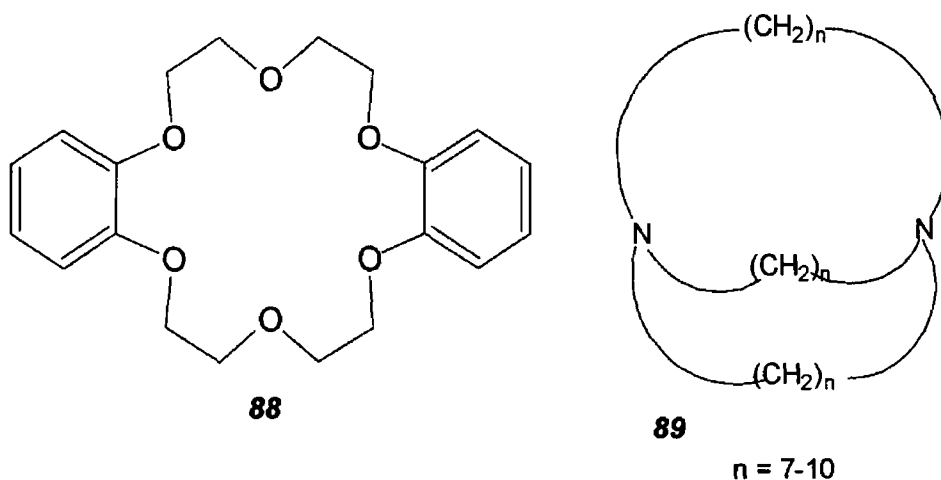


Figure 1 30 First Cation and Anion Receptors developed

Alkali cations, in particular Na^+ and K^+ exert an important influence in the regulation of biological processes, for example, the Na^+/K^+ gradient in animal cells controls cell volume, renders nerve and muscle cells electrically excitable and drives the active transport of sugars and amino acids. Alkaline earth metal cations such as Ca^{2+} play an important role in the regulation of muscle contraction. The development of specific chemosensors for the efficient detection of biologically relevant analytes is one of the most important areas of supramolecular chemistry [138]. For the recognition of such metal cations, specific ionophores developed have been based on the molecular platform of crown ethers, cryptands, spherands, and calixarenes [102,103,139].

Park and Simmons published details of a bicyclic diammonium katapinane (**89**) that encapsulated halide ions, with low stability constants [112,113].

These katapinand compounds marked the synthesis of the first artificial host molecule for anions. However, despite this early success, the field of anion coordination has been relatively slow to develop.

Biologically, 70-75% of substrates and co-factors in biological processes are anions. Anions control essential biological processes such as the activity of enzymes, protein synthesis, transport of hormones and DNA regulation. Cells exchange the energy released from the breakdown of ATP to carry out essential functions, converting chemical energy to electrical energy in transmitting nerve impulses and mechanical energy in muscle contraction. Adenosine triphosphate (ATP), the free energy of life's processes is an anion [114,138].

Environmental pollution is primarily caused by such anions as phosphates (PO_4^{3-}), nitrates (NO_3^-) and sulphates (SO_4^{2-}), commercially found in fertilisers. Rivers and lakes are polluted by these anions causing eutrophication and loss of aquatic life [114]. Developing selective anion receptors is therefore commercially attractive for example, in environmental pollution and wastewater management.

Receptors specifically designed for neutral molecular species have found huge biological applications in particular for the complexation of sugars, peptides and nucleotides [1,2,139]. Sugar derivatives serve as energy stores, as metabolic intermediates and may form part of the structural framework of RNA and DNA. Nucleotides play key roles in nearly all biochemical processes, act as activated precursors of DNA and RNA, as activated intermediates in many biosyntheses. They are components of three major coenzymes, NAD^+ , FAD and CoA . Peptides are subunits of proteins which play a crucial role in biological processes e.g. enzymatic catalysis, the transport and storage of small molecules and ions (O_2 , Fe). Evidently, the design of selective molecular receptors commands extensive research due to widespread potential applications [138].

1.2.2 Characteristics of Guest Species

To design a selective molecular receptor, each guest species must possess a discriminatory characteristic.

Cations are positively charged species and the focus of much calixarene research has been on the development of receptors for metal cations. Such metal cations include the 'hard' metal alkali and alkaline earth cations, Na^+ , K^+ , Ca^{2+} and 'soft' heavy metal ions, Ag^+ , Pb^{2+} , Hg^{2+} . There are also inorganic and

organic molecular cations, such as the ammonium cation, NH_4^+ . These cations vary considerably in size thus enabling size discrimination. Typical ionic radii are 69, 102, 138pm for Li^+ , Na^+ , K^+ respectively while Cs^+ , Ca^{2+} and NH_4^+ are 170, 100 and 148pm (Fig. 1.31).



Figure 1.31 Differing Sizes of the Alkali Metal Cations

Anions are distinguished from other guest species by their negative electrostatic charge. However, unlike cations discussed above, the ionic radii of H_2PO_4^- , PO_4^{3-} and SO_4^{2-} are very similar at 200, 238 and 230pm respectively, and consequently selective complexation of anions based on size discrimination is difficult. The discriminating characteristic of anions is their geometry, as they adopt different shapes (Fig. 1.33), including:

- Spherical (*chlorine (Cl^-)*)
- Linear (*azide (**90**)*)
- Trigonal planar (*nitrate (**91**)*, *acetate (**92**)*)
- Tetrahedral (*phosphate (**93**)*, *hydrogen phosphate (**94**)*, *dihydrogen phosphate (**95**)*)

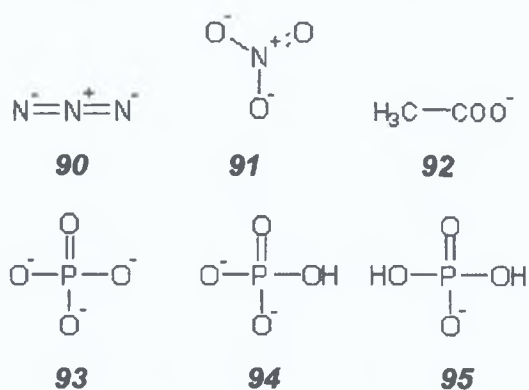


Figure 1.32 Various Anions

The nature of anions makes receptor design more challenging. Anions are larger than isoelectronic cations and therefore, have a lower charge to radius ratio. This decreases the effectiveness of electrostatic binding. Figure 1.33 displays the total charge density surface for the trigonal planar, **91** and the tetrahedrally

shaped, **94**. The total charge density surface is the best visible representation of a molecule's shape, as determined by its electronic distribution. It identifies the electron density in the space surrounding the nuclei of a molecule. As they have varying geometries, a higher degree of receptor design may be required for host-guest complementarity [111,112].

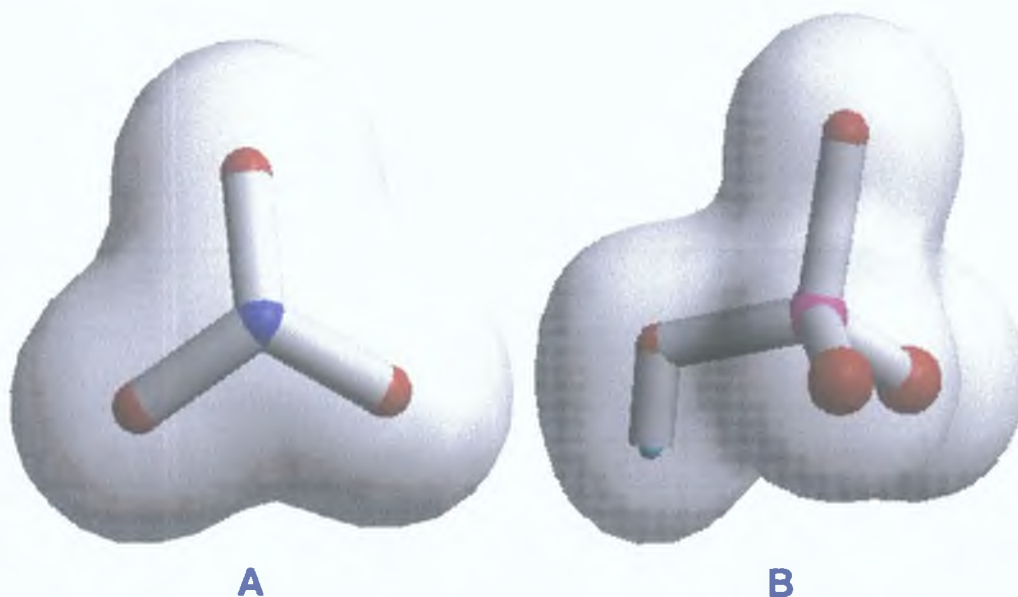


Figure 1.33 3D Shape of NO_3^- (**A**) and PO_4^{3-} (**B**)

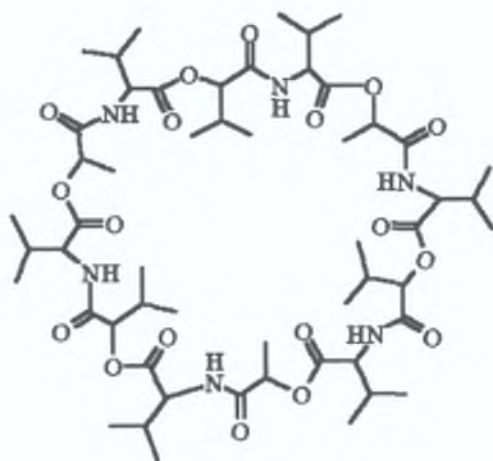
The binding and recognition of neutral molecules utilise electrostatic, donor-acceptor and hydrogen bonding interactions. Neutral species tend to be polyatomic and thus steric hindrance influences the design of receptors.

Attention has focused on the design of new abiotic host molecules that detect the binding event by transduction. The incorporation of an optical and/or redox signalling moiety close to the binding site of the host facilitates its use as a archetype sensor for a target guest species, as anion binding will perturb its electrochemical and/or photophysical properties [111].

1.2.3 Binding and Recognition of Guest Species

1.2.3.1 Complexation of Cations

Three main classes of selective cation receptors may be distinguished, natural macrocycles displaying antibiotic properties such as Valinomycin, **96** (Fig. 1.34). This gives a strong complex in which a K^+ ion is included in the macrocyclic cavity (Fig. 1.35) [139,202].



96

Figure 1.34 Ionophoric Valinomycin

This natural receptor inspired the development of synthetic macrocyclic polyethers (crown ethers, spherands) followed by the synthetic macropolycyclic ligands (cryptands).

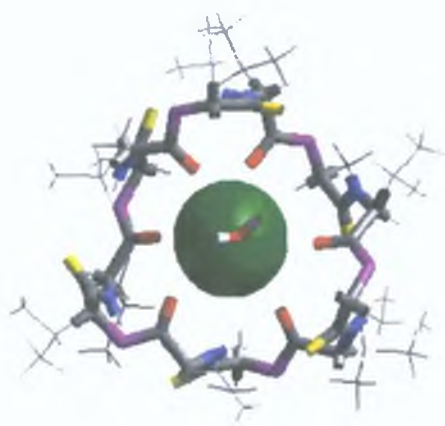


Figure 1.35 3d View of the Valinomycin- K^+ Complex [202]

Selectivity results as a function of the size complementarity between the spherical substrate and the intramolecular cavity, a feature termed spherical recognition. As the size of the cavity increases, the guest size must increase accordingly, Li^+ , Na^+ and K^+ [202].

Crown Ethers

Charles Pedersen discovered that crown ethers (dibenzo-18-crown-6 ether (**98**)) were an effective complexing agent for alkali and alkaline earth metal cations. They resemble a two dimensional binder as they provide the cation with a "ring" of donor groups. Figure 1 36 shows an 18-crown-6-ether (**97**) that forms a complex with a potassium ion by interaction with the six oxygen atoms of the polyether crown compound [102,103,107]

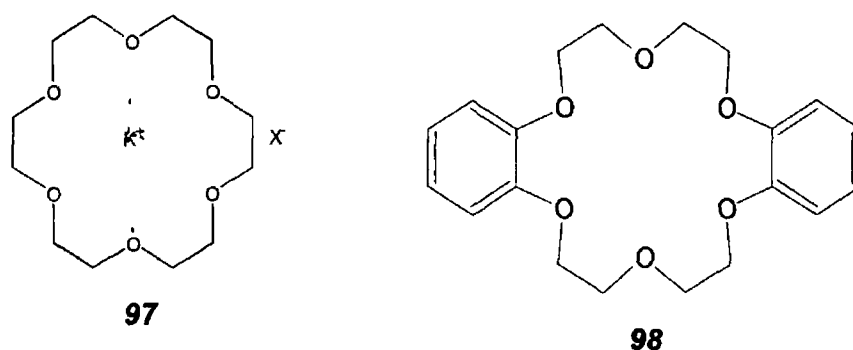


Figure 1 36 18-crown-6 ether- $[K^+X^-]$ complex & dibenzo-18-crown-6

Compound **97** can form a host-guest complex with a methyl ammonium ion, Fig 1 37. Prior to complexation, the host is disordered and contains no convergent binding sites but undergoes reorganisation upon complexation.

The three acidic hydrogen atoms of the methyl ammonium ion guest are hydrogen bonded to three alternate oxygen atoms of **97** in a tripod arrangement [106,107,138]

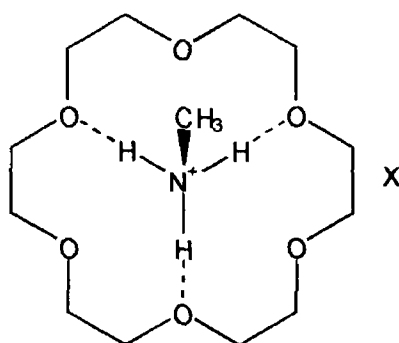


Figure 1 37 18-crown-6 ether- $[MeNH_3^+X^-]$ complex

Cryptands

Concurrent with Pedersen's discovery, Jean-Marie Lehn was researching complexing agents that could encapsulate cations. One design was that of modifying the crown ether by appending a third chain to the opposite ends of the macrocycle (*Fig 1 38*). These macropolycyclic structures are beneficial for the design of an artificial molecular host, as they are large in size and may contain cavities or clefts of appropriate size and shape for binding cations. Due to their polycyclic structure, the presence of branches, bridges and connections aid the construction of a host with desired features, they allow the arrangement of structural groups, binding sites and reactive functions.

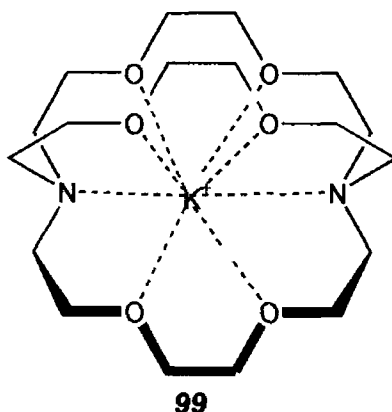


Figure 1 38 Lehn's [2 2 2] cryptand

Compound **99** does not contain either cavities or convergently arranged binding sites but reorganises itself to form a highly ordered potassium complex. The electron pairs of the eight heteroatoms coordinate to the potassium ion [102,104,105]

Spherands

In addition to these complexing agents, Cram et al. developed more complex structures. These macrocyclic molecules possess a preorganised ligand system. *Figure 1 38* illustrates a spherand complex, **100** whose oxygen atoms are octahedrally arranged around a spherical cavity, perfectly suitable to encapsulate sodium or lithium ions.

Crystal structures of **100** show that encapsulated lithium and sodium ions are in contact with six oxygen atoms.

These spherand complexes offer greater advantages for complexation as they provide more interaction sites and are highly preorganised. It has been shown

that combination of these two factors result in the spherand complexes exhibiting significant selectivity

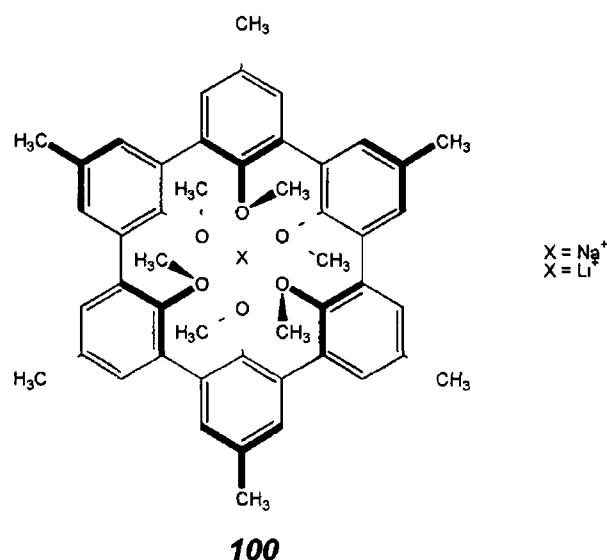


Figure 1.39 Encapsulation of a cation by a spherand complex

Although the crown-ether and cryptands are adequate complexing agents, the spherand complexes overshadow their complexing ability. Cram concluded that preorganisation is a central determinant of binding power. He proposed the principle of preorganisation which states that "the more highly host and guests are organised for binding and low solvation prior to their complexation, the more stable will be their complexes" [102,103,104]

Such soft heavy metal ions as Ag^+ , Pb^{2+} , Hg^{2+} exhibit great affinity for soft coordination centres, nitrogen or sulphur atoms. Replacement of the oxygen sites with soft coordinating atoms, N or S result in macrocycles that exhibit marked preference for transition metal ions, resulting in highly selective complexation of toxic heavy metals.

1 2 3 2 Complexation of Anions

Research into anion receptors may be divided into two categories

- those containing no metal ions
- those based on metal ion centres

The former are ligands that utilise hydrogen bonding and/or electrostatic interactions while the latter involve the metal acting as either a coordination site for the anion or an organisational element in the anion receptor [115,116,120]

1 2 3 2A Metal free Anion receptors

Anion receptors of this kind have been synthesised with coordination of the anion occurring by hydrogen bonding, electrostatic interactions or both. These receptors are categorised according to the functional groups present in the receptor, for example, amides, ammonium macrocycles, pyrroles, ureas and guanidinium.

Amide based receptors

Very simple amides, for example the isophthalic acid derivatives (**101**) are effective anion receptors for such spherical anions as chloride and bromide ions with an exclusive 1:1 host:anion stoichiometry. Stability constants for such complexes were $6.1 \times 10^4 \text{ M}^{-1}$ for chloride, $7.1 \times 10^3 \text{ M}^{-1}$ for bromide and $4.6 \times 10^2 \text{ M}^{-1}$ for iodide as determined by ^1H NMR titrations (Fig 1.40) [117].

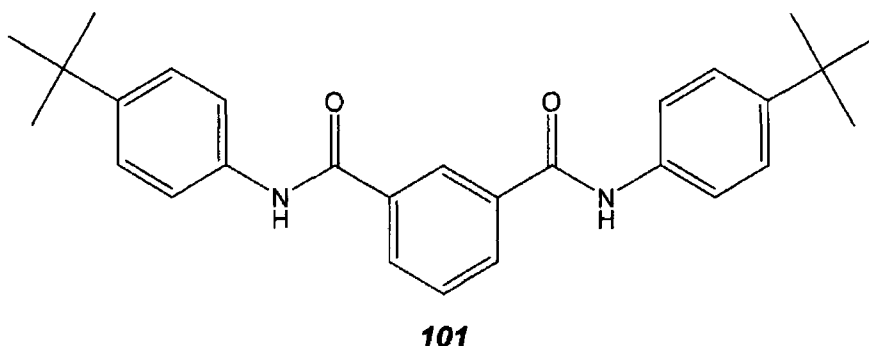


Figure 1.40 Isophthalic acid derivative

Functionalised calix[n]arenes, appended with amide groups have demonstrated interesting complexing abilities. Cameron and Loeb synthesised a calix[4]arene functionalised with varying numbers of electron withdrawing chloro-substituents in the 1 and 3 positions of the upper rim (Fig 1.41). Studies of these calix[n]arenes revealed that with increasing electron withdrawing groups, increased binding strength occurred, i.e. **102** binds benzoate with a stability constant of 107 M^{-1} whilst the **103**[benzoate] complex has a stability constant of 5160 M^{-1} . This increasing electron withdrawing trend failed for **104**, possibly due to the steric bulk of the CCl_3 groups preventing the anion approaching the upper rim anion binding site [118,119].

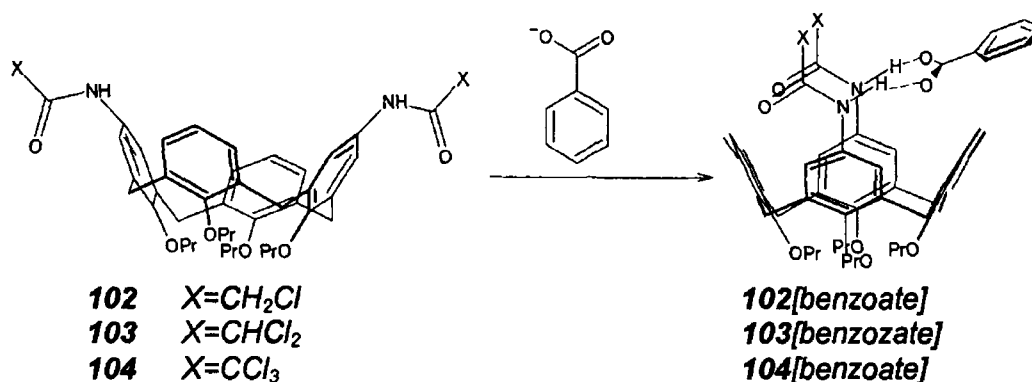


Figure 1 41 The upper nm substituted calix[4]arenes bind carboxylate anions selectively by the formation of a pinched cone conformation

Ammonium macrocyclic receptors

The earliest examples of synthetic anion receptors were protonated or alkylated polyammonium macropolycycles as demonstrated by Park and Simmons's "bicyclic diammonium katapinands" (Fig 1 42) [113]

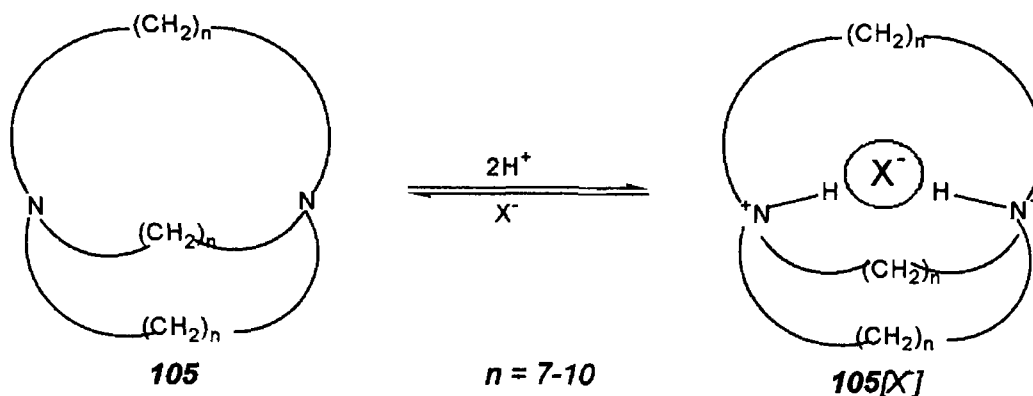


Figure 1.42 Encapsulation of halide ion by the diammonium katapinands

Open-chain polyammonium species **106-109** were investigated as receptors by NMR titrations, for such anions as aromatic and aliphatic dicarboxylates. The free energy of binding of such complexes ranged from -12.6 to -16.3 kJ mol⁻¹ (ΔG) (Fig 1 43)

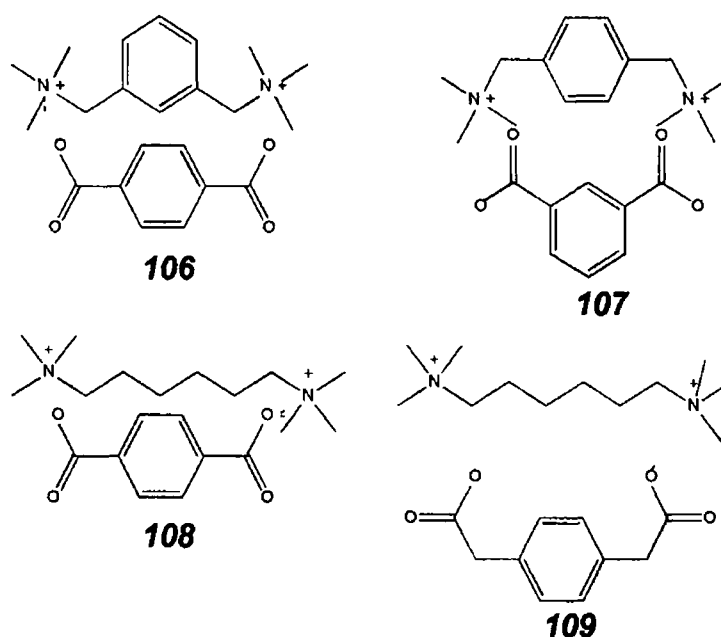


Figure 1 43 Complex formation between α,ω -dications and α,ω -dianions

Garcia-España, Celda, Bianchi et al, synthesised a protonated 1,4,7,10,13,16,19-heptaazacycloheptacosane ([21]aneN₇) (**110**) which interacted strongly with NAD⁺, (**111**) and NADP⁺, (**112**) with a degree of selectivity for NADP⁺. This selectivity is possibly due to the extra phosphate moiety binding with the two adjacent ammonium groups in the receptor (Fig 1 44) [116]

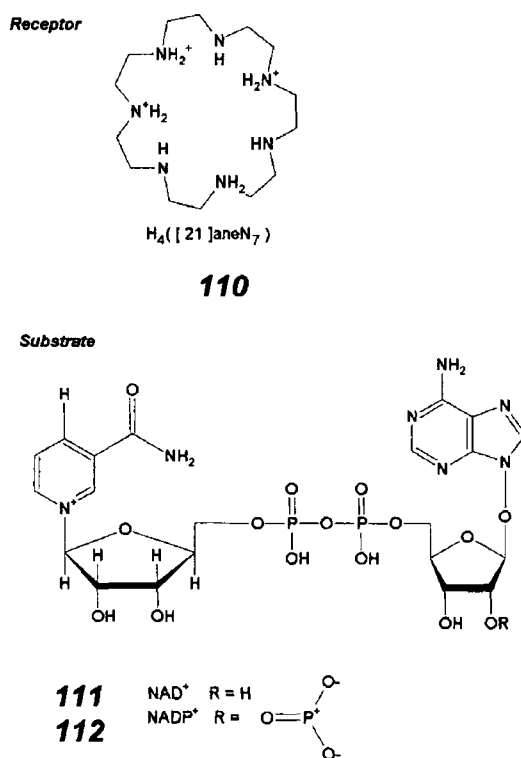


Figure 1 44 Receptor Substrate, [21]aneN₇, NAD⁺/NADP⁺ Complex

Pyrrole based anion receptors

Researchers such as Sessler, Gale and Král have pioneered studies in the area of anion binding abilities of calix[4]pyrrole macrocycles. Unlike calixarenes which cannot bind anions directly due to poor electrophilicity, calix[4]pyrroles can bind anions selectively through interaction with the pyrrolic hydrogen atoms.

A simple calix[4]pyrrole (**113**) displayed strong anionic responses towards Br^- , Cl^- and H_2PO_4^- . These tetrapyrrolic macrocycles bind anions by the formation of four pyrrole NH/Anion hydrogen bonds (Fig 1 45) [121]

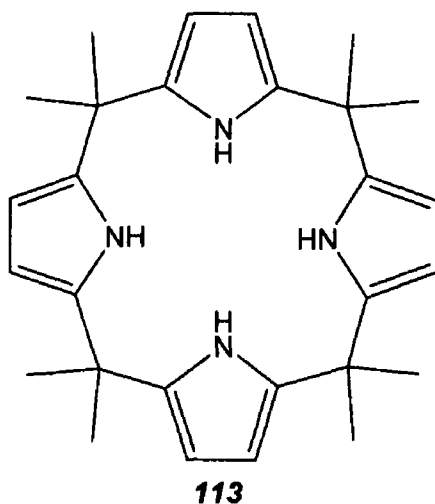


Figure 1 45 Calix[4]pyrrole

Urea based anion receptors

Urea and thioureas have exhibited binding abilities for anions such as carboxylates due to their excellent hydrogen bonding abilities.

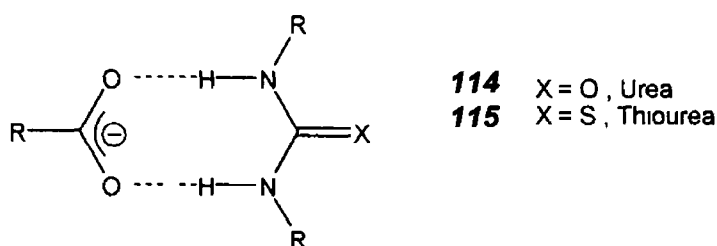


Figure 1 46 The ideal two-point interaction between (thio)urea and carboxylate anions

Umezawa and co-workers have resolved an important issue concerning the significance of preorganisation in anion binding. A range of acyclic thiourea cleft molecules were synthesised, from flexible receptors to some highly preorganised systems containing a xanthene spacer (Fig 1 47)

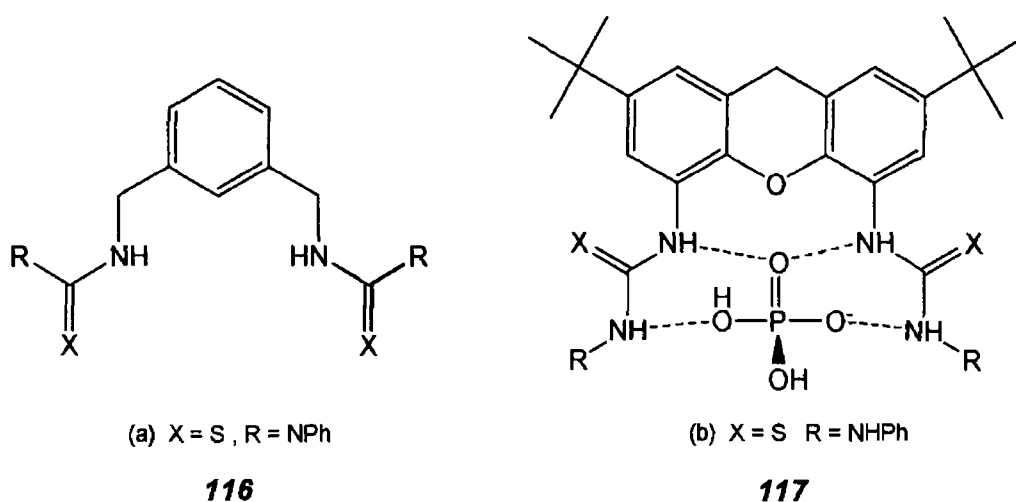
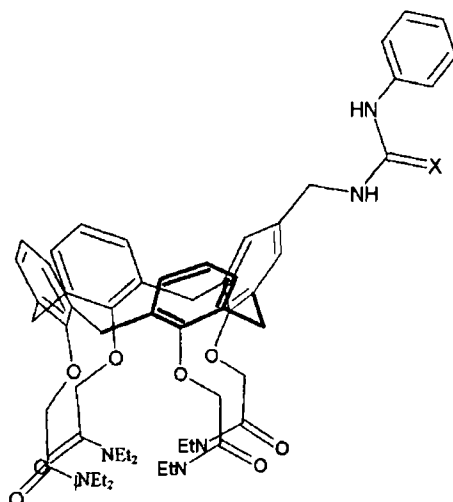


Figure 1 47 *Acyclic Thiourea Cleft Molecules*

Both receptors were selective for H_2PO_4^- over both CH_3CO_2^- and Cl^- . This selectivity trend was independent of the degree of preorganisation of the receptors but stability constants of $195,000\text{M}^{-1}$ for (b) in comparison to 4600M^{-1} for (a) were observed. This large difference is attributed to the difference in preorganisation. The xanthene spacer arranges the urea NH protons so that four hydrogen bonds can form to each H_2PO_4^- anion [132].

Investigating the importance of hydrogen bonding, Albrecht et al. synthesised a series of cleft-like receptors that contain (a) two amide, (b) one amide and one urea, (c) two urea groups. These receptors form 2, 3, and 4 hydrogen bonds to the NO_3^- . Each additional hydrogen bond contributes $2\text{--}3\text{kJmol}^{-1}$ to the stability of the resulting complex.

Ungaro et al. have synthesised a series of calix[4]arene based ditopic receptors containing urea or thiourea groups at the upper rim. Studies indicated that with the inclusion of cation binding amide groups at the lower rim, the efficiency of ion binding increases but with subsequent loss of selectivity (Fig 1 48) [115, 140].

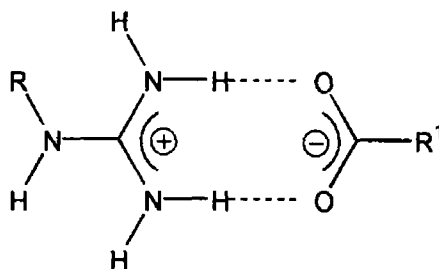


118

Figure 1 48 Calix[4]arene based Ditopic Receptor

Guanidinium based receptors

The guanidinium moiety is ubiquitous in enzymes that bind anionic substrates and is also involved in the stabilisation of protein tertiary structures via internal salt bridges with carboxylate functions (*Fig 1 49*)



119

Figure 1 49 The Guanidinium-Carboxylate Salt Bridge

There is a strong interaction with anions such as carboxylate and phosphate due to the peculiar binding pattern featuring two hydrogen bonds in addition to electrostatic attraction

The guanidinium group also offers pH independent binding power and amenability to structural elaboration. Guanidine remains in a protonated state over an extensive pH range due to its extreme basicity ($pK_a = 13.5$). The guanidinium moiety and its many derivatives have been extensively studied in the context of anion binding [131]

One such derivative is that of a pyrene functionalised monoguanidinium species (*Fig 1 50*) which forms a 2 : 1 receptor : anion complex with pyrophosphate

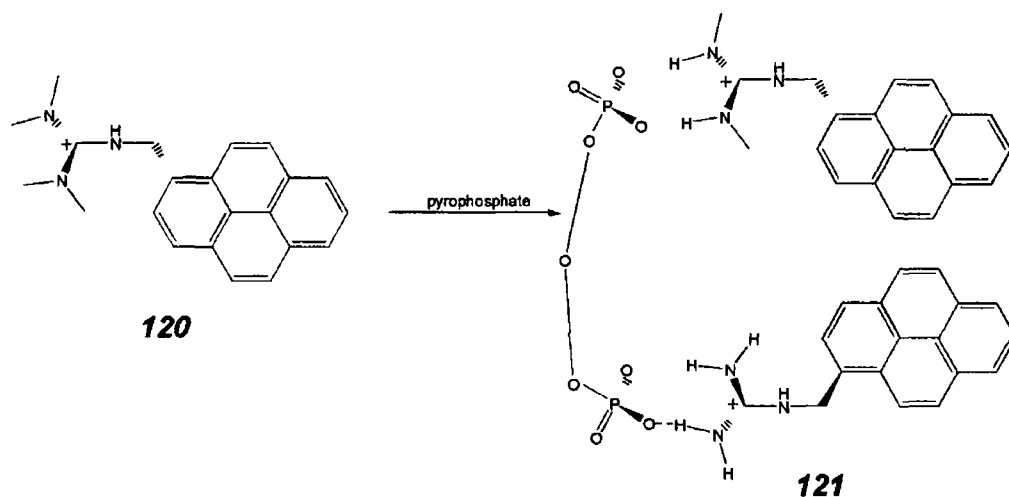


Figure 1 50 Self-assembly of the 2:1 complex between pyrene functionalised monoguanidinium species and pyrophosphate

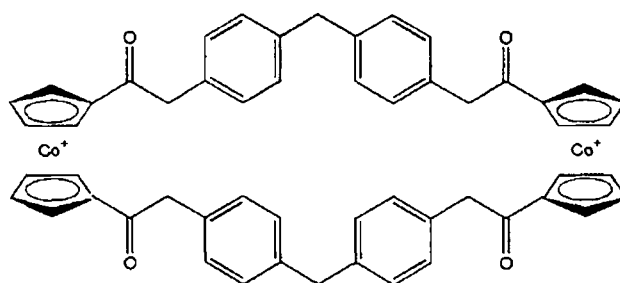
In the absence of anions, the spectrum shows a structured emission band at 370-450nm caused by the pyrene monomer emission. In the presence of pyrophosphate, a band with an emission maximum at 470nm and quenching of the monomer emission band was observed. Dramatic changes in the fluorescence of the pyrene moiety was observed which was not present for such anions as dihydrogen phosphate (H_2PO_4^-), acetate (CH_3CO_2^-), thiocyanate (SCN^-), chloride (Cl^-) or bromide (Br^-) [112,115]

1 2 3 2B Metal containing anion receptors

The metal ions in these receptors function as

- A coordination site for the anion,
- An element in the receptor that withdraws electron density from a π electron system and so increase the affinity of a hydrophobic receptor for anions,
- In anion sensors

The first transition metal centred anion receptor was reported in 1989. This receptor consisted of two positively charged, 18 electron, redox-active cobaltocenium moieties (**122**) (Fig 1 51) [127]



122

Figure 1.51 Cobaltocenium based anion receptor

Upon addition of excess bromide ions, the reduction potential of these redox active centres shifted cathodically, thus indicative of an electrostatic attraction between the bromide ions and the positively charged organometallic fragments Beer et al, synthesised a range of anion binding hosts containing electrochemically active cations tris(bipyridyl)-ruthenium(II), cobaltocenium and ferrocenyl moieties coupled to calixarenes. One such receptor is that of a cobaltocenium calix[4]arene receptor with a difunctionalised lower rim. Isomeric forms of such a receptor indicated that the anion coordination properties of this receptor are dependent upon the degree of preorganisation of the upper rim anion recognition site.

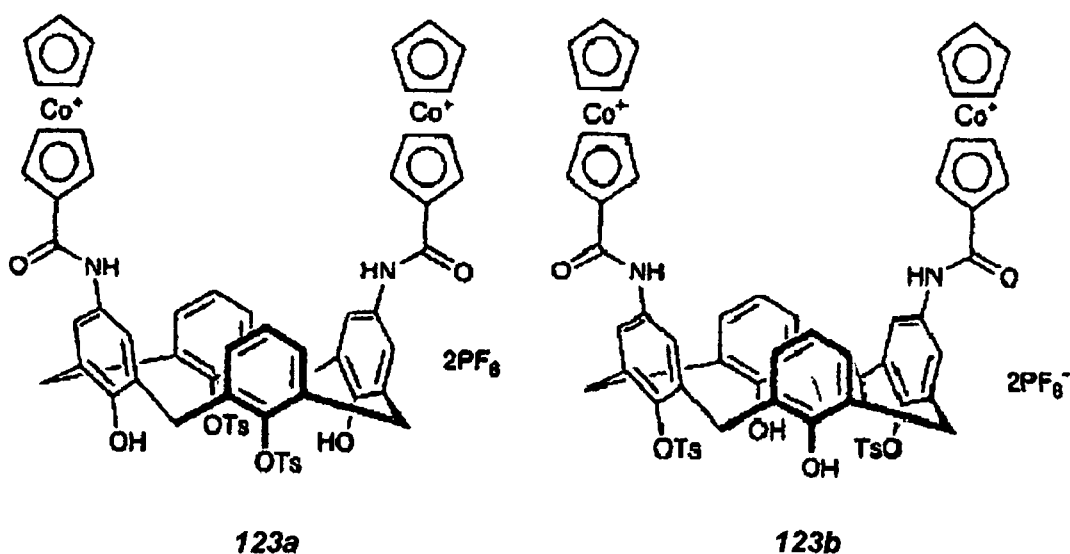


Figure 1.52 Cobaltocenium based calix[4]arene anion receptor

Compound **123a** exhibited a selectivity trend of $\text{MeCO}_2 \gg \text{H}_2\text{PO}_4$. Upon exchange of the positions of the tosyl substituent, **123b** the selectivity preference

was reversed. Changes of size, nature and position of lower rim substituents alter the topology of the upper rim anion recognition sites and consequently, the receptor's selective anion coordination properties [119,203]

Reinholdt and co-workers have incorporated a uranylsalophene bis-amide receptor into a CHEMFET and produced a fluoride selective anion sensing device. This receptor (*Fig 1 53*) contains a Lewis acidic uranium atom and amide NH groups that can form hydrogen bonds, stabilising the anion complex. The anion is bound at the fifth equatorial coordination site of the Lewis-acidic uranyl centre. It also contains lipophilic alkyl groups for immobilisation in an ISFET membrane ($C_{12}H_{25}$) [115,128]

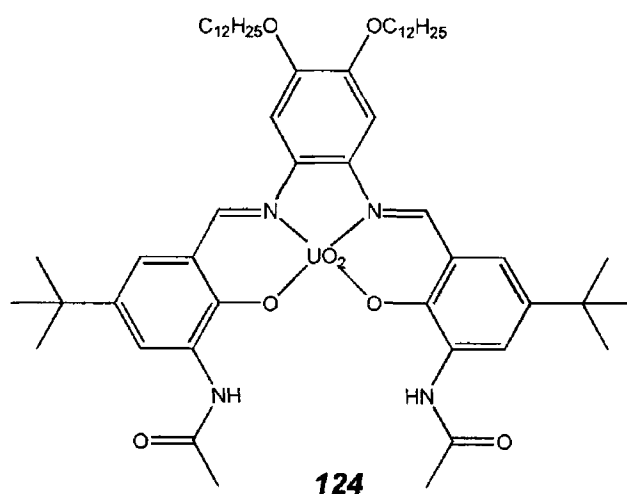


Figure 1 53 Uranylsalophene Bis-Amide Receptor

1 2 3 3 Complexation of Neutral Species

Recognition of neutral guests' result from the formation of specific hydrogen bonding patterns between complementary subunits, reminiscent of base pairing in nucleic acids. Typical receptors possess clefts or cavities in acyclic or macrocyclic receptors into which binding occurs by a complementary fit.

Figure 1 54 (a) illustrates a three sided cleft shape into which adenine sits and is retained due to three hydrogen bonds (**125**) while *Figure 1 54 (b)* displays a macrocycle that encapsulates barbituric acid through the formation of four hydrogen bonds (**126**) [139]

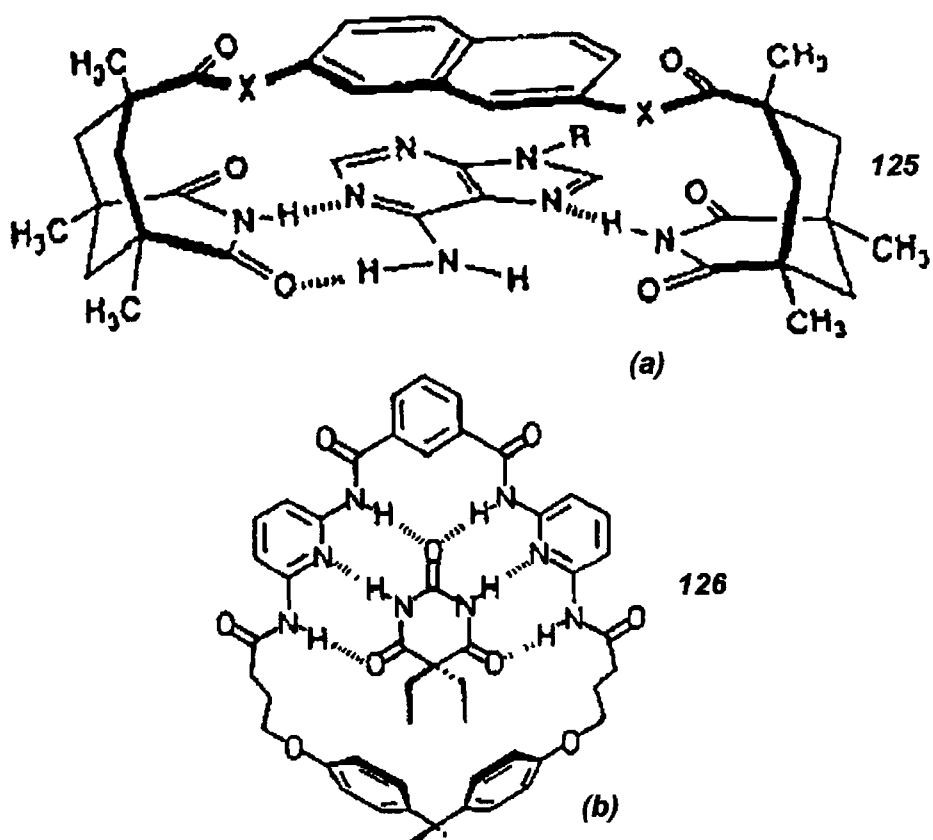


Figure 1 54 *Molecular Hosts for Neutral Species, Adenine (a) and Barbituric Acid (b)[139]*

Calix[4]resorcarenes have been found to complex sugar molecules Shinkai et al synthesised a bis-boronic acid calixcrown which complexed in a 1 : 1 ratio with such sugars as D-glucose, D-talose and D-allose (Fig 1 55) [141]

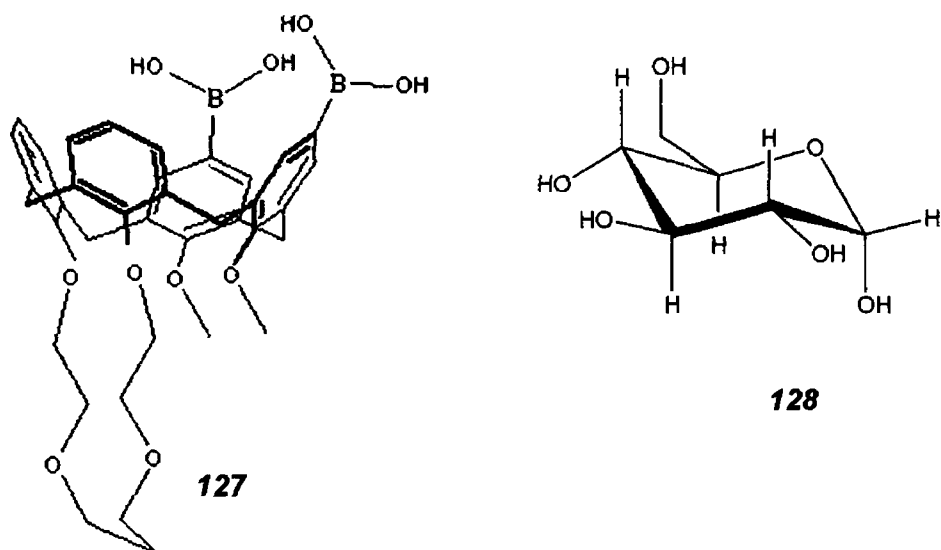


Figure 1.55 *Bis-Boronic Acid Calixcrown (Host) and α -pyranose form of D-glucose (Guest)*

1.3 Molecular Host-Guest Complexation

1.3.1 Concept of Molecular Host-Guest Chemistry

Supramolecular Chemistry is a highly interdisciplinary field of science, encompassing a multitude of features of chemical species of greater complexity than molecules themselves that result from the association of two or more chemical species held together by intermolecular (non-covalent) forces.

Complexation is an association, between two or more distinct molecules, host and guest, based on simultaneous non-covalent interactions between single binding sites, A (acceptor) and D (donor). The host component is defined as an organic molecule or ion whose binding sites converge in the complex whilst the guest component is that whose binding sites diverge in the complex or which is encapsulated by the host. Molecular complexes are held together by hydrogen bonding, electrostatic attraction, π - π stacking, van der Waals attractive forces and charge transfer interactions [102,103,139].

Several binding sites are essential for a strong and specific complexation of a guest molecule, as these non-covalent interactions are quite weak and hence, the greater number of binding sites, the maximum amount of interactions that are possible [101,103,104].

Paul Ehrlich recognised that molecules do not act if they do not bind, introducing the concept of a receptor. Complexation occurs by a geometrical complementary stereoelectronic arrangement of binding sites in the host and guest. Emil Fischer proposed the "Lock and Key" steric fit concept implying that complexation is most efficient and selective when the shape and arrangements of binding sites in the host and guest molecules fit together (*Fig. 1.56*) [114]. Selective complexation requires interaction, affinity between partners - coordination, first introduced by Alfred Werner.

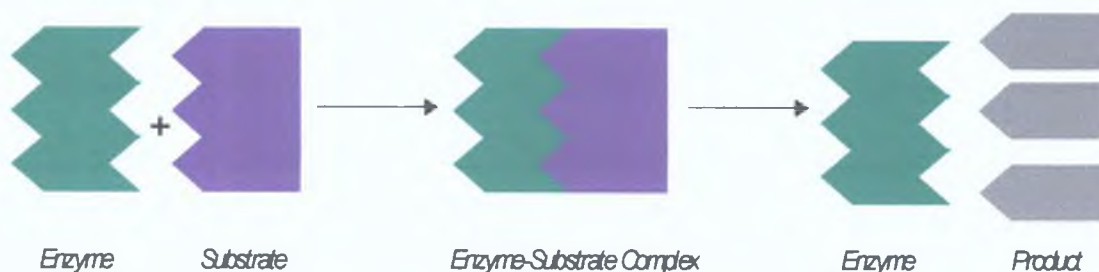


Figure 1.56 "Lock and Key model"

Complexation is categorised by the varying degree of interaction of host and guest [103].

"Capsular" : the guest is encapsulated completely by the host

"Nesting" greater than half of the guest surface contacts the host

"Perching" less than half of the guest surface contacts the host

In the early seventies, complexation of alkali metal cations developed rapidly due to the discovery of selective and powerful ligands including Pedersen's macrocyclic polyether "crown" compounds (*figure 1 36*), cryptands and cryptospherands

1 3 2 Application of Calixarenes as Molecular Receptors

Since the early 1980's, calixarenes have been extensively investigated as ideal molecular platforms for the construction of synthetic receptors in molecular recognition and supramolecular chemistry. This is predominantly due to the readily availability of the parent macrocycles and their amenability to modification. Due to the two possible conformational rotational modes the oxygen-through-the-annulus rotation and the *para*-substituent-through-the-annulus, conformational isomers are inevitable. The conformational isomers generated, afford a great number of unique cavities with different sizes and shapes, thus enhancing the use of calixarenes as molecular hosts [129, 130]

1 3 2 1 Calixarene-based Cation Receptors

Calixarene derivatives with carbonyl group containing substituents on the lower rim have proven effective hosts for alkali and alkaline earth metal cations [16,17, 126]. Calix[4] and [6]arenes derivatives proved the more useful derivatives. Such lower rim derivatives, **129** (*Fig 1 57*) were prepared by exhaustive alkylation of the parent calixarenes using an alkylbromoacetate [18, 134,135]

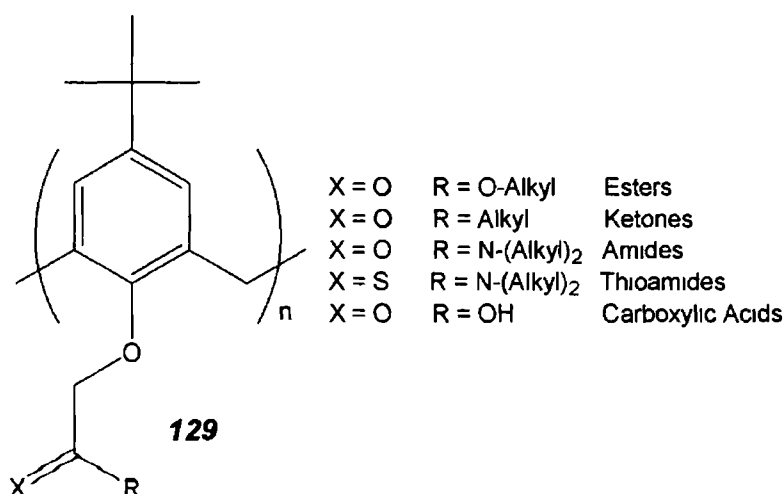


Figure 1 57 General Formula of Calixarene Derivatives Studied

Studies of calixarene ester and ketone derivatives concluded that they exhibited a broad spectrum of affinity for alkali metal cations which is a size related phenomenon. In the case of the calix[n]arene ethyl ester where $n=4$, there is a distinct preference for Na^+ in the extraction of alkali picrates from H_2O into CH_2Cl_2 . The pentameric ester derivative exhibits the highest level of extraction levels for all cations but shows little discrimination between large cations [22, 26]. The $n=6$ derivative favours Cs^+ , Rb^+ , K^+ with significant selectivity over Na^+ . The hepta- and octamer ethyl esters were poor extractants.

Due to efficient complexation and impressive selectivity of these ester derivatives, McKervey, Diamond and co-workers developed the first calix[n]arene based ion selective electrode sensor for Na^+ using tetraethyl-*p*-*t*-butylcalix[4]arene tetraacetate (**130a**), and tetramethyl-*p*-*t*-butylcalix[4]arene tetraacetate (**130b**). The latter compound exhibited excellent selectivity for Na^+ against K^+ whilst the hexaester derivatives (**130c** and **130d**) exhibited caesium selectivity [21,100,108]. These ISE sensors have found commercial applications for example, in blood analysis (**93a**).

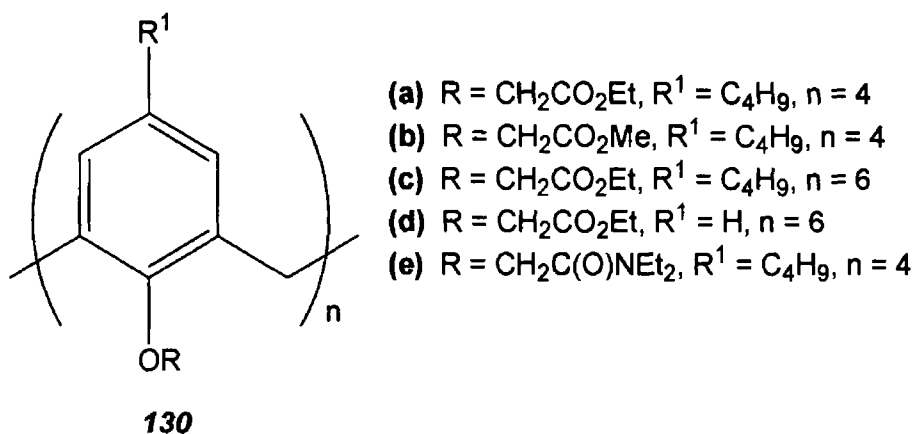


Figure 1 58 Calix[n]arene derivatives as ionophores

Tertiary tetraamides as shown in figure 1 58 complexed with Na^+ and K^+ but did not exhibit selectivity for Na^+ against K^+ as for that of the tetraester analogue. Modifying the type of amide function (primary, secondary, tertiary) was anticipated to modify the donor properties of the amide carbonyl groups and to allow intra- and intermolecular hydrogen bonding in the primary and secondary derivatives which could affect cation binding. A series of derivatives, a tetrasubstituted secondary derivative, a mixed tertiary/secondary and a mixed

tertiary/primary derivative was prepared which displayed no affinity for alkali or alkaline earth metal cations (*Fig 1 59*)[142]

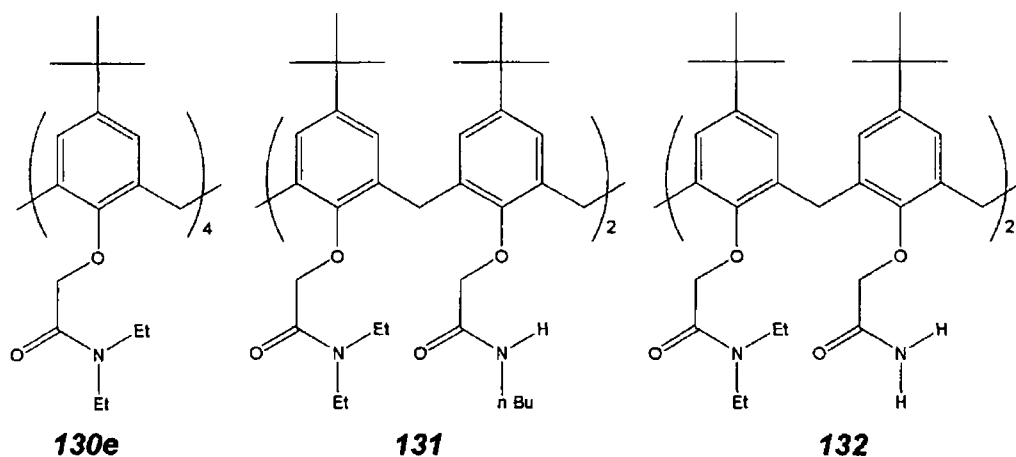


Figure 1 59 Calix[4]arene Derivatives bearing differing amide functions

Ion-selective electrodes for other cations, Pb^{2+} , Ag^{2+} and Cu^{2+} have been designed using calix[4]arenes bearing ligating groups such as thiol ethers and thioamides on the lower rim

Calix[n]arene phosphine oxides were first reported as cation receptors for the extraction of lanthanides and actinides from simulated nuclear waste but the tetrameric derivative discriminates in favour of calcium ions, against Mg^{2+} and alkali metal ions. Concurrent to these studies, ISE analysis of the calix[6]arene analogue showed excellent response characteristics towards Pb^{2+} . Conclusive from these complexation studies was that ligand selectivity varies dramatically with ring size (*Fig 1 60*) [109,125]

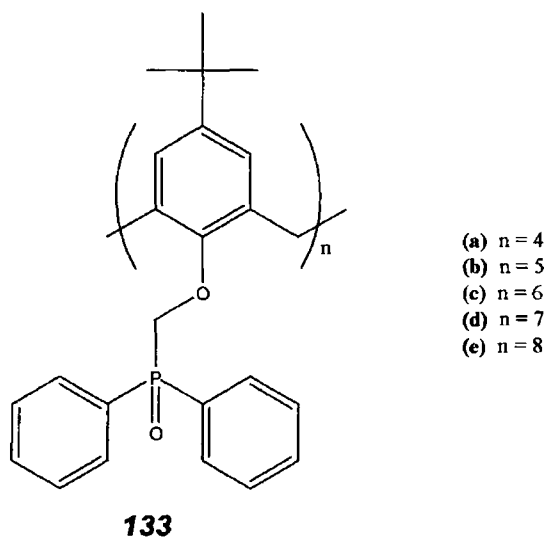


Figure 1 60 Calix[n]arene phosphine oxide derivatives

1 3 2 2 Calixarene-based Anion Receptors

The Calixarene-based Anion Receptors studied may be divided into organic and inorganic classes derived from the origin of the anion recognition site

Inorganic Calixarene based Anion Receptors

Beer and co-workers have advanced the field of inorganic based anion receptors by appending cobaltocenium/cobaltocene and ferrocene/ferrocenium redox couples, combined with amides to a calixarene, to electrochemically sense the anion

Calixarenes substituted with cobaltocenium, a positively charged organometallic, pH independent redox active unit may bind anions by favourable electrostatic interactions and amide hydrogen bonding. The 1,3 upper rim difunctionalised receptor is effective for complexing halides, nitrate, hydrogen sulphate and a series of dicarboxylates with typical $K_{\text{ass}} 11510\text{M}^{-1}$ for adipate [119,203]

In contrast, the 1,3 upper rim bridged receptor shows selectivity for monocarboxylates with $K_{\text{ass}} 41520\text{M}^{-1}$ for acetate. Crystal structure of this receptor halide complex indicates the calixarene is held rigidly in a pinched cone conformation with the cobaltocenium moiety pulling together the two phenyl units and arranging the amides for maximum hydrogen bonding interaction (Fig 1 61) [133]

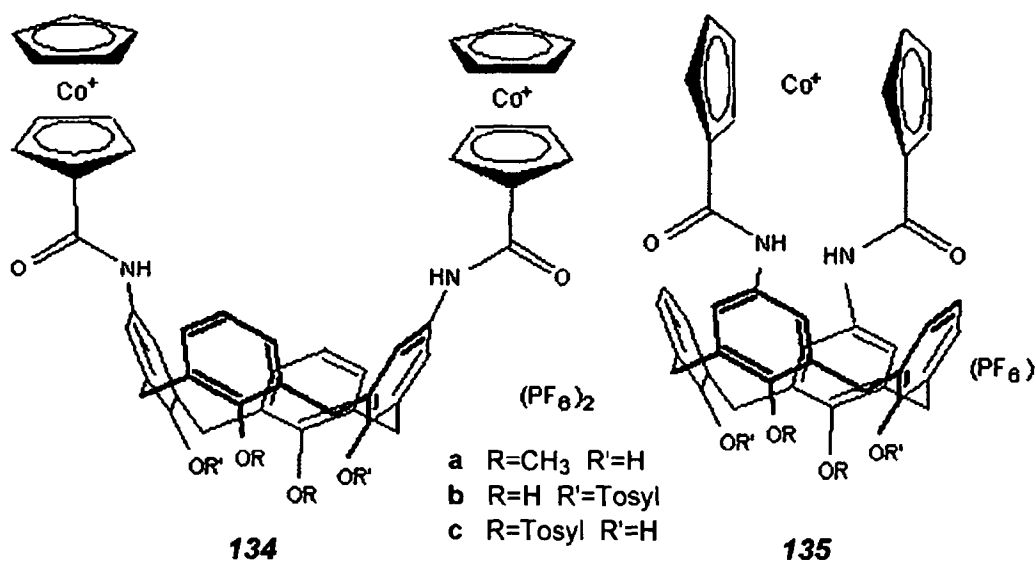


Figure 1 61 Cobaltocenium based Calix[4]arene Receptors

Organic Calixarene based Anion Receptor

Such organic anion receptors utilise amide, urea functionalities or calixpyrrole derivatives. An example of an amide calixarene receptor was that of a calix[4]arene bearing one sulfonamide hydrogen bonding unit appended to each phenol subunit, which displayed selectivity for the tetrahedral anion over both planar and spherical anions in CDCl_3 . Introducing a second amide unit to each phenol subunit enhances selectivity (Fig 1 62).

Association constants of K_{ass} 103400M^{-1} , 1250M^{-1} , 513M^{-1} were reported for HSO_4^- , Cl^- and NO_3^- respectively.

Urea based calixarene and calixpyrrolic derivatives function effectively as anion receptor as detailed in 1 2 3 2 (pp 39-40) [112].

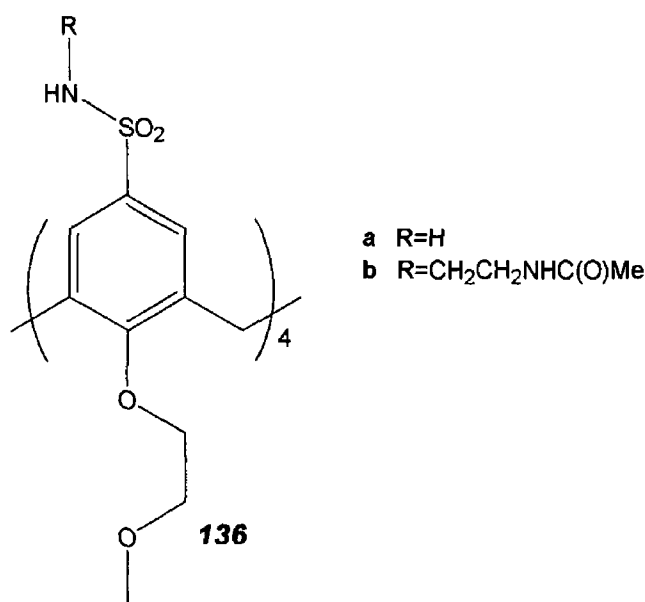


Figure 1 62 Upper Rim Amide based Calix[4]arene Receptors

1 3 2 3 Calixarene-based Neutral Receptors

The parent calix[4]arene, *p*-tetra-*t*-butylcalix[4]arene forms weak complexes with toluene and chloroform, expressing very little selectivity between the two guest species [1].

Functionalisation to such derivatives as the UO_2^{2+} complex of the calix-salophen-crown ether results in an effective host, the electrophilic uranyl cation serving as a binding site for such polar neutral compounds as urea. This receptor has been used to demonstrate urea transport through a supported liquid membrane with a flux of $18 \times 10^{-8} \text{mol cm}^{-2} \text{h}^{-1}$ (Fig 1 63) [143].

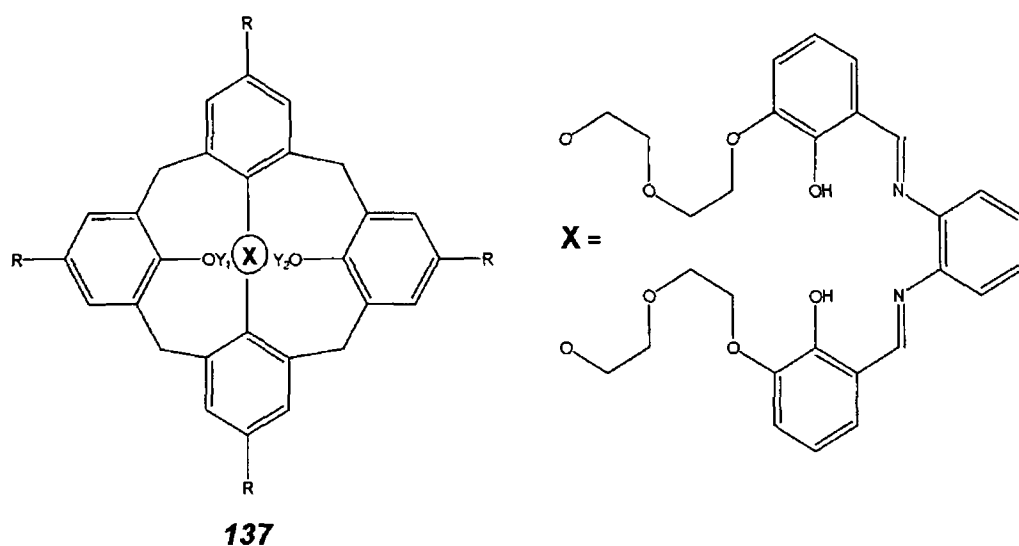


Figure 1.63 A Calix-Salophen-Crown Ether Receptor

1 3 3 Design of a Molecular Host

Molecular recognition is defined by the energy and information involved in the binding and selection of substrate(s) by a given receptor molecule

A Molecular receptor is defined as an organic structure held by covalent bonds, that is capable of binding selectively ionic or molecular substrates (or both), with greater preference than other molecular species and with a higher affinity than what would be expected from their molecular properties. This leads to an assembly of two or more species, a supermolecule [102,103]

In order to design a host, some important questions must be addressed. What is the chemical nature of the guest? and what particular environment or solvent will the host-guest complexation occur?

The first question involves the mutual recognition of host and guest for each other. Maximum discrimination of similar guest species is of paramount importance for a specific host. To achieve large differences in affinity, several factors must be considered [111]

- Steric (shape and size) complementarity between host and differing guests
- Interactional complementarity-presence of complementary binding sites (electrostatic, charge/dipole, dipole/dipole, hydrogen bond donor/acceptor)

- Large contact areas between host and guest so as to contain
- Multiple interaction sites, as non-covalent interactions are rather weak compared to covalent bonds
- Strong overall binding

The choice of solvent can affect complex stability, as association constants vary by orders of magnitude depending on the size of solvent molecules. A protic solvent could surround the charged species, stabilising them but also prevent interaction between host and guest.

Interaction and binding strength between host and guest may be maximised by the use of large, diverse structured hosts with good size, geometry and topological pattern of functional groups. Macropolycyclic structures are of beneficial interest for designing artificial receptors as they are large (macro), may contain cavities of appropriate size and shape, may possess numerous branches or bridges and provide means for the arrangement of structural groups, binding sites and reactive functions.

For example, a rigid host with all its anchor groups preorganised for guest binding should give strong interaction. However, if the guest is too large the host is inflexible and cannot interact strongly. A linear chain molecule, affixed with anchor groups has been synthesised which rearrange, to align the binding functions to their appropriate positions for complexation (*fig 1.64*). While the linear chain molecules are easy to synthesise compared to their macrocyclic counterparts, the disadvantage to a linear chain molecule is that it exhibits inferior selectivity towards competing guests, as energy is consumed in conforming a three-dimensional structure and is no longer available for guest discrimination [111,112].

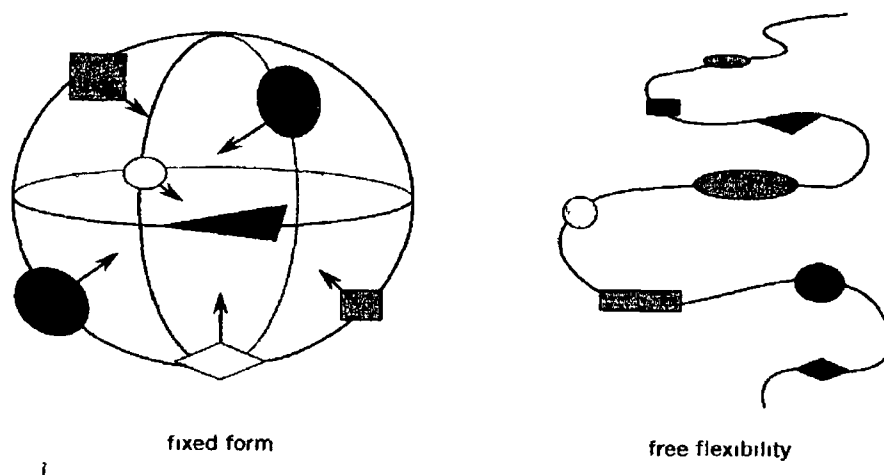


Figure 1.64 Opposing concepts of host design fixed form versus free flexibility

1.3.4 Design of a Molecular Host for Complexation of a Tetrahedrally Shaped Guest

Selective binding of tetrahedral substrates requires the construction of a receptor molecule with a tetrahedral recognition site. Positioning four suitable binding sites at the corners of a tetrahedron and linking them with six bridges may create such a recognition site. A macrotricyclic cryptand as featured in *figure 1.65* possess a tetrahedral spatial arrangement of binding sites and selectively forms strong complexes with the tetrahedral NH_4^+ cation, the ammonium cryptate. The ammonium ion fits into the cavity of **138** and is firmly held inside the cavity by a tetrahedral array of $\text{N-H} \cdots \text{N}$ hydrogen bonding and by electrostatic interaction with six oxygen atoms (*Fig 1.65*) [102,103,138]

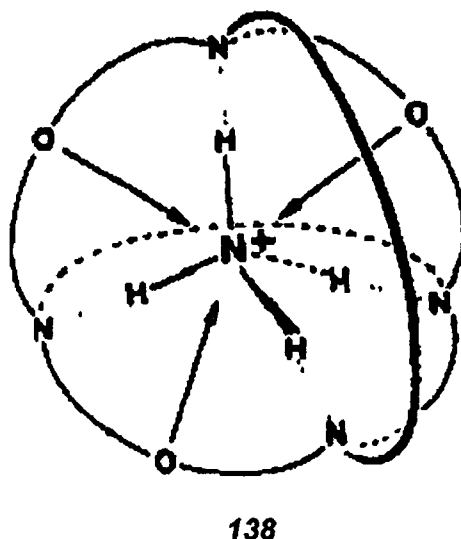


Figure 1.65 Molecular Host possessing a tetrahedral binding site [103]

The binding of tetrahedral anions e.g. phosphate, mono-, di-, tri-hydrogen phosphate has been achieved by protonated macrocyclic polyammonium ligands, tris-guanidinium macrocycles and non-cyclic di-, tri- and tetraguanidinium ligands. To date, the calixarene hosts predominantly studied are those functionalised at the lower rim with identical length and similar functionalities, thus creating an octahedral arrangement of binding sites. This spatial arrangement of binding sites enables complexation of cations of varying size [138].

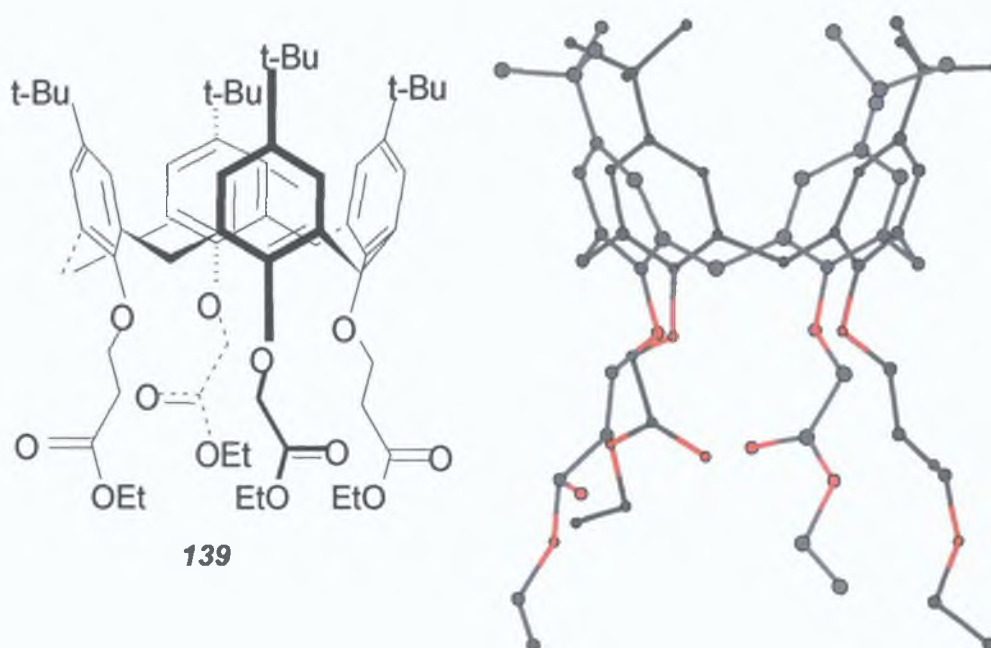


Figure 1.66 *Molecular Structure and 3d-View of a Calix[4]arene bearing a tetrahedral 'pocket'.*

Due to the extensive interest and success attained by calixarenes as a host molecule and the continuing quest for selective tetrahedral ion or molecular discrimination, it has inspired the design and synthesis of a calix[4]arene derivative affixed with a tetrahedral array of binding sites at the lower rim (Fig. 1.66). This structure represents a state of the art illustration of the molecular engineering involved in abiotic receptor chemistry.

**2. *LC-MS Optimisation of the Synthesis
of a Disubstituted Calix[4]arene
Derivative***

2.1 Introduction

Calixarenes provide a route to structures with well-defined cavities, offering simultaneous polar (lower rim) and non-polar (upper rim) character, rendering them effective complexing agents for various guest species. The appendage of four acid, amide or ester functionalities onto a *p*-tetra-*t*-butylcalix[4]arene induces a 'cone' conformation that demonstrates effective cation complexation e.g. with sodium, silver and caesium. The ester derivatives exhibit a broad spectrum of affinity for alkali and alkaline earth metal cations. The chemistry of the tetrameric calixarene has been explored intensively during the last two decades, with interest now focussed on developing methods of selective functionalisation of calixarenes, generating low-symmetry functionalised calixarene derivatives that may exhibit differing complexing abilities than a conventional calixarene derivative [1,2,134,135].

Obtaining reliable routes to partially substituted calixarene derivatives is necessary as they provide a template for generating more complex derivatives with mixed functionality and/or greater diversity in cavity geometry than conventional simultaneous substitution at all four positions at the lower rim.

To prepare the 'precursor molecule' or (1,3)-distal disubstituted calixarene derivative, *p*-tetra-*t*-butylcalix[4]arene (**4**) is regioselectively derivatised at position 1 and 3 using ethyl bromoacetate and carbonate base.

An array of derivatisation reactions of **4** and ethyl bromoacetate was carried out in order to prepare 5,11,17,23-*p*-tetra-*tert*-butyl-25,27-bis(ethoxycarbonyl methoxy)-26,28-dihydroxycalix[4]arene (**70**). Various reaction conditions were varied with respect to stoichiometry, base, solvent and reaction duration to optimise the synthesis of **70**. LC-UV-MS and LC-DAD methods were developed to successfully identify and characterise the compounds formed in these complex reactions [144].

2.2 Liquid Chromatography Mass Spectrometry (LC-MS) & Liquid Chromatography Diode Array Detection (LC-DAD)

LC-MS and LC-DAD are powerful analytical instruments allowing both separation (LC) and unambiguous identification (MS) of chemical compounds. LC is the separation of components of a reaction mixture, based on their relative affinity for the stationary and/or mobile phase. Usually peak identification is based on retention time provided there is a known standard and no co-elution.

Where this is unfeasible, LC detectors have evolved with increased specificity and enhanced identification abilities. The photo-diode array (PDA) detector is such an example, allowing identification of individual peaks by their UV-Vis spectra. UV detection is an example of a 'Class Specific' detector. It is used to confirm the presence of a known standard. UV-Vis detection is not always detailed or unique enough for positive compound identification. Mass Spectrometry (MS) provides the 'ultimate' identification, providing such peak information as a mass spectrum 'fingerprint' (compound molecular weight and fragmentation patterns). The rich chemical information available from mass spectra allows identification of unknown components of a reaction mixture, even when a standard is not available for comparison. MS offers greater sensitivity and specificity than the PDA detector and when coupled with LC separation allows separation, identification and characterisation of mixture components (Fig. 2.1)[145,146].

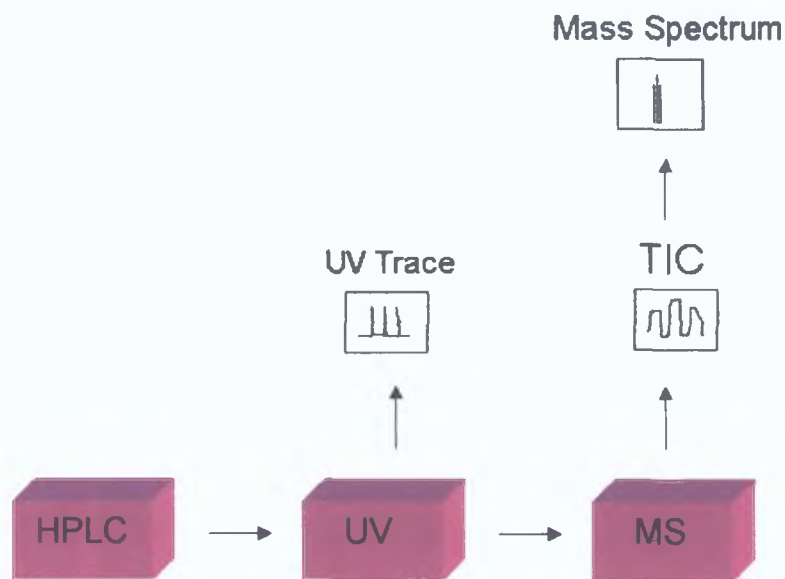


Figure 2.1 Schematic Diagram of an LC-MS

The LC module of the instrument was comprised of a variable wavelength detector, a low volume pump, an in-line degasser and an autosampler. Low flow rates, narrow bore columns and a micro flow cell in the UV detector were employed in the LC system. The peaks eluting from the HPLC column were detected in two ways by UV detection and a total ion current (TIC) chromatogram (from the mass spectrometer) [147].

The MS module of the instrument was comprised of the ionisation chamber, an ion trap mass analyser and the ion detector (*Fig. 2.2*). The Bruker Mass Spectrometer facilitates two types of ionisation – electrospray ionisation (ESI) and atmospheric pressure chemical ionisation (APCI) although ESI was the ionisation method of choice for this work.

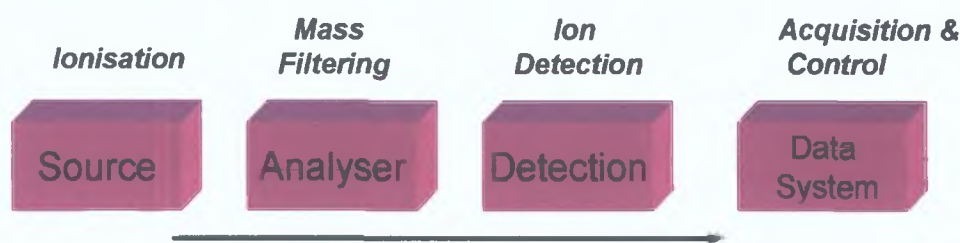


Figure 2.2 Common Components of a Mass Spectrometer

APCI creates gas phase ions at atmospheric pressure. Electron ionisation of the source gases, usually N_2 or O_2 leads to the formation of hydronium ion-water clusters, $H_3O^+(H_2O)^{n+}$. At atmospheric pressure there is significant interaction between the reagent ions and sample molecules which become ionised by the transfer of a proton to form $[M+H]^+$ or $[M-H]^-$. APCI is a very sensitive and rugged technique. It appears to be much less susceptible to chemical interferences than other ionisation methods. The ionisation process is very efficient and up to 98% of sample molecules are ionised.

In ESI, the solution enters the ionisation chamber through a needle which contains a fast-flowing nebulising gas. This produces a fine mist of droplets. In the spray chamber, the solvent is stripped away from the droplets by an inert warm gas, and the presence of a high-voltage gradient encourages this fine spray of charged droplets- the electrospray -to travel into the capillary which leads to the ion-trap and detector.

Electrospray ionisation is considered to be a 'soft' ionisation technique generating primarily pseudomolecular ions which in the positive mode are simply a

protonated, sodiated or potassiated molecular ion. Fragmentation does not usually occur, so this method is used when a molecular weight is required.

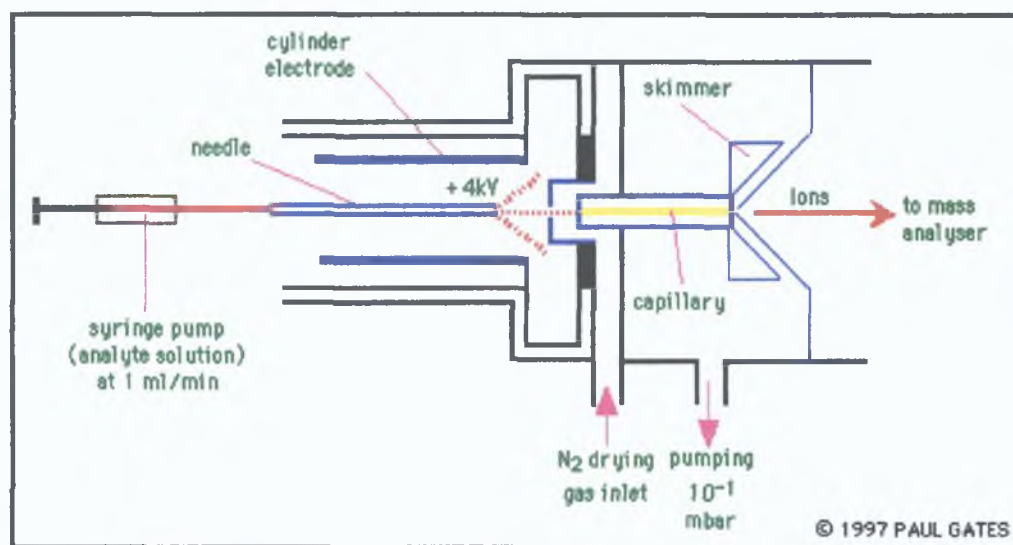


Figure 2.3 *Spray Chamber and Ion Trap*

ESI is a comparatively rugged ionisation technique and spectra are easy to obtain and it is sensitive and suitable for polar and ionic compounds. Polar compounds of low molecular weight (<1000 amu) such as those analysed in this work, preferentially form single charged ions by the loss of or gain of a proton to form $[M+H]^+$ or $[M-H]^-$ respectively although some compounds may form adducts with such additives or contaminants as sodium or potassium ions present in solution, leading to $[M + Na]^+$ or $[M + K]^+$ peaks.

'Ion Trap' mass analysers work by trapping ions and detecting them based on their mass to charge (m/z) ratio. The ion trap consists of two end caps and a ring. Ions produced from the source enter the trap through the inlet focussing system and the entrance endcap electrode. Various voltages are applied to the electrodes to trap and progressively eject ions according to their m/z ratio. An electron multiplier detector collects the ejected ions.

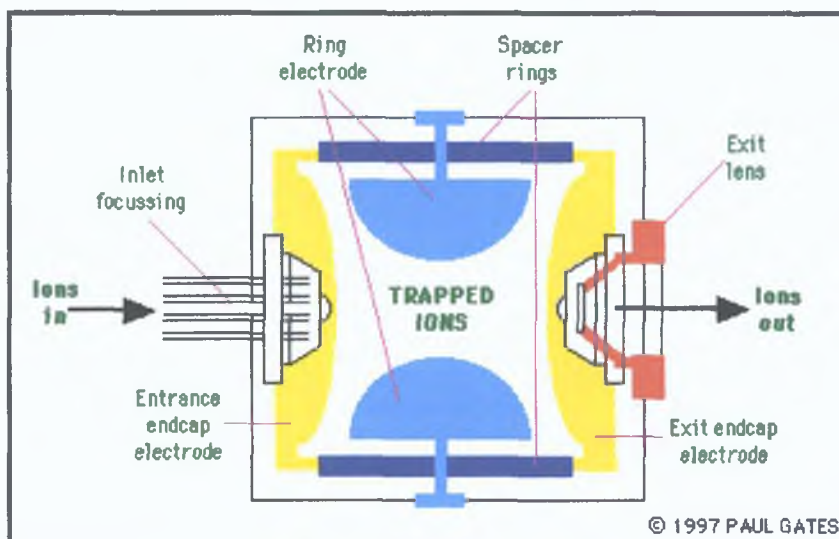


Figure 2.4 Ion-Trap Mass Analyser

The generated spectrum is a plot of ion abundance versus m/z value. There are three different scan ranges: the standard range is 50-2200 m/z , the extended range is 100-3400 m/z and the high range is 500-6000 m/z . As the scan range increases, resolution decreases. The MS instrument may be used in a stand-alone mode for direct injection of samples by syringe or in series with the LC for on-line LC-MS analysis [145,148,149].

The use of LC-UV-MS, LC-DAD instrumentation and the development of separation methods that can characterise the products of partial calix[4]arene derivatisation to **70** has been of great importance in this project, as there are many possibilities of forming other compounds during the reaction.

It is possible that

- The reaction may not proceed fully, yielding the mono-ester derivative;
- The reaction may continue beyond the disubstituted product, leading to the tri- or tetra-substituted products;
- Structural and conformational isomers may result, such as 1,2-diester and partial cone derivatives

LC-UV-MS and LC-DAD can aid in the determination of the product created during these reactions (Fig. 2.5) [144].

Outlined in *Figure 2 5* is a proposed synthetic route for the preparation of a 1,3-distal calix[4]arene. Previous workers have claimed that the 1,3-distal calix[4]arene is solely prepared by the described method [83]. For our purposes it is essential that we have 100% purity of the 1,3-distal before we can proceed to our tetrahedral pocket.

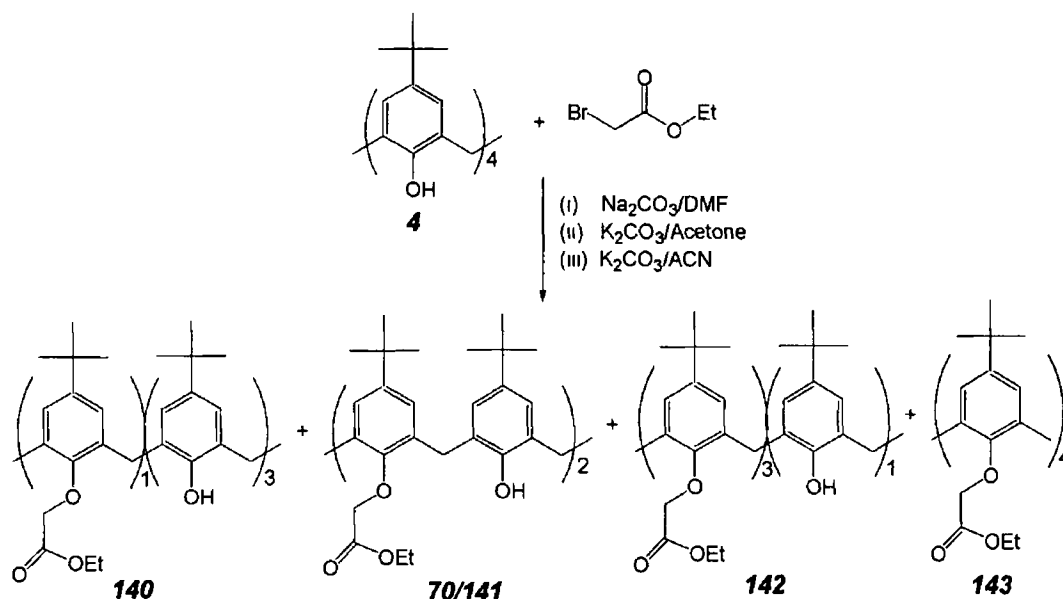


Figure 2 5 Structures of possible Derivatives synthesised

Table 2 1 and *Fig* details the different calix[4]arene derivatives that are possible from the reaction outlined in *Fig 2 5*

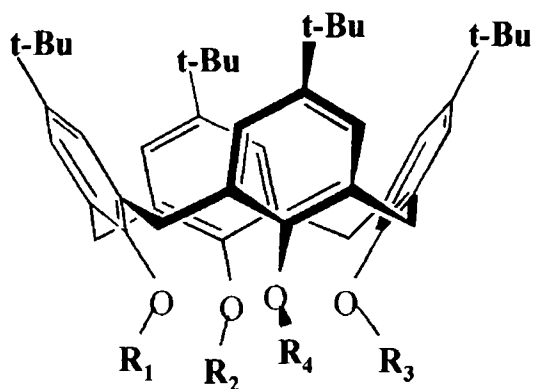


Figure 2 6 Structures of the Calix[4]arene Dervatives synthesised

Generic Chemical Name used in the Discussion of these Compounds	Mass (a m u)	Substituent Groups at Lower Rim	
		H	
p-t-butyl calix[4]arene (4)	648	R ₁ , R ₂ , R ₃ , R ₄	none
Mono-ethyl calix [4]arene ester (140)	734	R ₂ , R ₃ , R ₄	R ₁
1,3 Di-ethyl calix[4]arene ester (70)	820	R ₂ , R ₄	R ₁ , R ₃
1, 2 Di-ethyl calix [4]arene ester (141)	820	R ₃ , R ₄	R ₁ , R ₂
Tri-ethyl calix[4]arene ester (142)	906	R ₄	R ₁ , R ₂ , R ₃
Tetra-ethyl calix [4]arene ester (143)	992	none	R ₁ , R ₂ , R ₃ , R ₄

Table 2 1 Details of the Names, Structures and Molecular Weight of the Compounds in terms of substituents at the lower rim (R₁-R₄)

2 3 Results and Discussion

2 3 1 Synthesis of 5,11,17,23-Tetra-*t*-Butyl-25,27-bis(ethoxycarbonylmethoxy)-26,28-dihydroxycalix[4]arene

Exploring literature procedures for the synthesis of the aforementioned derivative resulted in employing two known methods. Procedure A employed sodium carbonate (Na_2CO_3) and N,N-dimethyl formamide (DMF) as base and solvent respectively, with a reaction stoichiometry of 1:10:2 of **4**, Na_2CO_3 and alkylating agent. Procedure B was the reported synthesis of **70** which involved treating **4** with ethylbromoacetate in a mole ratio of 1:2, with potassium carbonate (K_2CO_3) as base in refluxing acetone for 15h (Fig 2 7) [83]

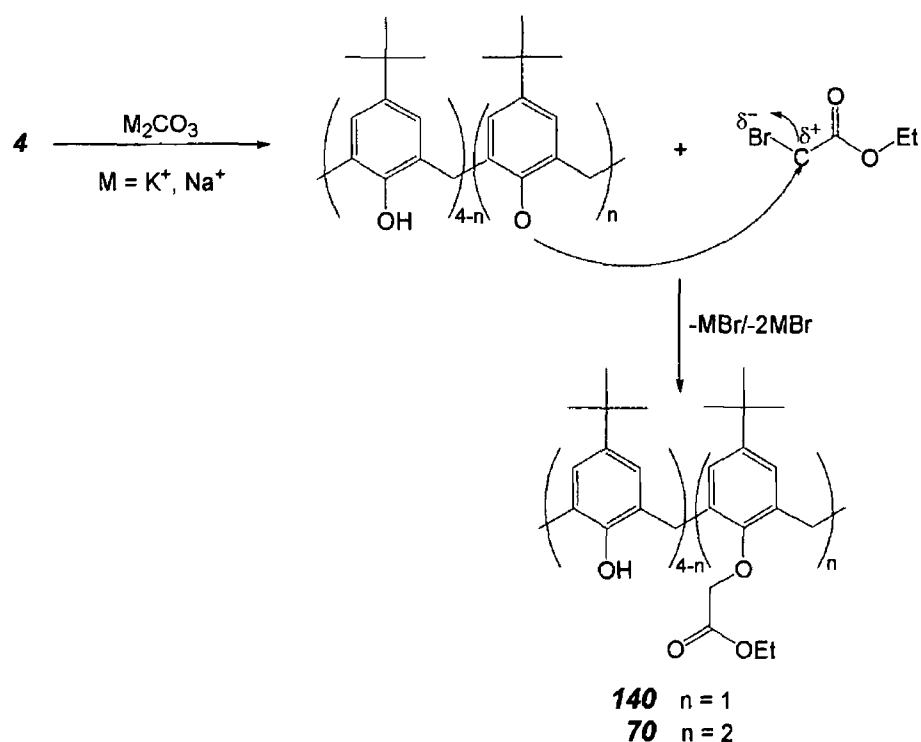


Figure 2 7 Reaction Mechanism for the synthesis of **140** and **70**

Direct Infusion (DI)-MS of these two reaction products appeared to indicate that they were rich in the desired product due to a high ion abundance signal in the mass spectrum (Fig 2 8)

LC-DAD was also carried out on the same sample and a number of reaction components was seen but as the impurities and the desired product have similar UV spectra, identification proved difficult. However, this presented a clearer picture than DI-MS of what was really in the reaction mixture. Online LC-UV-MS was then used to characterize the reaction products and a different picture

emerged. This technique confirmed that procedure A was superior to procedure B, yielding mainly **140** with only trace **70** present.

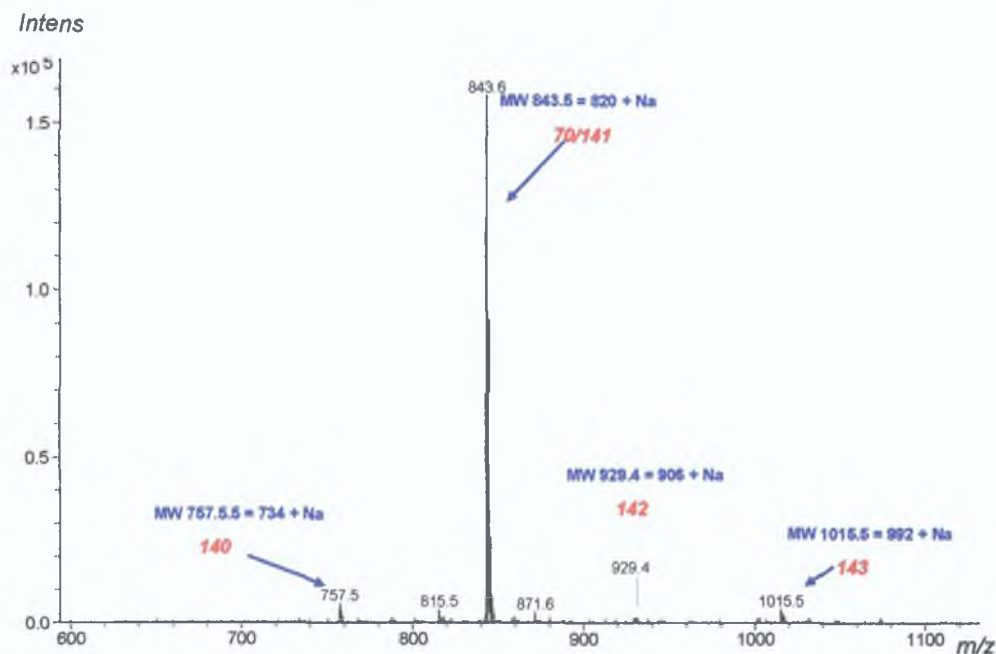


Figure 2.8 DI-MS of 24h sample of Synthesis of **70** (Procedure A)

Fig. 2.9 shows a chromatogram of the product of reaction E (Acetone, K_2CO_3 , table 2.4, pp. 77), according to Procedure B after 15h (spiked with additional **70** to confirm its absence). A number of products were obtained, with **140** being the predominant product with some **142** and **143**. It is quite apparent that none of these methods produce the target compound, **70** in high purity.

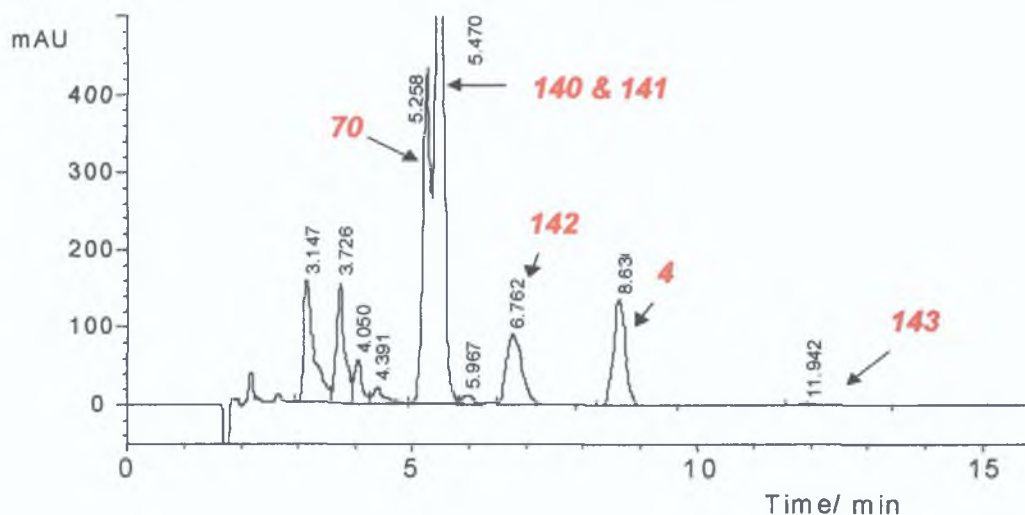


Figure 2.9 LC Chromatogram of a 15h sample of Reaction E (spiked with **70**)

We decided to explore various reaction conditions such as stoichiometry, base and timelength of the reaction in order to optimise the synthesis of **70** [144]

2 3 2 Reaction Stoichiometry

Table 2 2 details the optimisation reactions attempted (A-D) where the mole ratio of **4** to ethyl bromoacetate varies from 4 1 to 1 2, respectively. The relative area percent results demonstrated that as the stoichiometry of **4** ethyl bromoacetate varies from 4 1 to 1 2, the percent formation of **70** increased from 14 5% to 60 4% while the percentage of unreacted **4** ranges from 16 8% to 3 5%. An interesting observation from these experiments was that as the ratio of ethyl bromoacetate to **4** increases, the ratio of **70** to **140** increases also.

From the series of reactions described (Table 2 2), the largest formation of **70** was that of reaction C, an equimolar ratio of ethyl bromoacetate **4** resulting in a 72 8% relative area of **70**. Reaction D employing a twofold excess of ethyl bromoacetate to **4** gave a 60 4% relative area of **70**. The optimal stoichiometry lies between 1 1 and 2 1 ethyl bromoacetate **4**, respectively (Table 2 2).

Reaction Number	Ratio of EtBrOAc Calix[4] arene	Relative Area Percent Results				
		Calix[4] arene % (4)	Mono-ester % (140)	1,3-Diester % (70)	1,2-Diester % (141)	Sum of Diesters %
A	1 4	16 8	63 2	14 5	5 5	20 0
B	1 2	11 9	46 8	32 8	8 5	41 3
C	1 1	0 0	16 7	72 8	10 5	83 3
D	2 1	3 5	24 9	60 4	11 2	71 6

Table 2 2 LC Results of 24h samples taken from Reactions A to D
(Solvent DMF, Base Na₂CO₃, Sampling Time 24h)

2 3 3 Reaction Time

To investigate how this reaction proceeds with respect to time, reaction A, (4 1 **4** ethyl bromoacetate) was monitored at short intervals by LC. As time progressed, the concentration of **4** decreased with time over 24h while the area of **140** and **70** increased (Fig 2 10). Table 2 3 indicates that the 24h sample of reaction A consisted largely of **140** with trace levels of **70**. It is apparent that while this was

not the optimum reaction stoichiometry, as expected, the longer the reaction time the greater the formation of **140** and **70**

Reaction Time (min)	% Mono-ester (140)	% Di-ester I (70)	% Di-ester II (141)	% Di-ester I & II
20	97	3	0	3
40	88	10	2	12
60	83	15	2	17
80	74	22	4	26
100	72	23	5	28
300/5h	75	22	3	25
1440/24h	73	21	6	27

Table 2 3 *Reaction Time Studies of Reaction A (Solvent DMF, Base Na₂CO₃)*

When optimising a reaction there are a number of factors worth considering including consumption of the starting material and time length. A short time length is practical and viable. Table 2 3 indicated that 24h was a sufficient length of time for this reaction as the starting material is consumed, there is a high percent area formation of **70** and a longer reaction time introduces the risk of tri and tetra-substitution.

The optimum reaction stoichiometry and time length were established as those of reaction C, which was subsequently monitored by LC-MS.

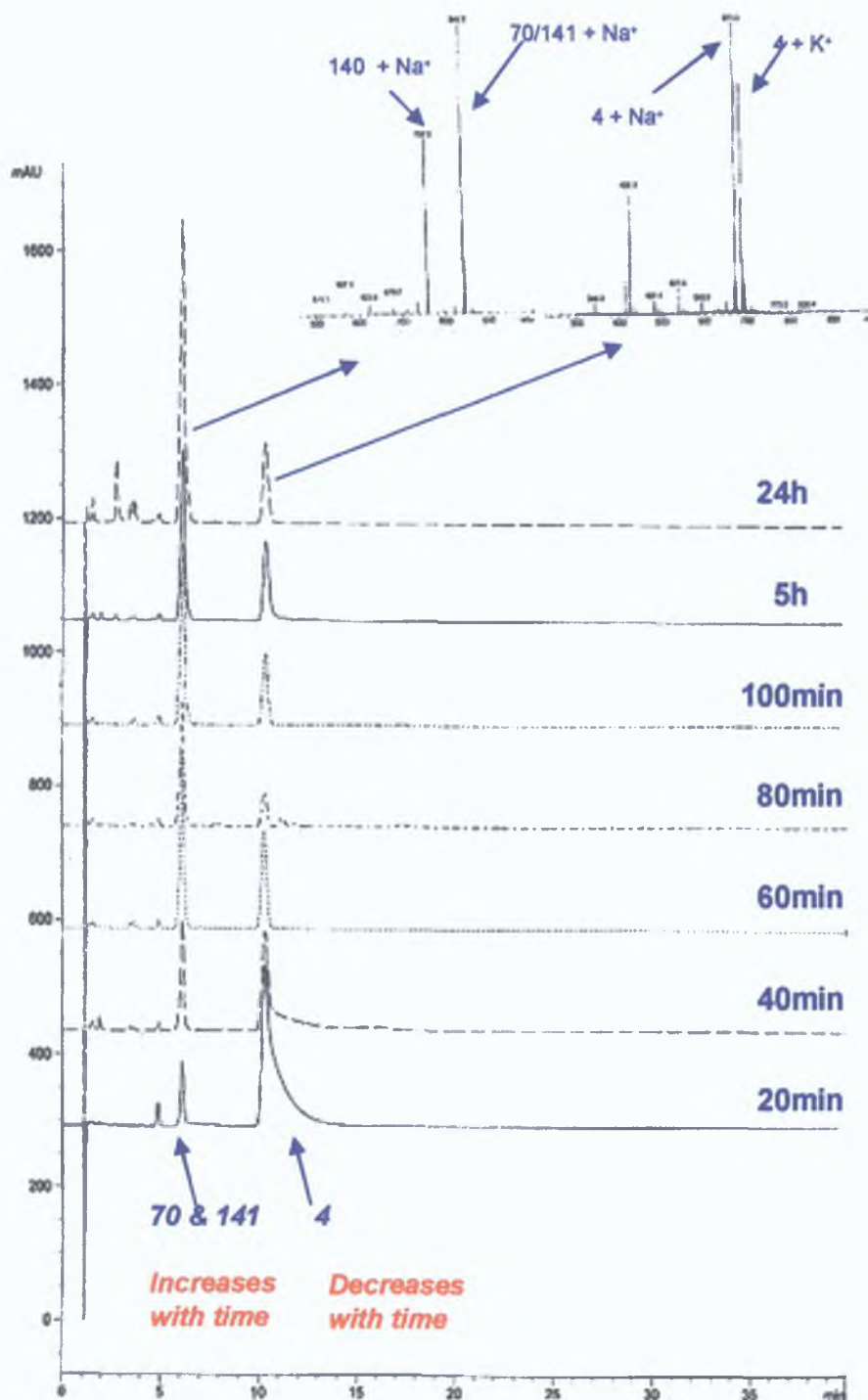


Figure 2.10 Chromatographic Data of the Time Studies of Reaction A

2.3.4 LC, DI-MS and LC-MS Monitoring of Reaction C

Fig. 2.11 shows the DI-MS and LC results of reaction C at three timepoints, 2, 5 and 24h. The DI-MS results showed a base peak at 843.5Da ($820 + \text{Na}^+$) correlating to **70** with a high ion abundance of 1.35×10^5 , 1.9×10^6 and 3.8×10^6 for 2, 5 and 24h respectively. Smaller peaks at 757.5, 929.5 and 1015.5Da confirmed the presence of the sodiated complex of **140**, **142** and **143**. These results suggested **70** was the main product from this reaction.

Examination of the LC-UV chromatograms led to conflicting results. The 2h LC chromatogram implied that there is one main peak with a retention time of 15.0min with a smaller peak preceding the main peak at 14.7min.

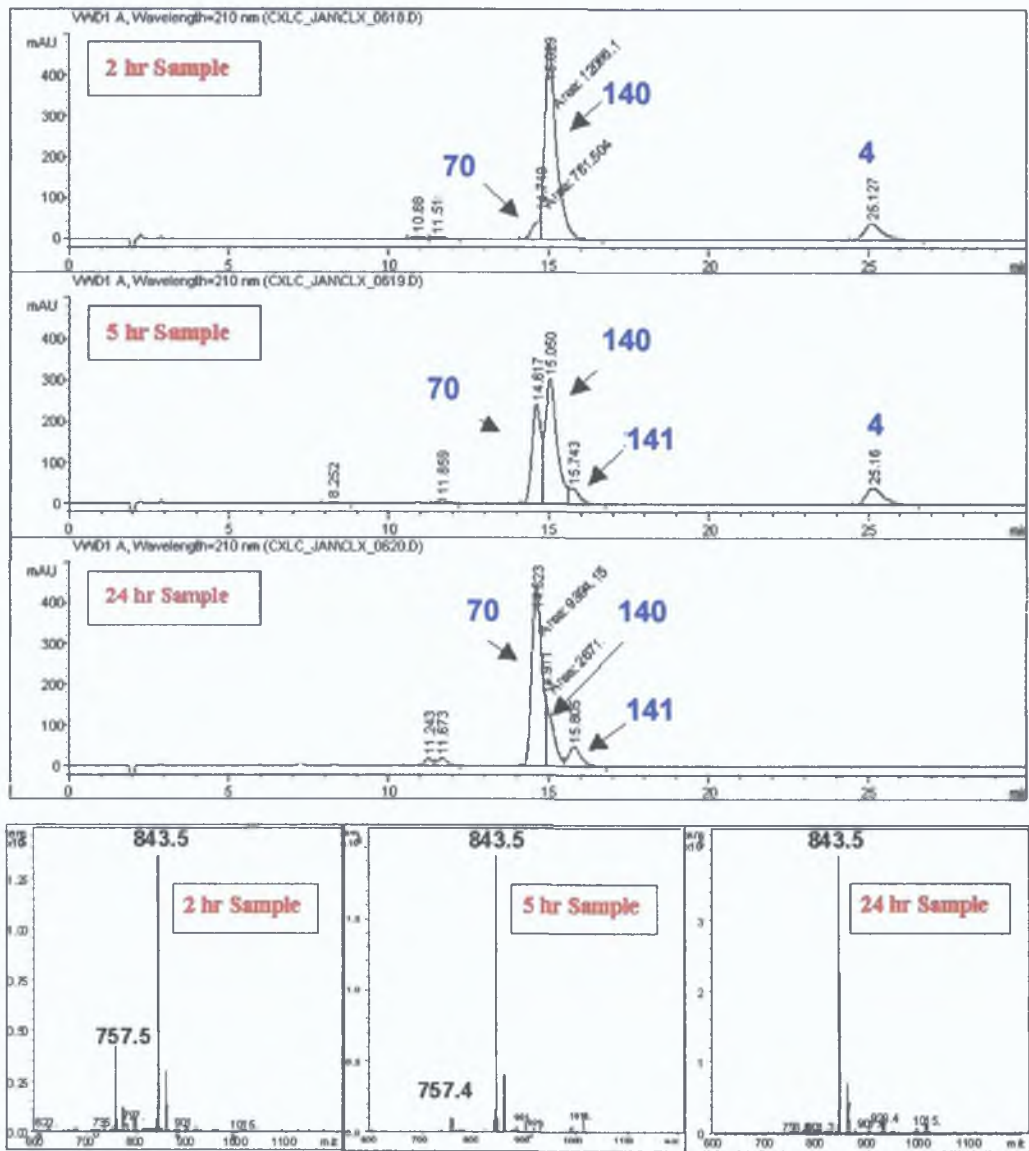


Figure 2.11 LC Chromatograms and Direct Infusion Mass Spectra for 2, 5, 24h samples from Reaction C

Trace starting material was observed at 25.1min. Progressing to the 5h sample, the LC chromatogram displayed a reduction in the area of the main peak at 15.0min with an increase in the area of the preceding peak, almost equal to the peak at 15.0min. Further evidence for this was the 24h chromatogram indicating that the peak area of the forepeak at 14.7min had surpassed the peak at 15.0min. Online MS of these peaks confirmed the main peak at 15.0min as **140**

and the growing forepeak was **70**. Over 24h, a higher yield of **70** (72.8%) to **140** (16.7%) was achieved with complete consumption of **4**.

The high intensity signals from the DI-MS of the 2 and 5h samples indicated that **70** was the main product whereas LC data conflicted. The 2h sample comprised of mainly **140** with trace quantities of **70** while the 5h sample contained almost equal quantities of **140** and **70**. All peaks in the DI-MS spectra were sodiated and the mass spectrometer is much more sensitive to **70** relative to **140** because **70** has a greater affinity for sodium ions than **140**. This may be attributed to their different shapes. The symmetrical arrangement of the two ligating groups in the 1 and 3 position at the lower rim of **70** facilitates encapsulation of the sodium ion in a manner similar to **143**, which is an excellent complexing agent for sodium. The shape of **140** with one ligating group hinders complexation with Na^+ ions (Fig. 2.12). Hence, **140** is almost 'invisible' in the mass spectrometer due to low ionisation efficiency whereas a more sensitive signal is obtained for **70** due to its ability to complex with Na^+ ions.

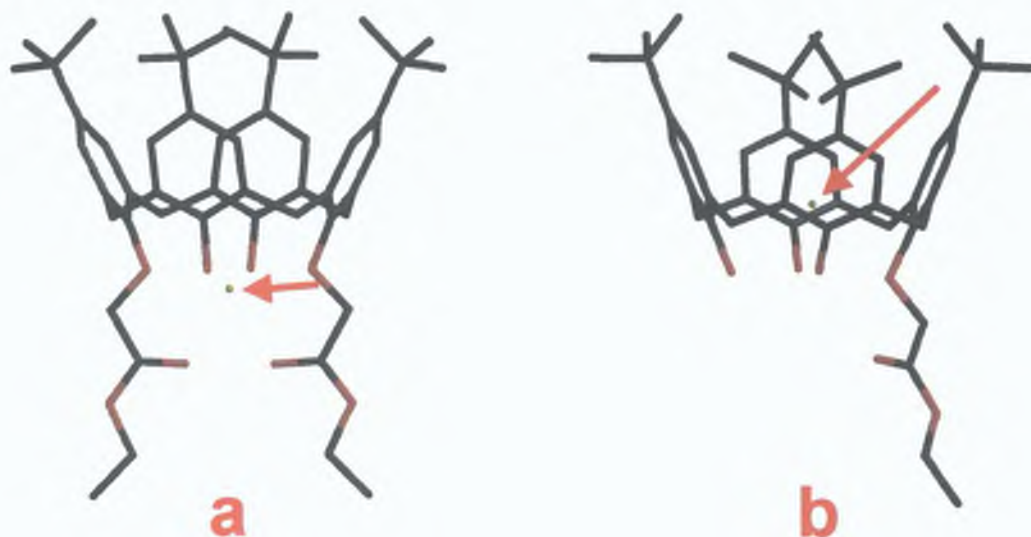


Figure 2.12 Energy minimised structures for the **70**- Na^+ complex (**a**) and **70**- K^+ complex (**b**) Position of cation indicated by arrow.

Thus, in the case of DI-MS, the mass spectrometer is more 'selective' for **70**. In conclusion, DI-MS is not a suitable tool for investigating mixtures of this series of calix[4]arenes and LC-MS was required to get a real picture of what the composition of the final reaction mixture was.

2.3.5 Development of an Alternative Route to Partially Functionalised Calixarene Derivatives

It was reported in the literature that a disubstituted calix[4]arene derivative may be readily prepared by employing ACN and K_2CO_3 as solvent and base respectively [150]. In parallel with the optimisation studies previously described, a reaction with a stoichiometric ratio of 1:2:1, (**4**:ethyl bromoacetate: K_2CO_3) was carried out at room temperature for 96h. LC-DAD analysis (Fig. 2.13) indicated that the predominant product was **70** with trace **140**. The actual product distribution (relative percent area) was 66.3% **70**, 26.9% **140** and 2.9% **141** which compared favourably to the relative percent area of 72.8% **70**, 16.7% **140** and 10.5% **141** for Reaction C (Table 2.4, pp. 77) at 24h.

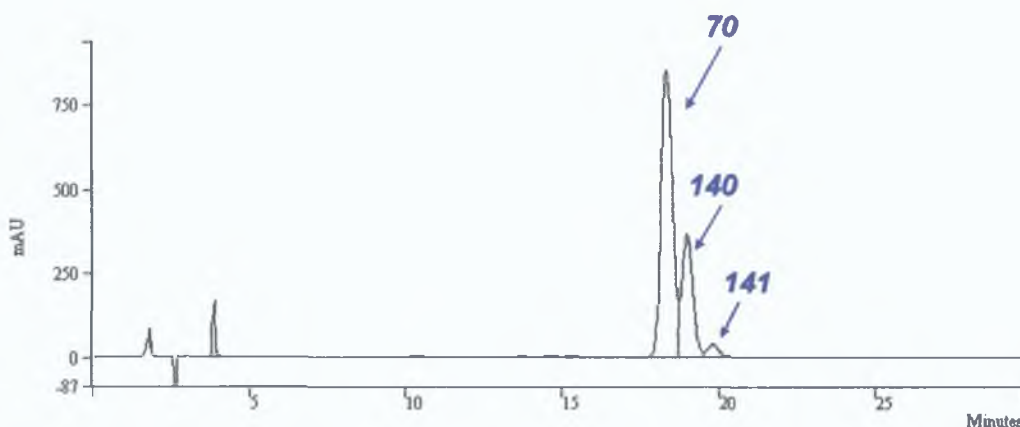


Figure 2.13 Chromatogram of 96h sample of Reaction G

A parallel reaction was set up using a stoichiometric ratio of 1:2:1, **4**:ethyl bromo acetate: K_2CO_3 in refluxing ACN. TLC analysis indicated that both sets of conditions yielded two derivatives, mono and disubstitution with unreacted **4**. Reaction G (Table 2.4, pp. 77) was the preferred synthetic procedure as no control of temperature was required, conditions were less hazardous and large scale amounts of **70** (2-5g) could be prepared. HPLC analysis of the differing reaction conditions, reaction D, F and G (Table 2.4, pp. 77) indicated that using acetonitrile as the solvent afforded a slightly lower yield of **70** than for DMF (Fig. 2.13).

2 3 6 Formation of 1,3- Vs 1,2-diester isomers

It is evident from *Fig 2 11* that two regioisomers, 1,2- and 1,3-disubstituted calixarene derivatives (**70** and **141**) are formed from the optimal reaction conditions [2]. Online MS assigned both of the peaks at 14.7 min and 15.8 min as the p-tetra-t-butylcalix[4]arene-diester, 843.5 Da ($820.5 + \text{Na}^+$). It was surmised that the preferential isomer formed was **70**, which was confirmed by spiking a reaction sample with **70**. The diester peak at 14.7 min increased in area, conclusive that this was **70** whereas there was no change in area after spiking for the peak at 15.8 min, assigned as **141**. As observed from *Fig 2 11*, the order of elution is **70**, **140** and **141** that may be attributed to the shape of the individual derivatives. **70** is symmetrical in shape with two ligating groups that may curl up into the cavity rendering it spherical in shape. Compound **140**, with its single ligating group may drag along the stationary phase, thus slowing it down relative to **70**. **141** has an arrangement with two ligating groups on the same side of the molecule causing some inflexibility relative to **70**, hence the effect is a slower elution than **70** (*Fig 2 14*).

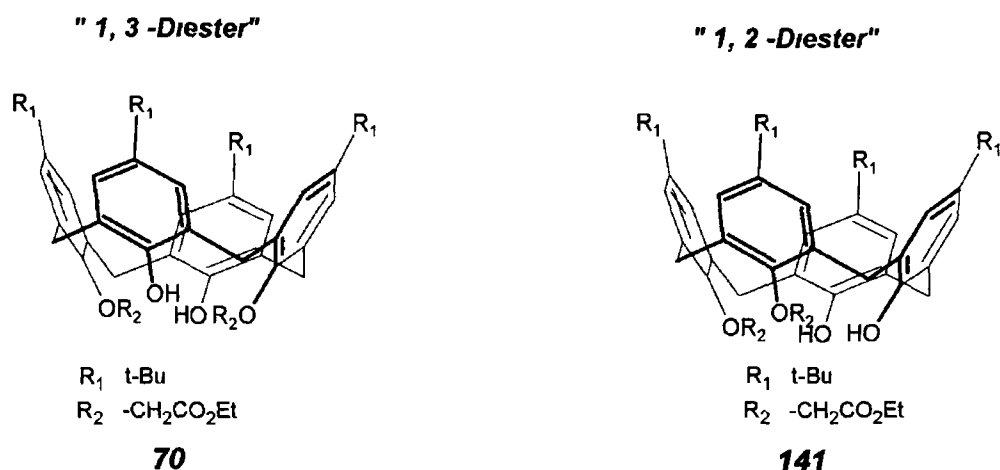


Figure 2 14 Distal-(1,3) and Proximal-(1,2) Disubstitution

Reinhoudt et al have suggested a mechanism to explain partial substitution patterns in calixarenes. From the pK_a values of calix[4]arenes, it was surmised that under weak basic conditions, Na_2CO_3 or K_2CO_3 , the reaction progresses via a sequential monodeprotonation step, forming a monoanion that is stabilised by hydrogen bonding, each followed by a monoalkylation step (*Fig 2 15a*). This sequence occurs preferentially at positions that give rise to a more stabilised monoanion, by contiguous hydrogen bonding. Following monoalkylation at position 1, a second deprotonation occurs. This may occur at position 2 or 3.

Deprotonation at position 2 affords a monoanion that is adjacent to both a hydroxyl and an alkoxyl group (*Fig 2 15c*) whereas at position 3, two hydroxyl groups flank the monoanion formed (*Fig 2 15b*) [28,30]

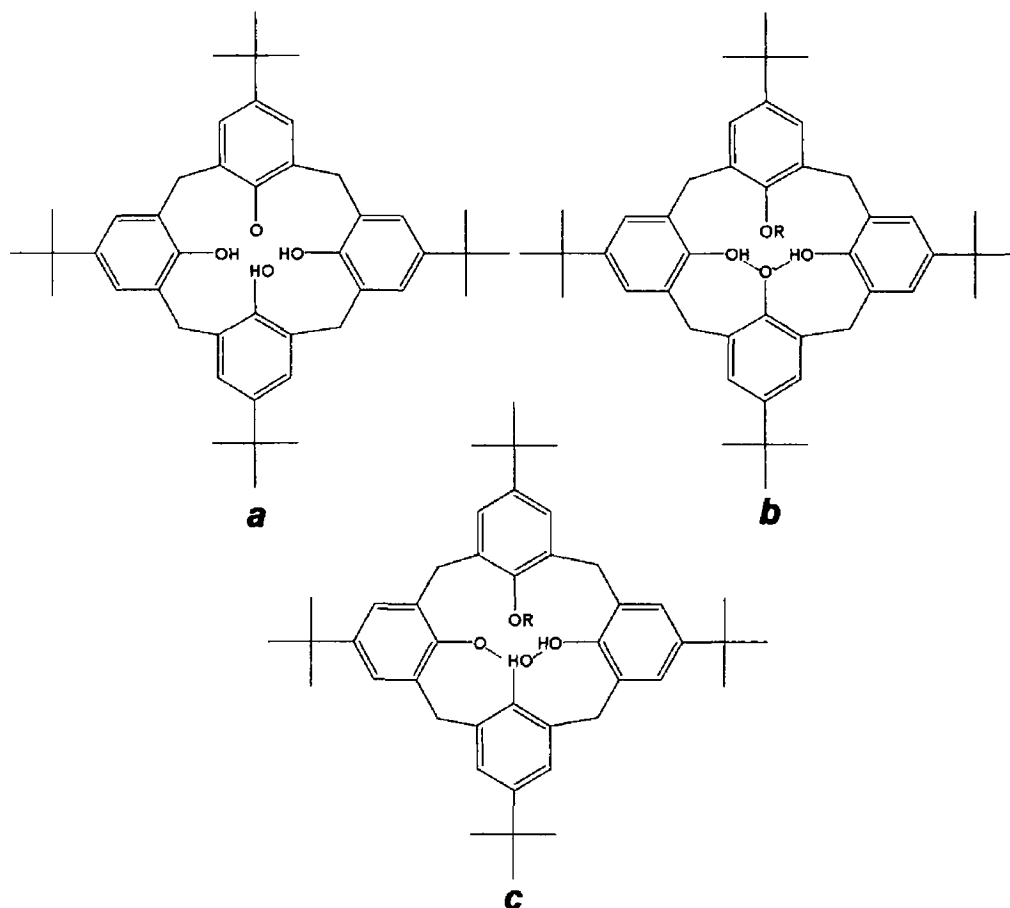


Figure 2.15 Anions arising from Mono-, (1,3)-, and (1,2)-Disubstitution (a),(b),(c)

Distal (1,3) selectivity is observed under weak basic conditions as the second deprotonation step at position 3 yields an oxyanion stabilised by strong intramolecular hydrogen bonds from the two adjacent hydroxyl groups [151] Proximal (1,2)-disubstitution has been achieved by using NaH in DMF with 2.2 equivalent of alkylating agent. A strong base such as NaH preferentially forms the dianion, which favours second alkylation in the proximal (1,2) position. The factors governing selective functionalisation undoubtedly are related to strength of the base, metal template effect and the possibility of forming mono- or polyanions of differing stability.

2.3.7 Effects of Reaction Conditions

It is apparent that this difunctionalisation reaction was sensitive to both the solvent and base used. The reactions studied employed identical stoichiometry; reactions D, E and F were carried out at 70°C while reaction G was carried out at room temperature (*Table 2.4, pp. 77*). These reactions were different in the choice of solvent and base used. *Fig. 2.16* exhibits the chromatographic data of reactions D-G (LC-MS for reaction D-F while LC-DAD for reaction G).

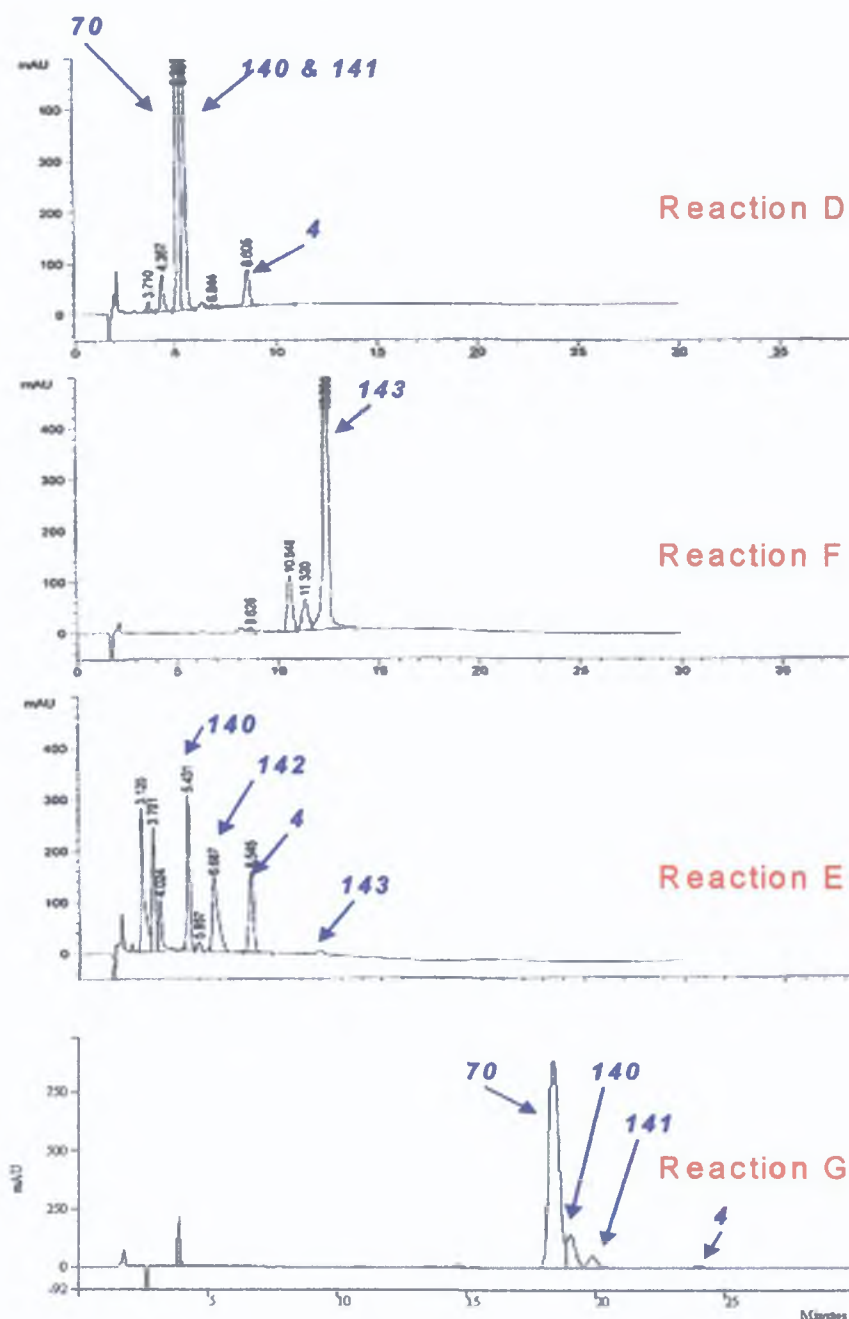


Figure 2.16 LC Chromatographic data of Reactions D-G, employing differing bases and solvents

Reaction F, employing Na_2CO_3 and acetone yielded primarily **143** whereas substituting K_2CO_3 for Na_2CO_3 led to a mixture of **140**, **142** and **143** derivatives. Both reactions gave a negligible amount of **70** after 15h. On increasing the polarity of the solvent, notable changes were observed. After 24h, reaction D and G yielded **140** and **70**. Substituting acetone for DMF or ACN drives the reaction further to almost complete conversion to **143**. It would thus appear that choice of solvent has a significant effect on the performance and product distribution of the alkylation reaction.

Rxn	Stoichiometry of EtBrOAc <i>p</i>-t-Butyl calix[4]arene	Solvent	Base	Time points for sampling	Rel. % Yield of 70
A	1 : 4	DMF	Na_2CO_3	20,40,60,80, 100min,2,5,2h	14.5
B	1 : 2	DMF	Na_2CO_3	2,5,24 h	32.8
C	1 : 1	DMF	Na_2CO_3	2,5,24 h	72.8
D	2 : 1	DMF	Na_2CO_3	2,5,24 h	60.4
E	2 : 1	Acetone	K_2CO_3	2,5,24 h	-
F	2 : 1	Acetone	Na_2CO_3	2,5,24 h	-
G	2 : 1	ACN	K_2CO_3	24,48,72,96h	66.3

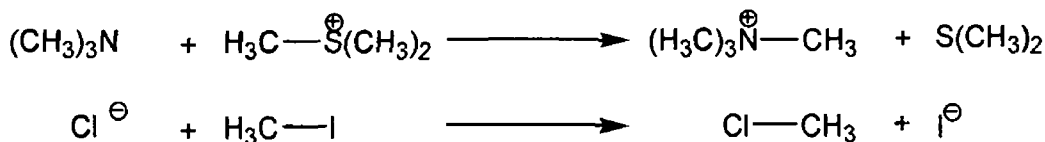
Table 2.4 Details of the Reactions carried out to optimise the synthesis of 5,11,17,23-Tetra-*tert*-butyl-25,27-bis(ethoxycarbonylmethoxy)-26,28-dihydroxycalix[4]arene

2.3.7.1 Influence of Solvent Polarity on $\text{S}_{\text{N}}2$ Reactions

Deprotonation of the *t*-butylphenol subunit generates the *p*-*t*-butylcalix[4]arene oxyanion which takes on the role of attacking nucleophile and attacks the ethyl bromoacetate. This reaction occurs via an $\text{S}_{\text{N}}2$ reaction (Fig. 2.17). There are three distinct $\text{S}_{\text{N}}2$ reactions distinguished by their nucleophile-leaving group charge types [152].

Type 1 Charge Dispersion

The nucleophile and the leaving group are both neutral and negatively charged



Type 2 Charge Separation

The nucleophile is neutral and the leaving group is negatively charged



Type 3 Charge Neutralisation

The nucleophile is negatively charged while the leaving group is neutral



A series of rules, the Hughes-Ingold rules of solvent effects were devised in order to express the principle in terms of the most important contribution to solvation, polar interactions

If the transition state is accompanied by an increase in electrical charge on the reactants, a change to a more polar solvent will cause a large increase in rate (charge separation)

If the transition state is accompanied by a decrease in electrical charge on the reactants, a change to a more polar solvent will cause a large decrease in rate (charge neutralisation)

If the transition state is accompanied by dispersion of electrical charges, a change to a more polar solvent will cause a small decrease in rate (charge dispersion)

Choosing a suitable solvent for an $\text{S}_{\text{N}}2$ reaction requires some thought. For an $\text{S}_{\text{N}}2$ reaction, the effect of solvent polarity is usually much less but the ability of the solvent to solvate the nucleophile is important. If a protic solvent (methanol, water) is used, it forces the equilibrium to the left as it stabilises the nucleophile by hydrogen bonding. Thus, the solvent must be stripped away from around the nucleophile in order for it to react. A polar aprotic solvent is more favourable, as it solvates both the nucleophile and the leaving group. The polar aprotic solvents chosen included acetone, ACN and DMF. Molecules with large dipole moments and high dielectric constants are considered polar. The dielectric constant for the

solvents chosen were ϵ 20.7, 36.6 and 38.3 for Acetone, ACN and DMF respectively. Thus, DMF and acetonitrile are very similar in polarity while acetone is less polar than the aforementioned solvents [153,154,155]

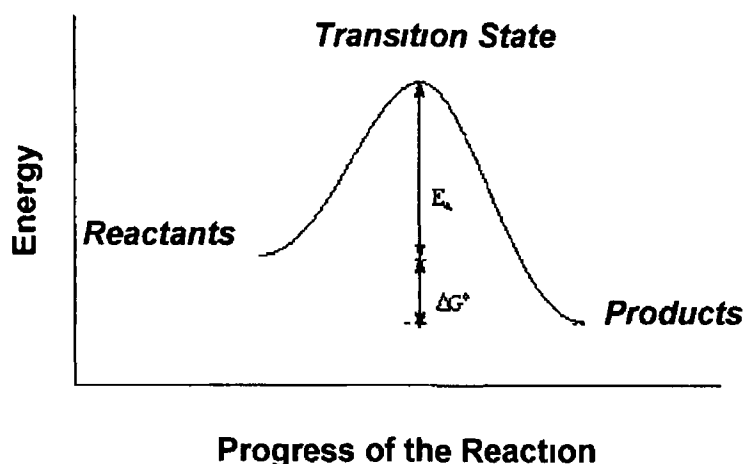


Figure 2.17 Reaction Profile of an S_N2 Reaction Mechanism

In this reaction there is charge dispersal in the transition state. An increase in the polarity of the solvent stabilises the reactants to a greater extent than it does the transition state, thus increasing the activation energy resulting in a decrease in the rate of the reaction. The change in the rate of reaction upon varying the solvent from a protic to an aprotic solvent is also related to the size of the attacking anion [156].

There are a number of possible explanations for the diverse product distribution observed for differing solvents. When choosing a solvent, it is important that the reactants are soluble in the solvent so that the molecules are dispersed, enabling molecules to collide. It was observed that **4** was less soluble in acetone than in DMF or ACN. Heating did not noticeably enhance its solubility in acetone. A smaller amount of **4** is dissolved in acetone and as there is a smaller amount of reactant solubilised, **4** may undergo a number of deprotonation steps to yield **142** or **143**. There is a greater proportion of **4** dissolved in the more polar DMF or ACN, hence there is a higher possibility of deprotonation of a second *p*-tetra-*t*-butylcalix[4]arene molecule as there is a greater amount of the reactants in the same phase which promote successful collisions. Polar aprotic solvents weakly solvate the anion, rendering the nucleophile, *p*-tetra-*t*-butylcalix[4]arene oxyanion 'naked'. Acetone may not stabilise the nucleophile as effectively as DMF or ACN causing the nucleophile to be unstable and reactive, favouring partial and complete substitution. The extra stabilisation of the nucleophile in DMF or ACN resulted in reduced reactivity leading to more selective partial substitution. In

general, the rates of S_N2 reactions decrease in solvents of increasing polarity [152]

2.3.7.2 Influence of Base

The most profound effects were observed for reactions E and F (*Table 2.4*, pp 77). Employing Na_2CO_3 as base gave mainly **143** while the use of K_2CO_3 gave a mixture of **140**, **142**, **143** with unreacted **4**. This may be attributed to the *p*-tetra-*t*-butylcalix[4]arene oxyanion complexing with the metal counterion of the base. Molecular dynamic simulations established that for polar solvents, for example ACN and acetone, exo complexation (sitting outside the 'cone' conformation) of the metal counterion is preferred. The calculated cation binding selectivities of the *p*-tetra-*t*-butylcalix[4]arene oxyanion exhibit a preference for the smallest ions in acetone and ACN, Li^+ , Na^+ , K^+ , Rb^+ , Cs^+ , following experimental trends [158-160].

The *p*-tetra-*t*-butylcalix[4]arene oxyanion complexes Na^+ more effectively than K^+ due to size restrictions (*Fig. 2.18*). The $[\text{M}^+][\text{A}^-]$ complex, where M^+ is the metal cation while A^- is the anion, may reduce the reactivity of the anion, rendering it less susceptible to attack ethyl bromoacetate. However, the substitution at the lower rim with long chained ligating tails (as the reaction proceeds) increases the size of the cavity, thus K^+ may then complex more strongly to this substituted oxyanion than Na^+ . The $[\text{K}^+][\text{substituted oxyanion}]$ complex which proceeds to the second alkylation step is less reactive, thus partial derivatisation results. The affinity of the substituted oxyanion to Na^+ may be reduced, thus increasing its reactivity at the subsequent alkylation steps which results in complete substitution [29].

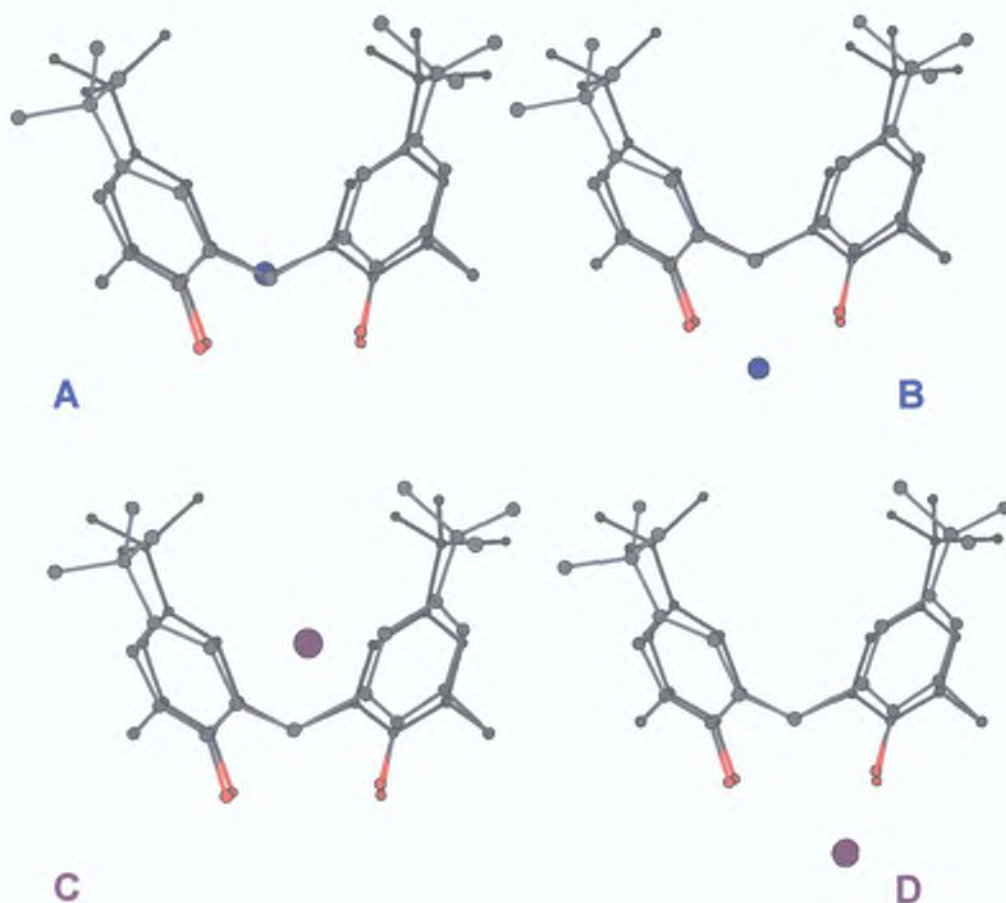


Figure 2.18 *p*-tetra-*t*-butylcalix[4]arene oxanion[Na⁺] endo (A), exo (B) & *p*-tetra-*t*-butylcalix[4]arene oxanion[K⁺] endo (C), exo (D)

2.3.7.3 A 'Metal Template' Effect

A difficulty that occasionally arises when carrying out nucleophilic substitution reactions is that the reactants do not mix due to solubility differences. This has a profound effect on reaction rates. Thus, to overcome this difficulty phase-transfer catalysis is often utilised. Crown ethers and varying cryptands have found use as catalysts improving reaction rates by complexing with the metal ion of a salt rendering the nucleophile 'naked' and soluble in an organic phase. For example, a salt like KCN is converted by dicyclohexano-18-crown-6 (Fig. 2.19) into a new salt whose anion is the same, but the cation is now a much larger species with the positive charge spread over a larger volume, enhancing its solubility in organic solvent [154].

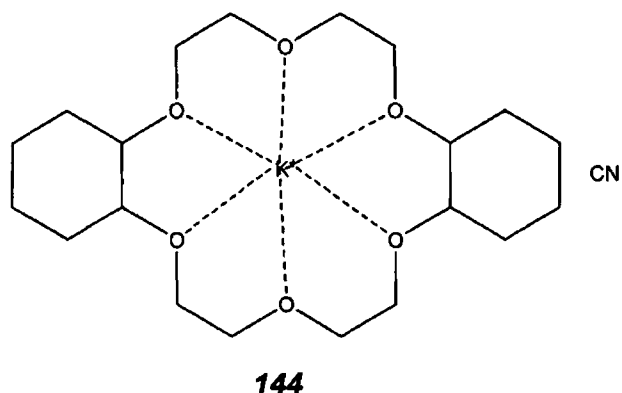


Figure 2 19 *Dicyclohexano-18-crown-6[K⁺] Complex (A Phase Transfer Catalysis)*

Potentiometric studies of **143** have established the ligand as an effective complexing agent for Na⁺, a characteristic that permits it to function as a phase transfer catalyst and thus, play a role in these reactions (Fig 2 20) [110]. Trace quantities of **143** in reaction F may complex to the Na⁺ ion of the base with a greater affinity than for the *p*-tetra-*t*-butylcalix[4]arene oxyanion. Subsequently, this increases the reactivity of the *p*-tetra-*t*-butylcalix[4]arene oxyanion as it becomes a 'naked' anion, driving the reaction towards complete alkylation. The atomic radius of a potassium ion is larger than that of a sodium ion. **143** exhibits high selectivity for Na⁺ over K⁺, which is attributed to the inner size of the ionophoric cavity, comparable with the ion size of Na⁺ rather than K⁺. The inability of **143** to complex to the potassium ion would seem to have implications on this reaction. Following deprotonation, potassium forms an ion-pair with the oxyanion. Any **143** present may not complex to the potassium ion as efficiently as that for sodium. Hence, the potassium remains bound to the phenoxide anion, reducing its nucleophilicity, as a result partial denaturation occurs.

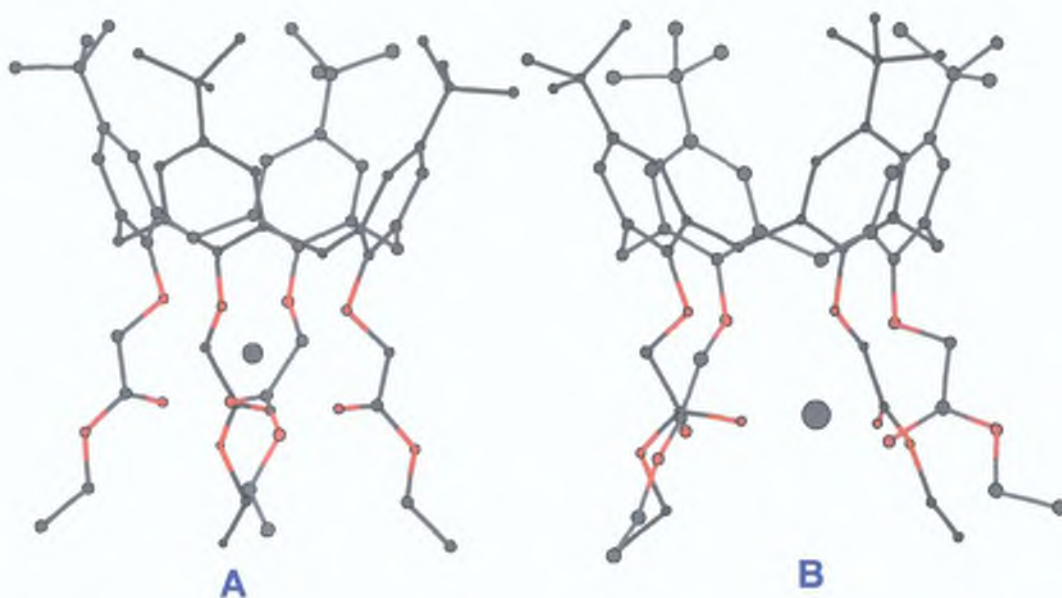


Figure 2.20 Energy minimised structures for the 143-[Na⁺] (**A**) and 143-[K⁺] (**B**) complex

2.3.8 Characterisation of Partially Substituted Calix[4]arene Derivatives

Figure 2.7 details the products, **140** and **70**, of the optimised reaction D and G (Table 2.4 pp. 77).

Upon purification, LC-DAD analysis indicated that 'pure' **70** was obtained with 99.6% relative peak area purity. DI-MS of this sample verified this with a molecular ion peak at 843.5 Da (820 + Na⁺). Collisional Ion Fragmentation, MSⁿMS demonstrated the loss of one ligating group (87amu) and MSⁿMSⁿMS demonstrated the further loss of the remaining ligating group (87amu).

Characterisation of **70** was straightforward as a symmetrical arrangement of ligating groups resulted in an uncomplicated NMR spectrum, with signals attributed to substituted and unsubstituted phenol subunits. The ¹H NMR spectrum **4** at room temperature consists of resonances from the aromatic, t-butyl and hydroxyl protons appearing as singlets. The most useful aspect of this spectrum is the information derived from the splitting pattern of the methylene linker (-CH₂-) protons. Often, the splitting patterns of these protons confirm the conformation of the calixarene and also, aid in the assignment of positional isomers (1,2- or 1,3-disubstituted) of partially substituted calix[4]arenes (Fig. 2.14) [1,2].

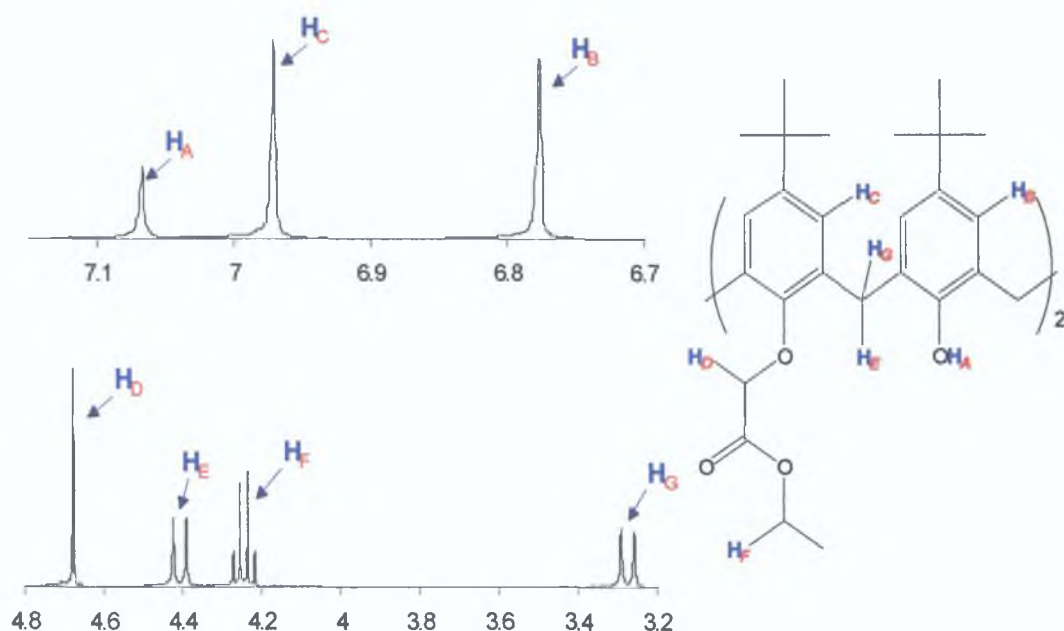


Figure 2.21 ^1H NMR of **70** (3-7ppm) in CDCl_3

The ^1H NMR spectrum of **70** exhibited two t-butyl singlets at δ 0.98 and 1.26, a single AB system for the bridging methylene groups at δ 3.32 and 4.45 ($J_{\text{HH}}=13.2$ Hz), a singlet for the OCH_2CO groups (δ 4.72) and two singlets for the aromatic protons (δ 6.82 and 7.02). This data confirmed that the substitution was of the 1,3-regioisomer (Fig. 2.13) as opposed to the 1,2-regioisomer but could not distinguish between a 1,3-alternate and a cone conformation (Fig. 2.21).

The high sensitivity of **70** to Na^+ implies that the diester is in the cone conformation. The related derivative, **143**, locked into a cone conformer is a selective Na^+ complexing agent. It has been reported in the literature that further alkylation of **70** with ethyl bromoacetate yielded **143** in the cone conformation suggesting that **70** possesses this conformation [83].

While it has been proven that the position of the singlet arising from the OH group (δ_{OH} value) may not be taken as a measure of the strength of intramolecular hydrogen bonding, it is interesting to observe that the δ_{OH} value of **4** is 10.34ppm. The substitution of two phenol subunits at the lower rim, resulting in the demise of the intramolecular hydrogen bonding network and a shielding influence by the two ligating groups is clearly demonstrated by the significant upfield shift of the resonance from the remaining OH group to 7.08ppm.

140 was isolated as a white solid, with a carbonyl stretch at 1744cm^{-1} and a molecular ion peak of 757Da ($734 + \text{Na}^+$), determined by MS LC-DAD demonstrated that this peak eluted at a retention time of 15.05min . The ^1H NMR spectrum of **140** exhibited two types of phenolic protons at 9.2 and 10.2ppm , with the phenolic proton adjacent to the substituted phenol shifted further upfield to 9.2ppm . Three different aromatic signals were observed, the substituted phenol, $\delta 7.7\text{ppm}$, the unsubstituted phenol distal to this substituted phenol at 7.11ppm and the two unsubstituted phenol units distal to each other at 7.06ppm .

There were three pairs of doublets corresponding to two types of axial (adjacent to a hydroxyl and an alkoxyl group, adjacent to two hydroxyl groups) and one equatorial proton with an integration of 2H_I , 2H_G , 4H_J , ax-ax-eq, $J_{\text{HH}} = 12.4\text{--}13.6\text{Hz}$. The equatorial proton is strongly influenced by the aromatic rings rendering it impervious to electron differences between the substituted and unsubstituted phenol subunits and hence, resonates at identical frequencies.

2.4 Conclusion

The optimal reaction conditions, **4** ethyl bromoacetate in K_2CO_3/ACN or Na_2CO_3/DMF were determined for the synthesis of **70**. From these studies, it was discovered that the selective functionalisation of calixarene derivatives does not proceed as anticipated but an insight into the direction and progression of this reaction can be ascertained by the use of such invaluable analytical techniques as LC-MS, LC-DAD and DI-MS. Direct injection MS of the reactions carried out gave misleading results due to differences in the relative sensitivity of the MS to the mono and diester derivatives. LC-DAD studies revealed the composition of these reactions. The amalgamation of these two analytical tools, LC-UV-MS, gives unequivocal identification of the reaction products.

It is apparent that the choice of base and solvent has a profound effect on the product distribution. From these studies, the mechanism of this reaction is clarified, stepwise alkylation is favoured for the weak bases, Na_2CO_3 and K_2CO_3 . LC-UV determined that the preferential regioisomer formed is the (1,3)-diester over the (1,2)-diester.

To conclude, LC-UV-MS has proven to be powerful for the identification and characterisation of the products obtained in these reactions and the optimisation of the reaction conditions for the preparation of **70**.

2 5 Experimental

2 5 1 Reagents and Chemicals

Spectranal grade acetonitrile and pestanal grade water for use with the LC-MS were supplied by Riedel-de-Haen Aldrich supplied HPLC grade acetonitrile and water for use with the LC-DAD Formic acid (A C S reagent), used in the preparation of mobile phase for LC-MS and LC-DAD, was supplied by Aldrich The solvents used for the synthetic work, including anhydrous DMF, HPLC grade ACN were supplied by Aldrich Acetone, supplied by Labscan, was dried over anhydrous calcium sulphate before use The *p*-tetra-*t*-butylcalix[4]arene was supplied by Diosynth Ltd and the ethyl bromoacetate and carbonate bases were purchased from Sigma-Aldrich

2 5 2 LC-MS Analysis

The LC-MS used was a Bruker/Hewlett-Packard Esquire instrument The LC was a HP 1100, with variable wavelength detector, a low volume pump, an in-line degasser and an autosampler linked to a Bruker Mass Spectrometer which was controlled by HP Chemstation software

2 5 2 1 LC Method 1

The HPLC column used was a reverse phase, Zorbax RX-C18, 150 x 2.1mm, 5µm in diameter The mobile phase used was 100/0.25 v/v Acetonitrile/Formic Acid at a flow rate of 0.2ml min⁻¹ The monitoring wavelength was 210nm and an injection volume of 4µl was used The samples were prepared in acetonitrile to a concentration of 0.5mg ml⁻¹

2 5 2 2 LC Method 2

A Supelco-C18, 250 x 2.1mm, 5µm column with a mobile phase of 92/8/0.25 v/v/v Acetonitrile/water/formic acid at a flow rate of 0.3ml min⁻¹ The monitoring wavelength was 210nm and an injection volume of 4µl was used Samples were prepared to a concentration of 0.5mg ml⁻¹ in acetonitrile

2 5 2 3 MS Method

The MS method employed for both LC methods used a positive ESI source The nebulisation gas and drying gas was set to 35psi and 9l min⁻¹ respectively The temperature of the source was maintained at 300°C The octapole voltage was 2.83V, the skimmer 1 voltage was 50 ± 5V and the trap drive voltage was 57 ±

2V Mass spectral data was collected in the scan range of 400-1200 m/z. When automated fragmentation information was required, the software was set up to subject the most abundant ion to MS/MS, using an isolation width of 4 Da and a collisional amplitude of 1.80 Da.

2.5.3 Direct Infusion Mass Spectral Analysis

Samples were injected into the ESI source (positive mode) at a rate of $5\mu\text{l min}^{-1}$. The nebulisation gas and drying gas were set to 15psi and 4 l min^{-1} respectively. The source temperature was maintained at 250°C . The octapole voltage was 2.83V, the skimmer 1 voltage was $50 \pm 5\text{ V}$ and the trap drive voltage was $57 \pm 2\text{ V}$. Mass spectral data was collected in the scan range of 400-1200 m/z. Samples were prepared in acetonitrile with 0.25% formic acid to a concentration of 0.1 mg ml^{-1} . When online MS/MS was being carried out, an isolation width of 4 Da and collisional amplitude of 1.60-2.10 were used depending on the ion being fragmented. Samples were prepared in acetonitrile with 0.25% formic acid to a concentration of 0.1 mg ml^{-1} .

2.5.4 LC-DAD Analysis

A Varian HPLC system comprising of a Varian Prostar 330 photodiode array detector and a gradient Prostar 230 pump was used to obtain UV-VIS spectra of the components of the reactions carried out. It was equipped with a manual operated switching valve with a $20\mu\text{l}$ injector loop and the system was controlled via Varian software.

Due to the availability of the Supelco column with standard dimensions, LC method 2 was set up. The parameters of LC-DAD analysis were a Supelco-C18, $250 \times 4.6\text{ mm}$, $5\mu\text{m}$ column with a mobile phase of 92/8/0.25 v/v/v acetonitrile/water/formic acid at a flowrate of 1.5 ml min^{-1} . The monitoring wavelength was 210nm and an injection volume of $20\mu\text{l}$ was used.

2.5.5 Synthetic Procedures

Table 2.2 details the reactions carried out for the optimisation of the synthesis of **70**. Reactions A – F were carried out at 70°C while reaction G was carried out at room temperature for 96h. Reactions A – D were run simultaneously on the same scale in a parallel synthesiser system (Radleys Carousel Reaction Station, Shire Hill, Saffron Walden, Essex, CB11 3AZ, UK). Reaction E was carried out according to the previously reported method for making **70**, employing a 2:1

stoichiometry of ethyl bromoacetate **4** using K_2CO_3 and Acetone Reaction F employed identical reaction conditions as for those stated for reaction E with the exception of Na_2CO_3 substituted for K_2CO_3

Synthetic Method for Reactions A – D

To a suspension of **4** (150mg, 3.09mM) in anhydrous DMF, was added Na_2CO_3 (0.33g, 3.09mM) followed by the dropwise addition of 2M excess ethyl bromoacetate. The mixture was heated to 70°C for the specified time length. Subsequently, the reaction was cooled to room temperature, poured onto ice and extracted with ethyl acetate (4 x 25ml), washed with water (4x25ml) and brine solution (4x25ml). The organic extract was dried over anhydrous magnesium sulphate ($MgSO_4$) and the solvent removed under reduced pressure.

Synthetic Method for Reaction G

To **4** (2.0g, 3.09mM) in HPLC grade ACN, potassium carbonate (K_2CO_3), (0.43g, 3.09mM) was added. This was stirred for 1h to which 2M excess ethyl bromoacetate was added. The reaction mixture was stirred at room temperature for 96h. The remaining insoluble reaction material was filtered and the solvent was removed under reduced pressure.

Purification of Partially Substituted p-Tetra-*tert*-Butylcalix[4]arene Ester Derivatives

Reaction mixtures were purified by flash column chromatography using 10/90 ethyl acetate/hexane as eluent to afford two main fractions.

5,11,17,23-Tetra-tert-butyl-25-(ethoxycarbonylmethoxy)-26,27,28-trihydroxycalix[4]arene (140)

Fraction A yielded a white solid (0.36g, 21%) mp 250–254 °C, IR (KBr) λ_{max} [cm^{-1}] 1744, 2954, 3326, R_f 0.39, 1H NMR (ppm, $CDCl_3$) δ 1.21, 1.22, 1.24 (s, 36H, CMe_3), 1.40 (t, 3H, $J=7.1$ Hz, CH_3), 3.43 and 3.46 (d, 4H, $J=12.4$ Hz, $ArCH_2Ar$), 4.30 and 4.33 (d, 2H, $J=13.6$ Hz, $ArCH_2Ar$), 4.41 (q, 2H, $J=7.2$ Hz, $C(O)CH_2$), 4.48 and 4.51 (d, 2H, $J=13.1$ Hz, $ArCH_2Ar$), 4.90 (s, 2H, OCH_2), 7.00 (s, 2H, $J=2.4$ Hz, ArH), 7.06 (s, 4H, $J=1.7$ Hz, ArH), 7.11 (s, 2H, ArH), 9.28 (s, 2H, OH), 10.25 (s, 1H, OH), ^{13}C NMR (ppm, $CDCl_3$) δ 14.1, 22.6, 31.2, 31.4, 31.5, 32.5, 33.0, 33.9, 34.0, 34.2, 61.9, 72.0, 125.6, 125.7, 125.8, 126.6, 127.7, 128.0, 133.3, 143.2, 148.2, 149.9, and 169.5, ESI m/z 757.4 ($M + Na^+$)

5,11,17,23-Tetra-tert-butyl-25, 27-bis(ethoxycarbonylmethoxy)-26,28-dihydroxycalix[4]arene (70)

Fraction B yielded a white solid (0.66g, 39%) mp 179–181 °C, IR (KBr) λ_{max} [cm⁻¹] 1751, 3424, R_f 0.21, ¹H NMR (ppm, CDCl₃) δ 0.98, 1.26 (s, 36H, CMe₃), 1.32 (t, 6H, $J=7.1$ Hz, CH₃), 3.30 and 3.34 (d, 4H, $J=13.2$ Hz, ArCH₂Ar), 4.29 (q, 4H, $J=7.1$ Hz, C(O)CH₂), 4.43 and 4.46 (d, 4H, $J=13.1$ Hz, ArCH₂Ar), 4.72 (s, 4H, OCH₂), 6.82 (s, 4H, ArH), 7.02 (s, 4H, ArH), 7.09 (s, 2H, OH), ¹³C NMR (ppm, CDCl₃) δ 14.1, 31.0, 31.6, 31.8, 33.8, 33.9, 61.2, 73.4, 125.0, 125.7, 127.9, 132.5, 141.5, 150.2, 150.7 and 169.2, ESI m/z 843.5 (M + Na⁺), 859.5 (M + K⁺)

2.5.6 Molecular Modelling

Molecular modelling calculations were carried out using Spartan software, SGI version 5.0.1 running on a Silicon Graphics workstation with a MIPS R10000 Rev 2.7, 195-MHz CPU, an IRIX operating system (release 6.3) and 128 MB of RAM. Partial charge surface maps based on extended Huckel calculations were generated using Chem-3d Pro (Cambridgesoft, Cambridge, MA, USA) after importing the energy minimised molecular coordinates.

3. Synthesis and Characterisation of Partially Functionalised Calix[4]arene Derivatives

3 1 Introduction

Reliable procedures for the synthesis of partially denvatised calixarenes have been developed as descnbed in Chapter Two. These conditions were used to synthesise various mono- and di-substituted calixarene derivatives as outlined in Table 3 1 [144]. These partially substituted derivatives prepared, contain both substituted (one or two) and unsubstituted (two or three) phenol subunits rendering them conformationally mobile but to a lesser extent than the *p*-tetra-*t*-butylcalix[4]arene derivative. Temperature NMR studies were used to investigate their conformational mobility.

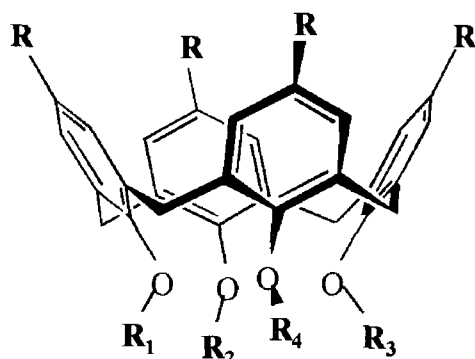


Figure 3.1 Structures of the Calix[4]arene Denvatives synthesised

No	Generic Name used for the Discussion of these Compounds	Substituent Groups at the Upper & Lower Rim				
		R	R ₁	R ₂	R ₃	R ₄
4	<i>p</i> - <i>t</i> -butylcalix[4]arene	CMe ₃	H	H	H	H
41	Calix[4]arene	H	H	H	H	H
140	<i>p</i> - <i>t</i> -Butyl monoester	CMe ₃	CH ₂ C(O)OEt	H	H	H
70	<i>p</i> - <i>t</i> -Butyl-1,3-Diester	CMe ₃	CH ₂ C(O)OEt	H	CH ₂ C(O)OEt	H
145	Calixdiester	H	CH ₂ C(O)OEt	H	CH ₂ C(O)OEt	H
146	<i>p</i> - <i>t</i> -Butyl monoamide	CMe ₃	CH ₂ C(O)NH ₂	H	H	H
147	<i>p</i> - <i>t</i> -Butyl-1,3-Diamide	CMe ₃	CH ₂ C(O)NH ₂	H	CH ₂ C(O)NH ₂	H
148	<i>p</i> - <i>t</i> -Butyl-1,3-Diacid	CMe ₃	CH ₂ C(O)OH	H	CH ₂ C(O)OH	H

Table 3 1 Names and Structures of the calix[4]arene derivatives synthesised

3 2 Results and Discussion

3 2 1 Characterisation of Partially Substituted Calix[4]arene Derivatives

The procedures discussed in Chapter Two (*Reaction C and G, Table 2 4, pp 77*) were applied for the synthesis of other partially substituted calixarene derivatives (*Fig 3 1*)

3 2 1 1 Disubstituted Calix[4]arene Derivatives

NMR characterisation of the disubstituted calix[4]arene derivatives **145**, **147**, and **148** was straightforward as a symmetrical arrangement of ligating groups bestows an uncomplicated NMR spectra, signals attributed to a substituted and unsubstituted phenol subunits. The most useful aspect of this spectrum is the information derived from the splitting pattern of the methylene linker ($-\text{CH}_2-$) protons. Often, the splitting patterns of these protons confirm the conformation of the calixarene and also, aid in the assignment of positional isomers (1,2- or 1,3-disubstituted) of partially substituted calix[4]arenes (*Fig 2 13*)

Treatment of **41** with ethyl bromoacetate using $\text{Na}_2\text{CO}_3/\text{DMF}$ or $\text{K}_2\text{CO}_3/\text{ACN}$ yielded **145** via nucleophilic attack of ethyl bromoacetate by calix[4]arene oxyanion (*Fig 3 2*). Recrystallisation from methanol afforded a crystalline solid in 40% yield that gave a molecular ion peak at 619Da ($596 + \text{Na}^+$) indicative of **145** which compares well with the relative yield of **70** (39%), demonstrating that the procedures developed in Chapter Two are suitable for the synthesis of other disubstituted calix[4]arene derivatives (*Fig 3 3*)

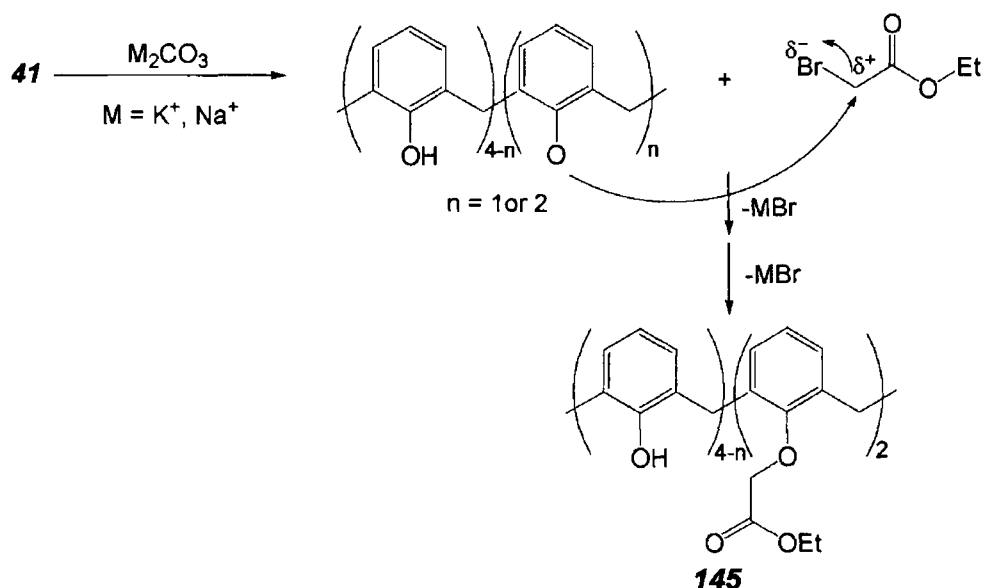


Figure 3 2 Reaction Mechanism for the synthesis of **145**

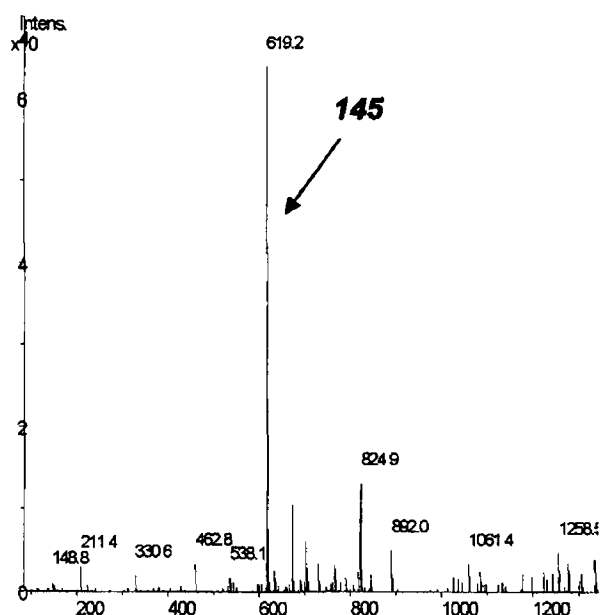


Figure 3.3 DI-Mass Spectrum of **145**

The ^1H NMR spectrum of **145** verified a distal (1,3)-disubstitution of two ethoxycarbonyl methylene groups. A triplet at δ 1.35, a quartet at δ 4.33 ($J_{\text{HH}}=7$ Hz) and a singlet at δ 4.73 ppm with appropriate integration of 3H 2H 2H were characteristic of the ligating tail, $\text{O}-\text{CH}_2-\text{C}(\text{O})-\text{O}-\text{CH}_2-\text{CH}_3$. Two sets of aromatic signals, the substituted and unsubstituted phenol subunits were observed in the region of δ 6.5-7.5 ppm. A pair of doublets for the $\text{Ar}-\text{CH}_2-\text{Ar}$, axial and equatorial protons at 3.40 and 4.48 ppm ($J_{\text{HH}}=13$ Hz) reaffirmed the conclusion that the substitution was a distal (1,3) type (Fig 3.4)

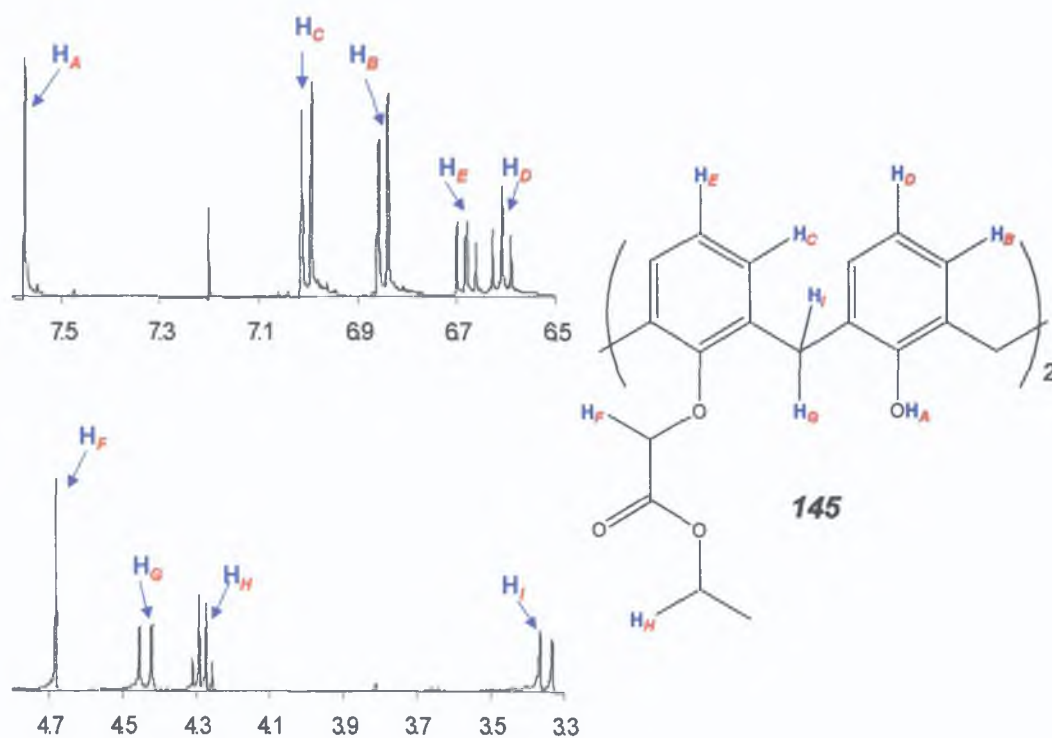


Figure 3.4 ^1H NMR Spectrum of **145** (3.3-7.5ppm) in CDCl_3

Employing 2-chloroacetamide as alkylating agent, **4** with K_2CO_3 and ACN yielded both the mono- and disubstituted derivative, **146**, **147** (Figure 3.5). Percentage yields of these derivatives, **146**, **147** were 13% and 34% which compared favourably to that of the ester derivatives, **140**, **70**, (described in Chapter Two) 21% and 39% respectively.

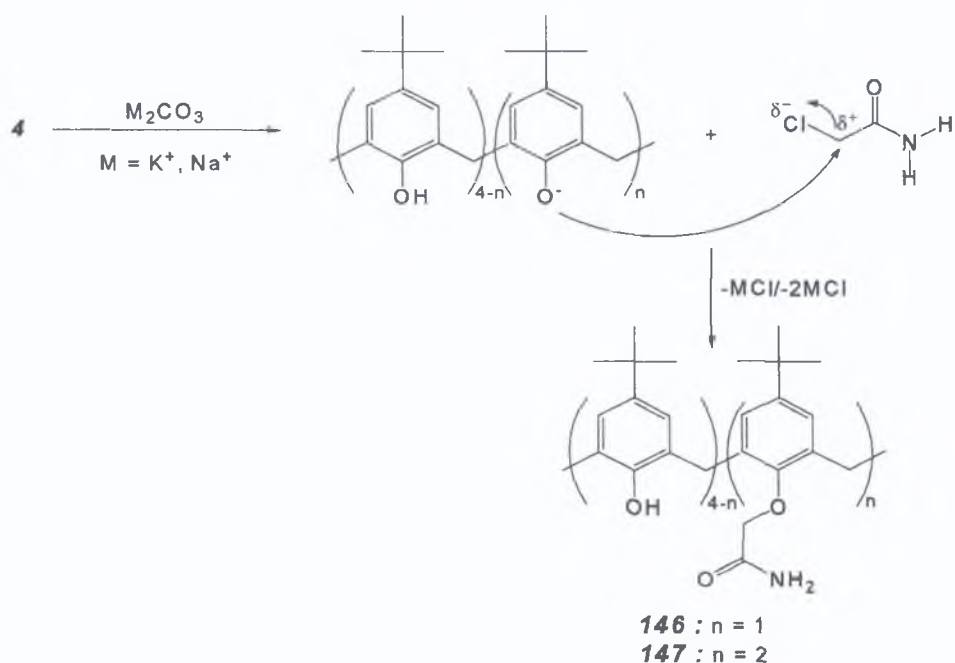


Figure 3.5 Reaction Mechanism for the synthesis of **146** and **147**

The ^1H NMR spectrum of **147** was very similar to that observed for **70** and **145** indicative of a distal (1,3)-disubstitution.

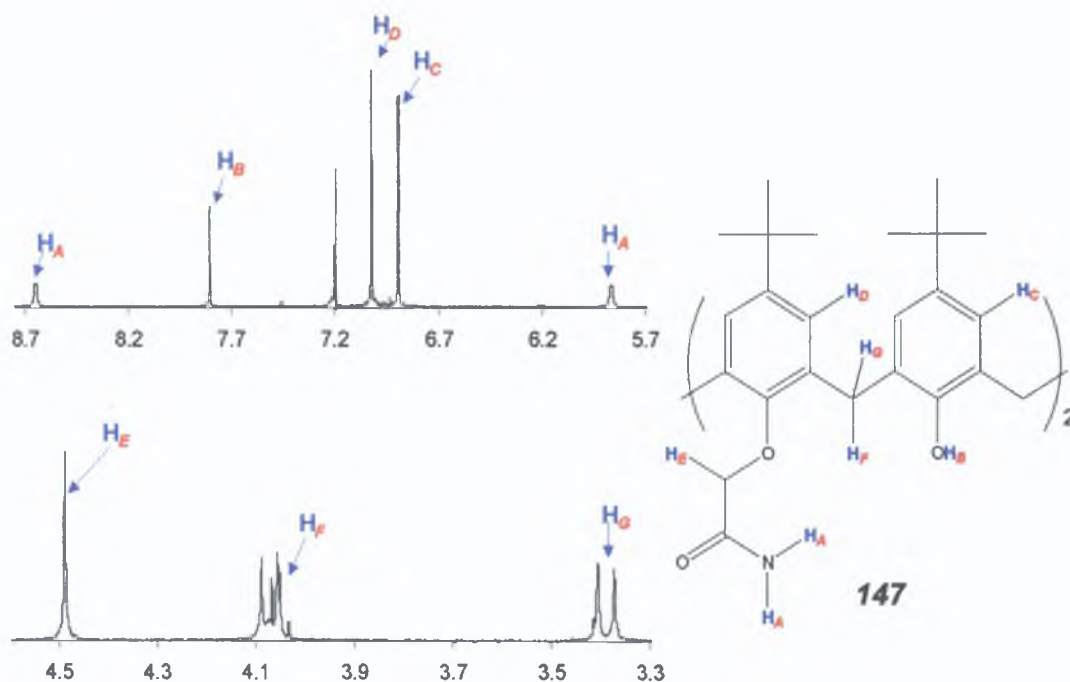


Figure 3.6 ^1H NMR Spectrum of **147** (3.3-8.7ppm) in CDCl_3

The amide protons of **147** resolve into two broad singlets resonating at δ 6.46 and 8.63ppm, indicative that one amide proton is in closer proximity to the deshielding, electron withdrawing carbonyl group. The appearance of two broad singlets for the amide protons indicates that the two amide protons are differently shielded (*Fig. 3.6*) and are also coupled to each other as confirmed by ^1H -H correlation (*Fig. 3.7*).

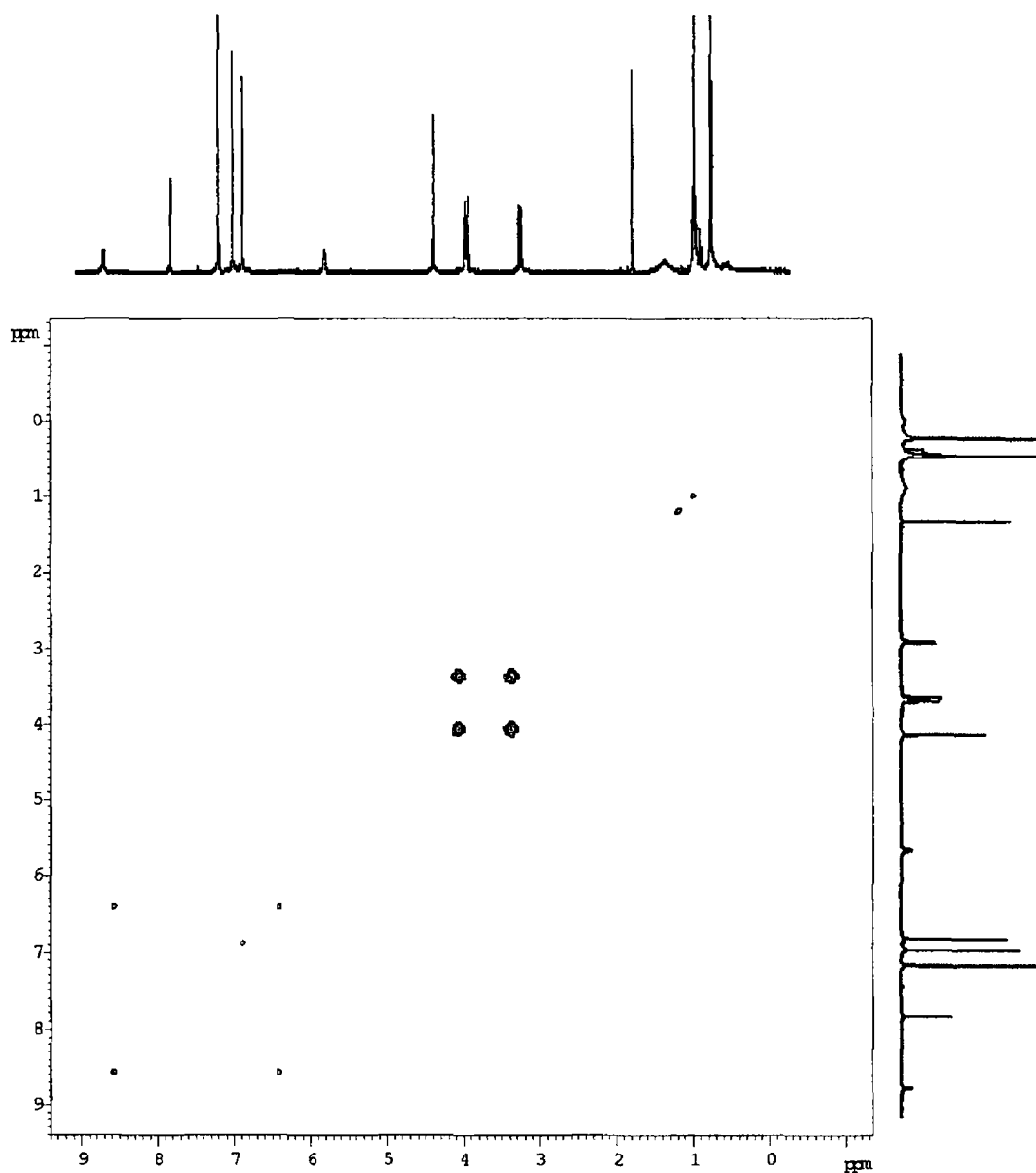


Figure 3 7 ^1H - ^1H Correlation Spectrum of **147** in CDCl_3

The coupling of the amide protons may be rationalised by examining the amide functionality. The CN bond has a high proportion of double bond character, resulting in hindering of rotation of the C-N bond so that the amino protons, H_a and H_b , are in different magnetic environments. This is represented in terms of its mesomeric canonical form (Fig 3 8)

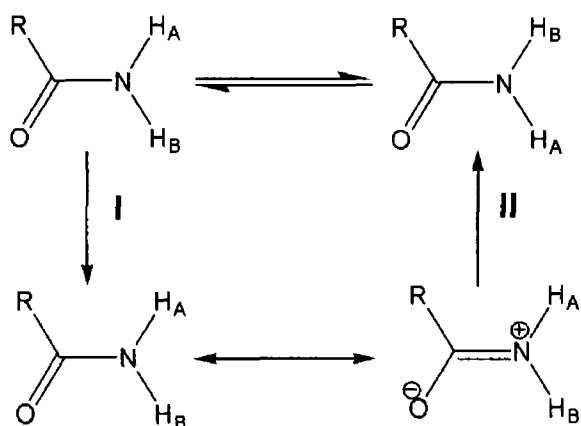


Figure 3 8 *Mesomeric Canonical Form of the Amide Functionality*

The electronic structure of the C=N bond makes bond rotation energetically unfavourable at room temperatures. Were it to occur, rotation would break the π part of the double bond by disrupting the sideways overlap of two parallel p -orbitals [162,164]. Figure 3 9 displays both the chromatographic and mass spectral results, a molecular ion peak at 785.5 Da ($762 + \text{Na}^+$) and 801.3 Da ($762 + \text{K}^+$) correlating to **147** which elutes at 9.00 min (96.6% relative area).

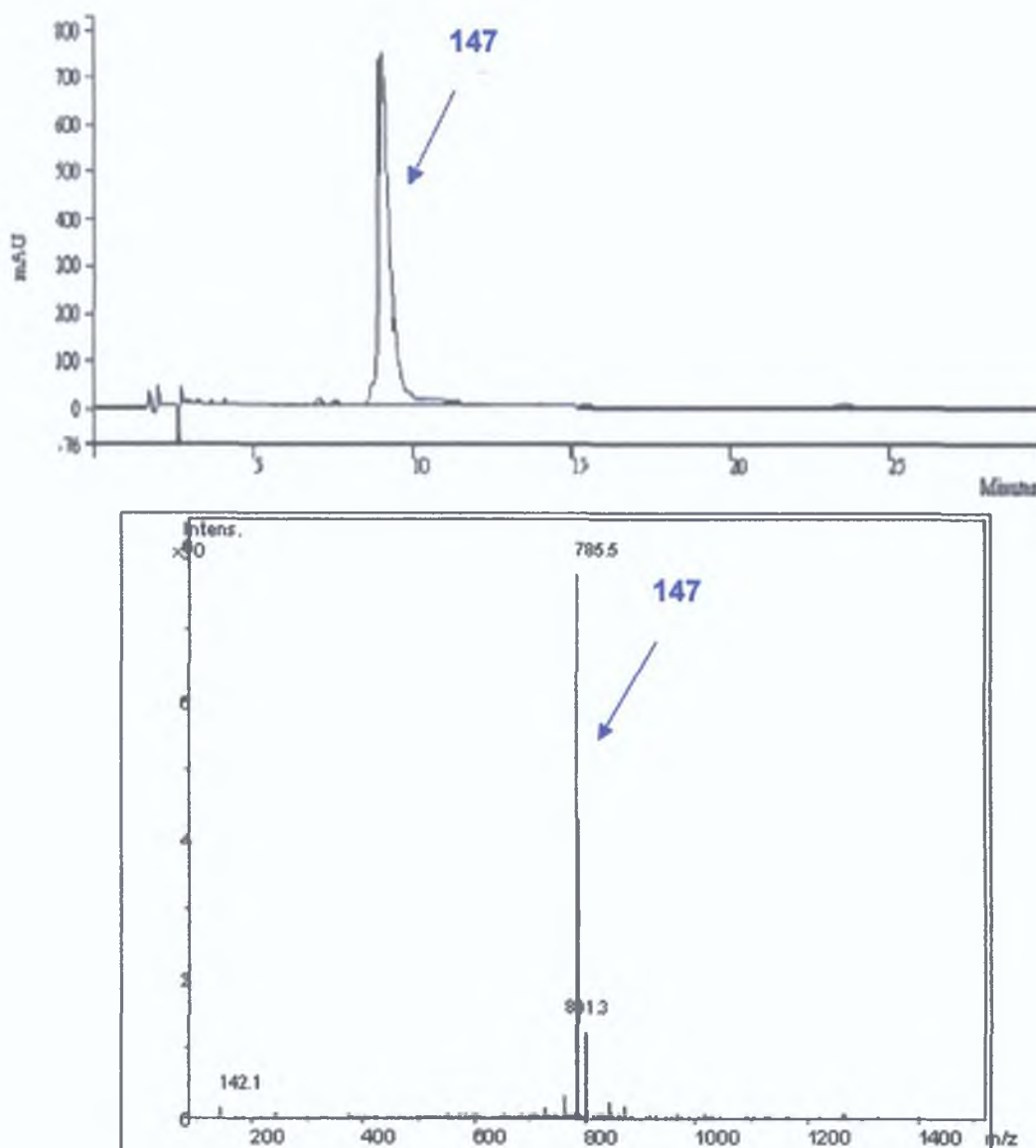


Figure 3.9 LC and DI-Mass Spectrum of **147**

Hydrolysis of 5,11,17,23-Tetra-*tert*-butyl-25, 27-bis(ethoxycarbonylmethoxy)-26,28-dihydroxycalix[4]arene (70**)**

Treatment of **70** with a strong alkaline solution resulted in hydrolysis of the ester functionalities to 5,11,17,23-Tetra-*tert*-butyl-25,27-bis(carboxymethoxy)-26,28-dihydroxycalix[4]arene, **148**. The nucleophilic hydroxyl group attacks the electropositive carbon of the carbonyl group, forming the unstable tetrahedral derivative. The carbonyl group reforms with expulsion of the ethoxy group, thus forming **148** (Fig. 3.10).

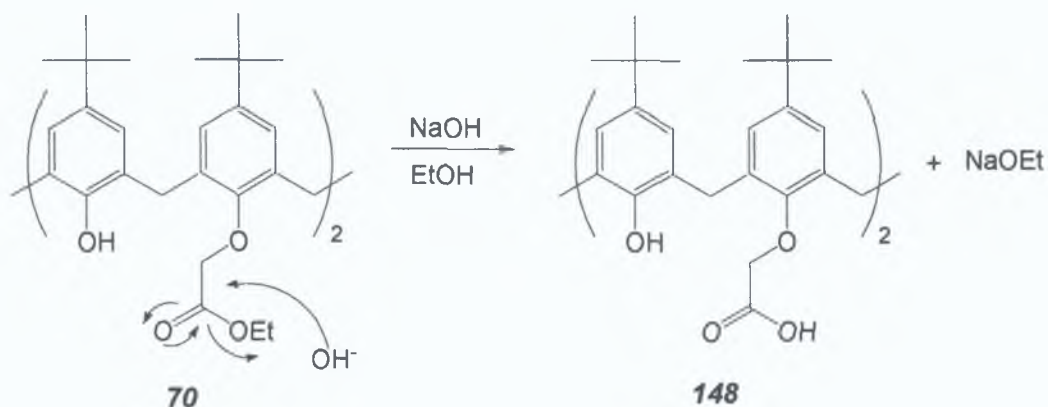


Figure 3.10 Reaction Mechanism for basic hydrolysis of **70**

Compound **148** exhibited significant signal broadening possibly due to extensive hydrogen bonding within the cavity. There are four exchangeable hydrogen atoms present in the molecule, intra- and intermolecular exchange processes leads to averaged signals, a broadening of peaks.

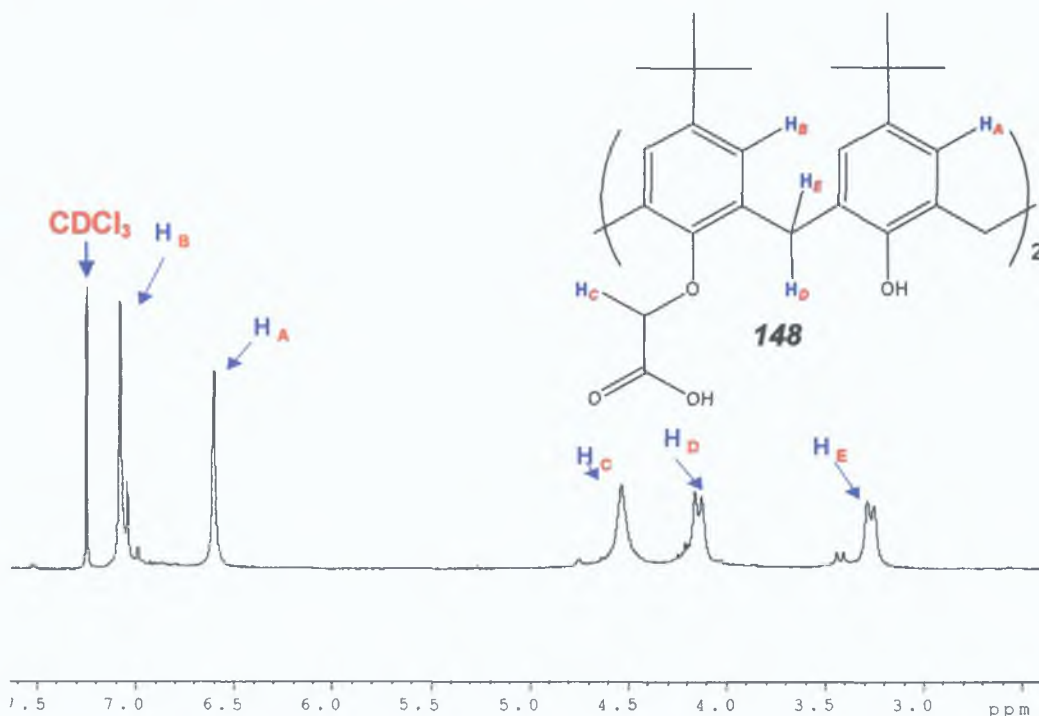


Figure 3.11 ¹H NMR Spectrum of **148** (3-7ppm) in CDCl₃

This trend was also observed for the *p*-tetra-*t*-butylcalix[4]arene tetraethyl acid (**143**). **148** eluted at 8 mins as a broad peak as it drags along the sorbent phase. De Mendoza and his co-workers proposed that ¹³C NMR spectra may aid conformational identification of calix[4]arenes. They showed that the resonance arising from the methylene linker is near δ 31ppm when the attached aryl groups

are in the *syn* orientation and near δ 37ppm when in the *anti* orientation [2]. The ^{13}C NMR spectrum of **148** verified that both groups are in the *syn* orientation with a resonance of δ 32.46ppm.

3.2.1.2 Monosubstituted Calix[4]arene Derivatives

The *p*-*t*-butylcalix[4]arene monoamide, **146** was recovered as a cream solid, with IR stretching frequencies at 1670 and 3365 cm^{-1} characteristic of a carbonyl and amide NH stretch respectively. As observed for **140** and **70**, both **146** and **147** eluted at a similar retention time, 8.94 and 9.0min respectively with a 56.9% relative peak area of monoamide. DI-MS of this solid gave a molecular ion of 728.4 [705 + Na^+] and 744.4 [705 + K^+] (Fig. 3.12).

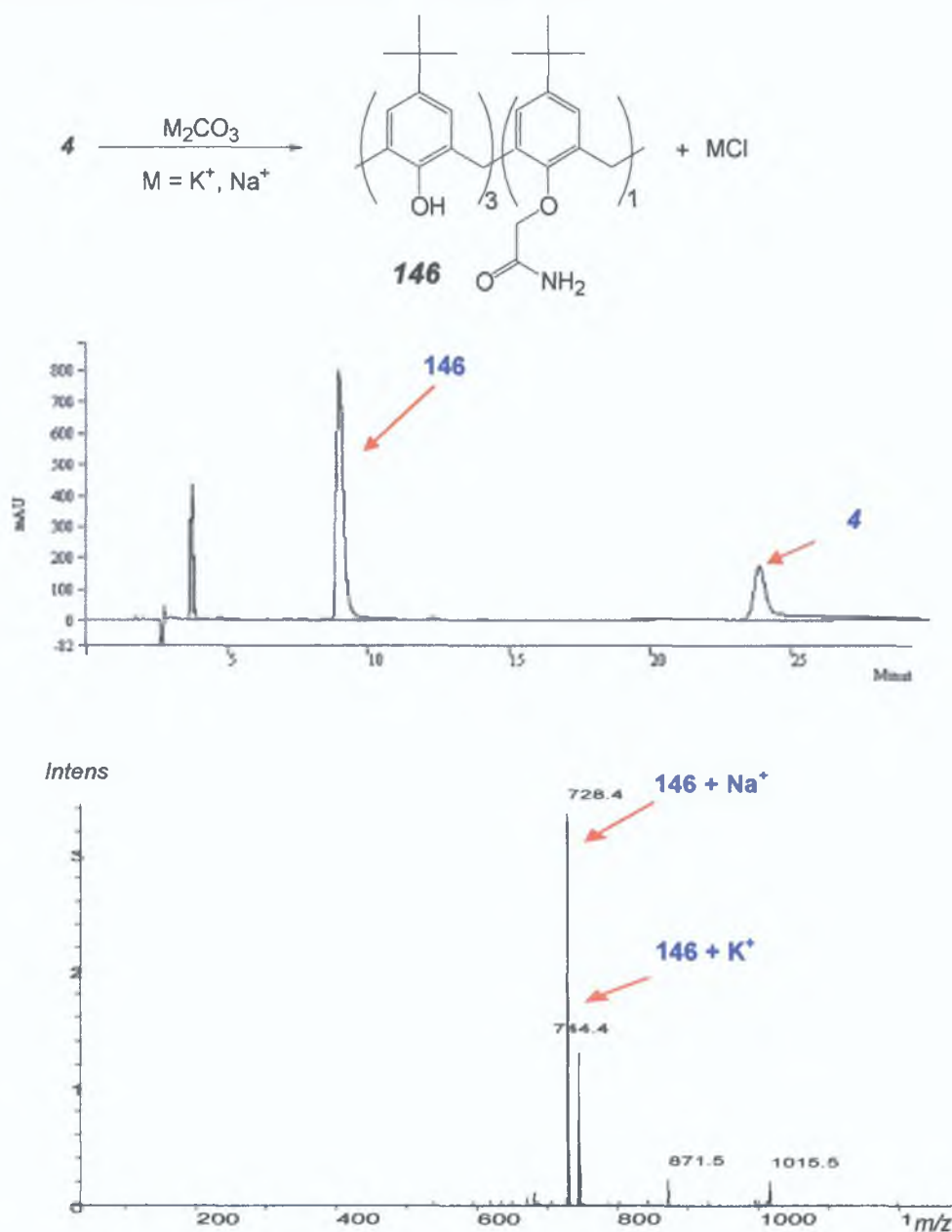


Figure 3.12 LC & DI-MS of **146**

^1H NMR verified this further with distinctive doublets, typical of the bridging methylene groups of a monosubstituted calix[4]arene derivative at δ 3.49, 4.21 and 4.24ppm ($J_{\text{HH}}=13.6, 9.3$ and 9.8Hz). The amide protons resonate as two broad singlets at δ 5.88 and 9.20ppm with three aromatic singlets at δ 7.01, 7.05 and 7.08ppm (Fig. 3.13). *Meta*-Coupling was observed for the aromatic protons of the unsubstituted phenols, with $J_{\text{HH}}=1.4$ and 1.9Hz as observed for **140**.

^1H -H correlation experiments exhibited direct spin-spin coupling between the two amide protons and also coupling of the methylene linker protons to each other, an AX system resulting in a doublet splitting pattern. These nuclei are non-equivalent due to their differing chemical environment i.e. the axial proton was deshielded due to its close proximity to the hydroxyl group whereas the shielding influence of the aromatic rings causes the equatorial protons to resonate further upfield [1]. Two broad singlets were observed for the two types of hydroxyl protons present in **146**. The hydroxyl proton, proximal to two hydroxyl protons was deshielded downfield to 10.1ppm whereas the remaining hydroxyl protons, proximal to a hydroxyl and an aminocarbonyl methoxy group are shielded further upfield to 9.4ppm.

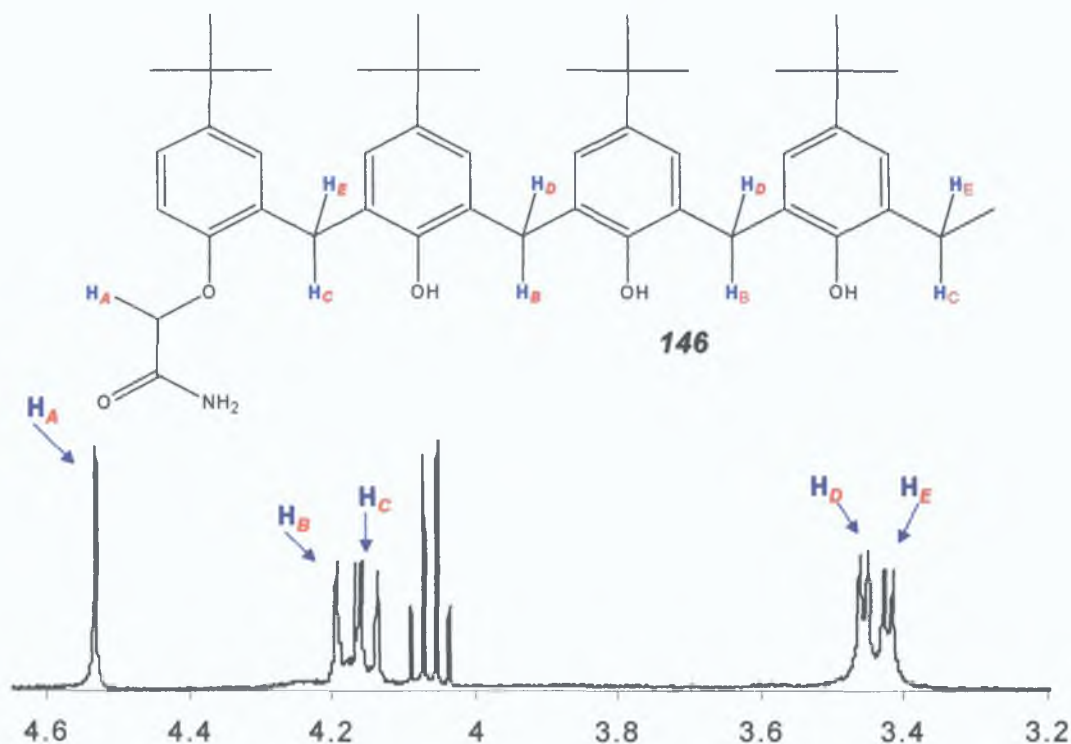


Figure 3.13 ^1H NMR Spectrum of **146** (3.2-4.6ppm) in CDCl_3

3 2 2 Investigation of the Conformational Mobility of Disubstituted Calix[4]arene Derivatives by Variable Temperature NMR Studies

Understanding the conformational properties of calix[4]arenes is of fundamental importance with respect to their utilisation as building blocks for the construction of supramolecular systems and artificial receptors. Recently, virtual molecular models based on the combination of molecular graphics with quantum chemical and molecular mechanics (MM) calculations have provided relevant information regarding intra- and intermolecular interactions and molecular stereochemistry. All the *p*-alkylphenol derived calix[4]arenes regardless of ring size are conformationally flexible in solution at room temperature on the ^1H NMR time scale. The four conformations (Fig 1 6) are obtainable by two pathways-Rotation via 'Upper Rim through the Annulus' and 'Lower Rim through the Annulus'. These calix[n]arenes including *p*-*t*-butylcalix[4]arene (**4**) and calix[4]arene (**41**) exist in solution, exclusively in the 'cone' conformation. The dominance of this 'cone' conformation is commonly ascribed to its stabilisation by the homodromic hydrogen bonding system in which each OH group acts simultaneously as a donor and acceptor. The cone \leftrightarrow cone interconversion is monitored by variable temperature ^1H NMR. In the ^1H NMR spectrum below $\sim 20^\circ\text{C}$, the methylene protons of **41** appears as a pair of doublets whereas above 60°C , a sharp singlet is observed. It is hypothesised that at lower temperatures, the cone conformation interconverts slowly on the NMR timescale and rapidly at higher temperatures. Para-substituents on **41** have a small though perceptible effect on the barrier to interconversion. This is demonstrated clearly as the conformational inversion of **41** occurs freely at 36°C with a free energy of activation (E_{act}) of $14.9 \text{ kcal mol}^{-1}$ whereas **4** converts freely at 52°C with an E_{act} of $15.7 \text{ kcal mol}^{-1}$ [3,165-167].

Variable temperature NMR studies were carried out on **70**, **145**, and **147**. Altering the temperature allows the study of exchange processes in three frequency ranges, slow, intermediate and fast exchanges. It has been demonstrated that partially derivatised calix[4]arenes are less conformationally flexible than their completely substituted counterparts or the parent calix[n]arenes. A case example is the methylation of **4**. In **4**, hydrogen bonding is at a maximum with cone conformation being favoured. Tetra O-methylation alleviates hydrogen bonding but introduces steric interference from the methoxy groups. These groups are not bulky enough to curtail conformational inversion as the conformation inversion barrier of the tetramethylated *p*-*t*-butylcalix[4]arene

149a ($\sim 15.7 \text{ kcal mol}^{-1}$) is almost identical to that of **4**, $15.7 \text{ kcal mol}^{-1}$. For partially substituted *p*-*t*-butylcalix[4]arene derivatives the E_{act} has been reported as $> 16 \text{ kcal mol}^{-1}$ for mono- (**149b**), (1,2) (**149c**), and (1,3)- (**149d**), dimethylated *p*-*t*-butylcalix[4]arene and as high as 18 kcal mol^{-1} for the trisubstituted (**149d**) derivative. This increase may be attributed to both hydrogen bonding and steric interference reducing their conformational mobility. Appending bulkier groups than a methyl group hinders conformational inversion and so, locks the calixarene derivative into a fixed conformation [1].

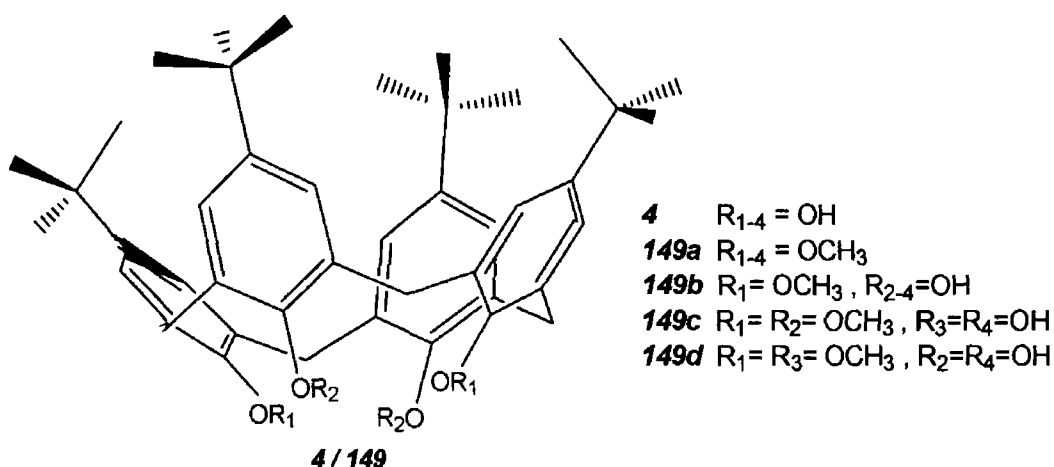


Figure 3 14 Structures of the Methylated *p*-*t*-Butylcalix[4]arene Derivatives

The conformational rotation of the disubstituted calix[4]arenes derivatives studied is influenced by steric strain and hydrogen bonding. At room temperature, the two unsubstituted phenol subunits may interconvert rapidly on the NMR timescale so that an average signal of the 'flipping' conformation is observed as sharp, distinctive signals (Fig 3 3). Hydrogen bonding involves a rapid movement of protons from one atom to another, with NMR recording an average signal. Reducing the temperature from 294 to 218K freezes ring inversion, slowing the 'flipping' conformation or exchange causing a broadening of the hydroxy proton signal as it predominantly partakes in 'flipping'. Low and high temperature NMR experiments were performed on *p*-*t*-butyl-(1,3) diester (**70**) (Fig 2 22), calix[4]-arene-(1,3)-diester (**145**) (Fig 3 4) and *p*-*t*-butyl-(1,3)-diamide (**147**) (Fig 3 6).

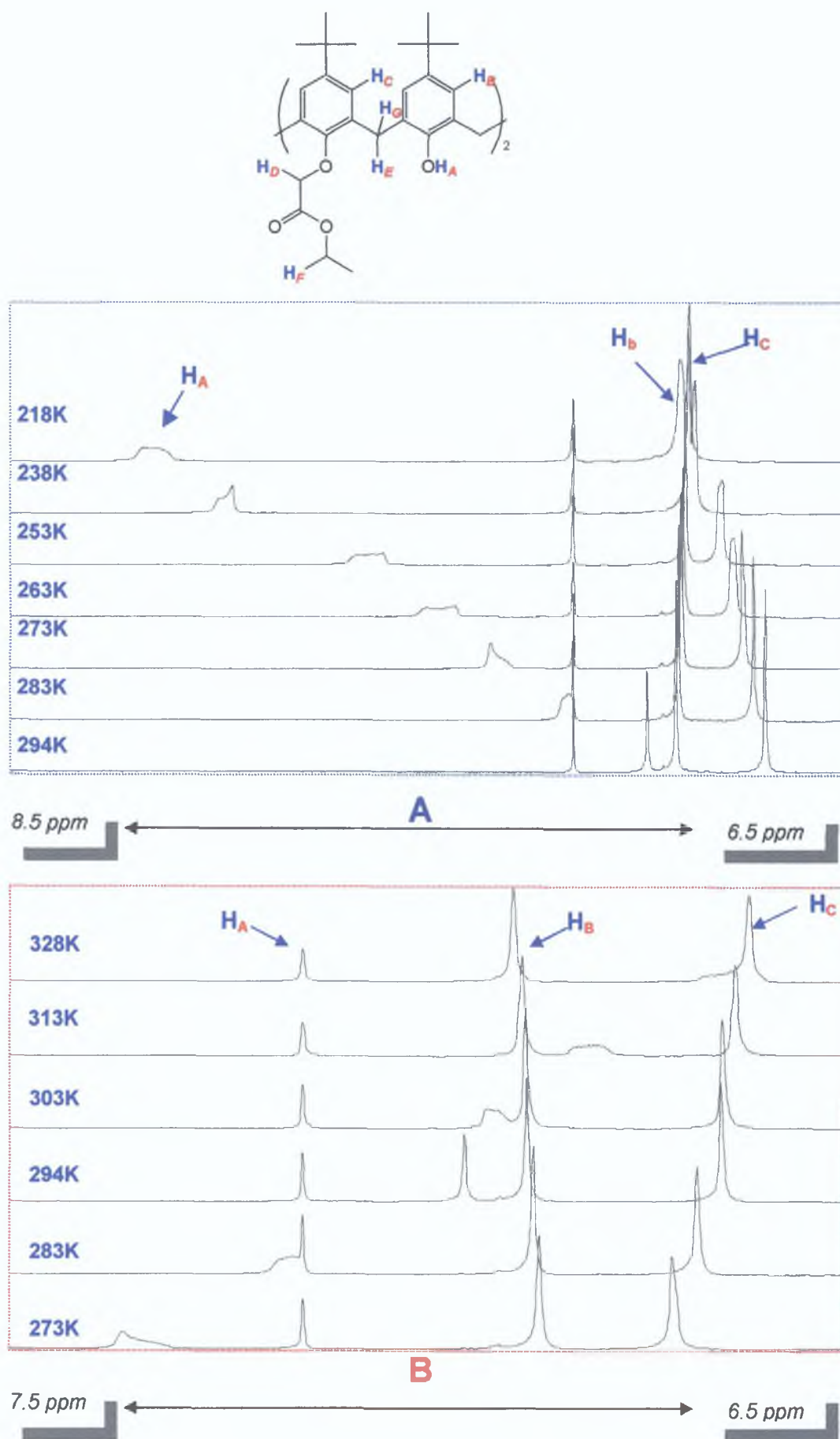
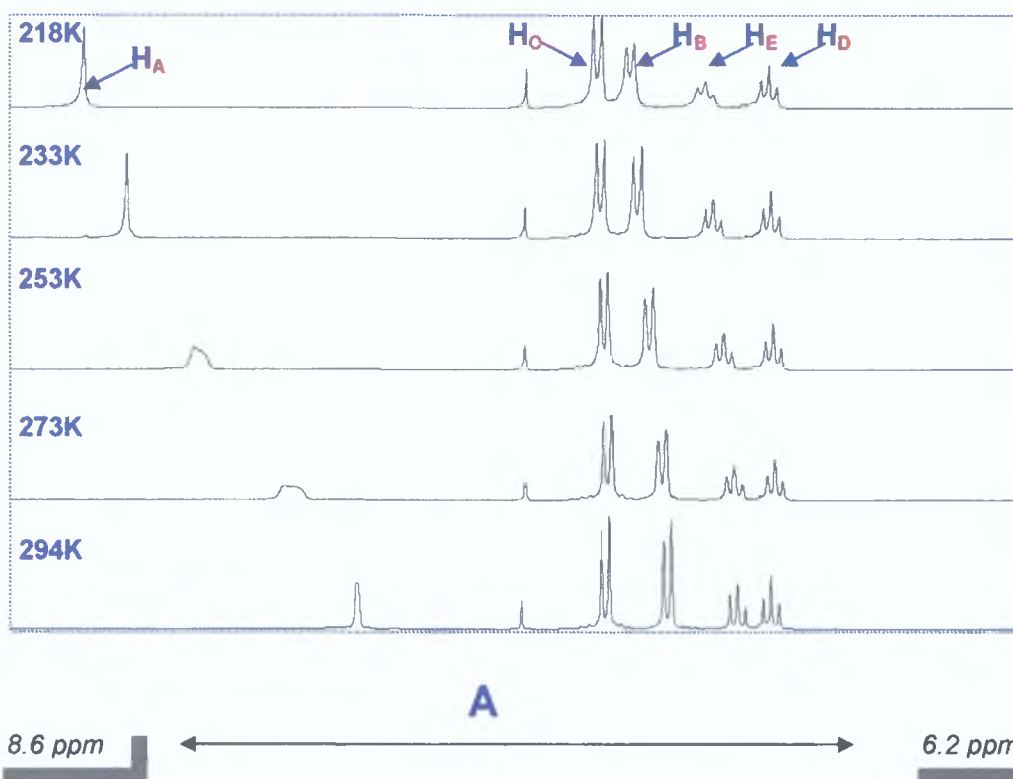
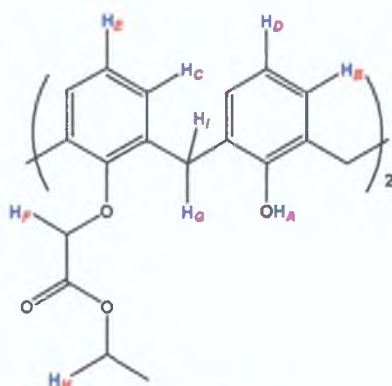


Figure 3.15 Low & High Temperature Studies of **70** (6.5-9ppm) in $CDCl_3$

As the temperature was reduced to 218K, the phenolic proton of **70** significantly broadens and is partially resolved into two peaks. Reducing the temperature does not affect the ^1H NMR spectrum of **147** as profoundly as observed for its other disubstituted counterparts. This may be attributed to strong hydrogen bonding within the lower rim cavity thus fixing its conformation and hindering the rotation of the t-butylphenol subunit.



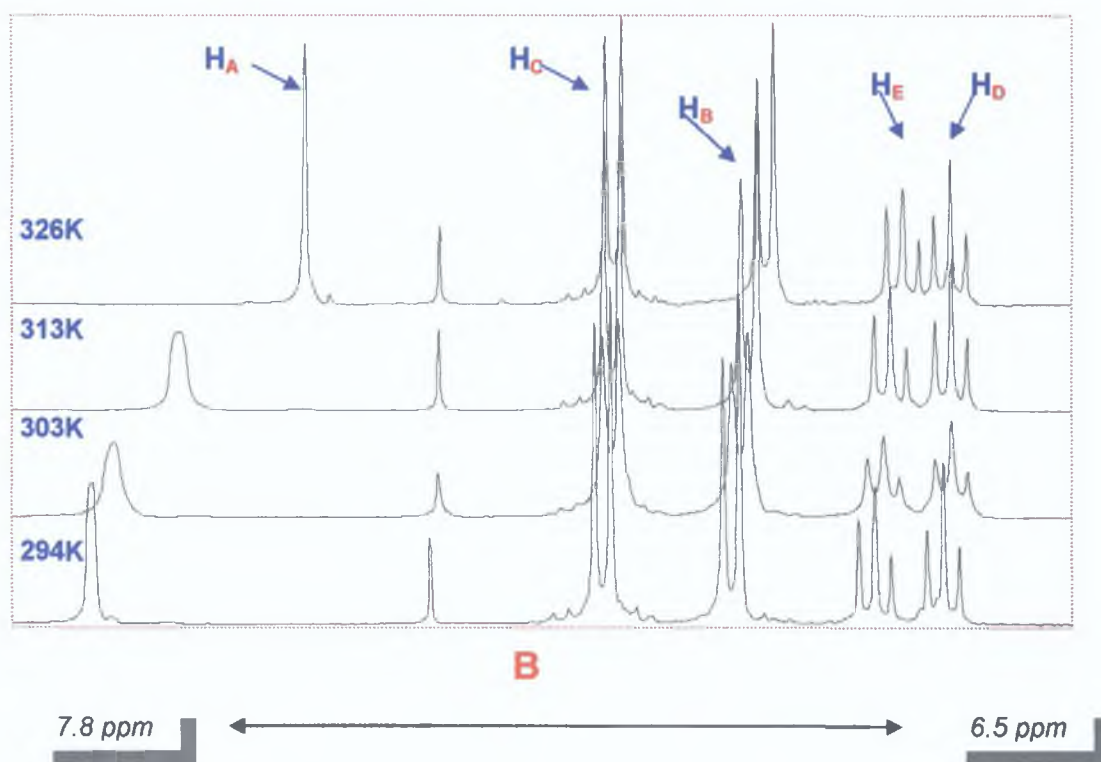
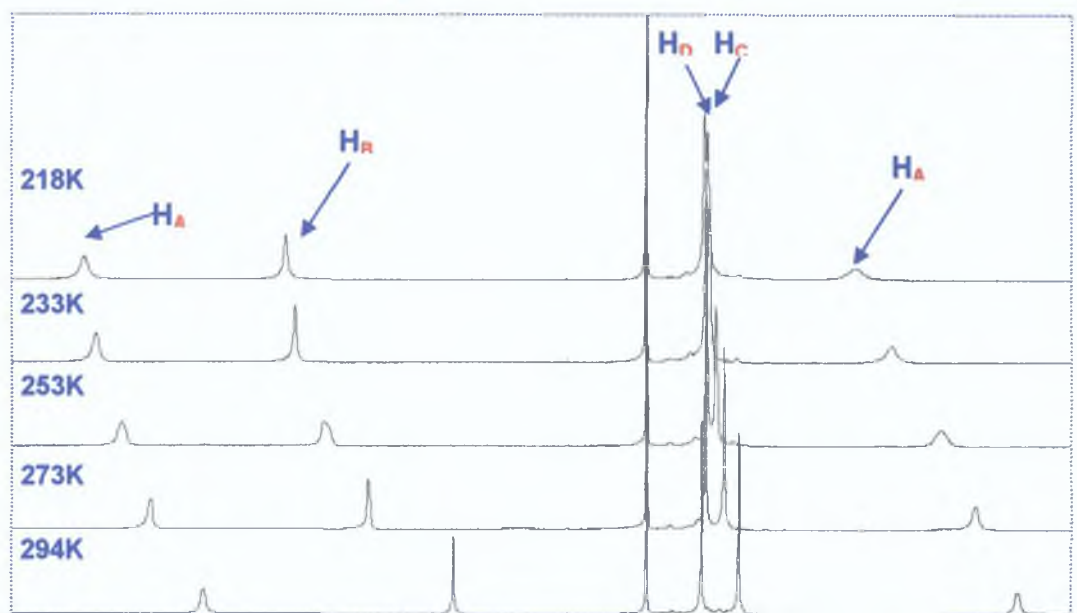
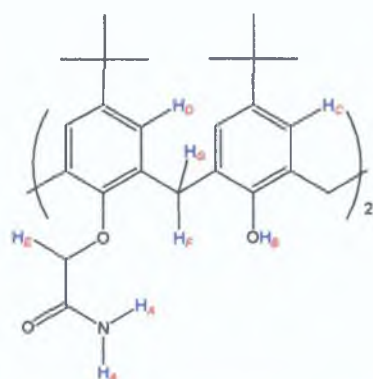


Figure 3.16 Low & High Temperature Studies of **145** (6.5-9ppm) in CDCl_3

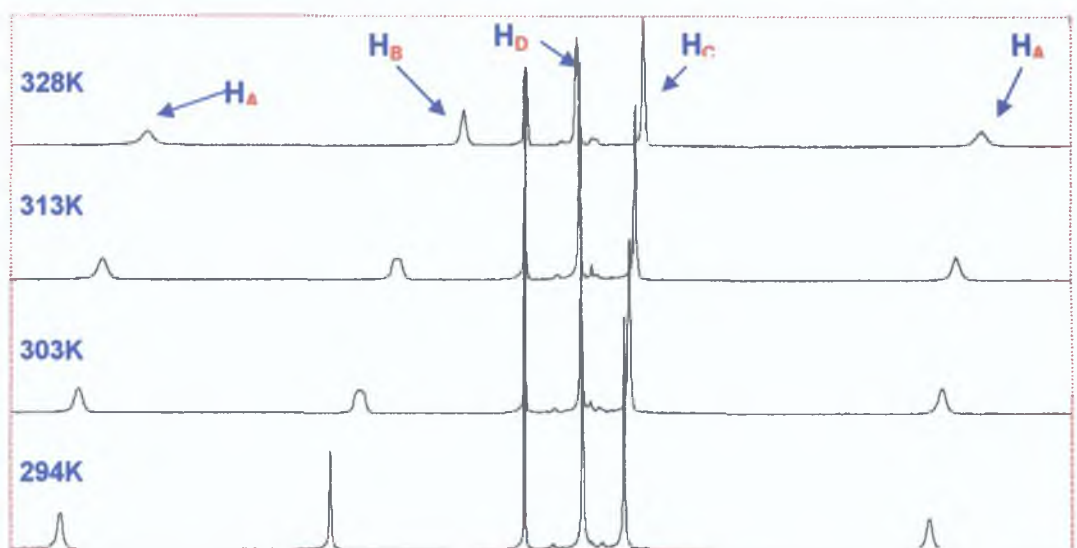
Common to all three spectra was the downfield shift of the proton signals of the unsubstituted phenol subunit. Upon slowing down interconversion, the 'cone' conformation is preferentially formed, causing an increase in the strength of hydrogen bonding observed by a downfield shift of the phenolic proton by ~0.8-1ppm.



A

9.3 ppm

5.7 ppm



B

8.7 ppm

5.7 ppm

Figure 3.17 Low & High Temperature Studies of **147** (6.5-7ppm) in CDCl_3

The antithesis to this is the upfield shift of the phenolic proton (~0.3-0.5 ppm) upon raising the temperature. As anticipated, increasing the temperature imparts greater energy that overcomes the strength of hydrogen bonding allowing greater conformational freedom, causing an upfield shift of the phenolic proton.

The ^1H NMR spectrum recorded for **145** at 218 K suggests that conformational freezing into the stable 'cone' conformation occurs as there is a dramatic downfield shift of the phenolic proton, approximately 0.8 ppm. This shift is caused by an increase in hydrogen bonding of the two ligating groups with the phenolic protons that is only possible in the 'cone' conformation.

The phenolic proton of **70** is broadened and shifted upfield by approximately 0.3 ppm and coalesces into the aromatic peak signal at 6.7 ppm. Compound **147** appears to be the most conformationally immobile derivative of the disubstituted derivatives studied with no apparent broadening of the proton signals. The aromatic proton signals of **145** were dramatically broadened with merging of the two triplet signals at 6.6 ppm. Conformational interconversion is rapid causing an almost indistinguishable chemical environment of the aromatic protons [3,166].

A general trend established for these disubstituted calix[4]arenes was defined: reducing the temperature freezes these conformationally mobile derivatives into conformationally stable multiple conformations, e.g. 'cone' and '1,3-alternate', which are strengthened by hydrogen bonding. Raising the temperature reduces the rotational barrier, causing 'flipping' of the unsubstituted phenol subunits, resulting in signal broadening. Removal of the tert-butyl groups afforded greater flexibility as demonstrated by the signal broadening and differing shielding observed for **145** compared to **70** (Fig. 3.15).

3 3 Conclusion

A series of partially functionalised calix[4]arene derivatives was synthesised and spectroscopically characterised

Procedure C and G, developed in Chapter 2, has proven a reliable method for the synthesis of various types of partially substituted calix[4]arene derivatives. Such diverse calix[4]arene derivatives included those functionalised at the upper rim, for example, Hydrogen or t-butyl groups. Partially substituted calix[4]arene derivatives bearing such pendant ligating groups as an acid, amide or ester were prepared. With percentage yields of **145**, **146** and **147** correlating closely to that of **70**, it is suggestive that the method, optimised for the synthesis of **70** is adaptable to differing calix[4]arene derivatives and allows the introduction of different functionalities onto the lower rim.

NMR characterisation, in particular ^1H NMR studies was simplified due to the symmetrical nature of the (1,3)-disubstituted derivatives. The monosubstituted derivatives, unsymmetrical in nature posed a greater challenge of interpretation. It was concluded from these studies that partial derivatisation of such macrocyclic compounds as calix[n]arene derivatives poses a challenging synthesis, often problematic. Unequivocal identification of products from partial substitution reactions may be achieved by LC-MS, LC to ascertain the product distribution of such reactions and MS to identify the products of these reactions.

Temperature NMR Studies probed the effect of varying temperature on the conformational rotational behaviour of such partially substituted calix[4]arene derivatives.

It was concluded that increasing the temperature imparts energy on the disubstituted calix[4]arene derivative which manifests as 'lower rim through the annulus' rotation of the unsubstituted phenol subunits. Peak broadening of the phenoxy and aromatic protons of the aforementioned subunits was observed whilst the protons attributable to the ligating groups and methylene linker groups remained unchanged in appearance.

Reducing the temperature resulted in slight resolution of the proton signals of the unsubstituted phenol subunits caused by the slowing down of conformational interconversion resulting in multiple conformations manifesting, for example, 'cone' and '(1,3)-alternate' conformation.

3 4 Experimental

3 4 1 General

Melting points are uncorrected ^1H and ^{13}C NMR spectra were recorded on a Bruker 400MHz and 100MHz Spectrometer using CDCl_3 as solvent unless stated otherwise IR spectra were recorded on a Perkin Elmer Spectrum GX FT-IR System A Bruker Mass Spectrometer, employing electrospray ionization was used to record the mass spectra of the derivatives synthesized The solvents used, anhydrous dimethyl formamide (DMF) and HPLC grade acetonitrile were purchased from Sigma-Aldrich Formic Acid (A C S reagent) purchased from Sigma-Aldrich was used for preparing mobile phase for the LC-DAD system The p-tetra-t-butylcalix[4]arene was supplied by Diosynth Ltd Other reagents used, ethyl bromoacetate, ethyl bromopropionate, sodium hydride and metal carbonate bases (Lithium, Sodium, Potassium) were supplied by Sigma-Aldrich

3 4 2 Synthetic Procedures

Partially substituted calixarene derivatives were prepared by two methods

3 4 2 1 Synthetic Procedure 1

To a suspension of **4** (2.0g, 3.09mM) in anhydrous DMF, was added sodium carbonate (Na_2CO_3), (0.33g, 3.09mM) followed by the dropwise addition of the alkylating agent, two molar excess The mixture was heated to 70°C for 24h Subsequently, the reaction was cooled to room temperature, poured onto ice and extracted with ethyl acetate (4 x 25ml), washed with water and brine solution (4x25ml) The organic extract was dried over anhydrous magnesium sulphate (MgSO_4) and the solvent removed under reduced pressure

3 4 2 2 Synthetic Procedure 2

To **4** (2.0g, 3.09mM) in HPLC grade ACN, potassium carbonate (K_2CO_3), (0.43g, 3.09mM) was added This was stirred for 1h to which the alkylating agent was added in two molar excess The reaction mixture was stirred at room temperature for 96h The remaining insoluble reaction material was filtered and the solvent was removed under reduced pressure

Disubstituted Calix[4]arene Ester Derivative 25,27-bis(ethoxycarbonyl methoxy)-26,28-dihydroxycalix[4]arene (145)

This was synthesized according to synthetic procedure 2 to which ethyl bromoacetate (1.58g, 9.43mM) was added to **41** (2.0g, 4.72mM) to yield a brown solid. Recrystallisation from MeOH afforded an off-whitish solid (1.12g, 40%) mp 170-173°C IR (KBr) λ_{max} [cm⁻¹] 1743, 3415, ¹H NMR δ 1.35 (t, 6H, *J*=7.1Hz, CH₃), 3.38 and 3.41 (d, 4H, *J*=13.2Hz, ArCH₂Ar), 4.33 (q, 4H, *J*=7.1Hz, C(O)CH₂), 4.47 and 4.50 (d, 4H, *J*=13.1Hz, ArCH₂Ar), 4.73 (s, 4H, OCH₂), 6.66 (t, 2H, *J*=7.5Hz, ArH), 6.73 (t, 2H, *J*=7.4Hz, ArH), 6.90 (d, 4H, *J*=7.6Hz, ArH), 7.1 (d, 4H, *J*=7.5Hz, ArH), 7.62 (s, 2H, OH), ¹³C NMR δ 14.1, 31.4, 61.4, 72.4, 119.1, 125.5, 128.1, 128.4, 129.1, 133.1, 152.3, 152.9 and 168.8, ESI, *m/z* 596.5 (M + Na⁺)

Partially Substituted p-Tetra-tert-Butylcalix[4]arene Amide Derivatives

This was synthesized according to both synthetic procedures to which 2-chloro acetamide (0.58g, 6.18mM) was added to **4** (2.0g, 3.09mM) yield a cream powder. This was purified by flash column chromatography using 1/1 ethyl acetate/hexane as eluent.

5,11,17,23-Tetra-tert-butyl-25-(aminocarbonylmethoxy)-26,27,28-trihydroxycalix[4]arene (146)

Fraction A yielded **146** (0.24g, 13%) as a cream solid mp > 280 °C, IR (KBr) λ_{max} [cm⁻¹] 1670, 2947, 3365, R_f 0.45, ¹H NMR (ppm, CDCl₃) δ 1.23, 1.25, 1.28 (s, 36H, CMe₃), 3.48 and 3.51 (d, 4H, *J*=13.6Hz, ArCH₂Ar), 4.21 and 4.22 (d, 2H, *J*=9.3Hz, ArCH₂Ar), 4.23 and 4.25 (d, 2H, *J*=9.8Hz, ArCH₂Ar), 4.58 (s, 2H, OCH₂), 5.88 and 9.20 (bs, 2H, NH₂), 7.01 (d, 2H, *J*=1.4Hz, ArH), 7.05 (d, 4H, *J*=1.9Hz, ArH), 7.08 (s, 2H, ArH), 9.4 (s, 2H, OH), 10.1 (s, 1H, OH), ¹³C NMR (ppm, CDCl₃) δ 31.1, 31.4, 31.5, 32.1, 32.6, 32.9, 33.9, 34.0, 118.9, 123.2, 125.9, 126.1, 126.9, 127.0, 127.7, 128.2, 129.7, 132.7, 143.9, 144.3, 146.6, 147.9 and 157.2, ESI, *m/z* 728.4 (M + Na⁺), 744.4 (M + K⁺)

5,11,17,23-Tetra-tert-butyl-25,27-bis(aminocarbonylmethoxy)-26,28-dihydroxycalix[4]arene (147)

Fraction B yielded **147** (0.62g, 34%) as an off-white solid mp > 280 °C, IR (KBr) λ_{max} [cm⁻¹] 1678, 2952, 3373, R_f 0.1, ¹H NMR (ppm, CDCl₃) δ 1.05, 1.25 (s, 36H, CMe₃), 3.41 and 3.45 (d, 4H, *J*=13.3Hz, ArCH₂Ar), 4.11 and 4.14 (d, 4H, *J*=13.3Hz, ArCH₂Ar), 4.53 (s, 4H, OCH₂), 6.47 and 8.63 (bs, 4H, NH₂), 6.94 (s,

4H, ArH), 7.07 (s, 4H, ArH), 7.86 (s, 2H, OH), ^{13}C NMR (ppm, CDCl_3) δ 30.9, 31.5, 32.0, 33.9, 34.1, 41.9, 74.5, 125.7, 126.2, 127.0, 132.2, 143.2, 148.2, 148.6, 149.4, 171.2, ESI m/z 785.5 ($\text{M} + \text{Na}^+$), 801.3 ($\text{M} + \text{K}^+$)

Disubstituted p-Tetra-*tert*-Butylcalix[4]arene Acid Derivatives

5,11,17,23-Tetra-tert-butyl-25,27-bis(carboxymethoxy)-26,28-dihydroxycalix[4]arene (148)

70 (2.0g, 2.44mM) was dissolved in ethanol to which 1.2M NaOH (0.24g, 6mM) was added. The mixture was brought to reflux and heating continued overnight. Subsequently, the reaction was cooled, acidified to pH 1 with 50% H_2SO_4 and stirred for 2h. The white solid was filtered, washed with H_2O and dried under vacuum. This was recrystallised in MeOH to result in a white solid, (1.0g, 54%) mp >280 °C, IR (KBr) $\lambda_{\text{max}}[\text{cm}^{-1}]$ 3417, 2952, 1730, ^1H NMR (ppm, CDCl_3) δ 0.99, 1.32 (s, 36H, CMe_3), 3.23 (bs, 4H, ArCH_2Ar), 4.16 (bs, 4H, ArCH_2Ar), 4.54 (bs, 4H, OCH_2), 6.60 (s, 4H, ArH), 7.01 (s, 4H, ArH), 8.00 (bs, 2H, OH), ^{13}C NMR (ppm, CDCl_3) δ 30.8, 30.9, 31.1, 31.4, 31.7, 33.8, 33.9, 125.3, 125.6, 131.9, 142.4, 149.4, ESI m/z 787.4 ($\text{M} + \text{Na}^+$), 803.3 ($\text{M} + \text{K}^+$)

3.4.3 Direct Infusion Mass Spectral Analysis

Using the syringe injector of the mass spectrometer, samples were infused into the ESI source (positive mode) at a rate of $2.5\mu\text{Lmin}^{-1}$. The nebulisation gas and drying gas were set at 15psi and 4Lmin⁻¹ respectively while the source temperature was maintained at 250°C. The octapole voltage was 2.83V, the skimmer 1 voltage was $50 \pm 5\text{V}$ and the trap drive voltage was $57 \pm 2\text{V}$. The scan range covered was typically 500-1500 m/z . Online MS/MS analysis was carried out using an isolation width of 4Da and a collisional amplitude of 1.8-2.3 was used depending on the ion being fragmented. Samples were prepared in acetonitrile to a concentration of 0.1mg/ml.

3.4.4 LC-DAD Analysis

A Varian HPLC system was used to obtain UV-Visible spectra of various components in the reaction mixture. It comprised of a Varian Prostar 330 PDA detector, a gradient Prostar 230 pump and a manually operated switching valve with a 20 μL injector loop. Prior to use, the mobile phase was degassed by sonication. The system was controlled by Varian software. The following parameters were used: Supelco-C18, 250 x 4.6mm, 5 μm column with a mobile phase of 95/5/0.1 v/v/v ACN/ H_2O /Formic Acid, flowrate of 1.5ml/min. The

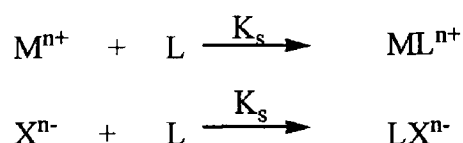
monitoring wavelength was 210nm and an injection volume of 20 μ l was used
Samples were prepared in ACN to a concentration of 0.5mg/ml

4. 'Host-Guest Chemistry' of Partially Functionalised Calix[4]arene Derivatives.

4.1 Introduction

Molecular Recognition is defined as the study of polymolecular entities and assemblies formed between two or more designed chemical species which are held together by noncovalent forces. The formation of a complex by host-guest interactions is one of the most fundamental and important processes in supramolecular chemistry. A molecular host is a species capable of binding another ionic or molecular species with a higher affinity than what is anticipated from their molecular properties. The guest is the substrate that the host will bind to and may include cationic, anionic, or neutral species of organic, inorganic, or biological nature [102,103].

Complexation of a cation (M^{n+}) or an anion (X^{n-}) by a neutral calixarene (L) in a solvent may be represented in its simplest forms as



A range of analytical techniques including spectroscopic (NMR, UV/Vis, MS, fluorescence/ phosphorescence), electrochemical (potentiometry, ISE measurement) and thermodynamic (calorimetry, extraction / distribution) methods has been used to investigate host-guest complexation. The determination methods chosen in these studies were ISE, MS and NMR spectroscopy. A large amount of equilibrium data regarding anion and cation complexation has been obtained in aqueous solution by potentiometry, which is useful as this medium is the one of greatest biological relevance. NMR allows determination of the stability constant and provides information at the molecular level, sites of interaction, conformation of receptor and guest species etc. This is one of the most widely used techniques for determination of complexation in a non-aqueous environment [112].

Computer modelling studies have probed molecular recognition, guest orientation and the role of various weak intramolecular forces. Although difficult to validate computer modelled structures of calixarene complexes, the structures shown have been validated by using X-ray structures as reference data sets.

4.2 Results and Discussion

4.2.1 Determination of Host-Guest Complexation by Ion Selective Electrode Analysis.

Potentiometric Sensors are a principal application of electrochemical transduction involving the use of electrodes to probe the sample and return an analytical signal. An Ion Selective Electrode (ISE) is a membrane electrode that responds selectively to one (or several) ionic species. ISE's are categorised by the type of membrane used i.e. homogeneous membrane electrode, heterogeneous membrane electrode, liquid ion-exchanger electrode and glass electrode. The type chosen for these studies was a liquid ion-exchanger electrode consisting of an ion sensitive solvent polymeric membrane, which is a water-immiscible liquid of high viscosity that is placed between two aqueous phases i.e. the sample and internal reference solution (Fig. 4.1) [168-171].

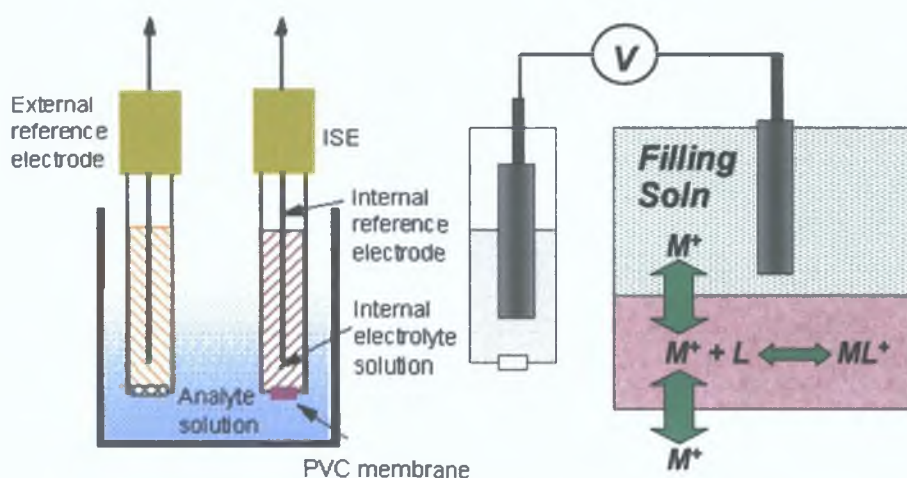


Figure 4.1 Schematic Diagram of an ISE Apparatus

Plasticised PVC remains the standard matrix for carrier based ISE for a number of reasons. PVC introduces elasticity, mechanical stability and also the fortuitous presence of ionic impurities enabling an electrode response. The addition of plasticiser results in lower cell resistance and minimises drift. Plasticised PVC is easily manipulated and used to support the various constituents of the ISE, typically the ionophore (ion-carrier) and an ion exchanger. Ionophores are defined as lipophilic complexing agents capable of reversibly binding ions. They may also catalyse ion transport across hydrophobic membranes. The ion exchanger, a salt of a lipophilic ion complexes to the ion it is sensing and establishes an equilibrium between the ion in the test solution and in the internal reference solution [172,173].

An excess of the ionophore should be maintained to prevent dominance in electrode response by the exchanger, which is responsive to larger ions. The sensor responds to the activity of the target ion and usually covers large sensitivity range, 1 to 10^{-6} M. At the membrane/sample interface, ion exchange equilibrium is established and a potential develops.

Figure 4.2 details the components of an electrode and the actual electrode used for the ISE analysis discussed.

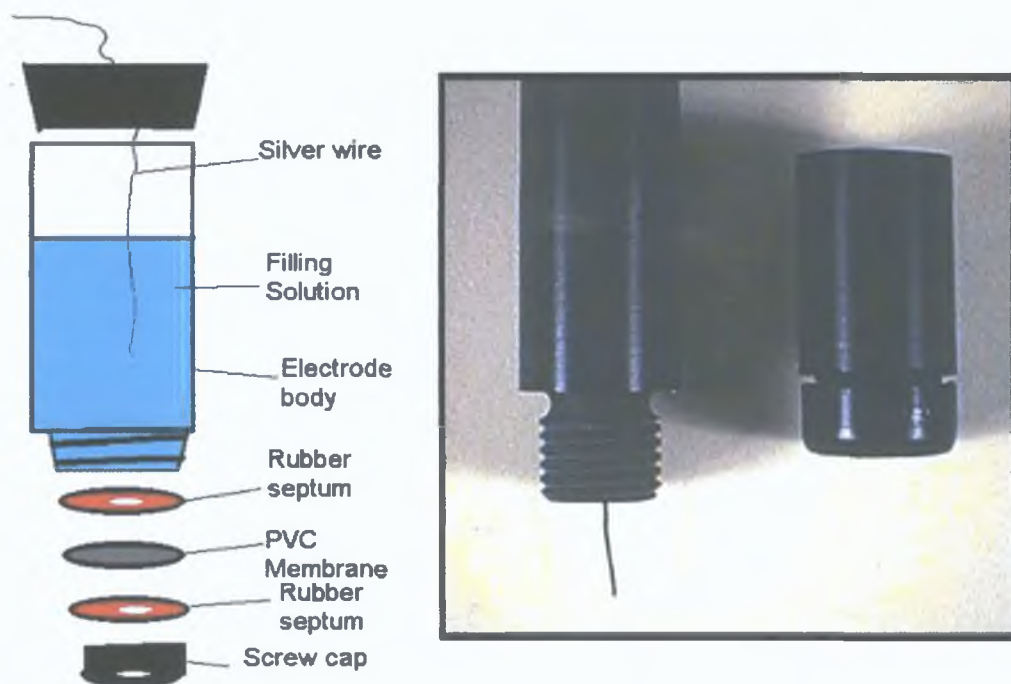


Figure 4.2 *Schematic of an Electrode Apparatus*

The Nernst Equation relates this potential to the activity of the primary ion.

$$E = E^0 + S \log a_i$$

where, E = measured potential in V

E^0 = a standard potential dependent on the entire cell measuring system and temperature but independent of a_i

a_i = activity of species i

S = a prelogarithmic factor (slope of E vs $\log a_i$ curve)

For true Nernstian response its value is $2.303RT/z_iF$ where R is the Gas constant, T is the absolute temperature, F is Faraday's constant and z_i is the charge of the ion. This equation predicts a response of 59.2mV to a decade change in the activity of a monovalent ion at 25°C. The Nikolskii-Eisenmann

equation has quantified the possibility of interfering ions penetrating the membrane and generating an additional response

$$E = E^0 + S \log[a_i + K_{ij}^{pot}(a_j)^{z_i/z_j}]$$

where, a_j = Activity of the Interfering Ion

K_{ij}^{pot} = Selectivity Coefficient

If the selectivity coefficient is less than one, the interfering species has a small effect on the potential whereas if it is greater than one, the interfering species has a large effect [171,173]

The ideal ionophore must

- (a) be capable of selectively binding with the target ion
- (b) should be unresponsive to other cations and anions
- (c) should preferentially be retained within the membrane phase
- (d) be able to diffuse freely in the direction of the potential gradient across the membrane
- (e) have a moderately large stability constant to ensure reversibility
- (f) have fast and reversible kinetics, of ion transfer between aqueous and membrane phases and of complexation with the ligand

Encompassing these criteria, calixarenes were proven to be effective ionophores due to their relative ease of chemical modification in terms of the nature and 3d arrangement of binding sites. Calixarenes functionalised with carbonyl containing ligating groups possess rigid cavities that are predisposed to selectively complex with cations, have rapid complexation-decomplexation kinetics for fast, reversible transduction processes, have high lipophilicity due to the non-polar tert-butyl groups at the upper rim ensuring retention of the ionophore and its complexed analogue from leaching from non-polar membranes into aqueous solutions [108,168,174]

4.2.1.1 ISE Analysis of 5,11,17,23-Tetra-*t*-butyl-25-(ethoxycarbonyl methoxy)-26,27,28-trihydroxycalix[4]arene (**140**) and 5,11,17,23-tetra-*t*-25,27-(bisethoxycarbonylmethoxy)-26,28-dihydroxycalix[4]arene (**70**)

The response of all four electrodes, a blank, mono-(**140**), di- (**70**) and tetraester (**143**) to differing NaCl concentrations, 10^{-6} to 1M is shown in Figure 4.3. The blank electrode was prepared with exclusion of the ionophore but with all of the other constituents in the membrane including the ion exchanger, Potassium tetrakis(4-chlorophenyl)borate (KTPClPB). This was to demonstrate that the potential response was due to the complexing abilities of the ionophore rather than the ion exchanger.

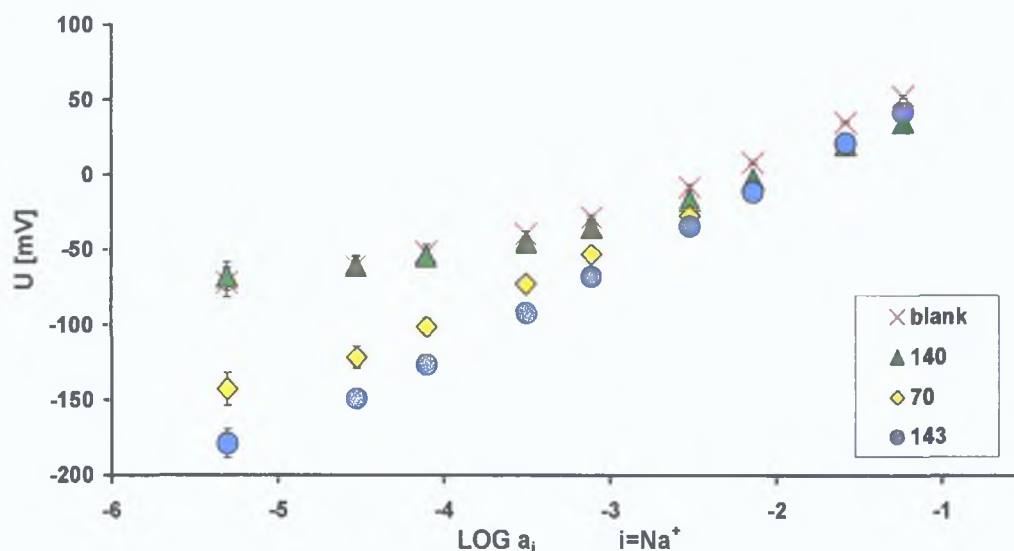


Figure 4.3 Response to sodium in the absence of any possible interferents

As anticipated, **143** exhibited a Nernstian response of 58.3mV per decade whereas the response profile of **70** was similar to that of **143** but with a slightly reduced slope. The potential response of **140** was almost identical to that of the blank electrode, exhibiting no affinity for Na^+ . To investigate the size selectivity of these ligands in particular, **70** to sodium, a series of calibrations was carried out in the presence of fixed interferents, 10^{-1} M LiCl, KCl and CsCl. Figure 4.4 shows the response of the four electrodes to sodium in a constant background of 10^{-1} M LiCl.

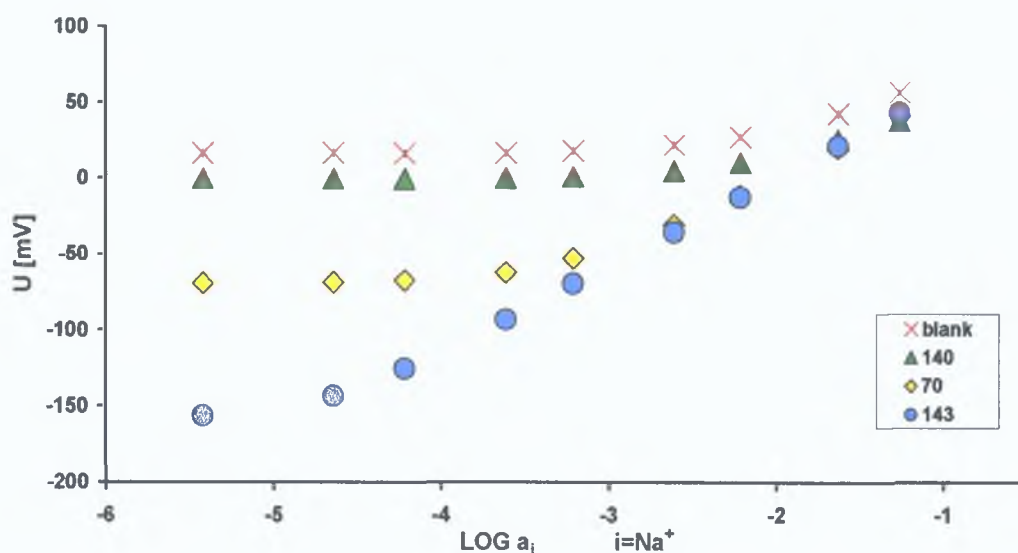


Figure 4.4 Response to sodium in the presence of 0.1M LiCl

Compound **143** has sufficient selectivity for Na^+ to remain almost unaffected by the Li^+ ions (tetraester slope of 56.22mV). **70** responds to Na^+ from a concentration of 10^{-3}M upwards in the presence of Li^+ implying that **70** exhibits selectivity to Na^+ , ~ 100 fold. Successive screening of **140** to Na^+ in such interferent backgrounds as Li^+ , K^+ and Cs^+ indicated that there was no selectivity or indeed response of **140** to any cations studied. These results suggested that the ion exchanger dominated the response of **140** and that **140** is a weak complexing agent. With a constant background of 10^{-1}M KCl and 10^{-1}M CsCl, the superior selectivity of **143** is evident whereas the selectivity of **70** to Na^+ , in the presence of larger cations, K^+ or Cs^+ is eliminated. This is apparent from Figure 4.5, where the potential response of **70** to Na^+ , in the presence of K^+ or Cs^+ resembles that of the blank electrode response. With such interferent ions as the alkaline earth metal cations, Ca^{2+} or Mg^{2+} , **70** exhibited good selectivity for Na^+ . Due to the insignificant response of **140** to the metal ions tested, ISE studies focussed on the remaining disubstituted derivatives prepared.

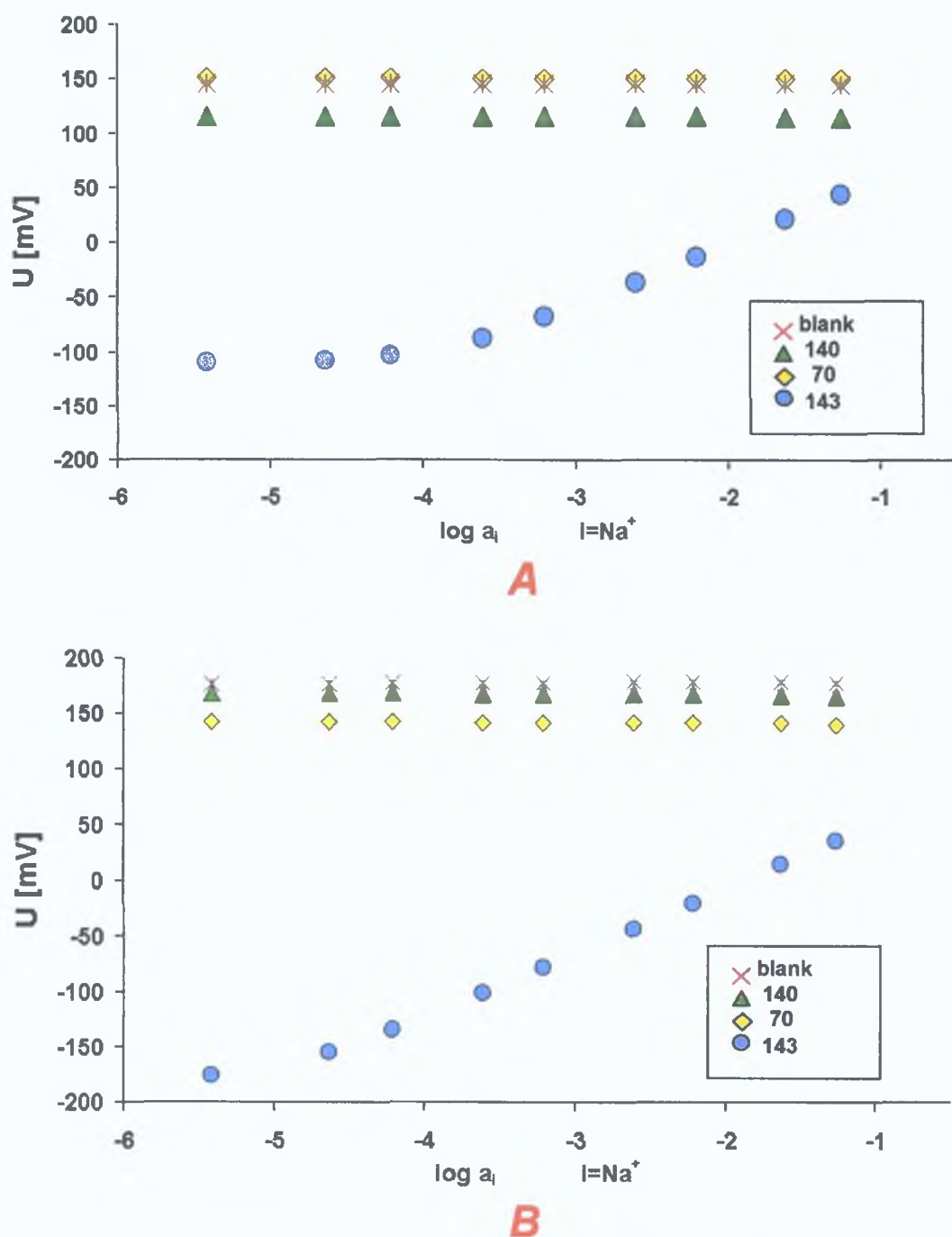


Figure 4.5 Response to Sodium in the presence of 0.1M KCl (**A**) and 0.1M CsCl (**B**)

The sensitivity difference exhibited by the partially substituted calix[4]arene derivatives in the MS and the ISE studies to Na^+ may be attributed to the shape of these derivatives. To confirm this, molecular modelling studies were performed. The 3D structure of calix[4]arene complexes has been previously studied within this group and have been validated using X-ray structures as

reference data sets. We were therefore confident that these structures are a reasonable approximation of the true geometry of the complexes. For **143**, the Na^+ ion is perfectly held in the centre of an octahedral cavity defined by the four phenoxy oxygen atoms at the calix[4]arene lower rim and the four carbonyl oxygen atoms of the ester ligating groups. **70** has a much more open structure than **143**. The Na^+ ion is held within the cavity by association with the phenoxy atom. Due to the greater flexibility of **70** it can accommodate the larger K^+ ion. For the larger ions the carbonyl oxygen atoms take an active role in complexation. Complexation of **140** with Na^+ is very weak which was attributed to the one ligating group failing to form a semi-enclosed cavity at the lower rim. Molecular modelling studies of the resultant complex indicates that the Na^+ ion associates more with the negative charge density of the aryl groups than the phenoxy oxygen atoms, thus explaining the relative weakness of the interaction compared to that of **70** and **143**- Na^+ complexes (Fig. 4.6) [175].

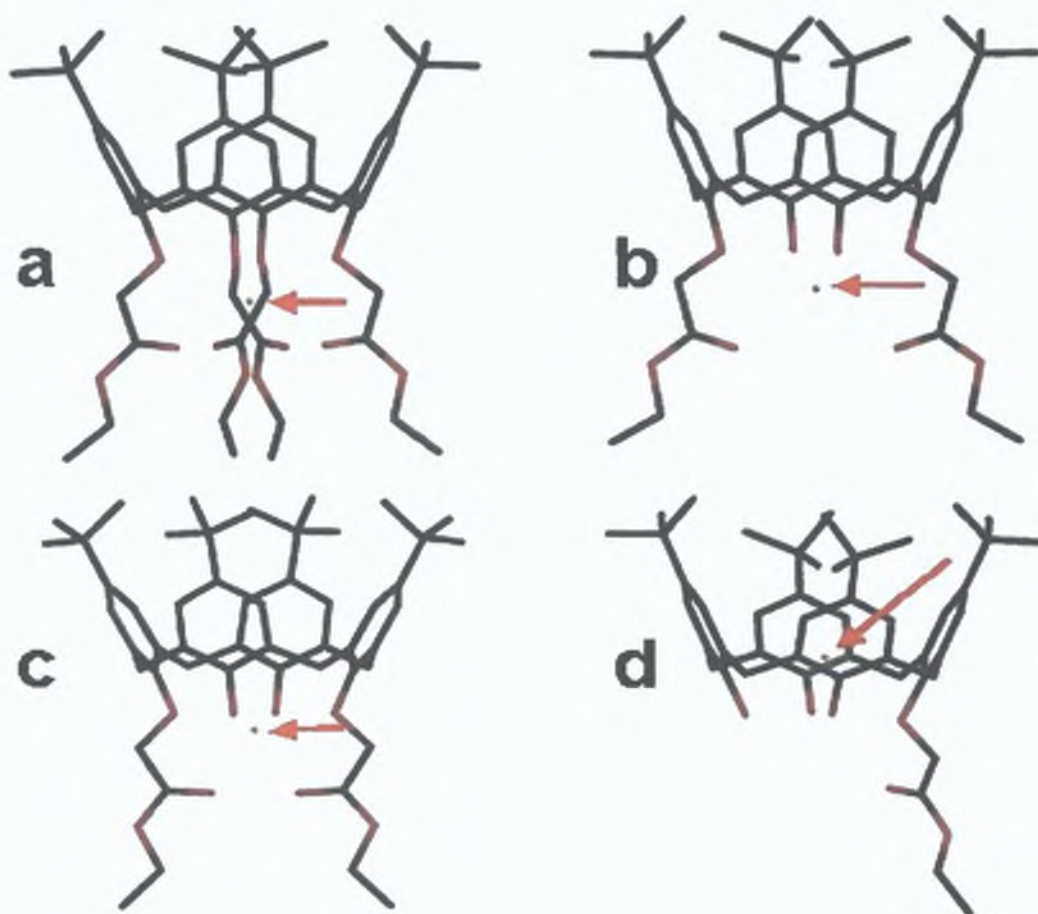


Figure 4.6 Energy minimised structures for **143**- Na^+ complex (a), the **70**- K^+ complex (b), **70**- Na^+ complex (c), and **140**- Na^+ complex (d). Position of cation indicated by arrow.

4.2.1.2 ISE Analysis of 5,11,17,23-Tetra-*tert*-butyl-25,27-bis(aminocarbonylmethoxy)-26,28-dihydroxycalix[4]arene (**147**) and 5,11,17,23-Tetra-*tert*-butyl-25,27-bis(carboxymethoxy)-26,28-dihydroxycalix[4]arene (**148**)

These two derivatives were incorporated into PVC membranes and screened for cations (due to their size and shape) and anions (due to the availability of hydrogen bonding). Both species, **147** and **148** exhibited no significant potential response to the cations (Na^+ , K^+ , Cs^+) tested with results comparable to that of the blank electrode (Fig. 4.7).

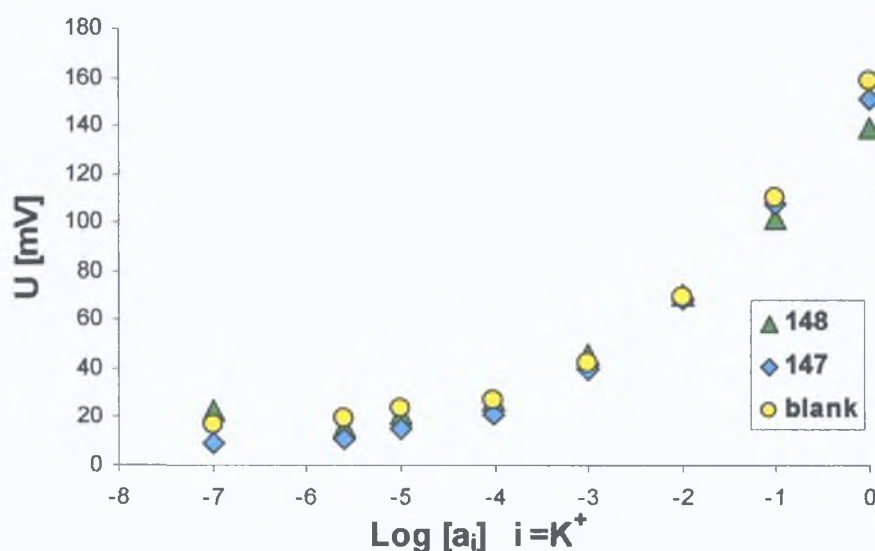


Figure 4.7 Response of **147** & **148** to Potassium in H_2O

Extraction studies have indicated that the tetracarboxylic analogue of **148** forms a stable complex with cations and extracts them efficiently [134, 176]. Whereas four such acid tails may encapsulate the cation and hold it in place, two such tails enhances flexibility and thus, may not form a rigid cavity to maintain encapsulation of the cation as observed for **70**. The hydrogen bonding stabilising influence at the lower rim between the phenoxy protons, the carbonyl oxygen, carboxylic acid proton and the phenoxy oxygen atoms may be disrupted upon complexation with a metal cation. The complexing abilities of *p*-*t*-butyldiacid with a wide range of anions encompassing spherical (Cl^- , I^-), trigonal planar (NO_3^-) and tetrahedral (H_2PO_4^- , HPO_4^{2-}) was investigated. There was no potential response of the **148** to any of the anions tested.

A positive response was observed for **147**. Even though there is little difference in the strength of hydrogen bonding between **147** and **148**, the shape of the lower rim cavity differs. The trigonal planar arrangement of the C-NH₂ and the two amide protons may facilitate encapsulation and complexation of an anion, by holding it in the cavity by a circular array of four amide protons and two phenolic protons that may hydrogen bond to the enclosed anion. The v-shaped arrangement of -C-O-H may not facilitate encapsulation as readily as **147**. The size of the cavity of **147** is slightly bigger than that for **148** due to the extra two protons, which may affect complexation.

From the spherical anions tested, **147** showed a sensitive response to I⁻ and Cl⁻ from 10⁻⁶M and 10⁻⁵M upward, (slope: -64mV and -55mV) respectively.

For NO₃⁻, a change in potential response of **147** occurred at 10⁻⁵M and was linear up to 10⁻¹M with a Nernstian response of -60mV. Compound **147** did not exhibit a sensitive response to the tetrahedral sulphate anion as a sub-Nernstian response of -27mV was obtained.

It is evident from these electrochemical studies that **147** is sensitive to such anions as the spherical, trigonal planar and tetrahedral shaped anions. The broad responses of **147** to a range of anions imply that selective discrimination of anions by **147** is improbable.

4.2.1.3 ISE Analysis of 25,27-(bisethoxycarbonylmethoxy)-26,28-dihydroxycalix[4]arene (**145**)

Exploratory ISE studies of **145** were carried out to investigate the effect if any, the tert-butyl groups at the upper rim may exert on complexation.

There was no Nernstian potential response of **145** to Li⁺, Mg²⁺ or Ca²⁺ while a small potential electrode response to Na⁺ was observed.

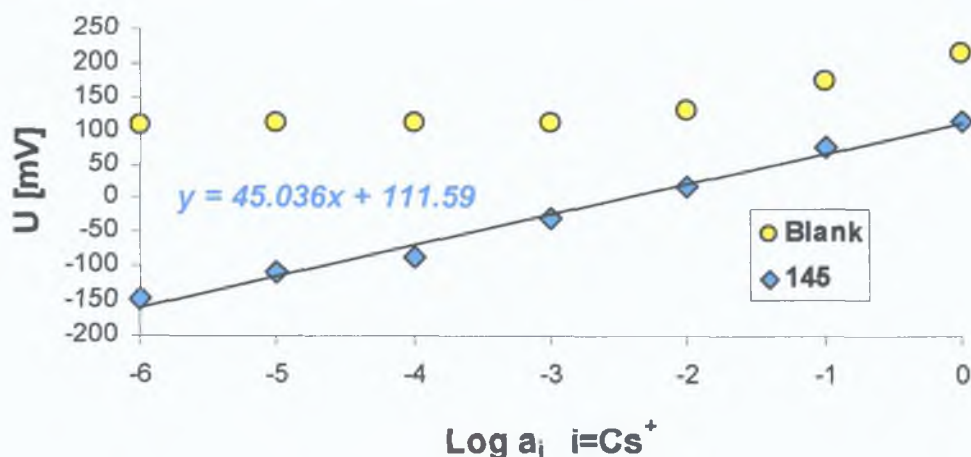


Figure 4.8 Response of **145** to Caesium in H₂O

A sub-Nernstian response to K^+ and Cs^+ , slope of 45.8 and 45mV was observed (Fig. 4.8 & 4.9).

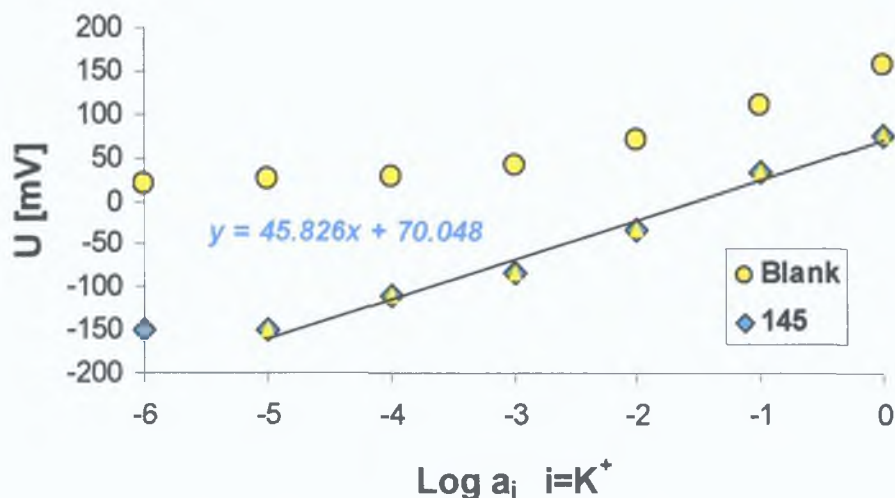


Figure 4.9 Response of **145** to Potassium in H_2O

These studies were repeated using two different discs from the same master membrane to ensure reproducibility and verification of the observed trend. Removal of the tert-butyl groups reduces the steric strain of **70**, enabling greater conformational freedom and generates a larger cavity at the lower rim that was demonstrated by basic ISE studies to complex larger cations (K^+ and Cs^+). As a Nernstian response was not obtained for **145** to group 1 and 2 metal ions, further selective ISE studies were not carried out.

Such was the nature of this work that basic exploratory ISE studies were only carried out to determine if the calix[4]arene derivatives synthesised were useful receptors for cation or anion guests.

4.2.2 Determination of Host-Guest Complexation by NMR Titration

The advantage of using NMR spectroscopy for binding studies is that it can provide information on the complex structures formed and supply several signals for the independent evaluation of stability constants. When the NMR method is applied to the study of complexation phenomena, two physical properties, chemical shift (δ) and relaxation time (T_1) are mainly concerned. To use chemical shift data, at least one site in both the free and complexed molecules must give significantly different chemical shifts. In a titration experiment, the stepwise addition of a varying concentrated solution of a cation/anion salt to a

dilute solution of a host in a deuterated aprotic solvent may result in either a large significant change in chemical shifts of the receptor protons or the evolution of a new set of resonances corresponding to a complexed species. Such a complexation-induced shift (CIS) is frequently observed when hydrogen bonding and/or inclusion with an aromatic ring are associated in the complexation [112,177]

4.2.2.1 ¹H NMR Coordination Studies of 5,11,17,23-Tetra-*tert*-butyl-25,27-bis(aminocarbonylmethoxy)-26,28-dihydroxycalix[4]arene (**147**)

The hydrogen bonding support available at the lower rim of **147** may facilitate anion complexation. A range of anions with differing shapes, spherical or tetrahedral, and varying stoichiometry, (0.25, 0.5, 0.75, 1, 2, 3, 4, 5) to a constant ratio of host (1) was tested [178].

Upon complexation, the ligating tails of the lower rim and the unsubstituted phenol subunits will experience a change in environment, expressed by a change in chemical resonances of the appropriate protons. **147** possesses a pseudo-tetrahedral cavity, with two short tails i.e. the unsubstituted phenol subunits and two longer tails i.e. O-CH₂C(O)NH₂ which may facilitate complexation of tetrahedral anions.

Addition of an equal stoichiometry of Br⁻ and I⁻ resulted in insignificant changes in the resonance of the two-amide protons and the phenolic proton, typically 0.006 ppm. Coordination studies of **147** suggested that it was indifferent to such large spherical guests as Br⁻ or I⁻ but favours the smaller spherical anion, Cl⁻, indicating that the size of the guest rather than shape predominates the coordination ability of the host with the halides. The amide protons were shifted downfield by 0.07, 0.09 and 0.17 ppm upon addition of 0.25, 0.5 and stoichiometric ratio of the chloride salt (Fig. 4.10). Addition of stoichiometric amounts of Cl⁻ i.e. 2 or 3 molar equivalents induced a change in chemical shift for one amide protons indicative that this proton is in closer proximity to this greater electron density and hence, is deshielded further downfield than the other amide proton.

In the gas phase, the association constants for a given complex are expected to increase in the order of Cl⁻ > Br⁻ > I⁻. For such solvents possessing weak anion-solvating properties, e.g. acetonitrile, the 'gaslike' conditions are approached and

the stability constants vary as predicted by the elementary electrostatic theory ($\text{Cl}^- > \text{Br}^- > \text{I}^-$) [112].

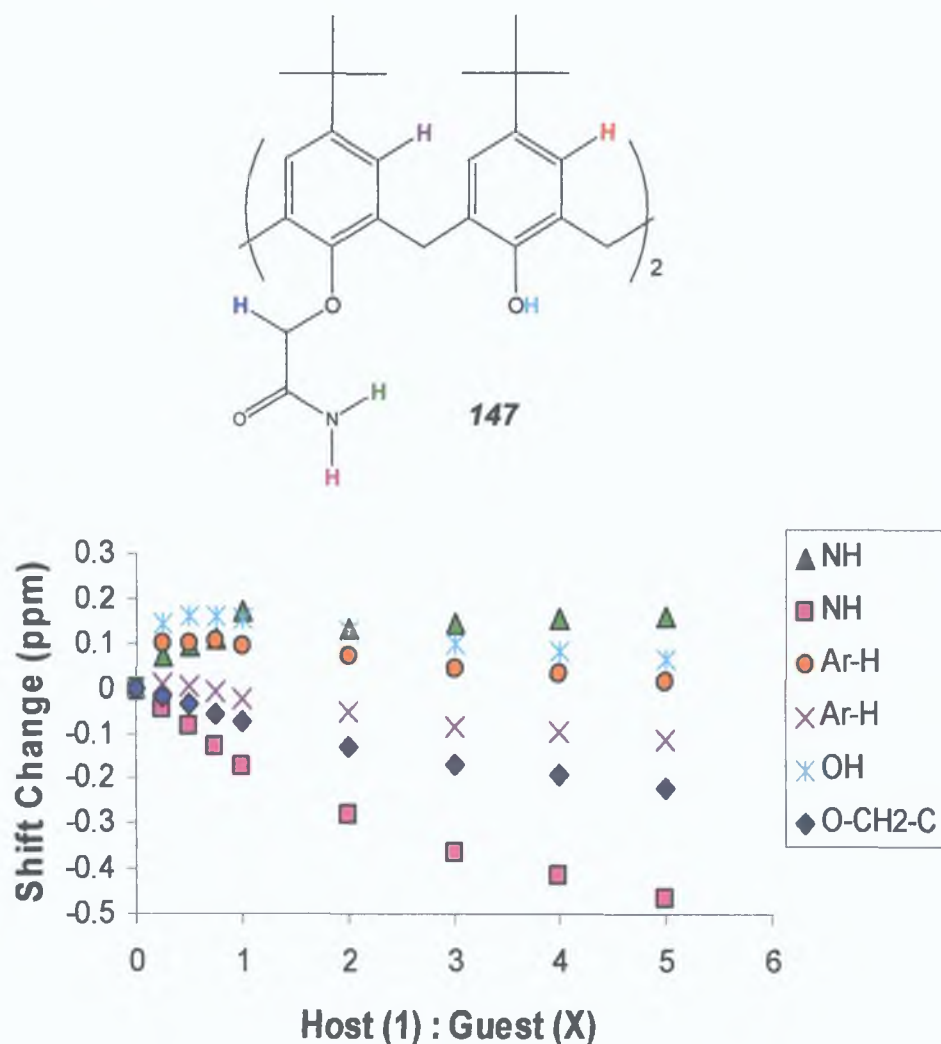


Figure 4.10 Schematic Diagram and Chemical Shift Change of **147** upon addition of stoichiometric amounts of $(\text{Et})_4\text{N}^+\text{Cl}^-$

The host **147** exhibited complexing ability to the trigonal planar, NO_3^- as a 1:1 host:guest stoichiometry induced a chemical shift change of 0.23 and 0.2ppm for the amide protons. The phenolic proton experienced a downfield shift of 0.15ppm while the methylene protons of the ligating tails were shifted upfield by 0.09ppm. The substantial change in chemical shift of the amide and phenolic protons in comparison to the methylene protons was suggestive that hydrogen bonding stabilises complexation, as the amide and phenolic proton can hydrogen bond to the electronegative oxygen atoms of the anion whereas the methylene protons do not participate in complexation. Complexation of the host to the anion

enriches the electron density at the lower rim of the host, causing the obligatory deshielding effect on the phenolic and amide proton

The most significant response of the coordination studies of **147** was with the tetrahedral anions, H_2PO_4^- or HSO_4^- in accordance with the pseudo tetrahedral binding site at the lower rim (*Fig 4 11*) Upon addition of an equal amount of the salts of H_2PO_4^- and HSO_4^- , a downfield chemical shift change of 0.53 and 0.75ppm of the amide proton was observed respectively. The other amide proton was shielded upfield by 0.16 and 0.38ppm suggestive that the arrangement in space of the amide protons facilitates a strong interaction of one amide proton with the guest and little interaction for the other amide proton. The shape of the titration plots shown in *Fig 4 11* elude to a 1:1 complex with HSO_4^- due to the regular chemical shift change of the amide proton up to 1:1 stoichiometric ratio and little successive chemical shift change of 2 or more equivalents of salt. With H_2PO_4^- , there was a constant regular change in chemical shift upon addition of 0.25 to 5 equivalents suggestive of non-stoichiometric interaction.

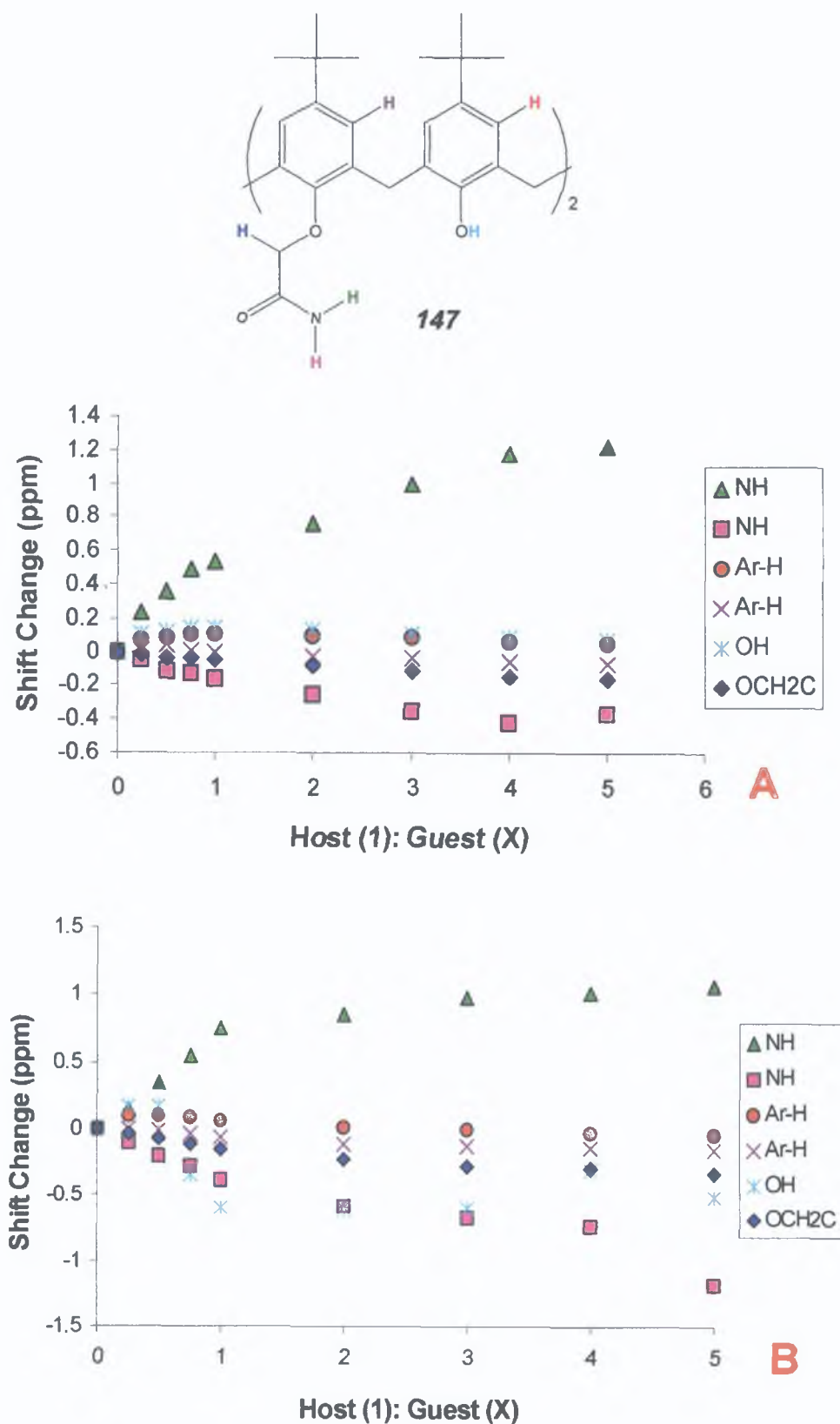


Figure 4.11 Chemical Shift Change of 147 upon addition of stoichiometric amounts of (Et)₄N⁺H₂PO₄⁻ (**A**) and (Et)₄N⁺HSO₄⁻ (**B**)

There is a range of non-covalent interactions to consider when discussing anion coordination. Electrostatic attraction is the driving force in anion complexation by positively charged receptors. For neutral receptors, electrostatic attraction between ions and permanent dipoles is weaker than ion-ion interactions. Consequently ion-dipole interactions in solution are easily hindered by competitive interaction with solvent molecules, especially in polar solvents where alignment of its dipole moment with the dipolar functionalities reduces their binding ability. Thermodynamic data for association via hydrogen bonding are not generally available. Consequently, the strength of these bonds is commonly discussed in terms of bond distances, physical properties such as vibrational changes in IR and chemical shifts in ^1H NMR spectroscopy, all of which are connected, within certain limits, with the strength of the interaction.

The upfield δ_{OH} shift of the 1:1 complex with H_2PO_4^- suggested that the geometrical shape of the host and anion does not facilitate stabilisation of the resulting complex by hydrogen bonding. Non-stoichiometric interactions were observed, upon addition of a two- to five-fold excess of guest, dramatic shifts of amide and phenolic protons (0.6–1.1 ppm) still occurs.

Reinholdt et al. designed a neutral receptor with hydrogen bond donor-acceptor and/or Lewis acid character that may mimic the extensive array of hydrogen bonding interactions found in natural anion binding proteins [57]. A range of calix[4]arene sulfonamides, **136b** (Fig. 4.12) was prepared and resulted in binding constants of up to $10^3,400\text{M}^{-1}$ with significant selectivity for HSO_4^- over Cl^- and NO_3^- . In the ^1H NMR spectrum the NH absorption has been shifted from δ 6.90 (free ligand) to δ 7.75 (complex). This striking result was attributed to the combination of a hydrophobic calix[4]arene cavity and an array of approximately preorganised amide functionalities which functionally mimic protein anion binding environment.

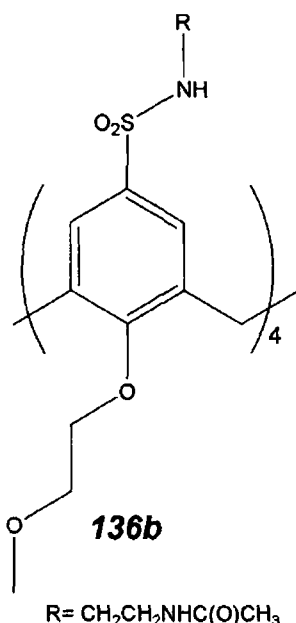


Figure 4 12 A Calix[4]arene Sulphonamide, a Neutral Anion Receptor

The predominant interactions available for this type of host, **147** are hydrogen-bonding interactions. ^1H NMR coordination studies of **147** have concluded that **147** does exhibit a degree of selectivity i.e. it will either complex with a guest (Cl^- , H_2PO_4^- , NO_3^- , HSO_4^-) or not (Br^- , I^-). The host guest complexes formed with the aforementioned salts, typically the 1 : 1 complex exhibited a chemical shift change ranging from 0.3 to 0.7 ppm. The complexed anion may lock the calixarene into a 'cone' conformation by complexing to the carbonyl oxygen donor atoms, the amide N-H acceptor atoms and the phenolic oxygen atoms. The chemical shift change is indicative of complexation.

4.2.2.2 ^1H NMR Coordination Studies of 5,11,17,23-Tetra-*tert*-butyl-25,27-bis(carboxymethoxy)-26,28-dihydroxycalix[4]arene (**148**)

This molecule adopts a 'pseudo' tetrahedral binding site but conformational rotation and rapid exchange is occurring as evident by the broad signals obtained in the ^1H NMR spectrum. The hydroxy proton of the acid ligating tail and the phenoxy proton are weak and broad due to the exchange processes and are not particularly evident in the ^1H NMR spectrum. Upon addition of an anion, the chemical resonance frequencies of the aromatic, methylene linker and methylene protons of the ligating tails may undergo a change in chemical shift, suggestive of a complexation process between host and guest.

A 1 : 1 stoichiometry of host : guest, where the guest was Br^- incurred a change 0.02-0.15 ppm for the aromatic protons, 0.1 ppm for the methylene protons of the

ligating tail and 0.2 ppm for the methylene linker protons. The trend of a small chemical shift change was observed upon addition of I^- to the **148**. The smaller spherical anion, Cl^- evoked an interesting response (Fig 4.13). The complexation of **148** to Cl^- was apparent by the change in δ , typically 0.2–0.3 ppm. This change in δ was indicative of complexation. Upon addition of Cl^- to the **148**, the broad peaks of the host sharpen to form narrow peaks, suggestive that the addition of the guest, Cl^- locks the host into a 'cone' conformation, thus reducing conformational flipping, sharpening the proton signals.

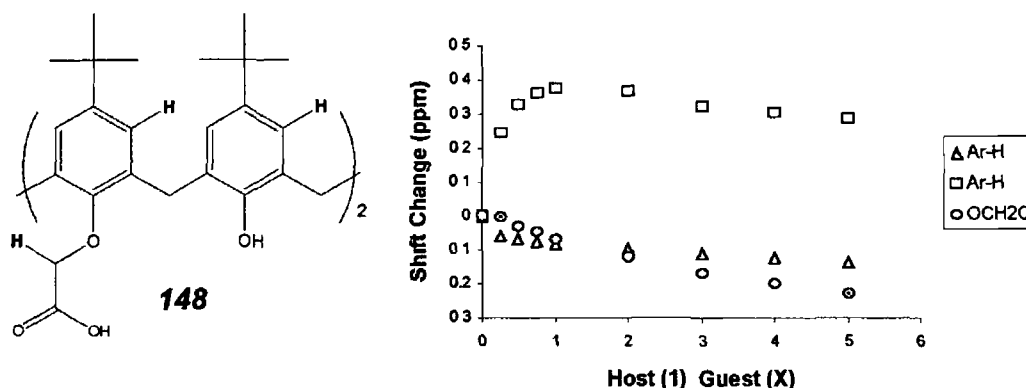


Figure 4.13 Chemical Shift Change of **148** upon addition of stoichiometric amounts of $(Et)_4N^+Cl^-$.

1H NMR spectrum of **148** with such tetrahedral anions as $H_2PO_4^-$ and HSO_4^- did not induce a great response with typical shift changes between 0.05 and 0.1 ppm for the methylene protons of the appended ligating groups upon addition of 1–3 molar excess of $H_2PO_4^-$ and HSO_4^- . There was a greater change in electronic environment of the axial proton than their equatorial proton counterparts due to the close proximity of the former protons to the lower rim. A similar chemical shift change was observed upon addition of HSO_4^- indicating that there was very little coordination occurring. These results concur with the results obtained by ISE analysis.

4.2.2.3 ¹H & ¹³C NMR Coordination Studies of 5,11,17,23-Tetra-*tert*-butyl-25,27-bis(ethoxycarbonylmethoxy)-26,28-dihydroxycalix[4]arene (**70**)

Previous complexation and molecular modelling studies on **70** support the theory that a metal cation is encapsulated at the lower rim by complexation with the ethereal and carbonyl oxygen atoms. Therefore resonance signals of the methylene (CH₂), methyl (CH₃) and phenolic protons should theoretically shift upon complexation, due to a change in their electronic environment. Titration of **70** with Na⁺ showed a change in chemical shift of the aforementioned proton resonance frequencies. Addition of an equimolar amount of a Na⁺ salt resulted in a change in resonance of ~0.5 ppm for the protons of the ligating tails while a shift change of 0.02 ppm for the phenolic proton. The protons of the substituted phenol subunit undergo a subtle shift change of 0.026 ppm whereas a shift change of ~0.001 ppm, typically within experimental error was observed for the proton signals of the unsubstituted phenol subunits (Fig. 4.14). A 1:1 **70**:Li⁺ stoichiometry incurred an upfield shift of 0.35 ppm for the methylene protons of the ligating tail alpha to the carbonyl and ethereal oxygen and 1.03 ppm for the methylene protons of the ligating tail alpha to the carbonyl group of the ester functionality. The axial proton closer in proximity to the lower rim were shifted upfield by 0.38 ppm whereas there was insignificant changes of chemical shift for the equatorial proton, typically 0.001 ppm.

¹³C NMR titrations were carried out to determine if the resonance frequency of the carbon atoms of the ligating groups were shifted. It was reasoned that if complexation occurred between the cation and the ethereal or carbonyl oxygen atom, the chemical environment of these carbon atoms should alter. This change in environment may be more profound for the ethereal and carbonyl carbon atoms rather than the methyl and methylene protons of the ester functionality.

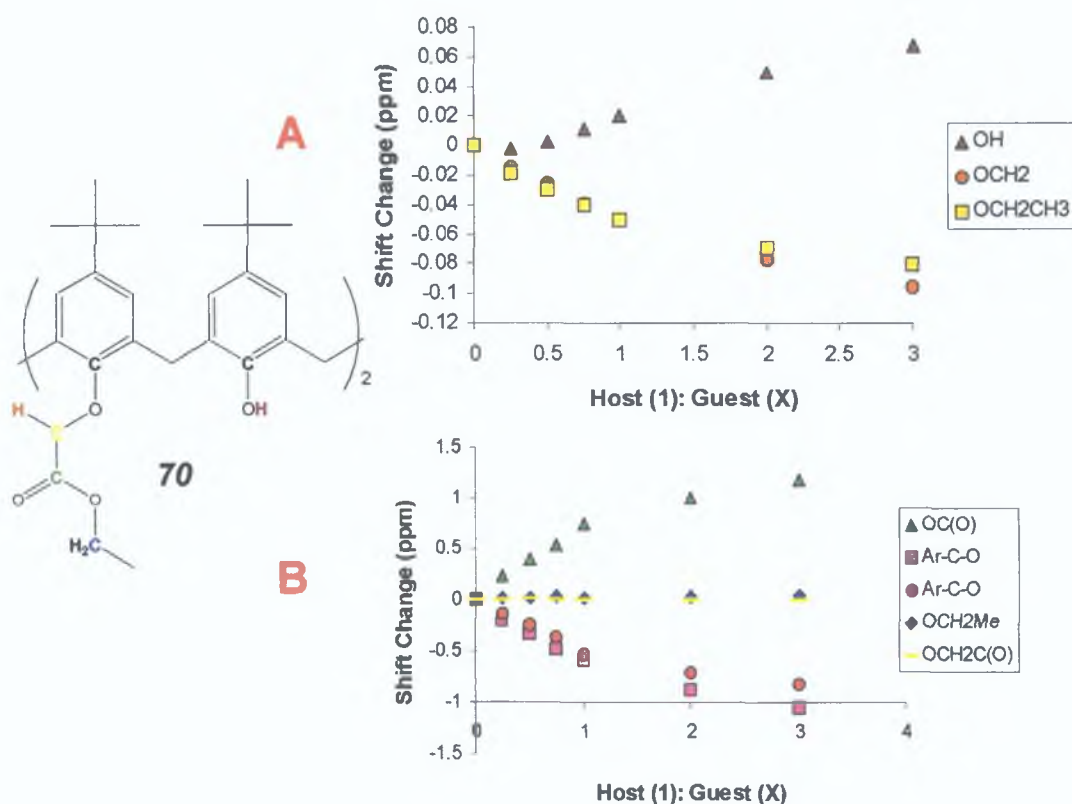


Figure 4.14 ^1H (A) and ^{13}C (B) NMR Titration of **70** and NaSCN

A stoichiometry of 1:0.25 of **70**:Na⁺ incurred a δ change ranging from 0.15-0.23ppm for the carbonyl carbon and the phenoxy carbon. An equimolar stoichiometry of host:guest invoked a δ change of 0.6-1.0ppm for the aforementioned ^{13}C signals (Fig. 4.14). It was apparent from ^{13}C NMR titrations of **70**:Na⁺ that complexation occurred proximally to the ethereal and carbonyl oxygen atoms. Upon addition of stoichiometric amounts of Na⁺, the chemical shift of some carbon atoms, those of the phenoxy and carbonyl carbon atoms continue to change, < 0.4ppm, suggestive that a 1:1 complexation is not occurring.

4.2.2.4 ^{13}C NMR Coordination Studies of 25,27-bis(ethoxy carbonylmethoxy)-26,28-dihydroxycalix[4]arene (**145**)

^{13}C NMR titrations of **145** with Group I metal ions led to some significant results. The 1:0.25 stoichiometric ratio of **145**:Na⁺ induced a δ change of 0.38, 0.57 and between 0.8-0.9ppm for the methylene carbon alpha to the carbonyl and ethereal oxygen, the carbonyl carbon and the quaternary phenoxy carbon. A 1:1

stoichiometry substantially changes the chemical shift by 0.75, 1.41 and between 1.8-2.0ppm for the previously stated carbon signals.

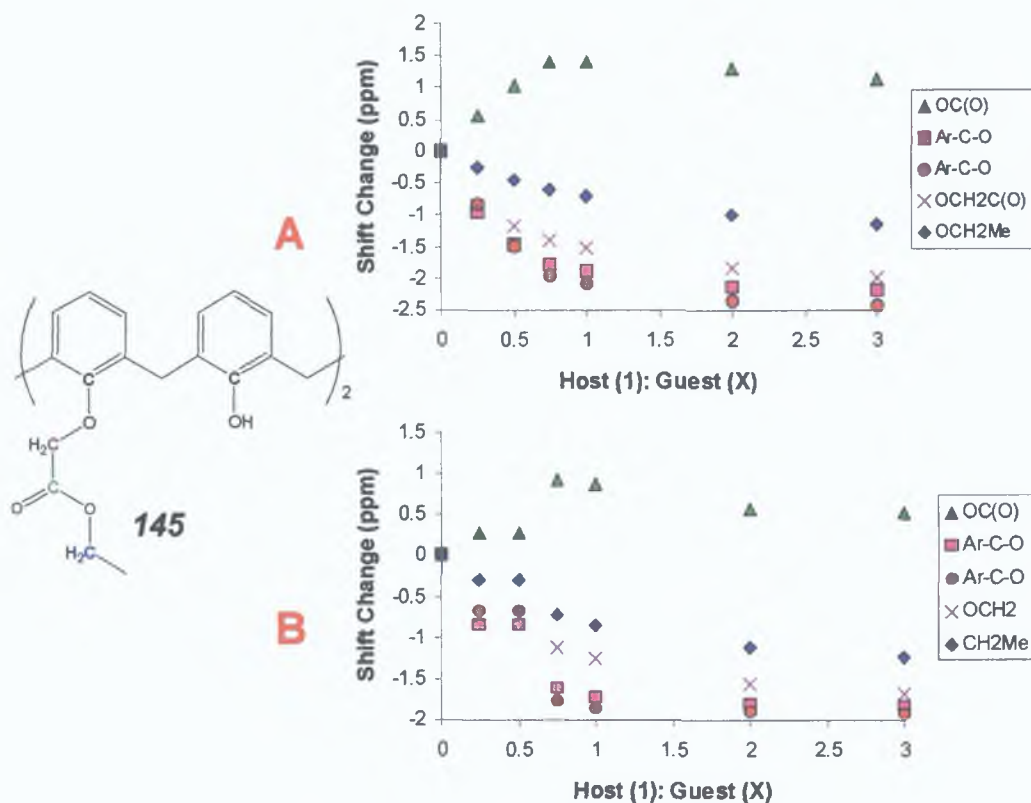


Figure 4.15 ^{13}C NMR Titration of **145** with Na^+ (A) and Li^+ (B)

The NMR titration studies precluded to a complexation to Li^+ and Na^+ as such dramatic downfield changes in resonance frequencies of 0.5-1.8ppm for a 1:1 **145** : Li^+ (Fig. 4.15 B) and 0.87-2.0ppm for a 1:1 **145** : Na^+ complex (Fig. 4.15 A). No significant change in chemical shift was observed for the titration of calix[4]arene diester with K^+ , with typical changes of 0.001-0.008ppm with increasing increments of K^+ (0.25, 0.5, 0.75, 1, 2, 3) suggestive that the change was within experimental error.

The complexation of a calix[4]arene derivative with a given guest is controlled by solvation. The choice of solvent was important as CDCl_3 stabilises the host by hydrogen bonding *exo*- to the cavity whereas CD_3CN is polar enough to solvate the ion and the use of a polar aprotic solvent eliminates the hydration sheath of the ion, rendering it 'naked' and susceptible to complexation [159].

4 2 3 Determination of Host-Guest Coordination

(Potentiometry V NMR Spectroscopy)

Potentiometry can be used to obtain reliable information on stability constants. Where spectroscopic and thermodynamic techniques for the determination of complexation often require special and sophisticated equipment, a considerable quantity of sample, and complicated computer-fitting programs, ISE measurement offers a more rapid and facile method for determining complexation. For ISE analysis, it is the induced membrane potential changes that are used as the basis of signal transduction. There are several established principles for discrimination at the membrane surfaces. Such principles involve

- (1) Potentiometric discrimination based on hydrogen bonding
- (2) Charged group interaction with specific functional groups present on the host
- (3) Shape discrimination arising from steric interaction between the targeted guest and the 'walls' of the receptor sites

In the case of NMR, the experimentally measurable parameters (chemical shift, coupling constants) depend on the NMR sensitive nuclei and their chemical environment as well as the exchange reaction rates occurring between them. The mode of NMR complexation is dependent on a number of factors including (a) a sufficient length of time may be required, complexation may not be instantaneous and (b) solvent dependency. A non-polar protic solvent aids the stabilisation of the host while a polar aprotic solvent may solvate the guest while eliminating the hydration sheath of the ion, rendering it 'naked' and susceptible to complexation.

Wherever possible, it is desirable to use more than a single experimental technique to quantitatively characterise solution equilibria. DI-MS results of **70** suggested that it was sensitive for Na^+ ion. This observation was reaffirmed by potentiometric analysis using ISE, **70** was proven as a sodium selective binding ionophore when in a competing ionic background of Li^+ / Mg^{2+} / Ca^{2+} . Molecular modelling studies hypothesised the complexation of a cation occurs by encapsulation at the lower rim and is held within the cavity by interaction with the phenoxy and carbonyl oxygen atoms at the lower rim. ^1H NMR titration studies was not sensitive to subtle changes of the ligating tails whereas ^{13}C NMR demonstrated small changes in the chemical environment of the binding

functionalities **70** does not reorganise itself greatly upon binding as it is quite open and flexible in structure

A strong hydrogen bonding effect accounts for the observed shift in NMR and electrochemical response, as the amide protons feel the deshielding effect of the electronegative anions present in the cavity while both techniques conclude that **148** is unresponsive to binding with the chosen ions studied

While both techniques yielded precise and accurate information on complexation behaviour, differing experimental conditions affect complexation behaviour, thus they may not be readily compared. In general, complexation phenomena are studied and stability constants determined by various physical methods including spectroscopic, electrochemical and thermodynamic methods. As stability constants have been determined in different solvents and by different methods, they cannot be readily compared [112,177,179]

4.3 Conclusion

A series of partially functionalised calix[4]arene derivatives, with pendant acid, amide or ester functionalities at the lower rim was synthesised. Their selectivity for group I and II metal ions and an array of differentially shaped anions was assessed by NMR and ISE measurements.

Principally, the ISE data of the partially substituted calix[4]arene esters explained the relative sensitivity of MS to these derivatives. Molecular modelling has assisted the rationalisation of the observed selective ion-binding behaviour. Compound **70** produces sensors that exhibit Nernstian behaviour with a number of ions. ISE analysis indicated that **147** was responsive to spherical, trigonal planar and tetrahedral anions, displaying little discrimination between differing geometries of the anions. **148** exhibited little affinity for any ion tested.

Comparison of the ISE analysis of **70** and **145** indicated they had different affinities for the cations tested. **70** exhibited a Nernstian response to Na^+ but the selectivity of this derivative to Na^+ , in the presence of larger cations, K^+ or Cs^+ is lost. Removal of the *t*-butyl groups imparts greater freedom to the cavity, resulting in greater accommodation of larger cations as manifested in the ISE studies of this derivative. **145** did not display any affinity for Li^+ , Na^+ ions but exhibited a sub-Nernstian response to K^+ or Cs^+ . Removal of the *t*-butyl groups of **70** resulting in **145**, does not influence the complexation behaviour of these two derivatives as the cavity is large enough to accommodate such larger cations as K^+ or Cs^+ .

^1H NMR titration studies indicated that **147** complexes to tetrahedral anions with no apparent affinity for spherical guest species. Compound **148** was verified by both techniques to exhibit no profound affinity for any ion tested.

The complexation of **70** and **145** to a metal ion results in the movement of the ligating tails, in order to accommodate the ion. ^{13}C NMR titration studies were more sensitive to the change in chemical environment than ^1H NMR. **145**-Metal complexation was confirmed by these titrimetric studies.

4 4 Experimental

4 4 1 General

Melting points are uncorrected ^1H and ^{13}C NMR spectra were recorded on a Bruker 400MHz and 100MHz Spectrometer using CDCl_3 as solvent unless stated otherwise HPLC grade Acetonitrile was purchased from Sigma-Aldrich

4.4 2 Direct Infusion Mass Spectral Analysis

Using the syringe injector of the mass spectrometer, samples were infused into the ESI source (positive mode) at a rate of $2.5\ \mu\text{Lmin}^{-1}$. The nebulisation gas and drying gas were set at 15psi and $4\ \text{Lmin}^{-1}$ respectively while the source temperature was maintained at 250°C . The octapole voltage was 2.83V, the skimmer 1 voltage was $50 \pm 5\text{V}$ and the trap drive voltage was $57 \pm 2\text{V}$. The scan range covered was typically 500-1500m/z. Online MS/MS analysis was carried out using an isolation width of 4Da and a collisional amplitude of 1.8-2.3 was used depending on the ion being fragmented. Samples were prepared in acetonitrile to a concentration of 0.1mg/ml.

4 4 3 Molecular Modelling

All molecular modelling calculations were carried out using Spartan software, SGI version 5.0.1 running on a Silicon Graphics workstation with a MIPS R10000 Rev 2.7, 195-MHz CPU, an IRIX operating system (release 6.3) and 128 MB of RAM. Geometry optimisations were carried out with the Merck Molecular Force Field (MMFF) until the terminating gradient of $1 \times 10^{-5}\ \text{kcal mol}^{-1}\ \text{\AA}^{-1}$ was reached. Partial charge surface maps based on extended Huckel calculations were generated using Chem-3d Pro (CambridgeSoft, Cambridge, MA, USA) after importing the energy minimised molecular coordinates.

4 4 4 NMR Titration Experiments

^1H and ^{13}C NMR titration experiments were carried out in a $\text{CDCl}_3/\text{CD}_3\text{CN}$ mixture at 298K using a constant host concentration of 5mM and a varying guest concentration of 1.25-25mM. The salts used, MClO_4 where $\text{M}=\text{Li}^+, \text{Na}^+, \text{K}^+$ and Et_4NA where $\text{A}=\text{Cl}, \text{Br}, \text{I}, \text{HSO}_4, \text{NO}_3, \text{HSO}_4, \text{HPO}_4^{2-}$ were of analytical grade, supplied by Sigma Aldrich.

4 4 5 Preparation of Electrodes

All membrane components with the exception of the calixarene compounds were, 'Selectophore'® grade obtained from FLUKA Chemicals. Metal nitrates were also

obtained from FLUKA and were of the 'puriss p a' standard or higher. Ultra Pure water from a Barnstead EASYpure water purification system was used throughout. A double junction calomel electrode was used as the reference electrode, with the outer junction containing saturated KNO_3 and the inner reference containing saturated KCl. All measurements were carried out at $25^\circ\text{C} \pm 0.5^\circ\text{C}$. Voltages were captured using an MIO-16 National Instruments data acquisition card, using an in-house developed virtual instrument (LabVIEW version 4.0, National Instruments, Austin, Texas) after impedance conversion. All PVC membranes used were fabricated using the method of Diamond et al. The ionophore (10 mg) and potassium tetrakis(4-chlorophenyl)borate (KTPClPB) ion exchanger (2 mg) were dissolved in 1g plasticiser (o-nitrophenyl octyl ether, o-NPOE). To this solution 500 mg high molecular weight PVC was added and stirred to give a thick slurry. Tetrahydrofuran (THF) was then added to the slurry slowly, with stirring until a clear solution was obtained. This solution was stirred for one hour to ensure thorough mixing. The membranes were then cast in glass rings (28mm i.d.) fixed on a glass plate and allowed to set overnight, loosely covered to allow for slow evaporation of the THF. From this master membrane, small discs were cut using a cork borer. Electrodes were prepared by clipping these discs into conventional ISE bodies containing Ag/AgCl wires as the internal reference.

Four electrodes were prepared with 0.1M NaCl internal filling solution: one with the monoester, one with the 1,3-diester, one with the tetraester, and one blank membrane with no ligand in the membrane (all other membrane components including KTPClPB were present in the amounts mentioned above). Sodium calibrations were carried out for all four electrodes with no interfering background to begin with, and then fixed interference studies were carried out in 10^{-1} M LiCl, KCl, CsCl, CaCl_2 and MgCl_2 .

**5. *Synthesis of a Calix[4]arene
Derivative possessing a ‘Tetrahedral’
Binding Site.***

5 2 Introduction

Calix[4]arenes, the well-known family of macrocyclic compounds frequently serve as molecular platforms for the construction of more elaborate supramolecular systems, such as various receptors possessing interesting complexation abilities towards target ions or molecules

The target ions or molecules we are interested in are those possessing a tetrahedral shape or geometry, for example, ammonium (NH_4^+), phosphate (PO_4^{3-}), or sulfate (SO_4^{2-}). Recognition of such tetrahedral ions as NH_4^+ has been obtained by complexation with the spherical macrocyclic cryptands, which contains four suitable binding sites at the corners of a tetrahedron. The NH_4^+ ion is encapsulated into the cavity of **138** (Fig 5 1) and is held by a tetrahedral array of $\text{N}^+ \cdots \text{H} \cdots \text{N}$ hydrogen bonds and by electrostatic interactions with six oxygen atoms [102,103,139]

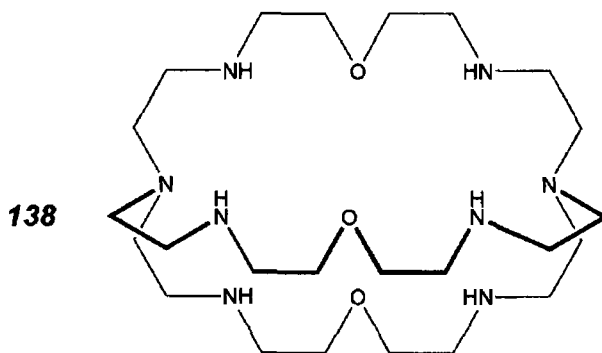


Figure 5 1 Structure of a Cryptate Molecular Receptor for NH_4^+

Such receptors as **150** bearing three guanidinium units have been shown to bind PO_4^{3-} in aqueous solution with a rather low affinity ($\log K_s = 2.4$). Open-chain polyamines, for example spermidine (**151**) that bind phosphate anions in water at neutral pH, most likely adopt a flexible extended conformation whereas polyprotonated azacrown ethers (**152**) possess a more rigid structure with greater charge density and thus, a greater predisposition to binding [180-183]

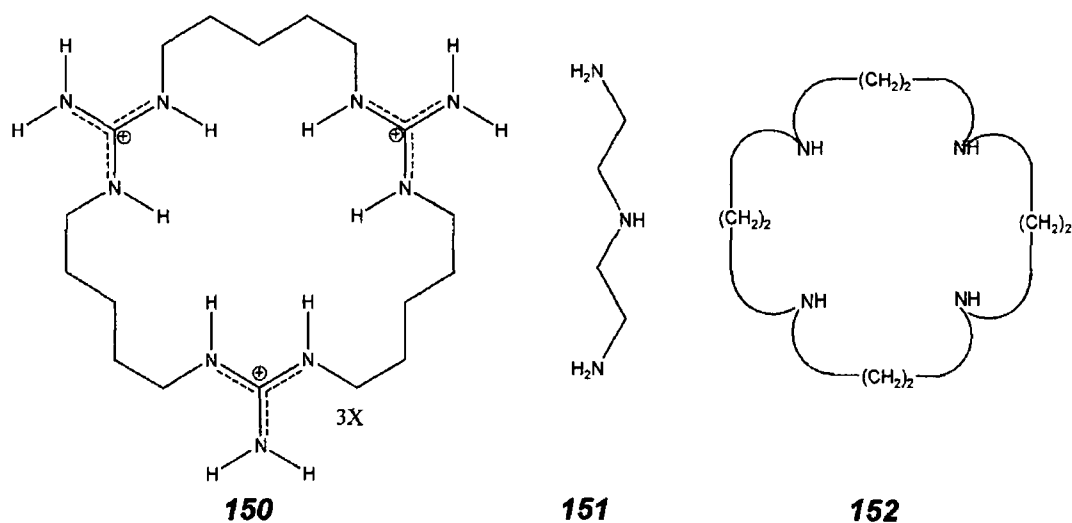


Figure 5 2 Structures of varying Anion Receptors

Calix[4]arene receptors for tetrahedral ions or molecules include the water soluble rigid cone peptidocalix[4]arene which complexes to benzyl trimethyl ammonium cations (*Fig 5 3*) [184]

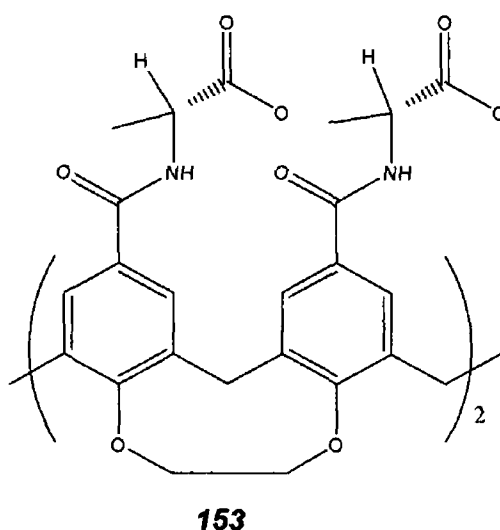


Figure 5 3 Structure of a Peptidocalix[4]arene

A Ru(II)-bis(bipyridine) complex of calix[4]arene, bridged at the lower rim with bipyridine units showed selectivity for dihydrogen phosphate over halides. Electrochemical studies on this receptor confirmed binding of the anion within the amide cavity. The advantage of appending charged Ru(II) or Rh(I) bipyridine units offers a number of sensing opportunities through electrochemical or luminescence methods. A marked cathodic shift of 175mV was observed for H_2PO_4^- , which was unaltered by the addition of a ten-fold excess of Cl^-/Br^- anions,

offering the possibility of selectively sensing H_2PO_4^- binding by cyclic voltammetry (Fig 5 4) [185,186]

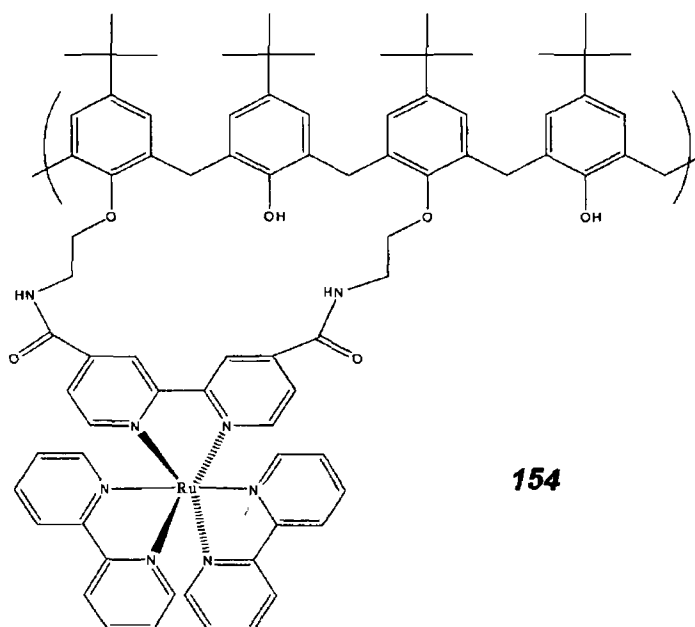


Figure 5 4 A Ru(II)-bis(bipyridine) Calix[4]arene complex

The objective of this part of the research was to synthesise an ion or molecular receptor with a tetrahedral spatial distribution of binding sites compared to the symmetrical tetrasubstituted calix[4]arenes that have been previously studied

A ligand employing tetrahedral coordination, 1,10-phenanthroline-2,9-bis(phenyl-2-acetic acid) was reported by Parker et al which may coordinate to zinc in preference to nickel (II), copper (II) and iron (III) by employing an L_2X_2 donor set (Fig 5 5) [190]

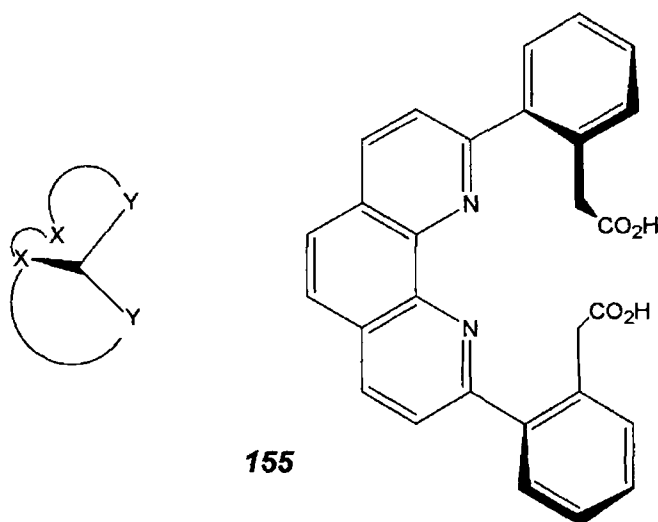


Figure 5 5 Diagrammatic representation of L_2X_2 binding geometry

To achieve this novel low symmetrical *p*-tetra-*t*-butylcalix[4]arene bearing a 'tetrahedral' pocket at the lower rim, the spacer units in the 1 and 3 positions of the calix[4]arene must be different in length than the spacer units in the 2 and 4 positions. This preorganisation of the binding sites may lead to preferential complexation with tetrahedrally shaped guest ions or molecules that have complementary charge distribution, leading to a new pattern of selectivity for the corresponding ion or molecular sensors.

Calix[4]arenes bearing a tetrahedral arrangement of binding sites is incredibly novel (Fig 5.6), with no known examples in literature and thus, presents a challenging synthesis.

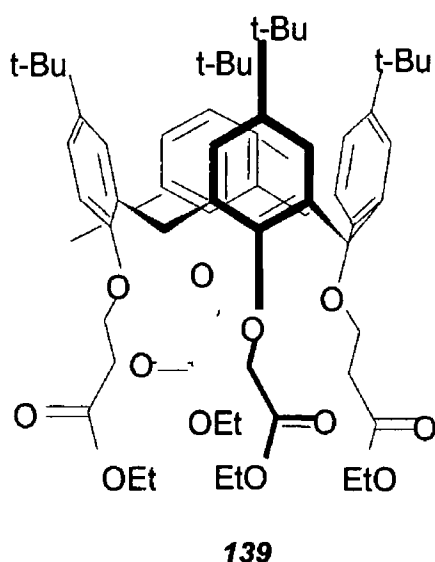


Figure 5.6 Schematic diagram of **139**

5.2 Results and Discussion

The synthetic route chosen was the alkylation of the *p*-tetra-*t*-butylcalix[4]arene-(1,3)-diethyl ester precursor (**70**) in the remaining 2 and 4 position with a longer chained ligating group that contains an extra methylene spacer group, ethyl-3-bromopropionate.

The solvent chosen was DMF as it readily solubilises the reactants but the choice of base remained problematic.

The general reaction sequence for functionalisation of **70** in the 2 and 4 position is that of two deprotonation steps, to form the phenoxide anion followed by nucleophilic attack on the electropositive carbon of the ethyl 3-bromopropionate (Fig 5.7) resulting in a differentially tetrasubstituted calix[4]arene derivative.

Due to hydrogen bonding at the lower rim between the ester ligating tails and the phenolic hydroxy groups, it was not known if a weak base would facilitate

deprotonation or if a strong base such as sodium hydride (NaH) would deprotonate the remaining 2 and 4 positions

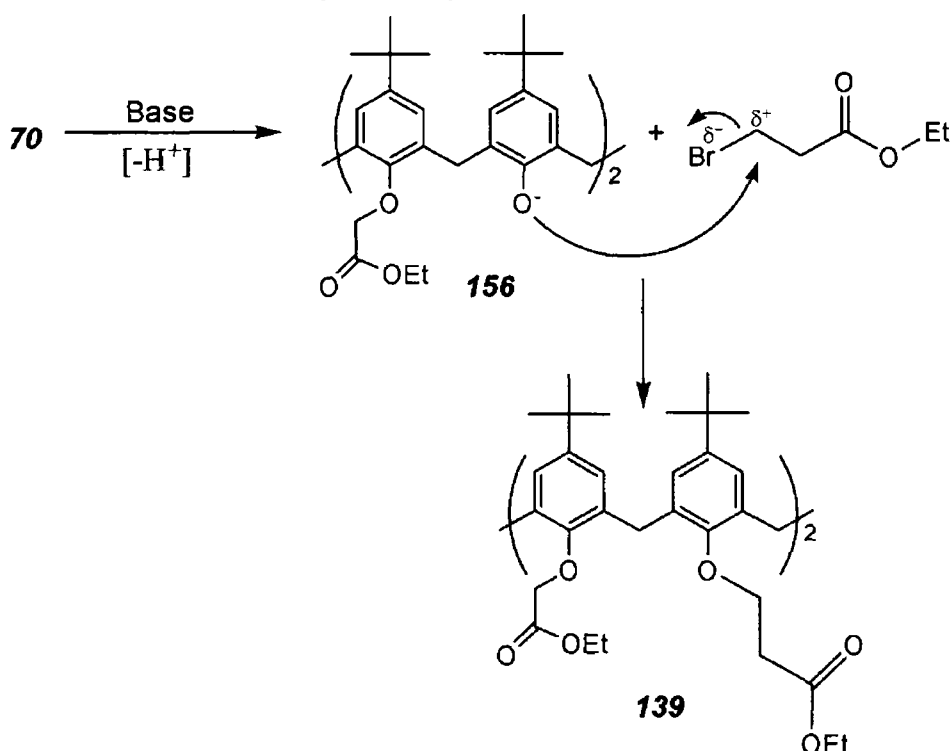


Figure 5 7 Functionalisation of the lower rim of 70

A procedure outlined by Cobben et al, detailed the reaction conditions that functionalised a disubstituted calix[4]arene in the 2 and 4 position. The reaction stoichiometry employed was a 10 molar and 15 molar excess of base and alkylating agent respectively, heated at 60-70°C for 24h. Subsequently, an extra aliquot of base and alkylating agent was added and heated for a further 24h [27].

Various bases were tested ranging from weak to strong basic character encompassing hindered and organic bases (Table 5.1). A range of metal carbonate bases, including Li⁺, Na⁺ and K⁺ carbonates was tested to investigate a potential 'metal template' effect, i.e. if a metal could exert an influence over the product distribution of this reaction.

Another experimental approach explored was the Michael Addition. The Michael Addition involves the nucleophilic addition of carbanions to α,β-unsaturated compounds, resulting in the formation of C-C bonds (Table 5.1).

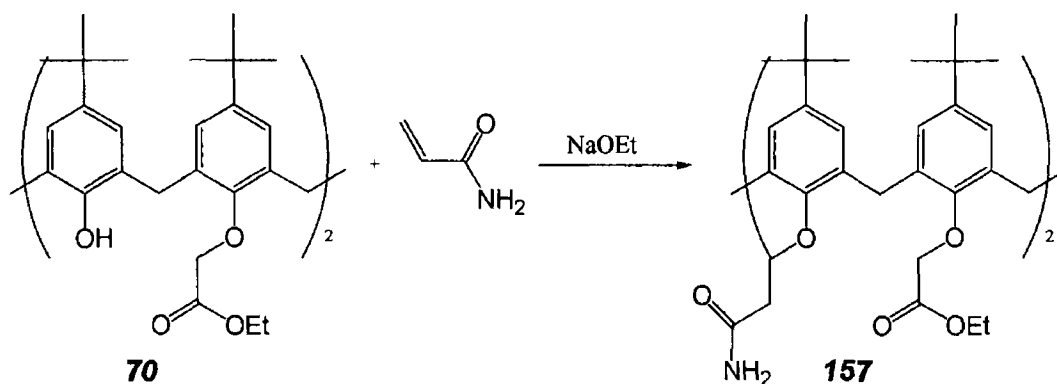


Figure 5 8 Reaction Scheme for the Michael Addition of **70** and Acrylamide

5 2 1 Use of Metal Carbonate Base

As previously stated, metal carbonate bases, M_2CO_3 where $\text{M} = \text{Li}^+$, Na^+ or K^+ were tested. The Li^+ ion is known to complex to tetrameric derivatives enforcing a 'cone' conformation. Due to the possibility of lower rim rotation through the annulus of the unsubstituted phenol, Li_2CO_3 was chosen as the base which could potentially yield a tetrasubstituted calix[4]arene locked into a 'cone' conformer ideal for complexation. Reaction A employing Li_2CO_3 was tested by TLC ~ every 24h. TLC at 48h indicated that unreacted **70** was present in the reaction mixture. It was thought that the addition of excess base and alkylating agent as the reaction progressed would be necessary to afford the tetrasubstituted derivative, **139**. Therefore, an extra aliquot of Li_2CO_3 and ethyl 3-bromopropionate was added and allowed to react for a further 72h. The LC chromatogram exhibited three peaks eluting at 8.92, 13.82 and 14.35 min. DI-MS gave 6 peaks (m/z), 787, 803, 815, 831, 843, 859.5Da indicative of 5,11,17,23-tetra-*t*-butyl-25,27-bis(carboxymethoxy)-26,28-dihydroxycalix[4]arene (**148**), 5,11,17,23-Tetra-*tert*-butyl-25-(ethoxycarbonylmethoxy)-27-(carboxymethoxy)-26,28-dihydroxycalix[4]arene (**160**) and **70** (sodiated and potassiated).

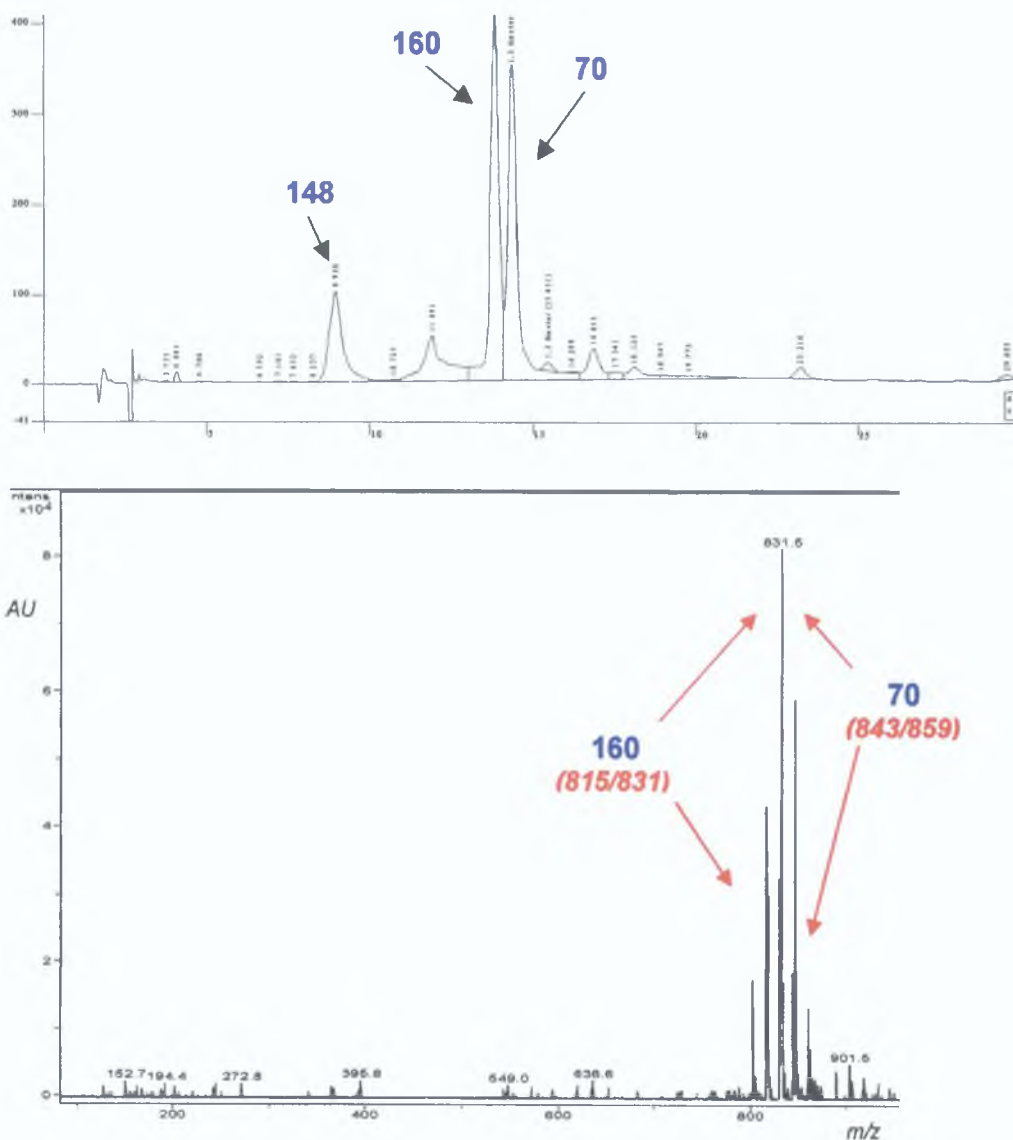


Figure 5.9 LC Chromatogram and DI-MS of crude product of Reaction A

Reaction B was carried out as for reaction A but Na_2CO_3 was chosen as base. DI-MS of the reaction product gave two ion peaks of 843.5 and 859.5Da, ($820 + \text{Na}^+/\text{K}^+$) indicative that **70** was unreacted. MS and ISE studies of **70** confirmed that it is selective for Na^+ , almost comparable to that of **143**. Thus, upon dissociation of Na_2CO_3 in DMF to form Na^+ and CO_3^{2-} ions, **70** may complex to the Na^+ ions forming a stable $[\text{70}][\text{Na}^+]$ complex, rendering CO_3^{2-} free to deprotonate.

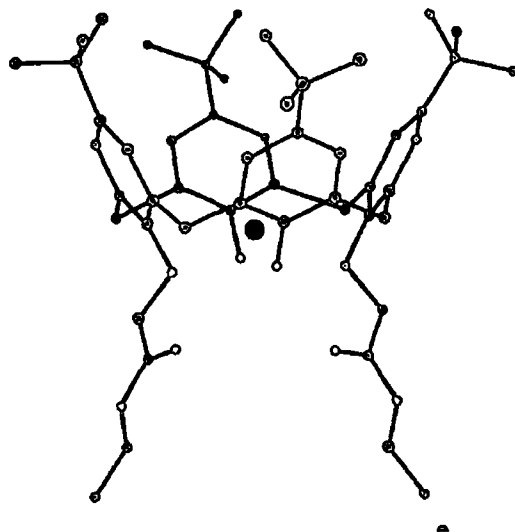


Figure 5 10 *Molecular Modelling Studies of 70 with Li⁺*

Molecular Modelling studies of **70** suggested that the Li⁺ ion, positioned quite high in the cavity, interacts strongly with both the substituted and the unsubstituted phenol subunits. A strong interaction of the two unsubstituted phenol subunits with Li⁺ may hamper the 'lower rim through the annulus rotation', thus reducing the number of conformations whilst encouraging a 'cone' conformation (*Fig 5 10*) [175]. Thus, Li₂CO₃ was chosen as base in order to synthesise the target derivative in a 'cone' conformation.

Na₂CO₃ was also tested in this reaction but both Li₂CO₃ and Na₂CO₃ resulted in a monoester, monoacid derivative (**160**) and **70**.

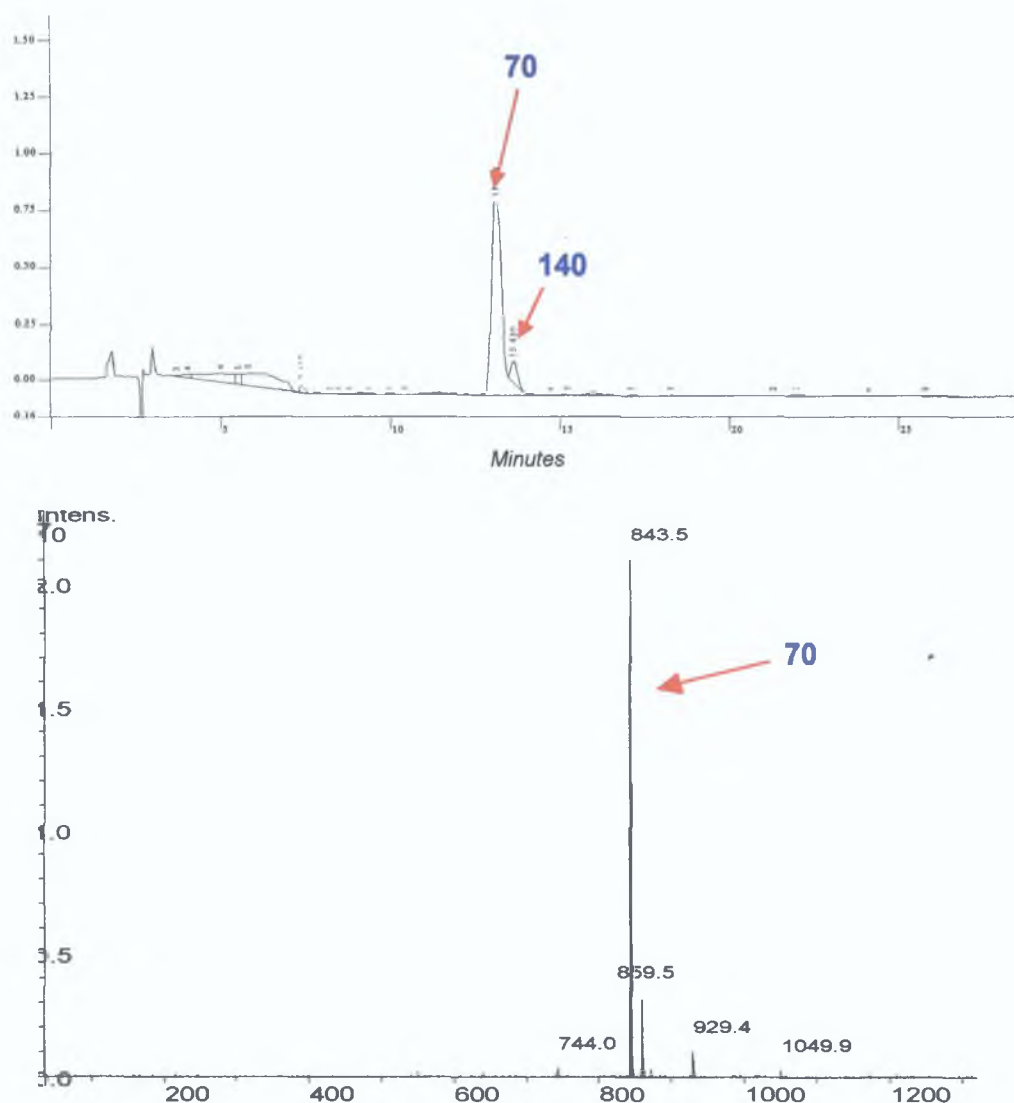


Figure 5.11 LC Chromatogram and DI-MS of Crude Product of Reaction B

K_2CO_3 was chosen as base for reaction C and was carried out as reaction A. A cream yellow solid was obtained that gave m/z ion peaks of 815.4, 831.4, 843.4 and 859.5Da indicative of two products recovered - **70** and an unidentified reaction product. This crude product was columned using 1:1 hexane:ethyl acetate as eluent, yielding two pure products. The first product to elute was identified as **70** while the second product to elute, gave an m/z ion peak of 815.4 and 831.4Da, correlating to a derivative with a molecular weight of 792.4 + Na^+/K^+ respectively, which correlates to **160**. The 1H NMR spectrum exhibited three doublet systems at δ 3.36, 4.02 and 4.22ppm, with an integration of 4H:2H:2H. There were two types of axial protons of the methylene linker protons, that of the proton proximal to an unsubstituted phenol subunit and an

ester ligating tail, 4.22 ppm, that of the proton adjacent to an unsubstituted phenol subunit and an acid ligating tail, 4.02 ppm. The equatorial protons, predominantly influenced by the aromatic shielding effect cannot distinguish between the different chemical environment at the lower rim and hence, a doublet with an integration of 4H was observed. Two singlets represent the methylene protons of the ligating tails at 4.57 and 4.61 ppm. Both DI-MS and ^1H NMR spectroscopy had confirmed that partial hydrolysis of **70** had occurred, affording **160** (Fig 5.11)

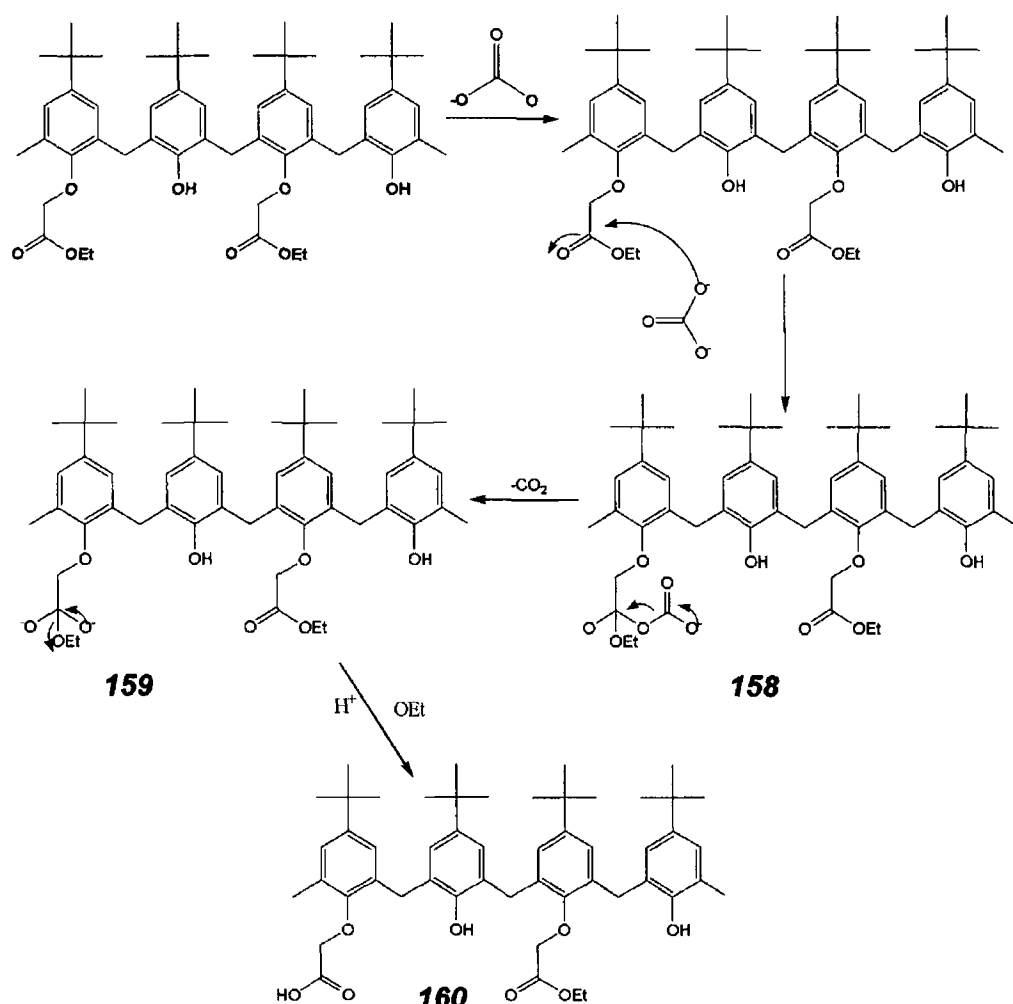


Figure 5.12 Proposed Reaction Mechanism for Partial Hydrolysis of **70**

Possible explanations for the synthesis of this derivative may be partial hydrolysis by (a) attack of CO_3^{2-} group at the carboxyl group of the ester to result in a tetrahedral intermediate (**158**) which reforms, with loss of the ethoxy group (and CO_2) to yield an acid functionality (**160**) (Fig 5.12)

or (b) trace moisture may react with CO_3^{2-} to form the bicarbonate ion (HCO_3^-) and a hydroxyl group that may attack the ethoxy group, causing the expulsion of the ethoxy group resulting in an acid functionality (**160**) (Fig 5 13)

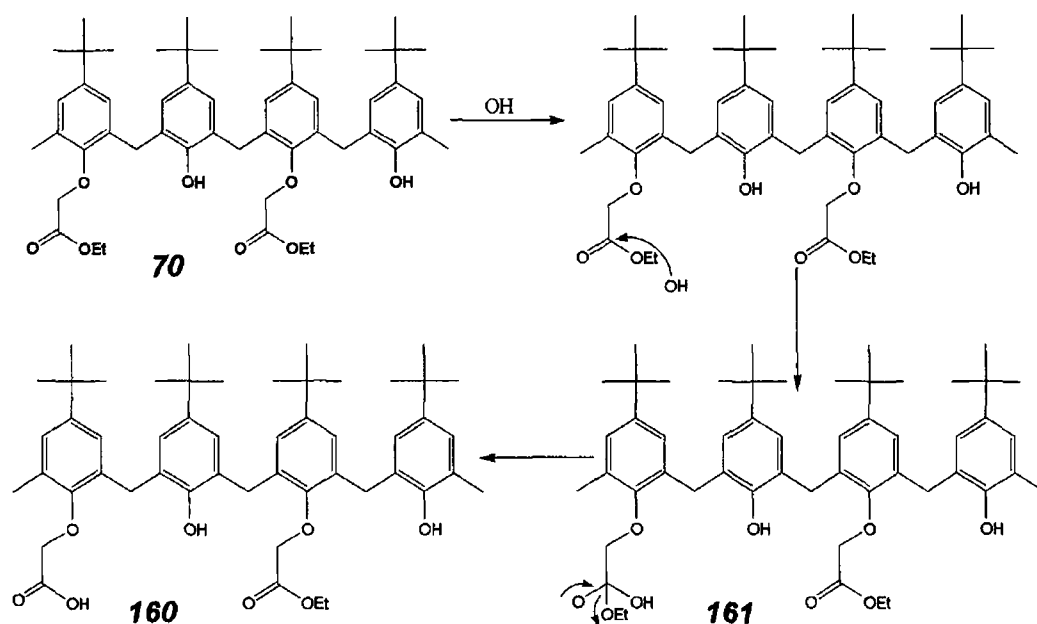


Figure 5 13 Proposed Reaction Mechanism for Partial Hydrolysis of **70**

It was concluded from this experimental data that carbonate bases were too weakly alkaline to remove the remaining phenoxy protons in the 2 and 4 position. Calixarenes are considerably stronger acids than their monomeric phenolic counterparts, but the accurate measurement of their pK_a values has posed some difficulties. The first dissociation of the calix[4]arene occurs quite easily, attributed to the stabilisation of the monoanion by the neighbouring hydroxy groups. Dissociation of a second proton of the calix[4]arene, distal to the previous deprotonated hydroxy group is favoured due to the adjacent stabilising influence of hydrogen bonding from the phenoxy groups in the 2 and 4 position [1,2]. The general observation was that of increasing pK_a values with consecutive dissociations. Deprotonation of a (1,3)-disubstituted calix[4]arene at position 2 and 4 is highly hindered, due to the absence of any hydrogen bonding stabilising influences from adjacent phenol subunits, causing an increase in pK_a values rendering the phenol subunits weakly acidic realizing a need for a stronger base than metal carbonate bases.

5 2 2 Use of an Organic Base

To eliminate calixarene-metal interactions in these reactions an organic, non-metal containing base, Triethylamine (TEA) was tested. The reaction was carried out as for 5 2 1 utilising TEA as base. After 120h, **70** remained unreacted as verified by TLC and DI-MS (*Fig 5 14* & *Fig 5 15*)

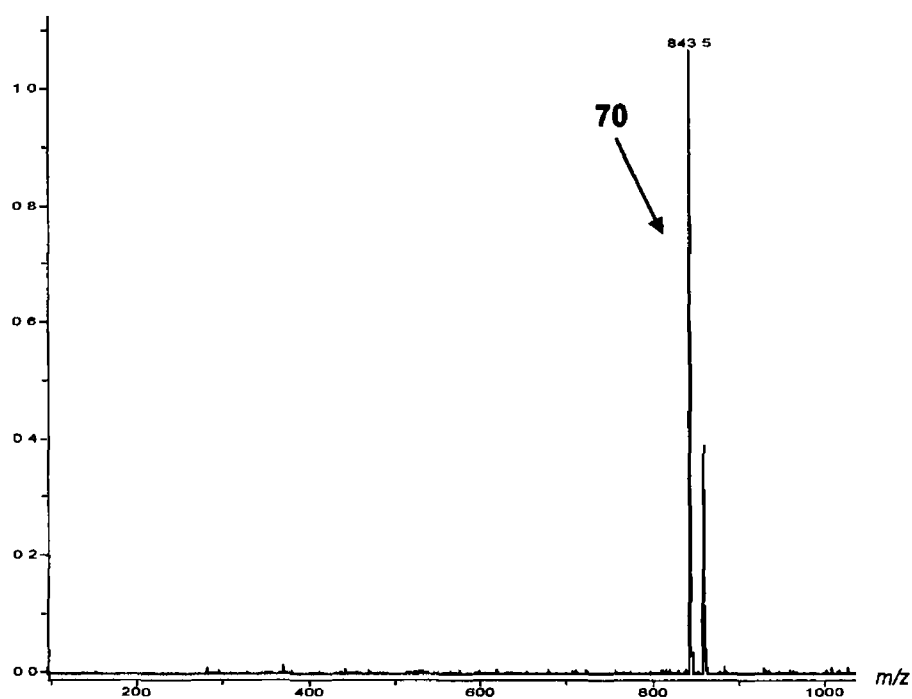


Figure 5 14 DI-MS Spectrum of **70**

Evidently, TEA was too weakly basic to remove the phenolic proton, with a pK_a value almost equal to CO_3^{2-} implying that a stronger base is required

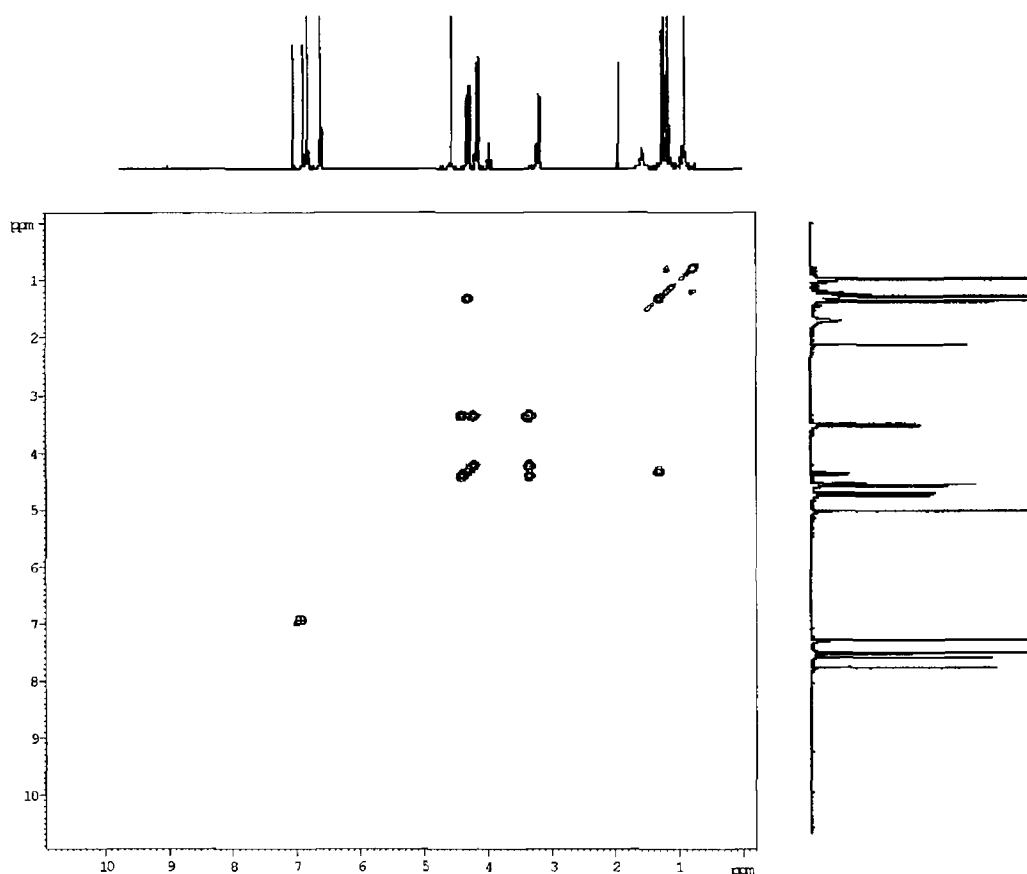


Figure 5 15 ^1H - ^1H COSY Spectrum of **70**

5 2 3 Use of an Hindered Base

Diaza(1,3)Bicyclo[5 4 0]Undecane (DBU) is a sterically hindered amidine base, commonly used where side reactions due to the inherent nucleophilicity of a basic nitrogen are a problem. Amidines are amongst the strongest neutral bases. The reactivity of amines (TEA) and amidines (DBU) is dependent upon the lone pair of electrons and this feature enables the amine or amidine nitrogen to behave as either a Bronsted base or a nucleophile [151, 187].

This varying degree of basicity was expressed by their pK_a values, measured in water, 10.75 and 12.0 for TEA and DBU respectively, indicative that DBU is a stronger base than TEA and can accommodate the abstracted proton by resonance stabilisation. The base can attack the phenoxy proton *endo*- or *exo*- to the lower rim. Due to its sheer bulk, we predicted it should attack *exo*- to the lower rim. The generated phenoxide anion is quite reactive as little stabilisation is imparted from the bulky DBU molecule compared to TEA and its metal containing base counterparts. The two m/z ion peaks of 843 and 859 for reaction E once again indicated that **70** remained unreacted (Fig 5 16).

The strength of hydrogen bonding between the hydroxyl group and the carboxyl group of the ester chain may be too strong. Also, the temperature of the reaction was $\sim 60\text{--}70^\circ\text{C}$. Temperature NMR studies of **70** at $\sim 55^\circ\text{C}$ in CDCl_3 (see *Chapter Three*) exhibited a broadening of the OH proton, suggestive of rapid movement of this unsubstituted phenol subunit by rotation of the OH group through the annulus. The reaction temperature ($60\text{--}70^\circ\text{C}$) and reaction solvent (DMF) renders it conformationally mobile. DBU may be too bulky and immobile to compete to abstract the proton and may not be a strong enough base.

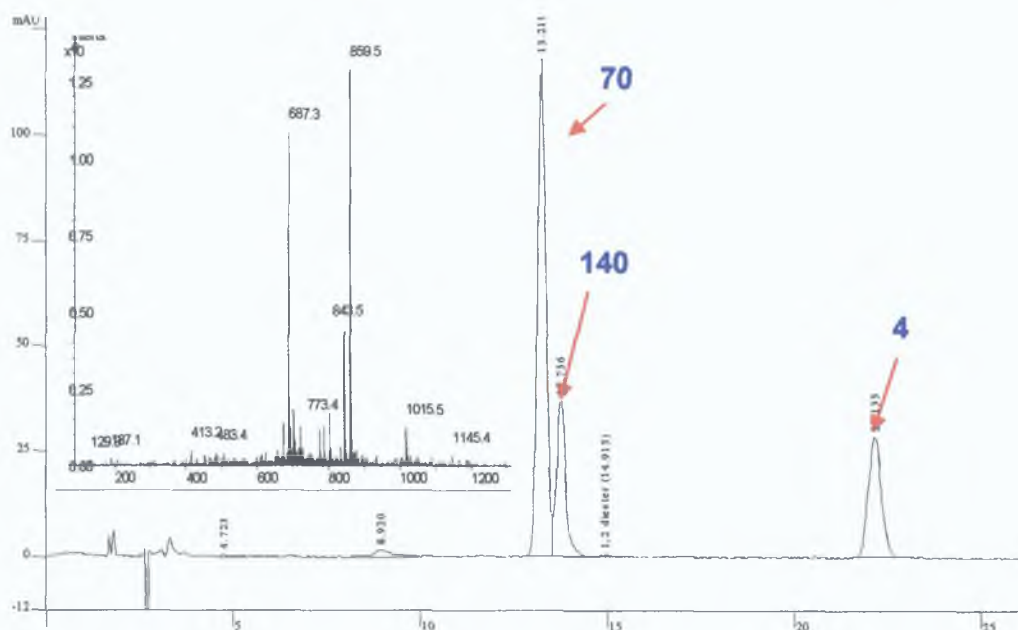


Figure 5.16 LC and DI-MS of Crude Product of Reaction E

5.2.4 Use of the Michael Addition Reaction

An alternative synthetic route to obtain the calix[4]arene bearing a tetrahedral binding site was attempted. This method was based on the Michael addition, where a nucleophilic addition of a carbanion to α,β -unsaturated carbonyl compounds. Compounds containing electron-withdrawing groups (CO_2R , CO_2H or CONH_2) in the presence of bases add to α,β -unsaturated carbonyl compounds predominantly in protic solvents [151]. The hypothetical Michael addition of **70** occurs by a mechanism of deprotonation of the phenoxy proton, of **70** generating a carbanion which acting as a nucleophilic reagent then attacks the conjugated system, acrylamide to form **157** (Fig 5.17).

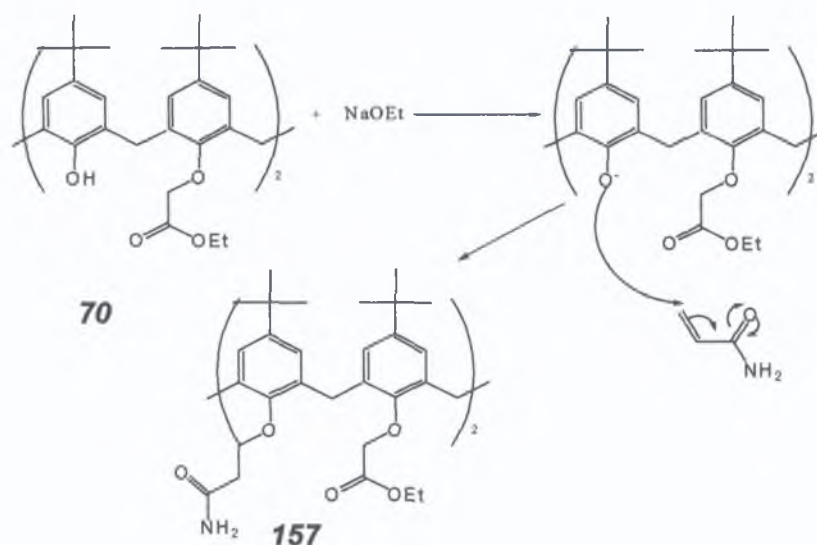


Figure 5.17 Reaction Mechanism of the Michael Addition of **70**

This negatively charged species would then become protonated to form the tetrasubstituted calix[4]arene derivative, with a tetrahedral array of binding sites. **70** was treated with sodium ethoxide (NaOEt) and then acrylamide in ethanol. The DI-MS and LC chromatographic studies indicated the presence of a number of products (Fig. 5.18 and Fig. 5.19)

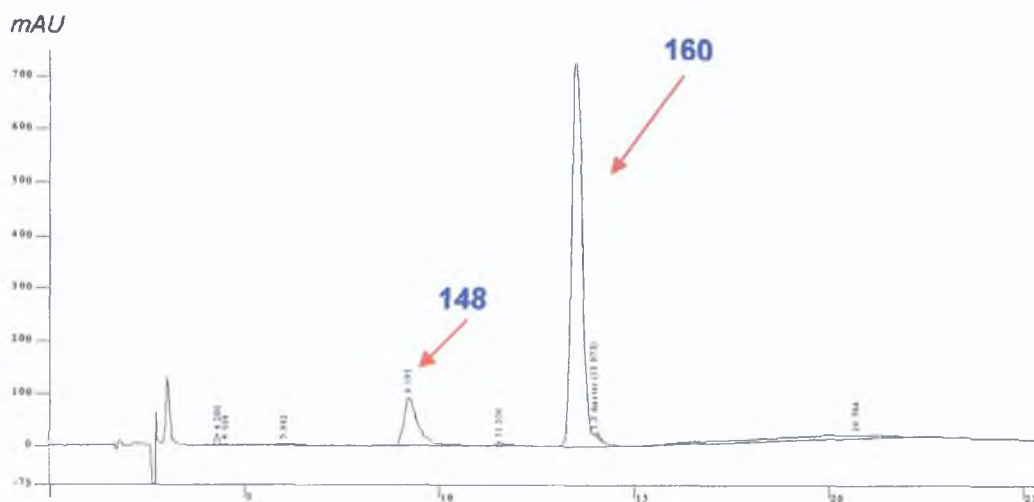


Figure 5.18 DI-Mass Spectrum of Crude Michael Addition Reaction of **70**

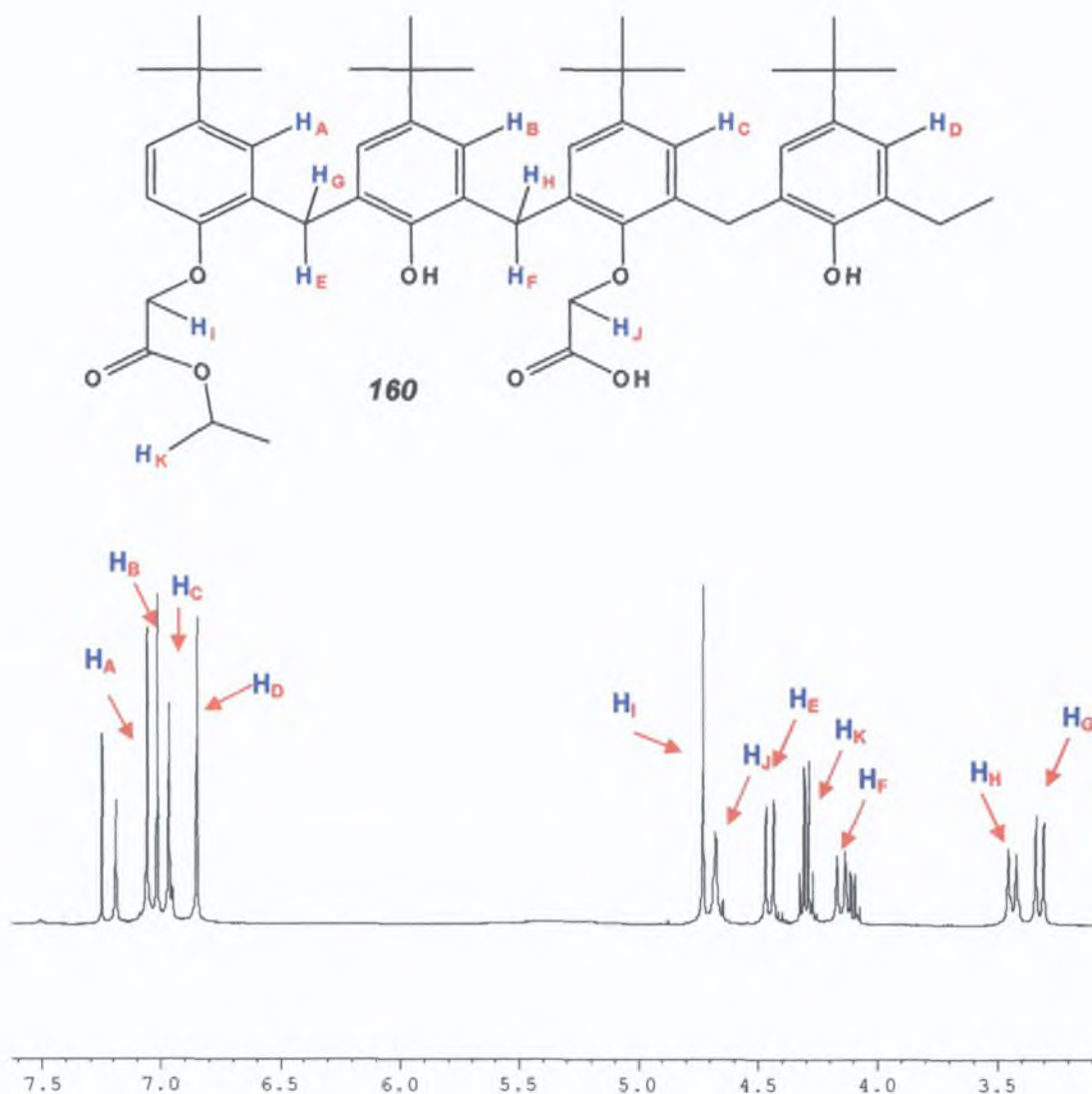


Figure 5.19 Schematic, DI-MS and ^1H NMR Spectrum (3-7.5ppm) of **160**

Columnning of this crude product using 1:1 hexane:ethyl acetate as the eluent afforded **70** and the partially hydrolysed, **160** as confirmed by LC, NMR and MS (Fig. 5.18 and Fig. 5.19). Partial hydrolysis of one ligating group had occurred.

5.2.5 Use of NaH Base

The experimental studies to date indicated that a stronger base for the deprotonation of the weakly acidic phenolic proton in the 2 and 4 position would be necessary. NaH was employed by Cobben et al. to deprotonate an inert dipropoxy calix[4]arene derivative for substitution of the 2 and 4 position by ethylbromoacetate or diethyl sulphide [27].

Compound **70** was a different molecule to that previously studied, considering the presence of ester ligating groups, thus increasing the possibility of additional

reactions at the appended ester tails or ethyl 3-bromopropionate **70** was treated with NaH, tenfold excess for 1h and subsequent treatment with ethyl 3-bromopropionate, 15-fold excess. The reaction was first monitored by TLC approximately every 24hr. After 48h, TLC indicated the presence of **70**, prompting the necessity for an extra aliquot of base and alkylating agent. TLC studies, following a further 72h, eluded to almost complete consumption of **70**. LC Analysis indicated the presence of two substantial peaks with retention times of 8.84 and 12.13min along with a peak at 14.92min indicative of **70** (Fig 5.22). Unambiguous identification of these unknown peaks from the LC chromatogram was obtained by DI-MS (Fig 5.20), with six principal m/z ion peaks of 787, 803, 887, 903, 987 and 1003 corresponding to three calix[4]arene derivatives with molecular weights of 764 (**148**), 864 (**162**) and 964Da (**1**), complexed to Na^+ (787, 887, 987Da) and K^+ (803, 903, 1003Da).

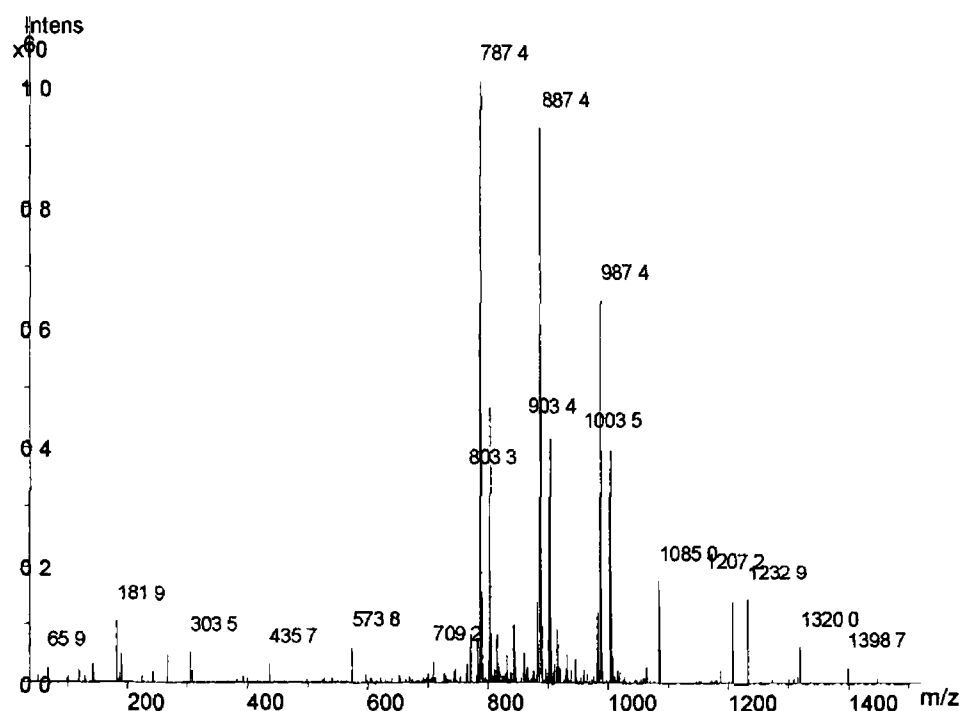


Figure 5.20 DI-Mass Spectrum of the crude product of Reaction G

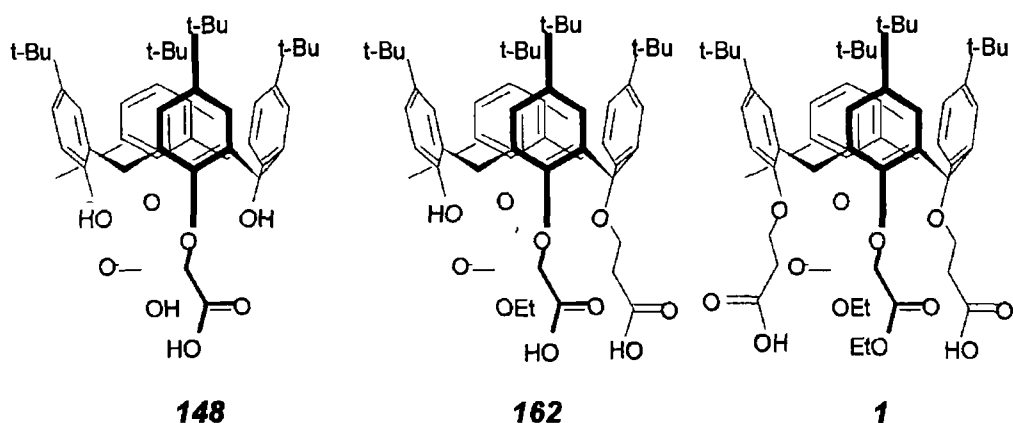


Figure 5 21 DI-MS and Structures of the Crude Product of Reaction G

Upon columning, a component of the mixtures adhered to the stationary phase, indicative of an interaction between the silica and some highly polar functionality present in the unknown derivative. HPLC of this derivative exhibited a large broad peak with a retention time of 8.19 min. DI-MS gave a single molecular ion peak of 787 Da while the ^1H NMR splitting and appearance pattern of the aromatic and methylene protons were characteristic of **148** (MW 764 Da).

The second unidentified component of the reaction mixture was shown by DI-MS to have a molecular weight of 864 Da. This derivative was not isolated for characterization but was deduced to be 5,11,17,23-tetra-*t*-butyl-25-mono(carboxymethoxy)-26-mono(carboxyethoxy)-27-mono(ethoxycarbonylmethoxy)-28-hydroxycalix[4]arene, **162** (MW 864 Da). Compound **70** undergoes a further substitution by the longer chained ester tail which undergoes hydrolysis to form **162**.

Efforts were made to eliminate any moisture present in this reaction. The reactions were performed under an inert atmosphere, the diester was oven dried prior to use, anhydrous DMF was dispensed under inert conditions, ethyl 3-bromopropionate and NaH were of high analytical reagent grade, typically $\leq 0.01\%$ H_2O . Though preventative methods were employed, hydrolysis still occurred, implicating that the reaction was indeed very sensitive to moisture.

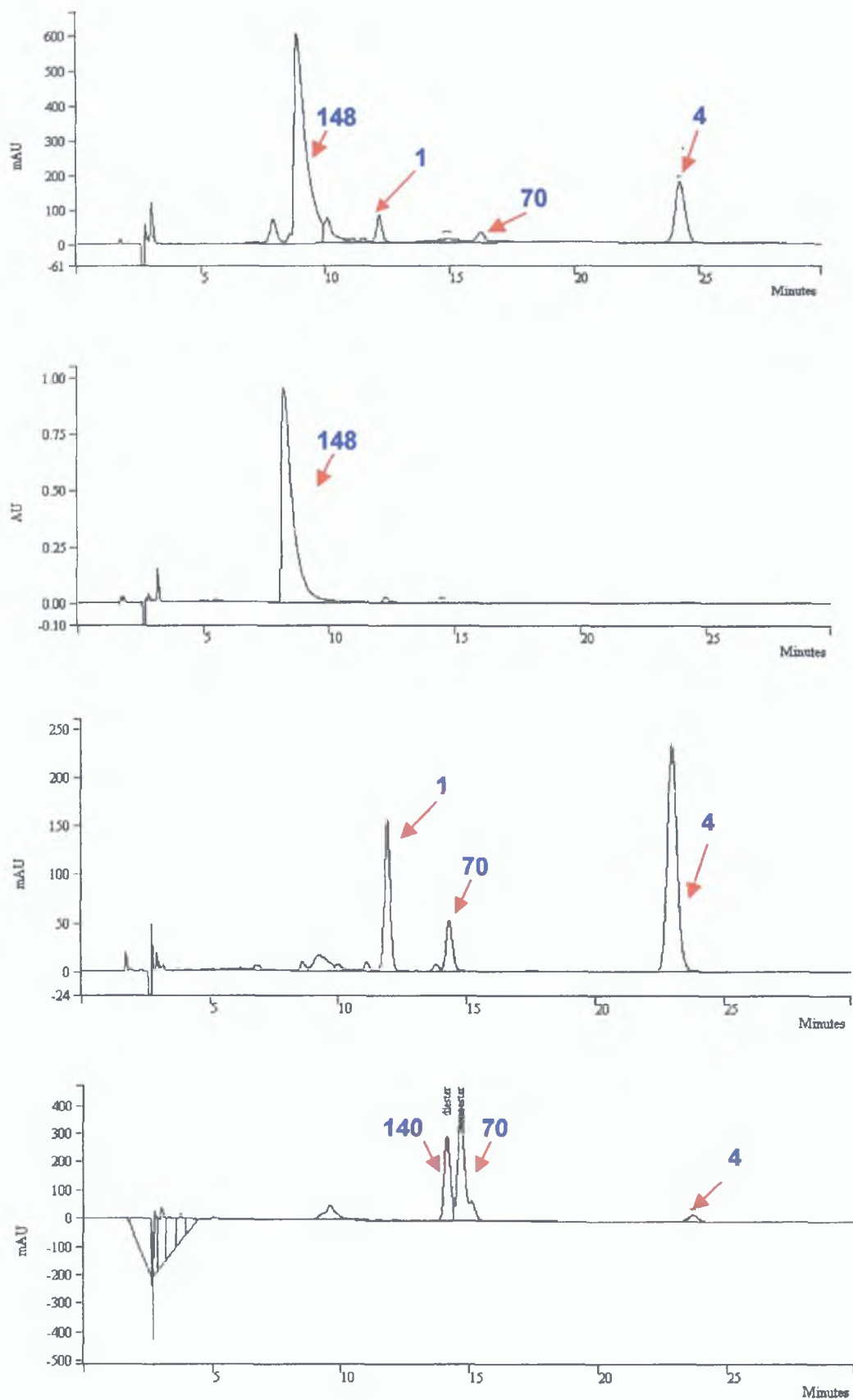


Figure 5.22 LC Chromatographic Studies of 'crude' (A) and 'pure' (B-D) products of Reaction G

5.2.6 Isolation and Characterisation of a Novel Tetrahedrally Shaped Calix[4]arene

Purification of this crude reaction mixture was carried out by column chromatography using 5:1 ethyl acetate:hexane as eluent. TLC studies showed that there was a spot with the solvent front and a large streak, which travelled up the plate. The fractions collected were analysed by TLC and HPLC. The chromatogram of the first fraction eluted exhibited three peaks with retention times at 11.89, 14.3 and 22.98 min. The slower two peaks were determined by a test injection mix to be that of **70** (14.3 min) and **4** (22.98 min). Recolumning this fraction using 9:1 hexane:ethyl acetate as eluent eluted **70** and **4**, with the third peak at 11.89 min remaining on the baseline.

The ^1H NMR spectrum of this third peak (11.89 min) exhibited an interesting splitting pattern of proton signals including two broad triplets at 2.76 and 4.51 ppm each integrating 4H proton. The proton signals characteristic of **70**, typically the methylene, $\text{OCH}_2\text{C}(\text{O})$, $\text{C}(\text{O})\text{OCH}_2$ and methyl, $\text{C}(\text{O})\text{OCH}_2\text{CH}_3$ protons of the ester tail are evident as a singlet, quartet and triplet at 4.71 (4H), 4.04 (4H) and 1.26 ppm (6H) respectively (Fig. 5.23).

Purification of this derivative proved difficult, as evident from Fig. 5.23 but DI-MS and MS² studies concluded that **70** had been functionalised in the 2 and 4 positions.

DI-MS of this peak gave a m/z ion of 987.5 Da. There were a number of possible arrangements of ligating groups at the lower rim that have a molecular weight in agreement with the observed molecular ion from the mass spectrum. Two possible derivatives were

- (a) 5,11,17,23-*p*-tetra-*tert*-butyl-25,27-bis(ethoxy-carbonylmethoxy)-26,28-bis(hydroxycarbonylethoxy)calix[4]arene (**1**)
- (b) 5,11,17,23-*p*-tetra-*tert*-butyl-25,27-bis(hydroxycarbonylmethoxy)-26,28-bis(ethoxycarbonylethoxy)-calix[4]arene (**163**) (Fig. 5.24)

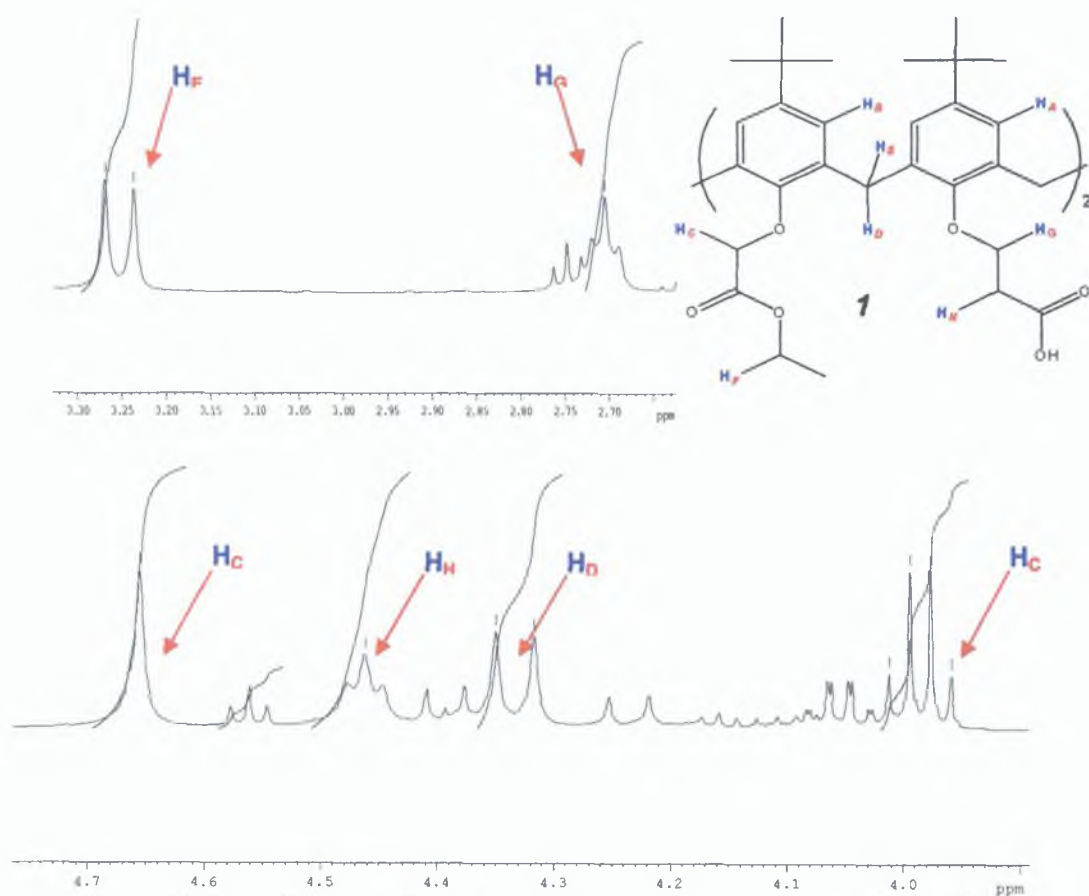


Figure 5.23 Schematic Diagram and ^1H NMR of 'pure' product of Reaction G

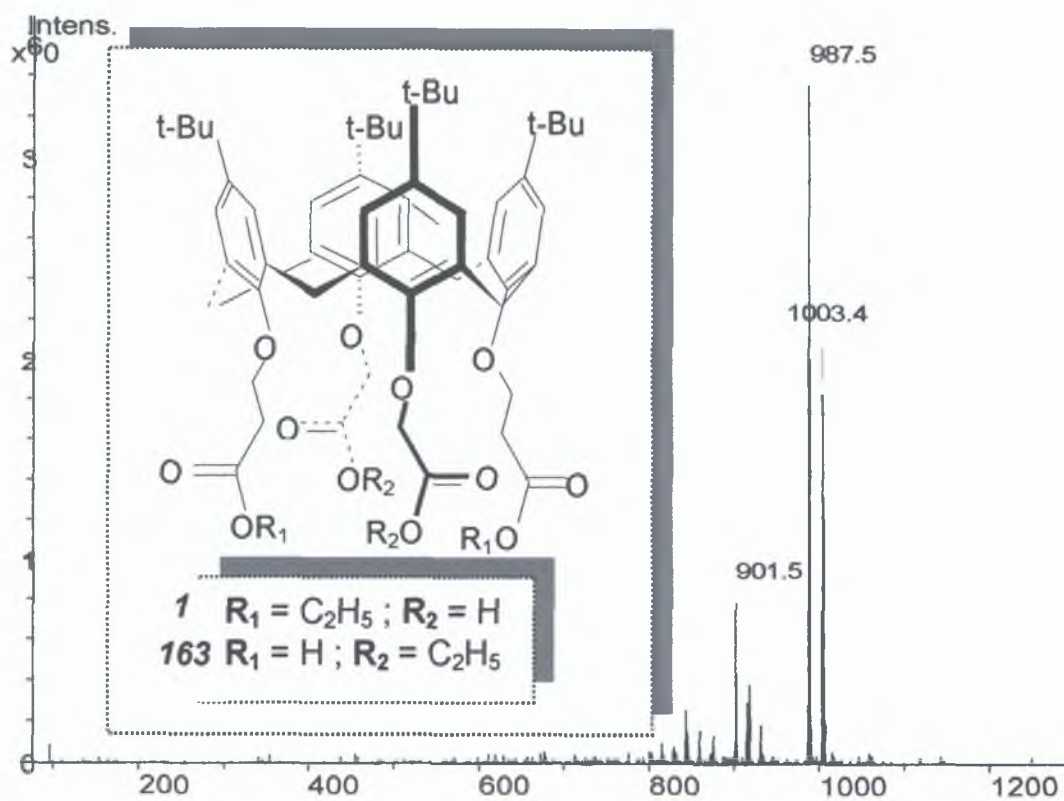


Figure 5.24 3d Structure and DI-MS of 'pure' product of Reaction G

Collisional Ion Fragmentation of this molecular ion gave a fragmentation ion of 914Da, resulting in a loss of 73amu, that of a propyl acid group, (-CH₂CH₂C(O) OH)

Sophisticated Mass Spectral Analysis was carried out by Bruker Daltonics Ltd. The MS data obtained from a 9 4 FTMS and an Esquire 3000 plus ion trap verified a molecular ion of 987 58 and 1003 50. MS/MS of m/z 987 58 indicated a fragmentation ion of 813 58, a 174amu - loss of two OCH₂CO₂C₂H₅ groups (see *Appendix, pp 201*)

Thus, complete characterisation has determined the new calix[4]arene derivative to bear a tetrahedral arrangement of such ligating groups as acid and ester, 5,11,17,23-p-tetra-tert-butyl-25,27-bis(ethoxycarbonylmethoxy)-26,28-bis(hydroxycarbonylethoxy)calix[4]arene (**1**)

The reaction conditions for the synthesis of a calix[4]arene derivative with a tetrahedral arrangement of its ligating tails have been determined. HPLC was used to monitor the progression of the reaction and also, gave an insight into the mechanism of the reaction and product formation, thus aiding the optimisation of the reaction conditions of the synthesis of this calix[4]arene derivative bearing a tetrahedral binding site (*Fig 5 25*)

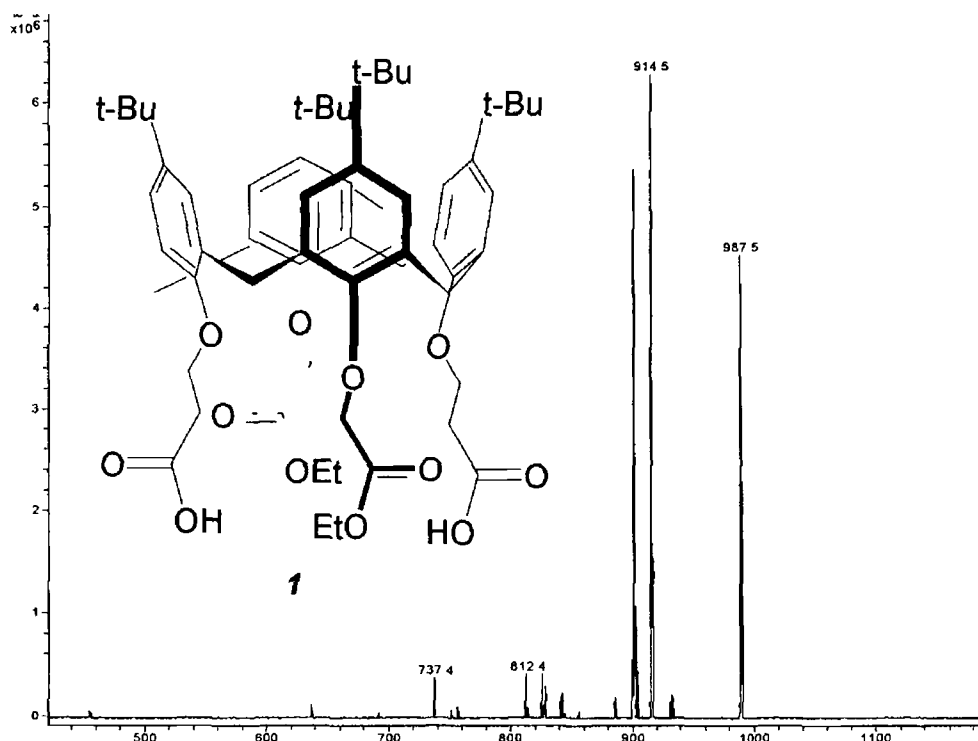


Figure 5.25 MS² Spectrum of **1**

5.2.7 Optimisation Studies of the Reaction of *p*-tetra-*t*-butylcalix[4]arene-(1,3)-diethyl ester and Ethyl 3-bromopropionate

The course of the reaction with varying reaction stoichiometry and NaH addition was studied at regular intervals, typically every 24h

Reaction G involved the reaction of **70** with NaH and ethyl 3-bromopropionate in a 10 and 15 molar excess respectively for 48h to which a second aliquot of base and alkylating agent were added and reacted for a further 72h. LC chromatographic studies gave interesting results. **70** was tested by HPLC to assess its purity prior to reaction. This derivative eluted at 13.7min with a relative peak area percent ~ 99.0-99.5% purity, with 0.1% **140** and 0.2% **4**.

As the reaction progressed, the relative percentage area of **70** reduced from 99.5% to 44% and then to 5%, following 0, 24 and 120h of reaction time. While the peak area of **148** dramatically increased from ~33% to 42% and then to 71% after 5h, 24h and 120h. The peak assigned as **1** was present in the 5h sample with a peak area of 0.19% which increased as the reaction progressed to 4.3% in area. Interestingly, even though **70** was 99.5% pure, **4** reappeared in the LC chromatogram after reacting for 24h. Following completion of the reaction, an LC chromatogram displayed a peak area of 15% for this species (Fig. 5.26).

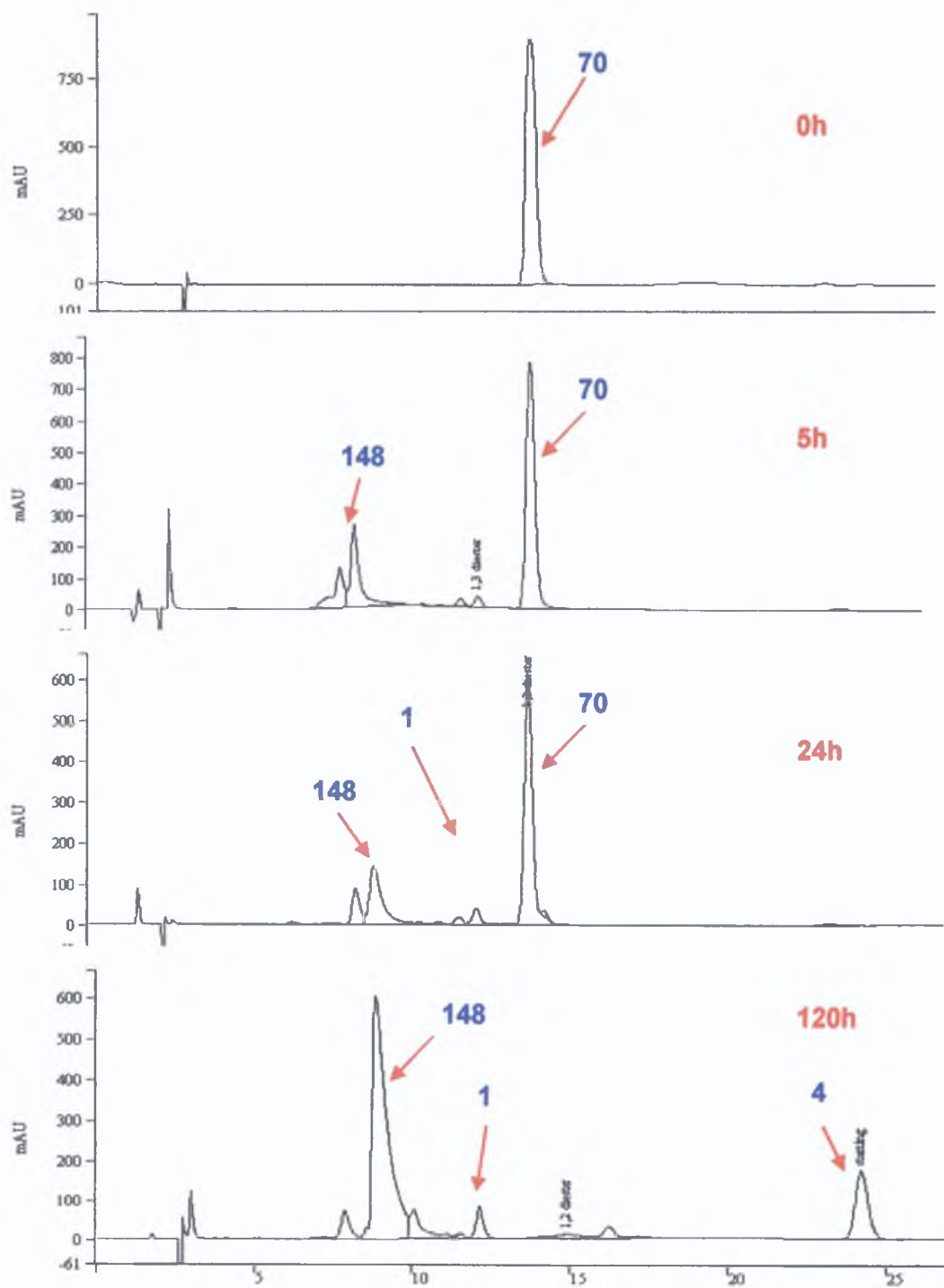


Figure 5.26 Chromatographic Data of Time Studies of Reaction G1

It was surmised that **70** is converted to **4** under the reaction conditions employed. To verify this observation and to alleviate the risk of decomposition, an LC study of the progression of this reaction was carried out. The effect of varying stoichiometry, the interval addition of the extra reagents and the mode of addition of NaH base were also studied.

5.2.7.1 The Influence of Stoichiometry and Time

As observed from preliminary LC studies of reaction G1 (*Table 5.3, pp 182*), the general trend that time incurred on this reaction, was that **70** was not completely consumed (~3.3-5%) while the formation of **148**, **1** and **4** was observed along with minor impurities. The predominant product formed was **148** and **4**.

Two reaction conditions were investigated, G2 and G3. Reaction G2 involved the regular 24h addition of 5 and 7½ times excess of NaH and ethyl 3-bromopropionate over 5 days whilst reaction G3 was as for G2, with half the stoichiometry. The trend observed for reaction G1 was observed for reaction G2 and G3. While reaction G2 exhibited appropriate peaks for **148**, **70** and **4**, there were additional impurities present. DI-MS of the crude product of reaction G2 and G3 indicated the presence of **70**, **148** and **1** in addition to some unidentified impurities.

It was thought that the regular addition of the extra aliquot of base and alkylating agent every 24h might inhibit the possibility of by-products, for example **148** or **4** as a larger excess of NaH and ethyl 3-bromopropionate was not available to react with **70**. On comparison of the LC chromatograms of the crude product of reaction G1 and G2, the former had a higher percent area for **148**, **1** and **4** than the latter, while there was an observed greater consumption of **70** in the former reaction than for G2. The addition of reactants for reaction G2 were different to reaction G1, by the addition of a smaller amount at more frequent intervals to possibly eliminate side reactions actually led to less consumption of the diester and introduced unidentified impurities. It was surmised that addition of extra aliquots of reactants more frequently leads to greater disturbance of the reacting system (*Fig 5.27*).

To minimise side reactions and to investigate the importance of stoichiometry on the distribution of products, a parallel reaction, G3 was carried out. The overall stoichiometry of reaction G1 and G2 was 1:20:30 **70**:NaH:Ethyl 3-bromopropionate whereas reaction G3 employed a 1:10:15 ratio of **70**:NaH:Ethyl 3-bromopropionate. The LC chromatographic data eluded that reducing the stoichiometry reduces the formation of **4**, **148** and **1**.

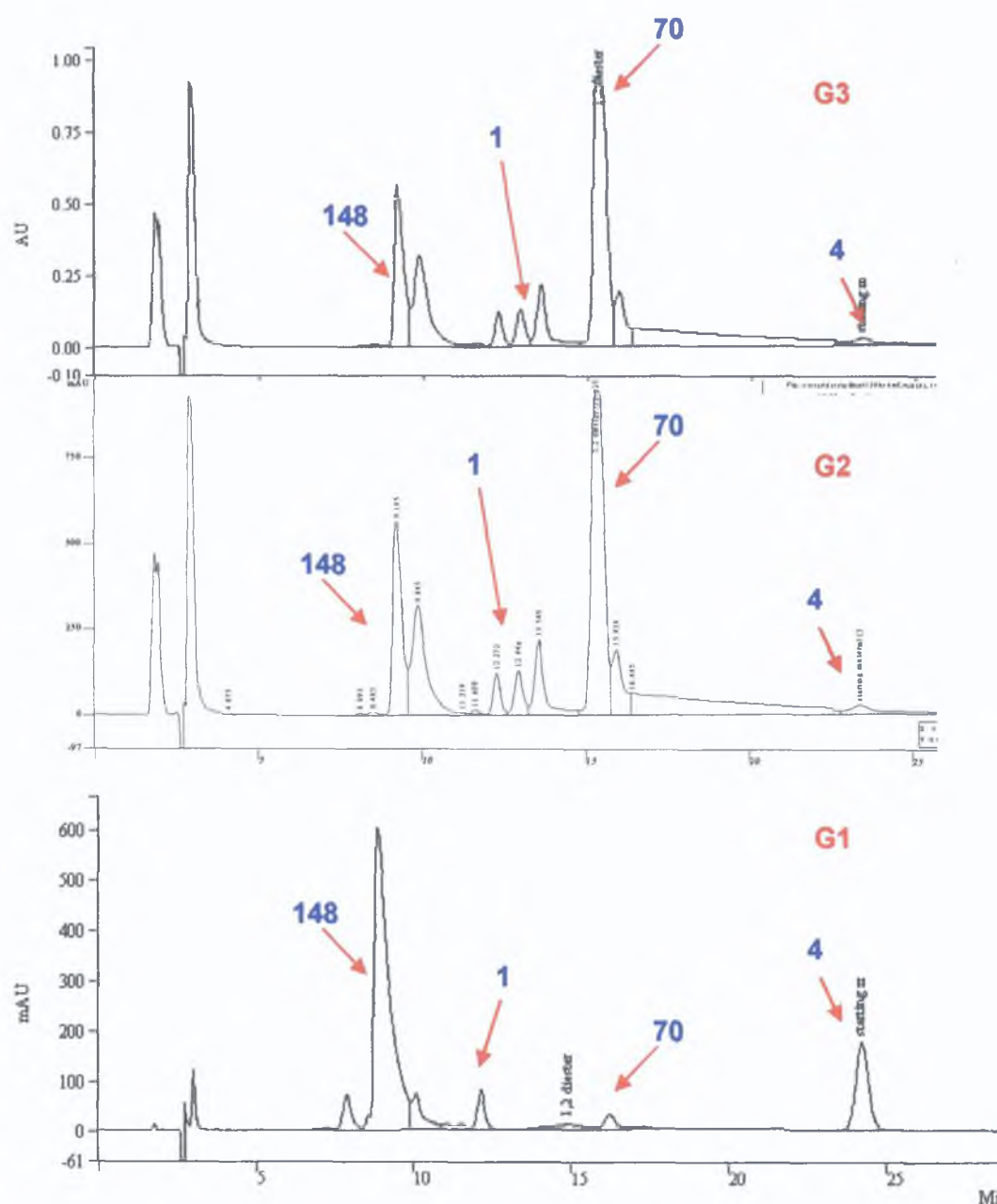


Figure 5.27 Chromatographic Data of Reactions G1-G3 (Deactivated form of NaH), sampling at 120h

Compound **70** was present in greater quantity, ~ 3.35, 33.4 and 66.5% peak area for reaction G1, G2 and G3 respectively. The DI-MS of the product of reaction G3 indicated the presence of **148** (787.4Da), **1** (815.4Da), **70** (843.5 and 859.5Da) and **162** (887.5Da).

Thus, it was surmised that reducing the stoichiometry did not enhance the synthesis of **1** or the yield of other side-products but resulted in a large amount of unreacted **70**. The addition of base and alkylating agent at more frequent intervals introduced an increased number of impurities. It was concluded from

the experiments performed, that the reaction G1, employing a 1:20:30 stoichiometry of **70**:NaH:Ethyl 3-bromopropionate with two regular additions of base and alkylating agent, spaced 48h apart yielded the greatest quantity of the target compound

5.2.7.2 The Influence of the Mode of Addition of NaH

The H⁻ ion is one of the strongest bases available and is very reactive with an acid, alcohol, aldehyde, ketone functionality or a water molecule. Thus, the mode of addition of NaH to the reacting system was considered important. The NaH used was 60% dispersed in mineral oil. Cobben et al. freed the NaH base from mineral oil by washing with petroleum ether (bp 40-60°C) prior to addition, thus activating it for reaction. It was proposed that activating the NaH incurred harsher reaction conditions as the NaH has a higher reactivity, maximizing the possibility of hydrolysis of the ester ligating tails and cleavage of the ethoxycarbonyl methylene (CH₂C(O)OEt) groups. Therefore, reaction G1, G2 and G3 were carried out in both the activated and deactivated NaH form i.e. freed and not freed from the mineral oil respectively. It was anticipated that the addition of NaH in its deactivated form would reduce the reactivity of the H⁻ base as it must dissociate first from the mineral oil and then react with **70**. The reaction occurs under milder conditions and over a longer period of time. For reaction G2, the NaH in the deactivated form did not react as quickly as for that in the activated form. This was apparent at 24h as the reported percent peak area of **70** for the activated form was 60.97% and 68.6% for the deactivated form while interestingly, the percent peak area for **4** at 24h for the activated and deactivated reaction was 0.67% and 0.2% respectively. After 72h, there was 51.58% and 1.0% of **70** and **4** for the reaction employing NaH in the activated form whereas the deactivated form gave a percent peak area of 61.65% and 0.65% for **70** and **4** (Fig. 5.28).

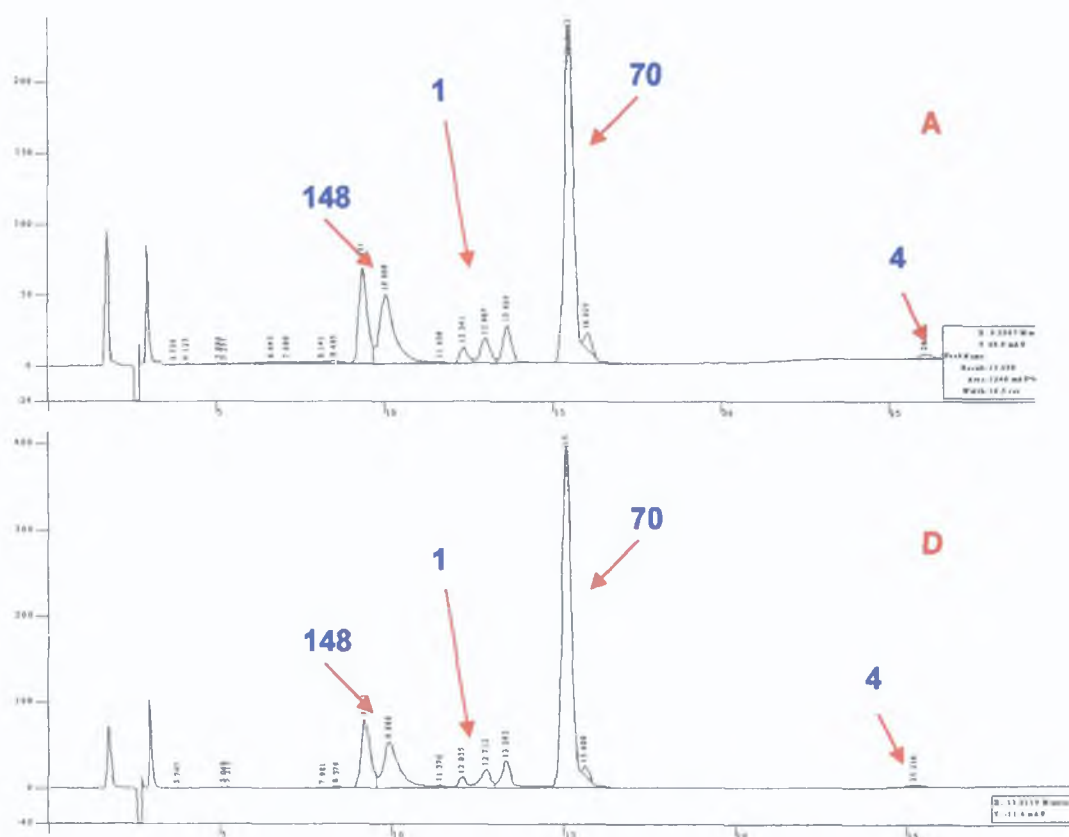


Figure 5.28 Chromatographic Data of Reaction G2 employing NaH in its Activated (A) and Deactivated (D) form, sampled at 72h

Completion of the reaction gave 33.4% and 7.5% **70** and **4** for the activated NaH reaction and 34.3% and 2.2% for the deactivated reaction. In terms of product distribution, the deactivated NaH reaction gave 13.2% **148** and 2.5% **1** whereas for the activated NaH reaction, the relative percent area for **148** was 21.0% while for **1** it was 3.4%. This trend was observed for reaction G3 as Figure 5.29 indicates that the deactivated form reduces the generation of **4** with reduced consumption of **70** compared to G3 in the activated NaH form.

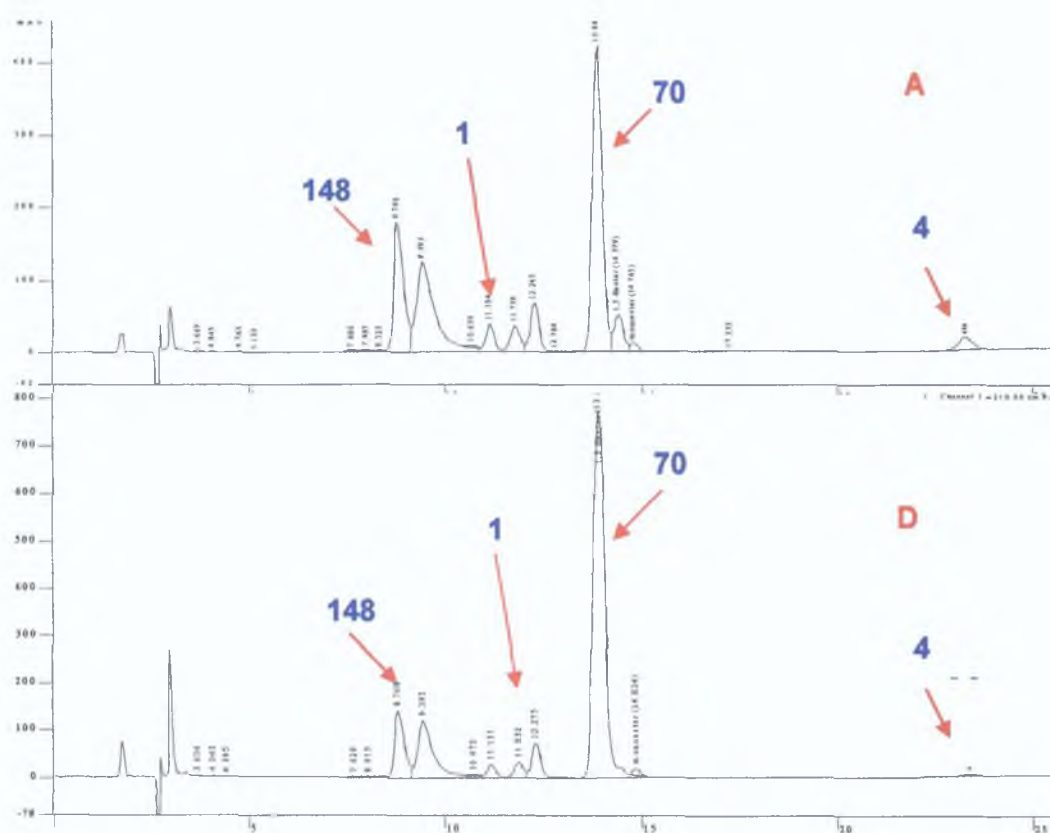


Figure 5.29 Chromatographic Data of Reaction G3 employing NaH in its Activated (A) and Deactivated (D) form, sampled at 72h

The mode of addition of NaH has a profound effect on product distribution. The observed increase in the yield of **1** may be attributed to the NaH added in its deactivated form, it takes longer to dissociate and does not attack **70** as strongly, thus reducing hydrolysis and cleavage of the ester ligating tails. The NaH added in its activated form may react immediately with **70**, causing rapid hydrolysis and cleavage at an enhanced rate, the NaH may be consumed before the addition of ethyl 3-bromopropionate and thus, the yield of **1** may be reduced. Similar results were obtained for reaction G3 where a greater proportion of **70** was consumed for the activated NaH form.

The activated NaH form of reaction G1 gave the following percent peak area results: 61.43%, 4.3%, 3.4%, 14.9% for **148**, **1**, **70** and **4** whereas for the deactivated NaH form, 82.7%, 6.2%, 2.8%, 5.9% for **148**, **1**, **70** and **4** were obtained.

The solubility of **4** in acetonitrile may incur inaccuracies in the LC data. Although the concentration of each sample prepared was identical, **4** was sparingly soluble in acetonitrile. Therefore, product distribution differences arising from NaH, used

in its activated and deactivated form were not based solely on the percent peak area of **4** but LC analysis was based on the complete product distribution encompassing **4** and the remaining products and starting material

It was decided that milder conditions i.e. the addition of NaH in the deactivated form was advisable in order to minimize side reactions and maximize the yield of **1**

It was thought that there might be good reasons to add NaH 1 hour before addition of the alkylating agent. This time could allow the NaH to deprotonate the phenoxy protons, generating the dioxyanion but may also allow side reactions to occur

Thus, the optimized reaction conditions found to date were the reaction of **70** with 10 and 15 molar excess of NaH and ethyl 3-bromopropionate for 48h to which an extra aliquot of base and alkylating agent were added and heated to 70°C for 72h, (compound **70** and NaH were added together and allowed to react for 1h to which the alkylating agent was subsequently added). All products obtained from the optimisation work are outlined in *Table 5.1* and *Fig. 5.30*

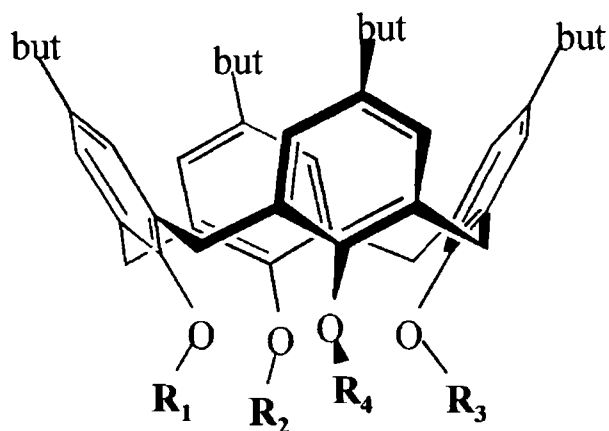


Figure 5 30 Diagram of the Calix[4]arene derivatives synthesised

Name used in Discussion Section	Mass (a m u)	Substituent Groups at the Lower Rim			
		R_1	R_2	R_3	R_4
<i>p</i> -t-Butyl-1,3-Diester (70)	820	CH ₂ C(O)OEt	H	CH ₂ C(O)- OEt	H
<i>p</i> -t-Butyl-1,3-Diacid (148)	764	CH ₂ C(O)OH	H	CH ₂ C(O)- OH	H
<i>p</i> -t-Bu-1-monoethyl acid-3-monoethyl ester (160)	792	CH ₂ C(O)OH	H	CH ₂ C(O)- OEt	H
<i>p</i> -t-Bu-1-monoethyl acid-2-monopropyl acid-3-monoethyl ester (162)	864	CH ₂ C(O)OH	CH ₂ CH ₂ - C(O)OEt	CH ₂ C(O)- OEt	H
<i>p</i> -t-Bu-1,3-diethyl ester-2,4-dipropyl acid (1)	964	CH ₂ C(O)OEt	CH ₂ CH ₂ - C(O)OH	CH ₂ C(O)- OEt	CH ₂ CH ₂ - C(O)OH

Table 5 1 Names, Masses and Structures of the Calix[4]arene Derivatives synthesised

5 2 8 Rationalisation of Product Formation

5 2 8 1 'A Hydrolysis Phenomenon'

As the reaction progresses the propionate ester group bound to the calix[4]arene appears to undergo hydrolysis to the propionic acid group. Efforts were made to eliminate any moisture present in these reaction, the reactions were performed under inert conditions, **4** was dried prior to use, anhydrous DMF was dispensed under inert conditions, ethyl-3-bromopropionate and NaH were analytical grade reagents. It is surmised that hydrolysis may occur during the reaction via three pathways. The first pathway may be hydrolysis of the ester functionalities following functionalisation in the 2 and 4 position by a hydroxyl group, in a manner similar to *Figure 5 13*. Also, the second pathway may be that trace moisture could attack ethyl-3-bromopropionate, expel the ethoxy group to form bromopropionic acid and subsequently is attacked by the oxyanion to result in a propyl acid substituted *p*-1-butylcalix[4]arene derivative (*Fig 5 31*)

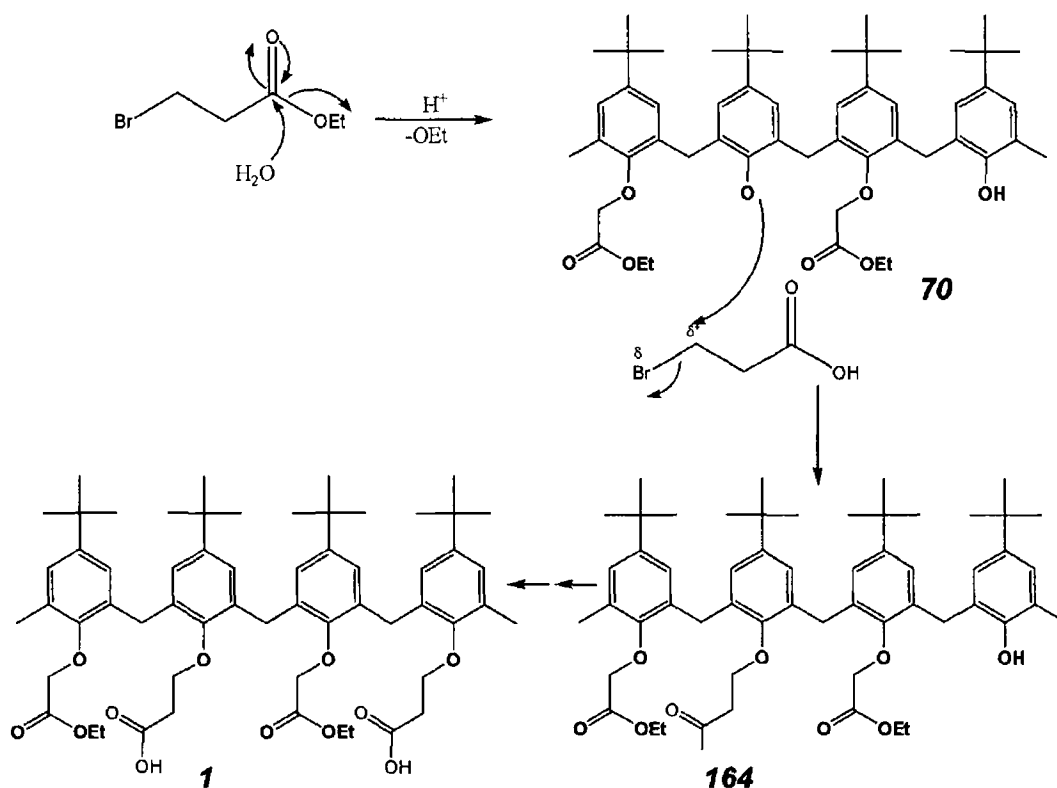


Figure 5 31 Proposed Reaction Mechanism for the synthesis of **1**

Another theory proposed was the arrangement of the tails of the lower rim may facilitate 'neighbouring group' hydrolysis. A tetra substituted ester calixarene derivative with two short and two long tails may result from this reaction. The carbonyl group of the shorter chain ester group may affect the electronegativity of the carbonyl group of the longer chain ester group, causing an increase of the

positive charge of this carbonyl carbon, thus increasing its susceptibility to hydrolysis by trace moisture (Fig 5 32)

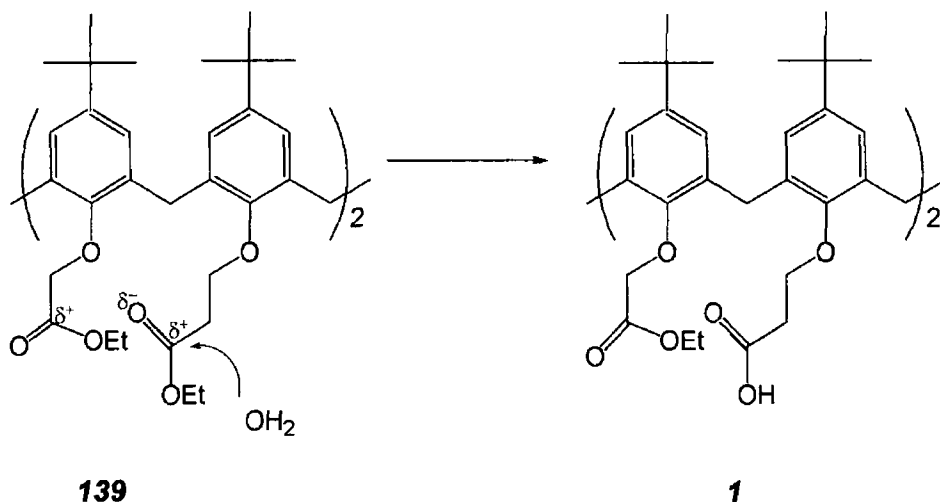


Figure 5 32 'Neighbouring Group' Hydrolysis resulting in a *t*-butyl diester, diacid calix[4]arene dervative

5 2 8 2 'A Cleavage Phenomenon'

Another phenomenon observed in this reaction was the apparent cleavage of the ethoxycarbonylmethylene group ($\text{CH}_2\text{C}(\text{O})\text{OEt}$) of the *p*-*t*-bucalix[4]arene diester resulting in the reformation of **4**. For the three reactions studied, G 1-3, the formation of **4** was documented over time (Fig 5 26) with an observed peak eluting at ~ 23-24min

Ethers are comparatively unreactive compounds, quite stable towards bases, oxidising and reducing agents. The ether linkage is generally cleaved under acidic conditions. Such alkyl-aryl ethers as the 1 and 3 position of **70** may be cleaved with concentrated acids or iodotrimethylsilane. The alkyl oxygen bond is broken to give an alkyl halide and a phenol. Alkyl aryl ethers can also be cleaved with LiI to give alkyl iodides and salts of phenols. While examples of such cleavage incurred by NaH are rare, other hydride containing reagents, LiAlH_4 or LiBHET_3 cause cleavage of other functional groups including amides.

It has been shown that by maintaining reactive hydroxyl groups at the lower rim, intramolecular hydrogen bonding predisposes these calixarene ligands to bind metal complexes on the periphery of the cyclic structure. Highly electrophilic metal complexes can frequently be isolated with calix[*n*]arenes. Flonani and co-workers in particular have prepared several novel, reactive organometallic

compounds. The preparation of metal complexes with the calix[n]arene ligand is severely limited by virtue of the build-up of charge at the metal centre by the 4 anionic aryloxy donors. Therefore, to prepare such metal complexes, it is often advantageous to alkylate 1 or 2 of the oxygen donor atoms to reduce the overall anionic charge of the ligand. Despite this protective measure, ether linkages are often susceptible to attack by the electrophilic metal centres, diminishing the reactivity of the metal to form a [Metal][Ligand] complex [188,189].

Considering this reported susceptibility of attack of such ether linkages, it is reasonable to propose that the Na^+ ion may attack the ethereal oxygen atom causing cleavage of the ether linkage. Deprotonation of the unsubstituted phenol subunits of **70** generates a di-phenoxide anion, increasing the electron density at the lower rim, causing a stronger attraction of the Na^+ ion to the lower rim thus enhancing the possibility of attack of this ion on the ether linkage.

A possible mechanism proposed for the observed reformation of **4** is shown in *Figure 5.33*.

The influencing effect of NaH must be addressed. Upon dissociation the H^- ion is readily reactive but may react via two modes, as a base or a nucleophile. The former mode results in deprotonation but there are a number of sites available for deprotonation. For *Figure 5.33 A* the implications of deprotonation have been previously discussed.

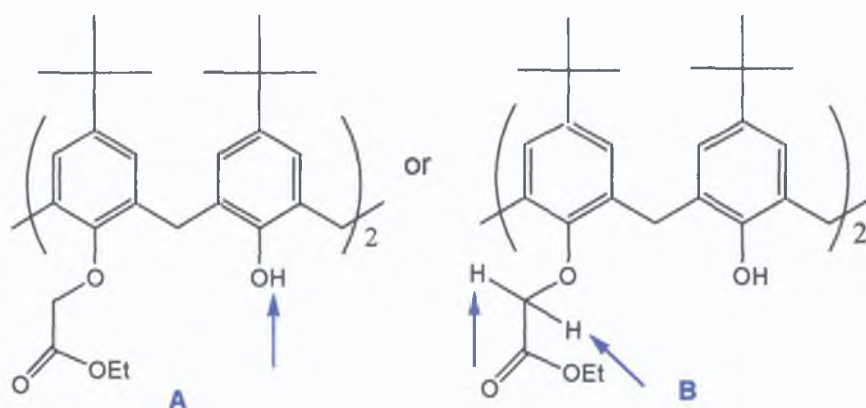


Figure 5.33 Deprotonation of the *t*-butyl diester at various sites

Deprotonation of the acidic proton α to a carbonyl group results in the formation of a carbanion. As the phenoxide is a good leaving group, this Alkyl-Aryl ether bond may cleave resulting in a phenoxy anion which may be stabilised by coordination to Na^+ . Therefore nucleophilic displacement is more likely by a hydroxide or hydride anion. From previous studies, **5.2.1**, trace amounts of hydroxide predominantly resulted in partial hydrolysis of the shorter chained carbonyl group. Therefore it is possible that the hydride may be causing the cleavage of the alkyl-aryl ether bond (Fig. 5.34 **A**).

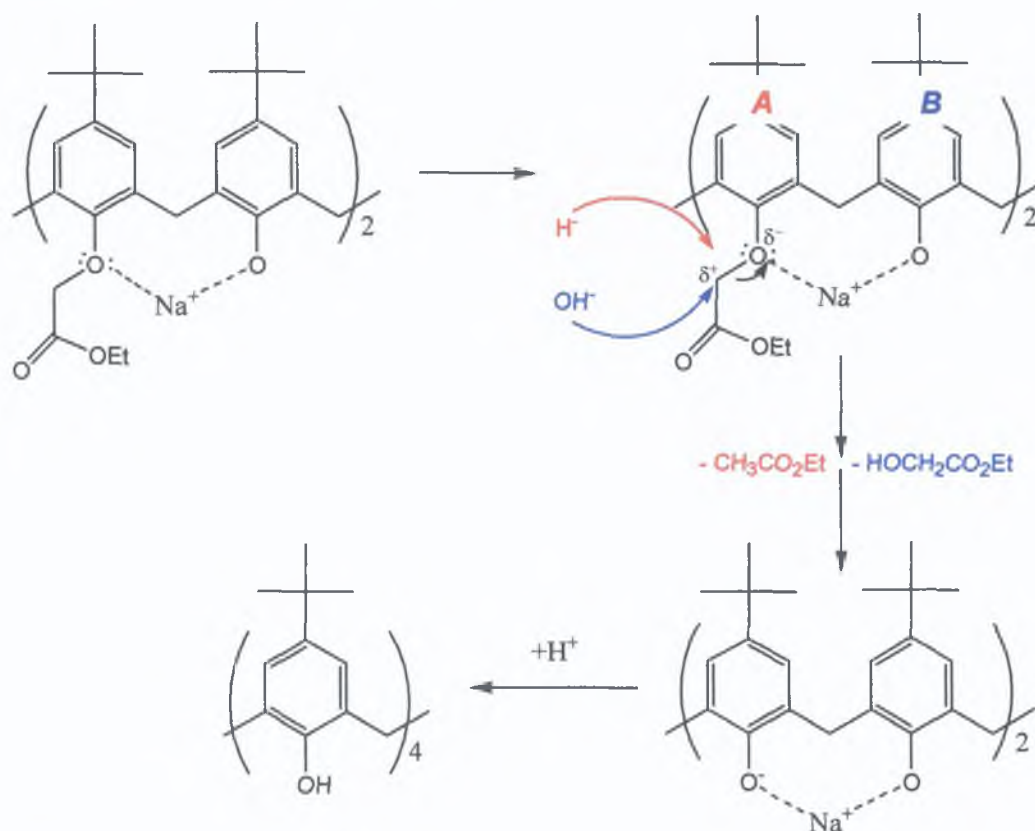
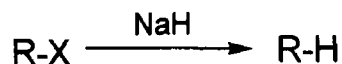


Figure 5.34 Proposed Reaction Mechanism for the observed 'Cleavage Phenomenon' of **70** (**A** & **B**)

Figure 5 34 B details an alternate proposal where a hydroxide ion, generated from trace moisture may displace the phenoxide resulting in a phenoxide anion which is further stabilised by coordination to Na^+

NaH may also attack as the nucleophilic H^- ion, involving the replacement of a leaving group by hydrogen. Reduction of alkyl halides (dehalogenation) has been accomplished with many reducing agents. This may be schematically represented by



The mechanism usually consists of simple nucleophilic substitution with attack by the H^- ion that may or may not be free. The H^- ion may attack the electropositive carbonyl of the alkyl halide (ethyl 3-bromopropionate) to form $\text{CH}_3\text{CH}_2\text{C}(\text{O})\text{OEt}$ and Na^+Br^- thus activating the Br^- to attack the electropositive carbon attached to the ethereal oxygen of the substituted phenol subunit causing cleavage of this ether linkage to form the phenoxide anion that is stabilized by Na^+ until it regains a proton (Fig 5 35)

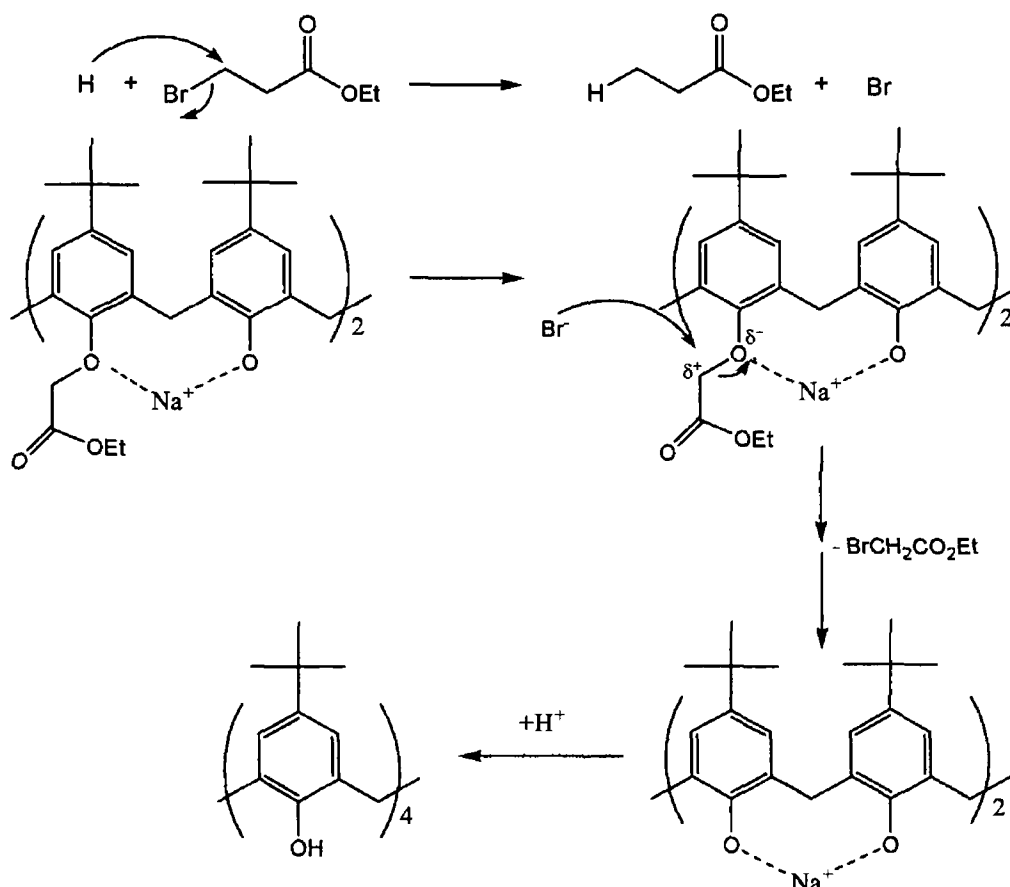


Figure 5 35 Proposed Reaction Mechanism for the observed 'Cleavage Phenomenon' of 70

To investigate this cleavage phenomenon, an exploratory reaction of **70** and NaH was set up and monitored periodically by HPLC. Over the course of the reaction hydrolysis of **70** to **148** (retention time: 8.9min) occurred along with cleavage of **70** to **4** (Fig. 5.36). As time progressed, the percent peak area of **4** increased from 0.72% to 1.13% to 3.35% for 48h, 96 and 120h respectively.

Compound **70** is a known selective complexing agent for Na⁺, with molecular modeling studies indicating that the Na⁺ ion is perfectly held in the centre of an octahedral cavity defined by the four phenoxy oxygen and four carbonyl oxygen atoms at the lower rim. Na⁺ complexes to **70** causing an induced partial positive charge to develop on the methylene group α to the phenoxy and carbonyl oxygen atom. This subsequently undergoes attack by the routes outlined in Fig. 5.34.

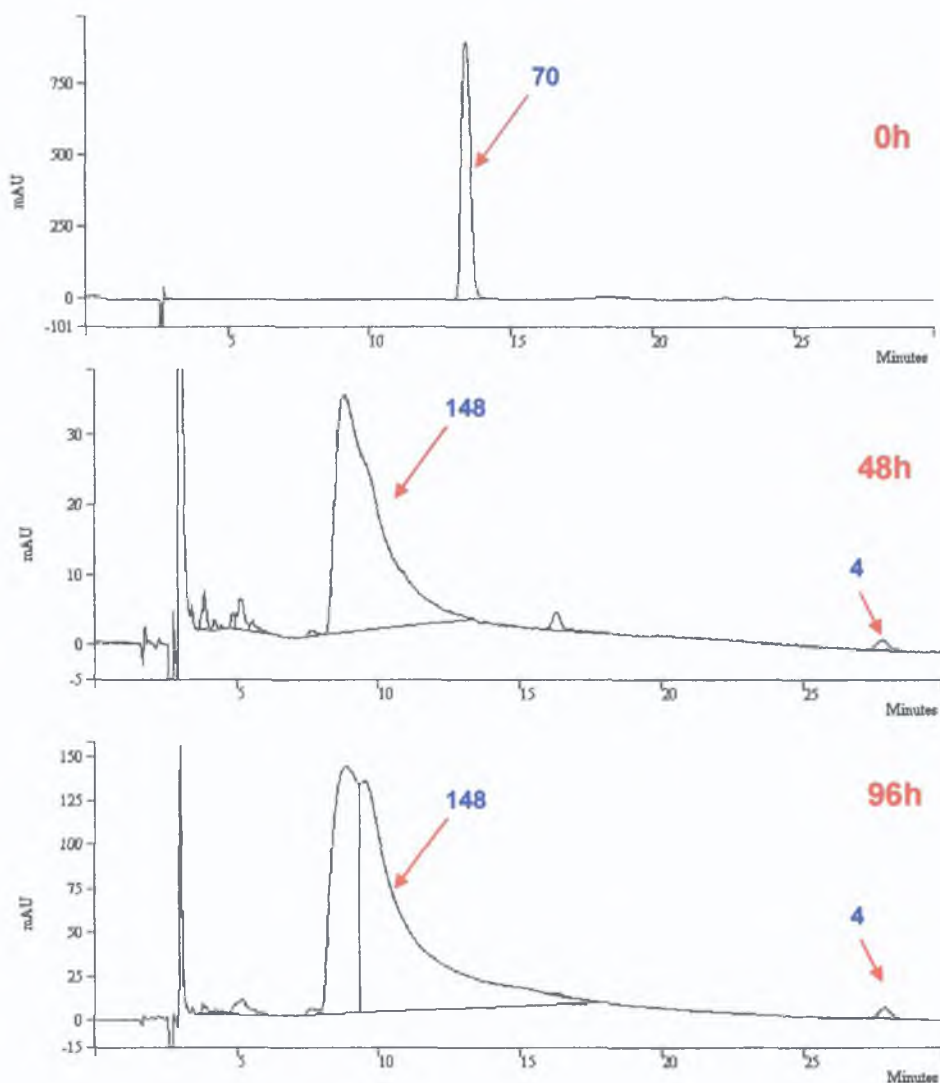


Figure 5.36 LC Chromatographic data of 'Control' reaction of **70** and NaH in DMF

As no alkylating agent was added, the halide of this group cannot undergo dehalogenation to form the halide ion and the protonated alkylating agent (*Figure 5 35*)

It was evident that NaH base was necessary for the observed cleavage phenomenon of **70** to **4**

5.3 Conclusion

The synthesis of a novel calix[4]arene derivative bearing a tetrahedral binding site, 5,11,17,23-*p*-tetra-*tert*-butyl-25,27-bis(ethoxycarbonylmethoxy)-26,28-bis(hydroxycarbonylethoxy)calix[4]arene (**1**) has been achieved

Though this synthetic step did not proceed according to the reaction mechanism, the synthetic conditions for the synthesis of this tetrahedrally shaped calix[4]arene derivative have been established although the yield is very low. Conditions must be optimised further to minimise the synthesis of by-products while maximising the synthesis of the tetrahedrally shaped calix[4]arene derivative.

LC-DAD Analysis has proven to be essential for providing the means to determine, explain and rationalise the progression of the reaction, by allowing the determination of what exactly is occurring in this reaction, by aiding the explanation of the product distribution of these reactions and rationalising the reformation of **4**.

This reaction has been carried out several times, consistently yielding **1**, indicative that hydrolysis of the long chained ligating tails appended onto the calix[4]arene scaffold is occurring. **1** is the first example of a low-symmetrical calix[4]arene derivative functionalised with a 'tetrahedral' binding site and represents a novel derivative with potentially unique complexing abilities towards tetrahedral molecules or ions such as NH_4^+ , PO_4^{3-} , or SO_4^{2-} .

5 4 Experimental

5 4 1 General

Melting points are uncorrected ^1H and ^{13}C NMR spectra were recorded on a Bruker 400MHz and 100MHz Spectrometer using CDCl_3 as solvent unless stated otherwise IR spectra were recorded on a Perkin Elmer Spectrum GX FT-IR System A Bruker Mass Spectrometer, employing electrospray ionization was used to record the mass spectra of the derivatives synthesized The solvent used, anhydrous dimethyl formamide (DMF), ethanol and HPLC grade acetonitrile were purchased from Sigma-Aldrich Formic Acid (A C S reagent) purchased from Sigma-Aldrich was used for preparing mobile phase for the LC-DAD system Ethyl 3-bromopropionate, sodium hydride and metal carbonate bases (Lithium, Sodium, Potassium), triethylamine, DBU, sodium ethoxide, and acrylamide were supplied by Sigma-Aldrich

5 4 2 Synthesis of a Differentially 1,3- and 2,4 Substituted *p*-Tetra-*t*-butylcalix[4]arene

A suspension of **70** (1.0g, 1.22mM) and base, 10 molar excess (*Table 5 2*) in DMF (35ml) was stirred at room temperature for 1h Subsequently, ethyl-3-bromopropionate (3.31g, 18.3mM) was added, and the mixture was stirred at 65-70°C for 48h Following this, the mixture was cooled to room temperature, an extra aliquot of base and alkylating agent were added This was then stirred at 65-70°C for a further 72hr Once again, the reaction was cooled to room temperature, poured onto ice and extracted with ethyl acetate (4 x 25ml), washed with water, saturated NH_4Cl and brine solution (4x25ml) The organic extract was dried over anhydrous magnesium sulphate (MgSO_4) and the solvent removed under reduced pressure

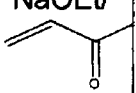
Reaction	Base	Observed Mass	Proposed Derivatives
A	Li ₂ CO ₃	815/831 843/859	t-Bu-1-monoethylacid-3-monoethylester (159) <i>p</i> -t-Butyl-1,3-Diethyl ester (70)
B	Na ₂ CO ₃	843/859	<i>p</i> -t-Butyl-1,3-Diethyl ester (70)
C	K ₂ CO ₃	815/831 843/859	t-Bu-1-monoethylacid-3-monoethylester (159) <i>p</i> -t-Butyl-1,3-Diethyl ester (70)
D	Triethyl-amine	843/859	<i>p</i> -t-Butyl-1,3-Diethyl ester (70)
E	DBU	843/859	<i>p</i> -t-Butyl-1,3-Diethyl ester (70)
F	NaOEt/ 	815/831 843/859	t-Bu-1-monoethylacid-3-monoethylester (159) <i>p</i> -t-Butyl-1,3-Diester (70)
G	NaH	787/803 887/903 987/1003	<i>p</i> -t-Butyl-1,3-Diethyl acid (148) <i>p</i> -t-Bu-1-monoethylacid-2-monopropyl acid-3-monoethyl ester (161) <i>p</i> -t-Bu-1,3-diethyl ester-2,4-dipropyl acid (1)

Table 5 2 *Details of the reaction conditions investigated*

5 4 3 Exhaustive Alkylation of 5,11,17,23-Tetra-tert-butyl-25,27-bis(ethoxy carbonylmethoxy)-26,28-dihydroxycalix[4]arene using NaH as base

Reaction	Stoichiometry Calix NaH EtBrProp	Interval Addition of NaH EtBrProp	Mode of Addition of NaH
G1	1 20 30	2 x 48h	Activated & Deactivated
G2	1 20 30	4 x 24h	Activated & Deactivated
G3	1 10 15	4 x 24h	Activated & Deactivated

Table 5 3 *Mechanistic Reactions attempted for the synthesis of a calix[4]arene dervative bearing a tetrahedral binding site*

The procedure was followed as stated above to which NaH (0.49g, 12.2mM) was added. The solvent was removed under reduced pressure to yield a waxy

orange solid This was purified by column chromatography [SiO₂, Ethyl Acetate/n-Hexane 5:1]

5,11,17,23-Tetra-*tert*-butyl-25,27-bis(ethoxycarbonylmethoxy)-26,28-bis(hydroxycarbonylethoxy)calix[4]arene (1)

Fraction A gave a cream solid (0.047g, 9.4%) mp 162-165 °C, IR (KBr) λ_{max} [cm⁻¹] 3417, 2947, 1725, 1748, R_f 0.92, ¹H NMR δ 0.95, 1.2 (s, 36H, CMe₃), 1.26 (t, J=7.2 Hz, 6H, CH₃), 2.76 (bt, 4H, J=5.3 Hz, CH₂), 3.29 and 3.32 (d, 4H, J=13.2 Hz, ArCH₂Ar), 4.03 (q, 4H, J=7.2 Hz, C(O)CH₂), 4.37 and 4.40 (d, 4H, J=13.2 Hz, ArCH₂Ar), 4.51 (bt, 4H, J=6.0 Hz, CH₂), 4.71 (s, 4H, OCH₂), 6.79 (s, 4H, ArH), 7.03 (s, 4H, ArH), ¹³C NMR δ 14.2, 22.7, 29.3, 31.2, 31.6, 33.8, 60.6, 60.8, 72.2, 125.1, 125.6, 126.6, 127.6, 127.9, 132.4, 141.5, 147.2, 150.2, 150.4, 146.6 and 170.5, m/z (EI) 987.5 and 1003.5

5,11,17,23-Tetra-*tert*-butyl-25,27-bis(carboxymethoxy)-26,28-dihydroxycalix[4]arene (148)

Fraction B gave a white solid mp >280 °C, IR (KBr) λ_{max} [cm⁻¹] 3417, 2952, 1730, R_f 0.37, ¹H NMR δ 0.97, 1.28 (s, CMe₃, 36H), 3.15 (bs, ArCH₂Ar, 4H), 4.17 (bs, ArCH₂Ar, 4H), 4.60 (bs, OCH₂, 4H), 6.64 (s, ArH, 4H), 6.96 (s, ArH, 4H), 7.79 (bs, OH, 2H), ¹³C NMR δ 30.8, 30.9, 31.1, 31.4, 31.7, 33.8, 33.9, 125.3, 125.6, 131.9, 142.4, 149.4, m/z (EI) 787.5 and 803.5

5,11,17,23-Tetra-*tert*-butyl-25-(ethoxycarbonylmethoxy)-27-(carboxymethoxy)-26,28-dihydroxycalix[4]arene (160)

To **70** (0.8g, 0.98mM) and sodium ethoxide (NaOEt) (0.13g, 1.951mM) in ethanol (35ml) was stirred at 50 °C for 2h. Subsequently, acrylamide (0.2g, 2.87mM) was added, and the mixture was stirred at 65-70°C for 8h. Following this, the mixture was cooled to room temperature, poured onto ice and extracted with ethyl acetate (4 x 25ml), washed with water and brine solution (4x25ml). The organic extract was dried over anhydrous magnesium sulphate (MgSO₄) and the solvent removed under reduced pressure. This was then purified by column chromatography using 1:1 Hexane Ethyl Acetate as eluent to afford a cream solid (0.39g, 50%) mp 206-210 °C, IR (KBr) λ_{max} [cm⁻¹] 3429, 2958, 1748, 1727, ¹H NMR δ 0.97, 1.01, 1.25 (s, 36H, CMe₃), 1.32 (t, 3H, J=7.1 Hz, CH₃), 3.30 and 3.34 (d, 2H, J=13.2 Hz, ArCH₂Ar), 3.42 and 3.46 (d, 2H, J=13.4 Hz, ArCH₂Ar), 4.14 and 4.18 (d, 2H, J=13.4 Hz, ArCH₂Ar), 4.29 (q, 2H, J=7.1 Hz, C(O)CH₂), 4.43 and 4.47

(d, 2H, $J=13$ Hz, ArCH₂Ar), 4.68 (bs, 2H, OCH₂), 4.72 (s, 2H, OCH₂), 6.83 (s, 2H, ArH), 6.97 (s, 2H, ArH), 7.02 (s, 2H, ArH), 7.06 (s, 4H, ArH), 7.13 (s, 2H, OH), ¹³C NMR δ 30.9, 31.0, 31.5, 31.6, 31.8, 32.3, 33.7, 33.8, 33.9, 34.1, 61.2, 72.3, 125.0, 125.6, 125.7, 126.2, 126.3, 127.2, 127.9, 132.5, 141.5, 143.0, 147.1, 148.4, 149.0, 149.1, 150.2, 150.6, 169.2 m/z (EI) 815.3 and 831.3

5.4.4 Direct Infusion Mass Spectral Analysis

Using the syringe injector of the mass spectrometer, samples were infused into the ESI source (positive mode) at a rate of 2.5 $\mu\text{L min}^{-1}$. The nebulisation gas and drying gas were set at 15 psi and 4 L min^{-1} respectively while the source temperature was maintained at 250°C. The octapole voltage was 2.83 kV, the skimmer 1 voltage was 50 ± 5 V and the trap drive voltage was 57 ± 2 V. The scan range covered was typically 500-1500 m/z . Online MS/MS analysis was carried out using an isolation width of 4 Da and a collisional amplitude of 1.8-2.3 V was used depending on the ion being fragmented. Samples were prepared in acetonitrile to a concentration of 0.1 mg/ml.

High Resolution Mass Spectra were carried out by Bruker Daltonics Ltd using a 9.4 FTMS system and an Esquire 3000 plus ion trap. The ESI source was set to a positive mode. The skimmer 1 voltage was 76.0 V and the trap drive voltage was 79.3 V. The scan range covered was 200-1200 m/z .

5.4.5 LC-DAD Analysis

A Varian HPLC system was used to obtain UV-Visible spectra of various components in the reaction mixture. It comprised of a Varian Prostar 330 PDA detector, a gradient Prostar 230 pump and a manually operated switching valve with a 20 μL injector loop. Prior to use, the mobile phase was degassed by sonication. The system was controlled by Varian software. The following parameters were used: Supelco-C18, 250 x 4.6 mm, 5 μm column with a mobile phase of 95/5/0.1 v/v/v ACN/H₂O/Formic Acid, flowrate of 1.5 ml/min. The monitoring wavelength was 210 nm and an injection volume of 20 μL was used. Samples were prepared in ACN to a concentration of 0.5 mg/ml.

Conclusion

The shape and size of calixarenes provide a unique molecular scaffold on which ionic or molecular receptors may be designed. Calixarenes with four identical ligating groups at either/both the upper and lower rim have sought recognition as effective ionic and molecular receptors, particularly for cationic species.

It was the objective to design and synthesise a novel receptor with a different spatial arrangement of binding sites at the lower rim (tetrahedral) than the conventional octahedral arrangement of binding sites. This preorganisation of the binding sites may encourage the preferential complexation with tetrahedrally shaped guest-ions that have complementary charge distribution, leading to new patterns of selectivity for the corresponding ion sensors.

The synthetic strategy chosen for this target calix[4]arene derivative was the selective alkylation of the 1 and 3 position of the parent *p*-tetra-*t*-butylcalix[4]arene with a short chain ligating group and subsequent alkylation of the 2 and 4 position with a longer chain ligating group.

A series of derivatisation reactions of *p*-tetra-*t*-butylcalix[4]arene and ethyl bromoacetate was carried out. The controlling reaction parameters, for example, base, stoichiometry, solvent and time were altered in order to maximise the yield of the disubstituted *p*-tetra-*t*-butylcalix[4]arene derivative. Preliminary MS results indicated that a number of products, mainly mono-, tri- and tetrasubstituted derivatives resulted.

Obtaining reliable routes to partially substituted calix[4]arene derivatives was essential as they provide a template for generating more complex derivatives. LC-UV-MS and LC-DAD methods were employed to identify and analyse the products obtained in these reactions and was valuable in the optimisation of the reaction conditions for the synthesis of a disubstituted *p*-tetra-*t*-butylcalix[4]arene derivative.

The reaction procedures developed by LC-MS and LC-DAD for the preparation of 5,11,17,23-Tetra-*tert*-butyl-25,27-bis(ethoxycarbonylmethoxy)-26,28-dihydroxycalix[4]arene were successfully applied to the synthesis of other partially functionalised calix[4]arene derivatives. Such derivatives included 5,11,17,23-Tetra-*tert*-butyl-25-(aminocarbonylmethoxy)-26,27,28-trihydroxycalix[4]arene (*t*-butylcalix [4]arene monoamide), 5,11,17,23-*p*-tetra-*tert*-butyl-25,27-bis(aminocarbonylmethoxy)-26,28-dihydroxycalix[4]arene (*t*-butylcalix[4]arene

diamide), 5,11,17,23-*p*-tetra-*tert*-butyl-25,27-bis(carboxymethoxy)-26,28-dihydroxycalix[4]arene, (*t*-butylcalix[4]arene diacid) and 25,27-bis(ethoxycarbonyl methoxy)-26,28-dihydroxy calix[4]arene (*calix*[4]arene diester)

LC-UV and DI-MS studies concluded that the mass spectrometer was much more sensitive to 5,11,17,23-*p*-tetra-*tert*-butyl-25,27-bis(ethoxycarbonylmethoxy)-26,28-dihydroxycalix[4]arene relative to 5,11,17,23-*p*-tetra-*tert*-butyl-25-(ethoxycarbonyl methoxy)-26,27,28-trihydroxycalix[4]arene. This was attributed to their differing shape which influences their relative affinity for sodium ions. The former is more predisposed to complex a sodium ion as the symmetrical arrangement of two ligating groups at the lower rim facilitates encapsulation of sodium whereas the latter, with a single ligating carbonyl group is less efficient at sodium complexation.

To verify this complexation behaviour, ISE and NMR studies were carried out on these disubstituted derivatives. The 5,11,17,23-*p*-tetra-*tert*-butyl-25,27-bis(ethoxy carbonylmethoxy)-26,28-dihydroxycalix[4]arene ionophore produces sensors that exhibit Nernstian behaviour with a number of ions. The calix[4]arene counterpart exhibited complexing affinity for the larger potassium and caesium cations. The disubstituted *p*-tetra-*t*-butylcalix[4]arene acid and amide derivatives did not exhibit complexing abilities for any Group I, II ions but due to the nature of the ligating tails, the latter derivative was proven by ISE and NMR to demonstrate complexing affinity for such anions as spherical and tetrahedral anions.

5,11,17,23-*p*-tetra-*tert*-butyl-25,27-bis(ethoxycarbonylmethoxy)-26,28-dihydroxycalix[4]arene served as a precursor for the synthesis of the tetrahedral shaped *p*-*t*-butylcalix[4]arene. HPLC-MS determined the reaction conditions required for the synthesis of this novel derivative and also, charted the progression of this reaction. The reaction conditions chosen whilst accomplishing the synthesis of the calix[4]arene bearing a tetrahedral pocket also incurred some interesting phenomena, namely 'Cleavage of the Alkyl-Aryl Ether linkage' and possible 'Intramolecular Hydrolysis'.

Synthesis and Functionalisation of Calixarene derivatives as demonstrated by this research is problematic but the combination of synthetic and analytical

procedures to synthesise, monitor, identify and characterise the products of such derivatisation reactions has proven invaluable to Calixarene Chemistry

Bibliography

- 1 C D Gutsche, *Calixarenes*, Monographs in Supramolecular Chemistry, Royal Society of Chemistry, Cambridge, UK, **1989**
- 2 C D Gutsche, *Calixarenes Revisited*, Monographs in Supramolecular Chemistry, Royal Society of Chemistry, Cambridge, UK, **1998**
- 3 C D Gutsche, *Acc Chem Res* **1983**, *16*,161-170
- 4 J Vicens, V Bohmer, Eds *Calixarenes A versatile class of Macrocyclic Compounds* Kluwer Academic Press Dordrecht, **1991**
- 5 A Pochini, R Ungaro, *Calixarenes and Related Hosts*, Supramolecular Chemistry, Pergamon Press, 2, 103-142
- 6 V Bohmer, *Angew Chem Int Ed Engl* **1995**, *34*, 713-745
- 7 V Bohmer, P Chim, H Kammerer, *Makromol Chem* **1979**, *180*, 2503-2506
- 8 V Bohmer, F Marschollek, L Zetta, *J Org Chem* **1987**, *52*, 3200-3205
- 9 J DeMendoza, P M Nieto, P Prados, C Sanchez, *Tetrahedron*, **1990**, *46*, 671-682
- 10 K No, K L Hwang, *Bull Korean Chem Soc* **1993**, *14*, 753-755
- 11 V Bohmer, L Merkel, U Kunz, *J Chem Soc, Chem Commun* **1987**, 896-897
- 12 C D Gutsche, L J Bauer, B Dhawan, K H No, J A Levine, *Tetrahedron*, **1983**, *39*, 409
- 13 A Arduini, A Pochini, S Reverben, R Ungaro, G D Andreetti, F Ugozzoli, *Tetrahedron*, **1986**, *42*, 2089-2100
- 14 F Arnaud-Neu, E M Collins, M Deasy, G Ferguson, S J Harris, B Kartner, A J Lough, M A McKervey, E Marques, B L Ruhl, M-J Schwing-Weill, E M Seward, *J Am Chem Soc* **1989**, *111*, 8681-8691
- 15 S-K Chang, I Cho, *Chem Lett* **1984**, 477-478
- 16 S-K Chang, I Cho, *J Chem Soc, Perkin Trans 1*, **1986**, 211-214
- 17 S-K Chang, S-K Kwon, I Cho, *Chem Lett* **1987**, 947-948
- 18 G Calestani, F Ugozzoli, A Arduini, E Ghidini, R Ungaro, *J Chem Soc, Chem Commun* **1987**, 344-346
- 19 A Arduini, E Ghidini, A Pochini, R Ungaro, G D Andreetti, G Calestani, F Ugozzoli, *J Incl Phenom* **1988**, *6*, 119-134
- 20 F Arnaud-Neu, M-J Schwing-Weill, K Ziat, S Cremin, S J Harris, M A McKervey, *New J Chem* **1991**, *15*, 33-37
- 21 G Ferguson, B Kartner, M A Mc Kervey, E M Seward, *J Chem Soc, Chem Commun* **1987**, 584-585

- 22 G Barrett, M A McKervey, J F Malone, A Walker, F Arnaud-Neu, L Guerra, M-J Schwing-Weill, C D Gutsche, D R Stewart, *J Chem Soc, Perkin Trans 2*, **1993**, 1475-1479
- 23 H Otsuka, K Araki, S Shinkai, *Chem Express*, **1993**, 8, 479
- 24 H Otsuka, K Araki, T Sakaki, K Nakashima, S Shinkai, *Tet Lett* **1993**, 34, 45, 7275-7278
- 25 K Iwamoto, S Shinkai, *J Org Chem* **1992**, 57, 7066-7073
- 26 F Arnaud-Neu, G Barrett, S Cremin, M Deasy, G Ferguson, S J Harris, A J Lough, L Guerra, M A McKervey, M-J Schwing-Weill, P Schwinte, *J Chem Soc, Perkin Trans 2*, **1992**, 1119-1125
- 27 P L H M Cobben, R J M Egbenk, J G Bomer, P Bergveld, W Verboom, D N Reinhoudt, *J Am Chem Soc* **1992**, 114, 10573-10582
- 28 J-D van Loon, W Verboom, D N Reinhoudt, *Org Prep, Proceed Int* **1992**, 24, 437
- 29 S Shinkai, *Tetrahedron*, **1993**, 49, 40, 8933-8968
- 30 L C Groenen, B H M Ruel, A Casnati, P Timmerman, W Verboom, S Harkema, A Pochini, R Ungaro, D N Reinhoudt, *Tet Lett* **1991**, 32, 2675
- 31 L C Groenen, J-D van Loon, W Verboom, S Harkema, A Casnati, R Ungaro, A Pochini, F Ugozzoli, D N Reinhoudt, *J Am Chem Soc* **1991**, 113, 2385-2392
- 32 K Iwamoto, K Araki, S Shinkai, *Tetrahedron*, **1991**, 47, 25, 4325-4342
- 33 K Araki, K Iwamoto, S Shinkai, T Matsuda, *Chem Lett* **1989**, 1747
- 34 K Araki, K Iwamoto, S Shinkai, T Matsuda, *J Org Chem* **1991**, 56, 4955-4962
- 35 K Iwamoto, K Fugimoto, T Matsuda, S Shinkai, *Tet Lett* **1990**, 31, 49, 7169-7172
- 36 K Araki, K Iwamoto, S Shinkai, *J Chem Soc, Perkin Trans 1*, **1991**, 1611-1613
- 37 F Arnaud-Neu, G Barrett, S J Harris, M Owens, M A McKervey, M-J Schwing-Weill, P Schwinte, *Inorg Chem* **1993**, 32, 2644-2650
- 38 J K Moran, E M Georgiev, A T Yordanov, J T Mague, D M Roundhill, *J Org Chem* **1994**, 59, 5990-5998
- 39 H Kammerer, G Happel, V Bohmer, D Rathay, *Monatsch Chem* **1978**, 109, 767
- 40 C D Gutsche, J A , Levine, *J Am Chem Soc* , **1982**, 104, 2652-2653

- 41 M Tashiro, G Fukato, S Mataka, K Or, *Org Prep Proced Int* **1975**, 7, 231
- 42 M Tashiro *Synthesis*, **1979**, 921
- 43 M Tashiro, T Yamato, *J Org Chem* **1981**, 46, 1543-1552
- 44 M Tashiro, T Yamato, *J Org Chem* **1985**, 50, 2939-2942
- 45 C D Gutsche, J A Levine, P K Sujeeth, *J Org Chem* **1985**, 50, 5802-5806
- 46 S G Rha, S-K Chang, *J Org Chem* **1998**, 63, 2357-2359
- 47 F Hamada, S G Bott, G W Orr, A W Coleman, H Zhang, J Atwood, *J Incl Phenom* **1990**, 9, 195
- 48 K Park, H-J Kim, S-K Chang, *Supramol Chem* **1995**, 5, 83
- 49 K Park, H Ihm, *Chem Lett* **1996**, 311
- 50 W Verboom, R J Bodewes, G van Essen, P Timmerman, G J van Hummel, S Harkema, D N Reinhoudt, *Tetrahedron*, **1995**, 51, 499
- 51 S Shinkai, T Anmura, K Araki, H Kawabata, H Satoh, T Tsubaki, O Manabe, J Sunamoto *J Chem Soc , Perkin Trans 1*, **1989**, 2039-2045
- 52 D M Rudkevich, W Verboom, D N Reinhoudt, *J Org Chem* **1994**, 59, 3683-3686
- 53 G Misin, E Graf, M W Hosseini, *Tet Lett* **1996**, 37, 26, 4503-4506
- 54 S Shinkai, K Araki, T Tsubaki, T Anmura, O Manabe, *J Chem Soc , Perkin Trans 1*, **1987**, 2297
- 55 S Shinkai, H Koreishi, K Ueda, T Anmura, O Manabe, *J Am Chem Soc* **1986**, 108, 2409-2416
- 56 S Shinkai, K Araki, O Manabe, *J Chem Soc , Chem Commun* **1988**, 187-189
- 57 Y Morzhenn, D M Rudkevich, W Verboom, D N Reinhoudt, *J Org Chem* **1993**, 58, 7602-7605
- 58 M H B Gansey, W Verboom, D N Reinhoudt, *Tet Lett* **1994**, 35, 7127
- 59 S Shinkai, T Tsubaki, T Sone, O Manabe, *Tet Lett* **1985**, 26, 3343
- 60 S Shinkai, H Koreishi, K Ueda, O Manabe, *J Chem Soc , Chem Commun* **1986**, 233
- 61 P Sykes, *A Guidebook to Mechanism in Organic Chemistry*, Longman Scientific & Technical Press
- 62 D J Reif, H O House, *Org Syn* , **1963**, Coll Vol, IV, 375
- 63 J P Schafer, J G Higgins, P K Sheney, *Org Syn* **1973**, Coll Vol V, 249
- 64 C D Gutsche, K C Nam, *J Am Chem Soc* **1988**, 110, 6153-6162

- 65 M Almi, A Arduini, A Casnati, A Pochini, R Ungaro, *Tetrahedron*, **1989**, *45*, 7, 2177-2182
- 66 C D Gutsche, I Alam, *Tetrahedron*, **1988**, *44*, 15, 4689-4694
- 67 I Alam, S K Sharma, C D Gutsche, *J Org Chem* **1994**, *59*, 3716-3722
- 68 A Arduini, A Casnati, M Fabbi, P Minan, A Pochini, A R Sicuri, R Ungaro, *Supramol Chem* **1993**, *1*, 235
- 69 T Nagasaki, K Sisido, T Anmura, S Shinkai, *Tetrahedron*, **1992**, *48*, 5, 797-804
- 70 S Armon, T Nagasaki, S Shinkai, *J Chem Soc , Perkin Trans 1*, **1993**, 887-889
- 71 K Araki, K Sisida, K Hisaidi, S Shinkai, *Tet Lett* **1993**, *34*, 8297
- 72 A M Yuldashev, B T Ibragimov, S A Tallpov, H L Gapparov, *J Struct Chem* **1996**, *37*, 470
- 73 Y S Zheng, Z T Huang, *Synth Commun* **1997**, *27*, 1237
- 74 A Arduini, A Pochini, A Rizzi, A R Sicuri, F Ugozzoli, R Ungaro, *Tetrahedron*, **1992**, *48*, 905
- 75 C D Gutsche, S K Sharma, *Tetrahedron*, **1994**, *50*, 14, 4087-4104
- 76 C D Gutsche, S Kanamathareddy, *J Org Chem* **1995**, *60*, 6070-6075
- 77 L C Groenen, B H M Ruel, A Casnati, W Verboom, A Pochini, R Ungaro, D N Reinhoudt, *Tetrahedron*, **1991**, *47*, 39, 8379-8384
- 78 A Casnati, A Arduini, E Ghidini, A Pochini, R Ungaro, *Tetrahedron*, **1991**, *47*, 12/13, 2221-2228
- 79 J Ruhwn, N Wong, *Chem Rev* **1989**, *89*, 1599-1615
- 80 G A Olah, S C Nareig, *Tetrahedron*, **1982**, *38*, 15, 2225-2227
- 81 Z T Huang, G-Q Wang, *Synth Commun* **1994**, *24*, 1, 11-22
- 82 J-D van Loon, A Arduini, W Verboom, R Ungaro, G J van Hummel, S Harkema, D N Reinhoudt, *Tet Lett* **1989**, *30*, 20, 2681-2684
- 83 E M Collins, M A McKervery, *J Chem Soc , Perkin Trans 1*, **1989**, 372-374
- 84 V Bohmer, A Wolff, W Vogt, *J Chem Soc , Chem Commun* **1990**, 968-970
- 85 C D Gutsche, M Iqbal, K S Nam, K See, I Alam, *Pure Appl Chem* **1988**, *60*, 483-488
- 86 C D Gutsche, M Iqbal, K S Nam, T Rogers, I Alam, T J Mangiafico, *J Incl Phenom Mol Recognition Chem* **1989**, *7*, 73-81
- 87 C D Gutsche, L-G Lin, *Tetrahedron*, **1986**, *42*, 6, 1633-1640
- 88 C D Gutsche, M Iqbal, T Mangiafico, *Tetrahedron*, **1987**, *43*, 21,

4917-4930

- 89 S Shinkai, T Otsuka, K Fujimoto, T Matsuda, *Chem Lett* **1990**, 835
- 90 K Iwamoto, K Fujimoto, T Matsuda, S Shinkai, *Tet Lett* **1991**, 32, 830
- 91 K Iwamoto, K Fujimoto, T Matsuda, S Shinkai, *Tet Lett* **1990**, 31, 7169-7172
- 92 G Ferguson, J F Gallagher, L Giunta, P Nen, S Pappalardo, M Parisi, *J Org Chem* **1994**, 59, 42-53
- 93 C-M Shu, W-S Ching, *J Org Chem* **1999**, 64, 2673-2679
- 94 K A See, F R Franczek, W H Watson, R P Kashyap, C D Gutsche, *J Org Chem* **1991**, 56, 7256-7268
- 95 J-D van Loon, A Arduini, L Coppi, W Verboom, A Pochini, R Ungaro, S Harkema, D N Reinhoudt, *J Org Chem* **1990**, 55, 5639-5646
- 96 P D Beer, M G B Drew, C Hazlewood, D Hesek, J Hodacova, S E Stokes, *J Chem Soc, Chem Commun* **1993**, 229-231
- 97 Z-T Huang, G-Q Wang, *J Chem Soc, Perkin Trans 1*, **1993**, 167-168
- 98 C D Gutsche, L-G Lin, *Tetrahedron*, **1986**, 42, 6, 1633-1640
- 99 C D Gutsche, *Organometallics*, **1994**, 13, 5157-5159
- 100 K O'Connor, G Svehla, S J Harns, M A McKervey, *Talanta*, **1992**, 39, 325
- 101 H-J Schneider, A K Yatsimirsky, *Principles and Methods in Supramolecular Chemistry*, Eds, John Wiley & Sons, Ltd
- 102 D J Cram, *Angew Chem Int Engl* **1988**, 27, 8, 1009-1020
- 103 J-M Lehn, *Angew Chem Int Engl* **1988**, 27, 1, 89-112
- 104 D J Cram, *Angew Chem Int Ed Engl* **1986**, 98, 1041
- 105 D Parker, *Macrocyclic Synthesis*, Oxford University Press, 1996
- 106 C Pedersen, *J Am Chem Soc* **1967**, 89, 7017
- 107 D Semlyen, *Large Ring Molecules*, John Wiley & Sons, Ltd
- 108 D Diamond, K Nolan, *Anal Chem* **2001**, 73, 23-29
- 109 F Cadogan, P Kane, M A McKervey, D Diamond, *Anal Chem* **1999**, 71, 5544
- 110 D Diamond, G Svehla, E M Seward, M A McKervey, *Anal Chim Acta*, **1988**, 204, 223
- 111 D Schmidtchen, G Berger, *Chem Rev* **1997**, 97, 5, 1609-1646
- 112 A Bianchi, K Bowman-James, E Garcia-España, *Supramolecular Chemistry of Anions*, Eds, Wiley-VCH Press
- 113 C H Park, H Simmons, *J Am Chem Soc* **1968**, 90, 2431
- 114 J R Holum, *Organic & Biological Chemistry*, Wiley Press

- 115 P A Gale, *Coord Chem Rev* **2000**, *199*, 181-233
- 116 P A Gale, *Coord Chem Rev* **2001**, *213*, 79-128
- 117 R H Crabtree, *J Am Chem Soc* **1997**, *119*, 2325-2326
- 118 B R Cameron, S J Loeb, *J Chem Soc, Chem Commun* **1997**, 573-574
- 119 P D Beer, M G B Drew, D Hesk, K C Nam, *J Chem Soc, Chem Commun* **1997**, 107-108,
- 120 P A Gale, Z Chen, M G B Drew, J A Heath, P D Beer, *Polyhedron*, **1988**, *17*, 405-412
- 121 P A Gale J L Sessler, V Kral, V , Lynch, *J Am Chem Soc* **1996**, *118*, 5140-5141
- 122 P A Gale, J L Sessler, V Lynch, P I Sansom, *Tet Lett* **1996**, *37*, 7881
- 123 P A Gale J L Sessler, W E Allen N A Tvermoes, V Lynch, *J Chem Soc, Chem Commun* **1997**, 665
- 124 J F J Valiyavethil, W Engbersen, *Angew Chem Int Ed, Engl* **1993**, *32*, 900
- 125 J F Malone, D J Marrs, M A McKervey, P O'Hagan, N Thompson, A Walker, F Arnaud-Neu, O Maupnvez, M-J Schwing-Weill, J-F Dozol, H Rouquette, N Simon, *J Chem Soc, Chem Commun* **1995**, 2151-2153
- 126 T McKittrick, D Diamond, D J Marrs, P O'Hagan, M A McKervey, *Talanta*, **1996**, *43*, 1145-1148
- 127 P D Beer, *Acc Chem Res* **1998**, *31*, 2, 71-80
- 128 M M G Antonisse, B H M SnellinkRuel, J F J Engerbrsen, D N Reinhoudt, *Sens Actuators B-Chemical*, **1998**, *47*, 9-12
- 129 F Arnaud-Neu, M-J Schwing-Weill, *Synth Metals* **1997**, *90*, 157-164
- 130 A Ikeda, S Shinkai, *Chem Rev* **1997**, *97*, 1713-1734
- 131 D M Perreault, L A Cabell, E V Anslyn, *Biorg & Med Chem* **1997**, *5*, 6, 1209-1220
- 132 P Buhlmann, S Nishizawa, K P Xiao, Y Umezawa, *Tetrahedron* **1997**, *53*, 5, 1647-1654
- 133 S E Matthews, P D Beer, *Calixarenes 2001*, Kluwer Academic Publishers, **2001**, 421-439
- 134 M A McKervey, M-J Schwing-Weill, F Arnaud-Neu, *Cation Binding by Calixarenes*, Supramolecular Chemistry, Pergamon Press, *1*, 538-600
- 135 F Arnaud-Neu, M A McKervey, M-J Schwing-Weill, *Calixarenes 2001* Kluwer Academic Publishers, **2001**, 385-406
- 136 C D Gutsche, M Iqbal, D Stewart, *J Org Chem* **1986**, *51*, 742-745

137. C.J. Pedersen, *J. Am. Chem. Soc.* **1967**, *89*, 7017
138. L. Stryer, *Biochemistry*, 3rd Edition, W.H. Freeman & Co.
139. J-M. Lehn, *Supramolecular Chemistry*, VCH Press.
140. N. Pelizzi, A. Casnati, A. Friggeri, R. Ungaro, *J. Chem. Soc., Perkin Trans. 2*, **1998**, 1307
141. F. Ohseto, H. Yamamoto, H. Matsumoto, S. Shinkai, *Tet. Lett.* **1995**, *36*, 6911
142. F. Arnaud-Neu, S. Barbosa, F. Berny, A. Casnati, N. Muzet, A. Pinalli, R. Ungaro, M.J. Schwing-Weill, G. Wipff, *J. Chem. Soc., Perkin Trans. 2*, **1999**, 1727-1738
143. W.F. Nijenhuis, A.R. van Doorn, A.M. Reichwein, F. de Jong, D.N. Reinhoudt, *J. Am. Chem. Soc.* **1991**, *113*, 3607; W.F. van Straaten-Nijenhuis, A.R. van Doorn, A.M. Reichwein, F. de Jong, D.N. Reinhoudt *J. Org. Chem.* **1993**, *58*, 2265; A.M. Reichwein, W. Verboom, S. Harkema, A.L. Spek, D.N. Reinhoudt, *J. Chem. Soc., Perkin Trans. 2*, **1994**, 1167.
144. G. McMahon, R. Wall, K. Nolan, D. Diamond, *Talanta*, **2002**, *57*, 1119-1132.
145. R. Willoughby, E. Sheehan, S. Mitrovich, *A Global View of LC/MS*, Global View Publishing.
146. http://www.waters.com/Waters Website/Applications/LCMS/lcms_cc.htm
147. http://www.waters.com/Waters Website/Applications/LCMS/lcms_hpl.htm
148. http://www.waters.com/Waters Website/Applications/LCMS/lcms_itq.htm
149. http://www.waters.com/Waters Website/Applications/LCMS/lcms_fra.htm
150. B.S. Creaven, M. Deasy, J.F. Gallagher, J. McGinley, B.A. Murray, *Tetrahedron*, **2001**, *57*, 8883-8887.
151. P. Neri, C. Geraci, M. Piattelli, *J. Org. Chem.* **1995**, *60*, 4126-4135.
152. http://www.usm.maine.edu/~newton/Chy251_253/Lectures/Sn2Solvents/sn2solvents.html
153. G.W. Klumpp, *Reactivity in Organic Chemistry*, Wiley Interscience.
154. M.B. Smith, J. March, *Advanced Organic Chemistry: Reactions, Mechanisms and Structure*, 5th Edition, Wiley Interscience.
155. T.H. Lowry, K.S. Richardson, *"Mechanism and Theory in Organic Chemistry"*, Harper and Row.
156. <http://www.chem.ucalgary.ca/courses/350/Carey/Ch08/ch8-8.html>
157. <http://www.usm.maine.edu/~newton/Chy251/Lectures/Solvents.html>
158. F. Benevelli, W. Kolodziejski, K. Wozniak, J. Klinowski, *Chem. Phys. Lett.* **1999**, *308*, 65-70

- 159 R Abidi, M V Baker, J M Harrowfield, D S-C Ho, W R Richmond, B W Skelton, A H White, A Varnek, G Wipff, *Inorg Chim Acta*, **1996**, 246, 275-286
- 160 G Wipff, *Calixarenes 2001*, Kluwer Academic Publishers, **2001**, 312-333
- 161 R Freeman, *A Handbook of Nuclear Magnetic Resonance*, Longman Scientific & Technical
- 162 H Freibolin, *Basic One- and Two-Dimensional NMR Spectroscopy*, 3rd Rev Ed , Wiley VCH
- 163 P J Hore, *Nuclear Magnetic Resonance*, Oxford Science Publications
- 164 E J Haws, R R Hill, D J Mowthorpe, *The Interpretation of Proton Magnetic Resonance Spectra*, Heyden Publishers
- 165 C D Gutsche, B Dhawan, K H No, R Muthuknshnan, *J Am Chem Soc* **1981**, 103, 3782-3792
- 166 C D Gutsche, L J Bauer, *J Am Chem Soc* **1985**, 107, 6052-6059
- 167 K Araki, S Shinkai, T Matsuda, *Chem Lett* **1989**, 581-589
- 168 D Diamond, M A McKervey, *Chem Soc Rev* **1996**, 15-24
- 169 G Svehla, *Electrochemistry, Sensors and Analysis*, M R Smyth, J G Vos, Eds Analytical Chemistry Symposia Series 25, Elsevier Amsterdam, The Netherlands, **1986**, 131-140
- 170 D B Hibbert, *Introduction to Electrochemistry*, Macmillan Physical Science Senes, 190-205
- 171 D A Skoog, D M West, F J Holler, *Fundamentals of Analytical Chemistry*, 5th Ed , Saunders College Publishing, 290-367
- 172 E Bakker, P Buhlmann, Erno Pretsch, *Chem Rev* **1997**, 97, 3083-3132
- 173 D Diamond, *Electrochemistry, Sensors and Analysis*, M R Smyth, J G Vos, Eds Analytical Chemistry Symposia Series 25, Elsevier Amsterdam, The Netherlands, **1986**, 155-161
- 174 F Cadogan, K Nolan, D Diamond, *Calixarenes 2001* Kluwer Academic Publishers, **2001**, 627-641
- 175 A Lynch, K Eckhard, G McMahon, R Wall, P Kane, K Nolan, W Schuhmann, D Diamond, *Electroanalysis*, **2002**, 14, 19, 1-8
- 176 T Grady, A Cadogan T McKittrick, S J Harns, D Diamond, M A McKervey, *Analytica Chimica Acta*, **1996**, 336, 1-12
- 177 H Tsukube, H Furuta, A Odani, Y Takeda, Y Kudo, Y Inoue, Y Liu, H Sakamoto, K Kimura, *Comprehensive Supramolecular Chemistry*, Pergamon Press, Vol 8, Ch 10, 426-479
- 178 V Bocchi, D Foina, A Pochini, R Ungaro, *Tetrahedron*, **1982**, 38, 373

179. Z. Brzózka, *Comprehensive Supramolecular Chemistry*, Pergamon Press, Vol. 10, Ch. 8, 187-211.
180. B. Dietrich, T.M. Fyles, J-M. Lehn, L.G. Pease, D.L. Fyles, *J. Chem. Soc., Chem. Commun.* **1978**, 934.
181. R. Lahti, R. Hannukainen, H. Lönnberg, *Biochem. J.* **1989**, 259, 55.
182. M.S. Searle, M.S. Westwell, D.H. Williams, *J. Chem. Soc., Perkin Trans. 2*, **1995**, 141.
183. B. Dietrich, M.W. Hosseini, J-M. Lehn, R.B. Sessions, *J. Am. Chem. Soc.* **1981**, 103, 1282.
184. F. Sansone, S. Barbosa, A. Casnati, D. Sciotto, R. Ungaro, *Tet. Lett.* **1999**, 40, 4741-4744.
185. P.D. Beer, Z. Cheng, A.J. Goulden, A. Grieve, D. Hsek, F. Szemes, T. Wear, *J. Chem. Soc., Chem Commun.* **1994**, 1269-1271
186. F. Szemes, D. Hsek, Z. Cheng, S.W. Dent, M.G.B. Drew, A.J. Goulden, A.R. Graydon, A. Grieve, R.J. Mortimer, T. Wear, J.S. Wrightman, P.D. Beer, *Inorg. Chem.* **1996**, 35, 5868-5879.
187. http://users.ox.ac.uk/~mwalter/tutorial_web/year2/nitr/amines.shtml
188. B. Castellano, E. Solari, C. Floriani, *Organometallics*, **1998**, 17, 2328-2336.
189. M.K. Nayak, A.K. Chakaborti, *Tet. Lett.* **1997**, 38, 50, 8749-8752.
190. G. S. Bates, D. Parker, *Tet. Let.* **1996**, 37, 2, 267-270.

Appendix

Display Report

Analysis Name KN1_0000 d

Acquisition Date 03/14/03 14 45 23

Operator

Administrator

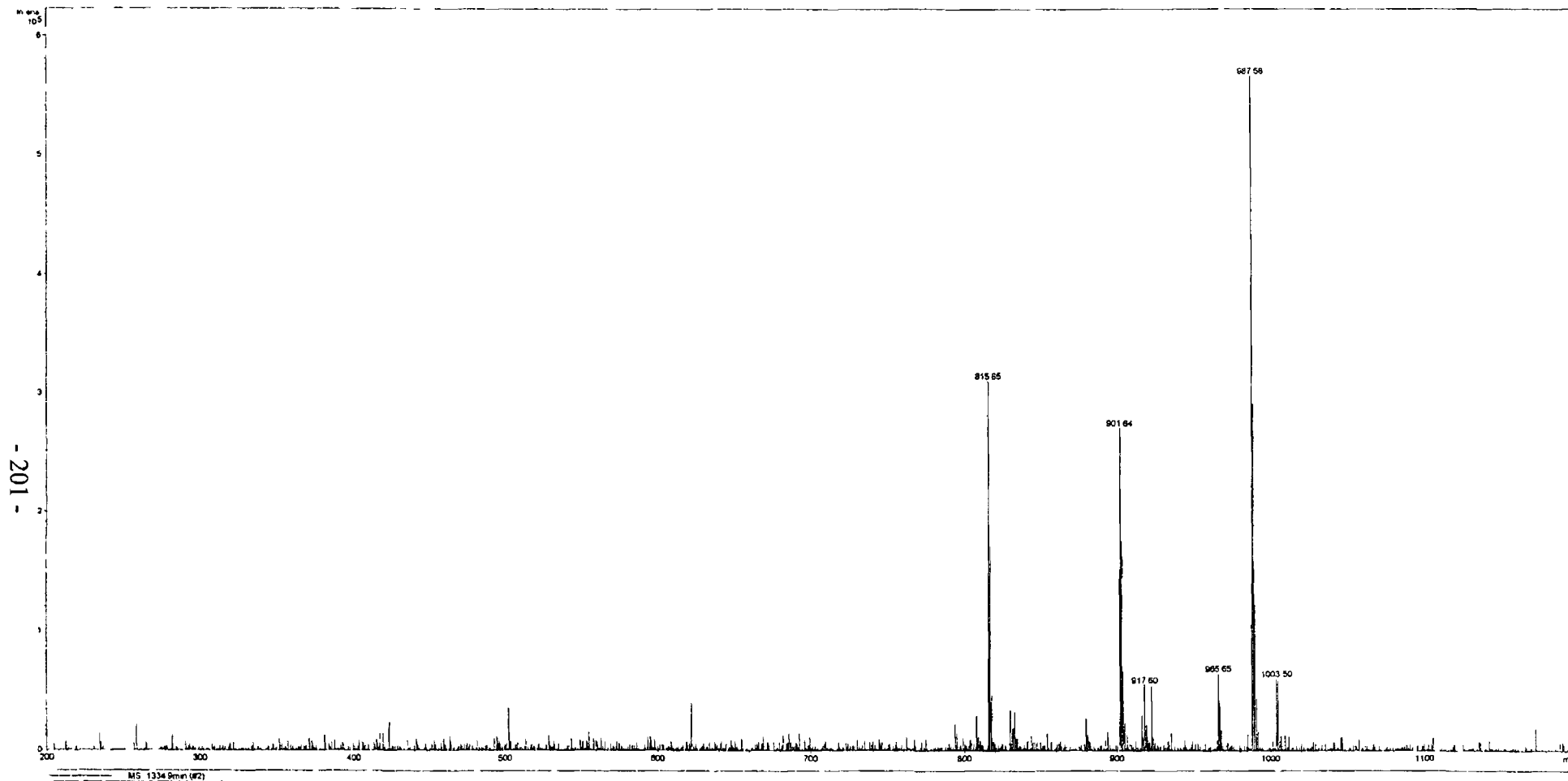
Sample Name Default

Method DCU MS

Instrument

esquire3000plus

Comment KN001 diluted 1 part in 10 000 in ESI solvent Maximum resolution mode full scan MS



Display Report

Analysis Name KN1_0000 d

Sample Name Default

Comment KN001 diluted 1 part in 10,000 in ESI solvent Maximum resolution mode full scan MS

Acquisition Date 03/14/03 14 45 23

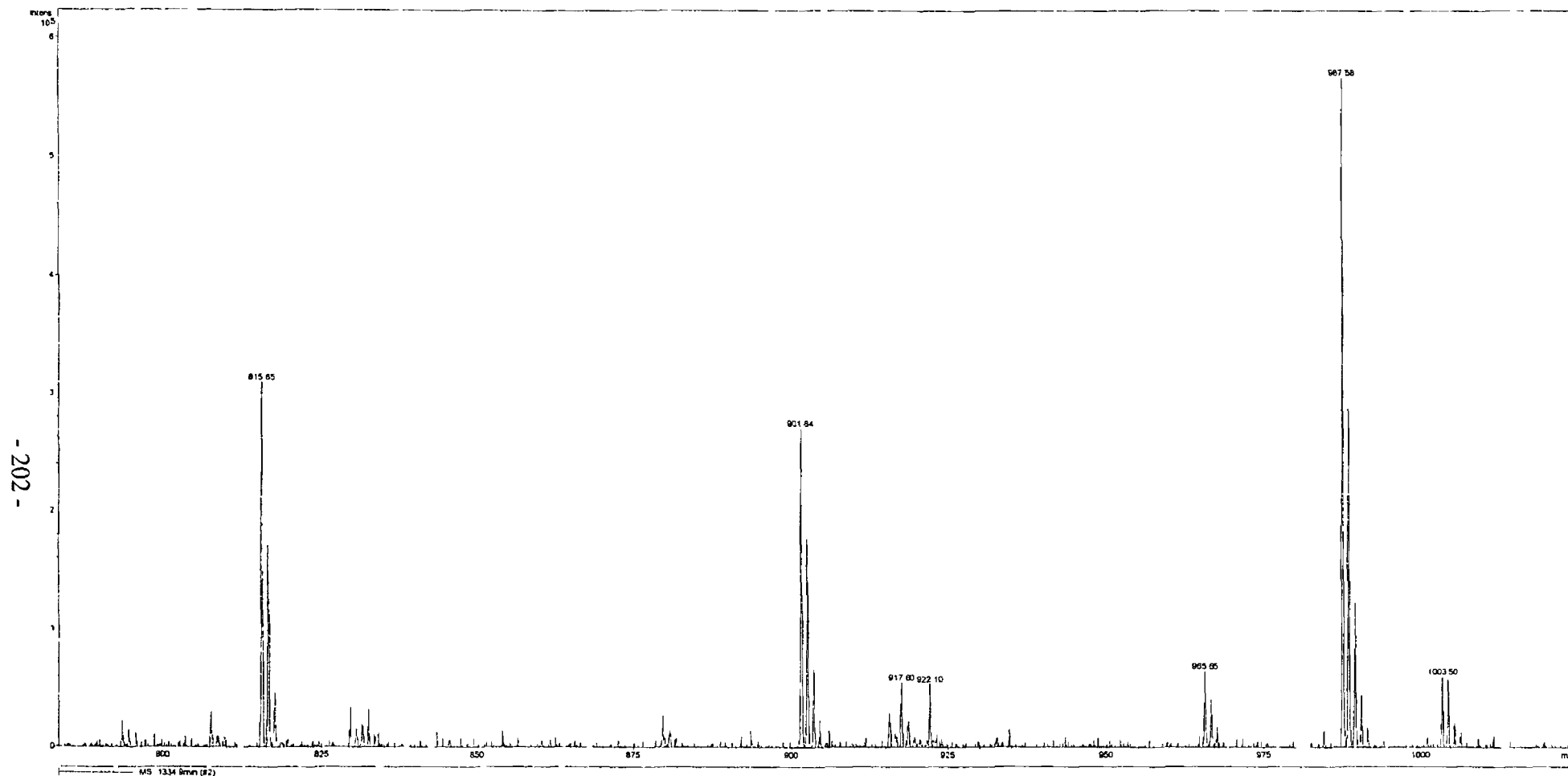
Method DCU MS

Operator

Instrument

Administrator

esquire3000plus



Display Report

Analysis Name KN1_0001.d

Acquisition Date 03/14/03 14:47:07

Operator

Administrator

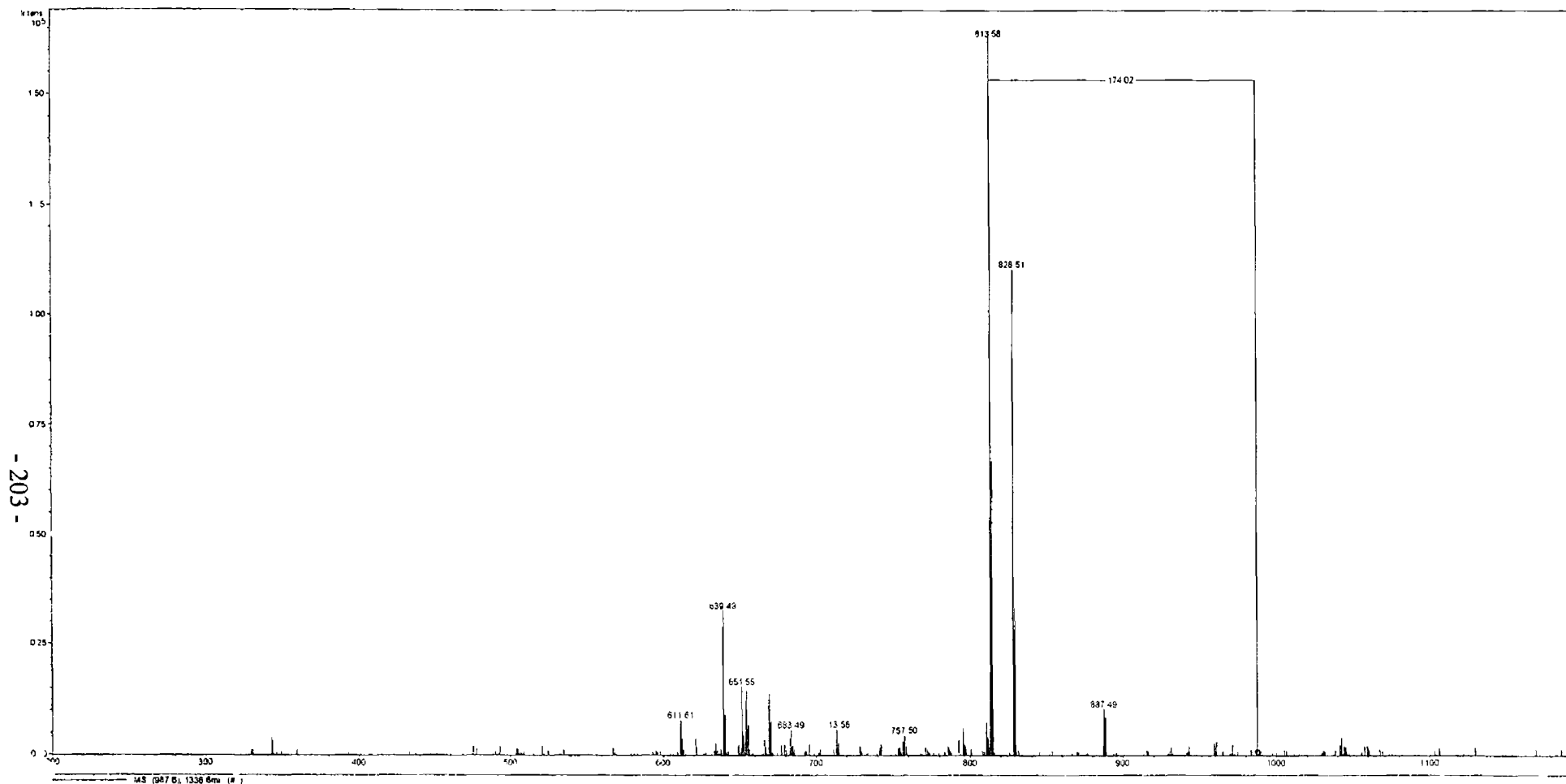
Sample Name Default

Method DCU MS

Instrument

esquire3000plus

Comment KN001 diluted 1 part in 10 000 in ESI solvent Maximum resolution mode, MS/MS of 987.6



Display Report

Analysis Name KN1_0001.d

Acquisition Date 03/14/03 14:47:07

Operator

Administrator

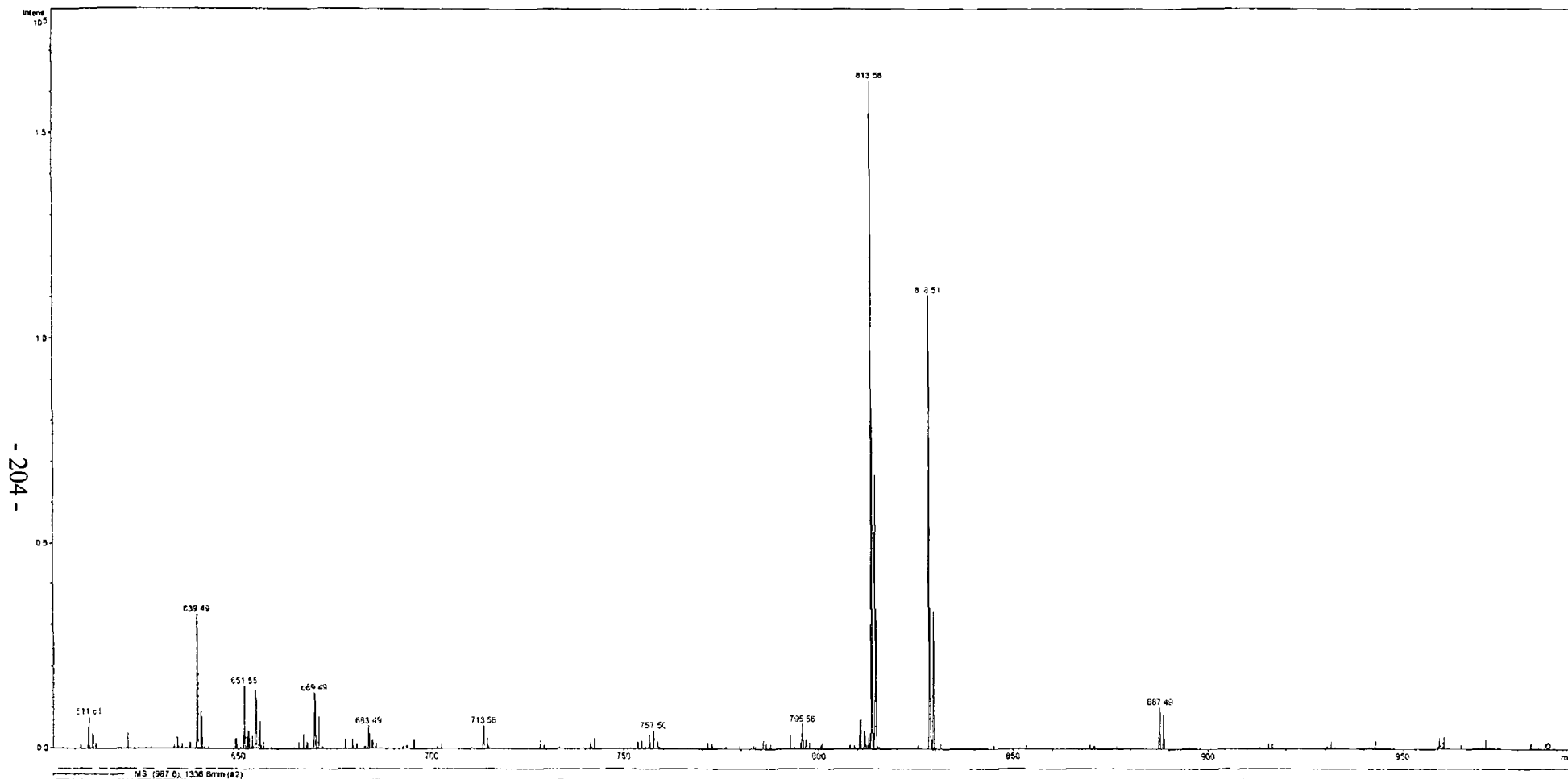
Sample Name Default

Method DCU MS

Instrument

esquire3000plus

Comment KN001 diluted 1 part in 10 000 in ESI solvent Maximum resolution mode, MS/MS of 987.6



Characterisation of the ester-substituted products of the reaction of p-t-butyl calix[4]arene and ethyl bromoacetate using LC-UV-MS and LC-DAD

Gillian McMahon *, Rachel Wall, Kieran Nolan, Dermot Diamond

National Centre for Sensor Research Dublin City University Glasnevin, Dublin 9 Ireland

Received 28 December 2001 received in revised form 8 April 2002 accepted 8 April 2002

Abstract

A series of derivatisation reactions between p-t butyl calix[4]arene and ethyl bromoacetate were carried out in order to prepare 1,3 diester substituted calix[4]arene. Mass spectral data, obtained from direct injection of samples, indicated that the reactions were rich in the desired product. Since the ultra violet (UV) spectra of the desired product and possible impurities are very similar, liquid chromatography (LC) chromatographic data seemed to corroborate these results. However, when on-line LC UV MS was carried out and each LC peak subjected to MS analysis as it eluted, a very different picture emerged. It was found that many of these reactions actually contained high levels of the monoester product which, having less affinity for sodium in the MS, is therefore seriously underestimated in any direct injection assay. LC-diode array detection (DAD) methods were also used to help successfully identify and characterise the compounds being formed in these complex reactions. The overall results obtained in this paper allowed the optimal reaction conditions to be determined for this reaction. LC-MS analysis of the chromatographic peaks also identified the presence of two isomers of the diester substituted calix[4]arene (1,3 and 1,2 diesters). The combination of LC and UV/MS detection is required for accurate analysis of the products of such reactions. © 2002 Elsevier Science B.V. All rights reserved.

Keywords: Calix[4]arene; Liquid chromatography; Mass spectrometry; Diode array detection

1 Introduction

Calixarene compounds, because of their unique ‘bowl-like’ structures, have attracted much attention, especially in host–guest and analytical chemistry [1–6]. Although calixarenes with 3–20

repeat units have been reported in the literature, the majority of analytical activity to date has focussed on tetramers (four phenolic units), called calix[4]arenes (see Table 1). The most commonly used conformation of calix[4]arenes is that of the ‘cone’, where the four phenoxy groups are all positioned on the lower rim of the molecule, and are held in place by a network of intra-molecular hydrogen bonds. In order to reduce the formation of rotamers, it is common practice to attach bulky

* Corresponding author. Tel. +353 1 700 8774; fax. +353 1 700 5503.

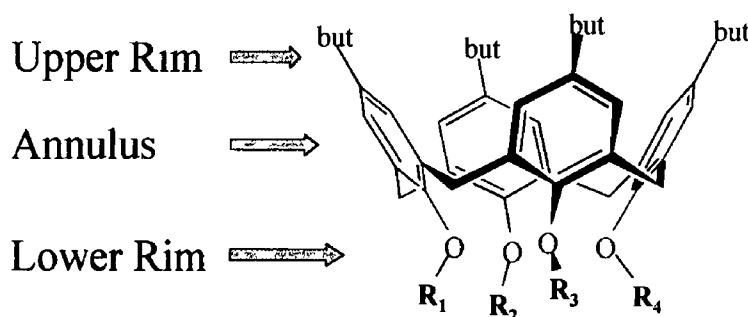
E-mail address: gillian.mcmahon@dcu.ie (G. McMahon).

t-butyl groups at the upper rim, as these cannot pass through the annulus of the tetramers. Calix[4]arenes thus provide a route to molecules with well-defined cavities offering simultaneous polar character (lower rim) and non-polar character (upper rim) capable of forming inclusion complexes with a wide range of guest species, depending on the nature and number of substituted moieties. Applications of tetrameric calixarenes and their derivatives include their use as selective agents for cations such as sodium [7–9], calcium [10,11], silver [12–14] and caesium [15,16], or to a lesser extent anions [17] in ion-se-

lective electrodes. They have also been used as optical sensors [18–21] and in chiral recognition [22–25]. They lend themselves well to these applications because of the multiplicity of options for structural elaboration, which has led to the generation of a number of highly selective hosts for important 'guest' ions/molecules. Due to their inherently non-polar structure, they do not leach into aqueous test samples from non-polar membranes, a property which can be important for chemical sensor and waste purification applications. Calixarenes have also been used as stationary phases themselves in chromatographic

Table 1

Details of the names and structures of the compounds formed in this research in terms of substituents at lower rim positions R_1 – R_4



Chemical Name	Name used in this Paper	Mass (a.m.u.)	Substituent Groups at Lower Rim	
			H	
<i>p</i> -t-butyl calix[4]arene	Calix[4]arene	648	R_1, R_2, R_3, R_4	none
Mono-ethyl calix[4]arene ester	Monoester	734	R_2, R_3, R_4	R_1
1,3 Di-ethyl calix[4]arene ester	1,3 Diester	820	R_2, R_4	R_1, R_3
1,2 Di-ethyl calix[4]arene ester	1,2 Diester	820	R_3, R_4	R_1, R_2
Tri-ethyl calix[4]arene ester	Triester	906	R_4	R_1, R_2, R_3
Tetra-ethyl calix[4]arene ester	Tetraester	992	none	R_1, R_2, R_3, R_4

columns for the analysis of compounds such as nitroanilines [26], uracil derivatives and estradiol epimers [27], peptides [28] and barbiturates and xanthine derivatives [29]

There have been many publications about the characteristics of calixarenes, which have been investigated using instrumental techniques such as nuclear magnetic resonance spectrometry (NMR), infrared spectrometry (IR), ultraviolet spectrometry (UV) and more recently, X-ray analysis. The isolation and purification of these compounds from synthetic mixtures has generally been carried out by simple recrystallisation or column chromatography. In order to evaluate the purity of the synthesised products, the first chromatographic methods were developed over 10 years ago and included thin layer chromatography (TLC) [30], flash chromatography [31] and liquid chromatography (LC) [32]. More recently there have been a few references in the literature about the use of capillary electrophoresis (CE) for the analysis of the more polar calixarenes [33–35]. However, LC offers the most possibilities for analysis of these compounds, allowing separation of polar and non-polar substances. Table 2 summarises some LC methods that have been used for the analysis of calixarenes [36–44].

Obtaining reliable routes to partially substituted calixarene derivatives, such as the compounds discussed in this paper, is of growing interest as they provide templates for generating more complex derivatives with mixed functionality, and/or greater diversity in cavity geometry than conventional simultaneous substitution at all four lower rim positions. For example, 1,3-disubstituted calix[4]arenes can be regarded as precursors for molecular sensors with different spatial distributions of receptor groups at the 1,3 and 2,4 positions. When further groups are linked to the molecule, those on the 2,4 positions will be of shorter chain length than those in the 1,3 positions, allowing selective 3-dimensional binding. These compounds should have significantly different host–guest properties compared to more conventional symmetrically functionalised calix[4]arenes. This preorganisation of structure will be able to accommodate, for example, tetrahedral molecules or ions such as am-

monia or phosphate. The development of separation methods that can more completely characterise the products of partial calix[4]arene derivatisation to the 1,3 diester is of great importance, as there are many possibilities for forming other compounds during the reaction. For example:

- The reaction may not proceed fully, leading instead to the monoester derivative,
- The reaction may continue beyond the diester substituted product, leading to the tri- or tetra-substituted products,
- Structural and conformational isomers may form (e.g. 1,2 diester, and partial cone derivatives).

Table 1 summarises the possible products that could be formed during esterification of the calix[4]arene starting material. In this paper we demonstrate that LC, mass spectrometry (MS), LC-diode array detection (DAD) and LC-UV-MS (commonly referred to as LC-MS) have generated important new analytical information about the products formed in these esterification reactions, and provide a convincing means to optimise the reaction conditions.

2 Experimental section

2.1 Reagents and chemicals

Spectranal grade acetonitrile (ACN) and tetrahydrofuran (THF), and pestanal grade water, for use with the LC-MS, were supplied by Riedel-de-Haen. LC grade ACN, THF, and water, for use with the LC-DAD, were supplied by Aldrich. Formic acid (ACS reagent) was purchased from Aldrich and was used for preparing mobile phases for both the LC-MS and the LC-DAD systems. Solvents for the synthetic work, i.e. anhydrous dimethylformamide (DMF) and acetone were purchased from Aldrich. The acetone was dried over calcium sulphate before use. The starting material p-t-butyl-calix[4]arene (catalogue number 34,752-3) and ethyl bromoacetate (EtBrOAc) were purchased from Aldrich.

Table 2
Literature LC methods for calixarenes and related compounds

Reference no year and author	Type of calixarene(s) analysed	Type of LC	Column used	Mobile phase and flowrate	Detection method
[36], 1995 Vocanson et al	p t butyl calix[n]arenes $n = 4, 6, 7, 8$ LC method was not applicable to other alkyl calixarenes	Reversed phase	Spherisorb ODS1, 250 × 4.6 mm, 5 μm	(ACN/DCM/acetic acid 95/5/1 v/v/v) MTBE 9 l, 0.8 ml/min	UV @ 287 nm
[37] 1996 Saito et al	Calix[n]arenes $n = 4, 6, 8$	Reversed phase	C ₆₀ bonded silica 150 × 0.32 mm, 5 μm vs Develosil ODS 5	Toluene/methanol 2/3 or Toluene/ACN 2/3 2 μl min ⁻¹	UV @ 320 nm
[38] 1997 Jinno et al	Calixarenes and their sulphonated derivatives	Reversed phase	C ₆₀ bonded silica 150 × 0.32 mm vs Develosil ODS 5	Toluene/methanol 30/70 or water, 2 μl min ⁻¹	UV @ 280 nm
[39] 1997 Kalchenko et al	Calixarenes ($n = 4, 6, 8$) and their phosphoryl derivatives	Reversed phase	Lichrosorb C18 250 × 1 mm	ACN/water 86/14 0.04 ml min ⁻¹	UV @ 254 nm
[40] 1997 Rodriguez et al	p t butyl calix[n]arenes $n = 4-10$	Reversed phase	Spherisorb ODS 150 × 4.6 mm, 3 μm	ACN/MeOH/EtOAc/TF A Gradient system 1 ml min ⁻¹	UV @ 288 nm
[41] 1997 Graham et al	p t butyl calix[n]arenes Total separation time only 5 min	Reversed phase	Spherisorb ODS 150 × 4.6 mm 3 μm	ACN/EtOAc/acetic acid 800/199/1 1 ml min ⁻¹	UV @ 288 nm
[42] 1999 Thibodeaux et al	Chiral N acylcalix[4]arene amino acid derivatives mono di tri and tetrasubstituted were separated	Reversed phase	Biorad Biosil ODS 5S, 250 × 4 mm	ACN /water/H ₃ PO ₄ 65/35/0.1 1 ml min ⁻¹	UV @ 274 nm
[43], 2000 Feng et al	Calix[n]arenes ($n = 4, 6, 8$) and various calixcrowns	Reversed phase	C ₆₀ bonded silica 150 × 4.6 mm	Cyclohexane/propan 2 ol 39/1–99/1, 0.5 ml min ⁻¹	UV @ 288 nm
[44] 2000 Dodi et al	Dioctyl calix [4] crown 6	Normal phase	Silica Uptisphere 5 μm 250 × 4.6 mm	Hexane/propan 2 ol 17/3 1.2 ml min ⁻¹	UV @ 228 nm

2.2 Sample preparation

Worked up samples from reactions A to F (see Section 2.7 below and Table 3) were prepared in ACN to a concentration of 0.5 mg ml⁻¹ for analysis by LC-MS and/or LC-DAD. For direct injection onto the MS, samples were prepared in ACN with 0.25% formic acid to a concentration of 0.1 mg ml⁻¹ as appropriate. Samples with high residual levels of the starting material were

difficult to dissolve fully due to the relative insolubility of the calix[4]arene in ACN. In these cases, THF was used to prepare the stock samples and they were subsequently diluted to the required concentrations with ACN. As long as the final proportion of THF in the samples was less than 50%, the peak shapes on the LC system were not affected.

Samples of calix[4]arene and tetraester for UV-Visible spectral scanning were prepared in ACN

to a concentration of 0.02 mg ml^{-1} and in mobile phase (from LC method 2, see Section 2.3 below) to a concentration of 0.02 mg ml^{-1} .

2.3 LC-MS analysis

The instrument used was the Bruker/Hewlett-Packard Esquire LC—a Bruker mass spectrometer linked to a HP liquid chromatograph. The LC module of the instrument was a HP1100 with a variable wavelength detector, a low-volume pump, an in-line degasser and an autosampler. It was controlled via user-friendly HP ChemStation software. This LC system generally uses low flow rates, narrow bore columns and a micro flow cell in the UV detector. Because of this, the exit flow from the UV detector can be sent directly into the mass spectrometer's ionisation chamber without having to be split. The MS module of the instrument comprised the ionisation chamber, the ion-trap to collect the ions and then to release them according to mass, and the ion detector to generate the spectrum. The Esquire-LC is capable of two types of ionisation—electrospray (ESI) and atmospheric pressure chemical ionisation (APCI), although in this work, we used only ESI. With ESI, samples are subjected to 'gentle' ionisation such that in-source fragmentation generally does not occur to any great extent. Neutral compounds will not be detected unless they acquire a charge—usually a proton, sodium or potassium.

Two LC methods, employing two different columns, were required for these experiments. The LC methods had the following parameters:

Table 3
Details of the reactions carried out for this paper

Reaction no	Stoichiometry of EtBrOAc calixarene	Solvent	Base	Time points for sampling (h)
A	1:4	DMF	Na_2CO_3	2, 5, 24
B	1:2	DMF	Na_2CO_3	2, 5, 24
C	1:1	DMF	Na_2CO_3	2, 5, 24
D	2:1	DMF	Na_2CO_3	2, 5, 24
E*	2:1	Acetone	K_2CO_3	15
F	2:1	Acetone	Na_2CO_3	15

* Literature method Ref [45]

2.3.1 LC Method 1

Based on a Zorbax RX-C18, $150 \times 2.1 \text{ mm}$, $5 \mu\text{m}$ column with a mobile phase of 100/0.25 v/v ACN/formic acid at a flowrate of 0.2 ml min^{-1} . The monitoring wavelength was 210 nm and an injection volume of $4 \mu\text{l}$ was used.

2.3.2 LC Method 2

Based on a Supelco-C18, $250 \times 2.1 \text{ mm}$, $5 \mu\text{m}$ column with a mobile phase of 92/8/0.25 v/v/v ACN/water/formic acid at a flowrate of 0.3 ml min^{-1} . The monitoring wavelength was 210 nm and an injection volume of $4 \mu\text{l}$ was used.

After passing through the UV detector, the samples were introduced directly into the mass spectrometer, with the ESI source in the positive mode, enabling simultaneous UV and total ion current (TIC) based chromatograms to be obtained. The nebulisation gas and drying gas were set to 35 psi and 9 l min^{-1} , respectively. The temperature of the source was maintained at 300°C . The octopole voltage was 2.83 V, the skimmer 1 voltage was $50 \pm 5 \text{ V}$ and the trap drive voltage was $57 \pm 2 \text{ V}$ (depending on the chosen target mass). Mass spectral data was generally collected in the scan range 400–1200 m/z . When automated fragmentation information was required, the software was set up to subject the most abundant ion to MS^2 , using an isolation width of 4 Da and a collision amplitude of 1.80.

2.4 Direct infusion MS analysis

Using the syringe injector of the mass spectrometer, samples were infused into the ESI source (positive mode) at a rate of $5 \mu\text{l min}^{-1}$. The nebulisation gas and drying gas were set to 15 psi and 4 l min^{-1} respectively and the source temperature maintained at 250°C . The nebulisation gas pressure, drying gas flowrate and temperature were reduced in comparison to the LC-MS parameters. This is because these parameters are required to be higher when the MS is connected in series with the LC, so that the incoming LC eluent would be successfully converted into the gas phase. The octopole voltage was 2.83 V, the skimmer 1 voltage was $50 \pm 5 \text{ V}$ and the trap drive voltage was $57 \pm 2 \text{ V}$. The scan range covered was

400–1200 m/z When on-line MS–MS was being carried out, an isolation width of 4 Da and a collision amplitude of 1.60–2.10 were used depending on the ion being fragmented

2.5 LC-DAD analysis

A Varian HPLC system was used to obtain UV-Visible spectra of various components in the reaction mixture. It comprised a Varian Prostar 330 PDA detector, a gradient Prostar 230 pump and a manually operated switching valve with a 20 μ l injector loop. Pre-mixed mobile phases were degassed by sonication. The system was controlled via Varian software.

Only LC method 2 was set up on the Varian LC-DAD due to the availability of the Supelco column with standard dimensions. The following parameters were used: a Supelco-C18, 250 \times 4.6 mm, 5 μ m column with a mobile phase of 92/8/0.25 v/v/v ACN/water/formic acid at a flowrate of 1.5 ml min⁻¹. The monitoring wavelength was set at 210 nm and an injection volume of 20 μ l was used.

2.6 UV reference spectrum

A Perkin-Elmer Lambda 900 UV/VIS/NIR spectrometer was used for obtaining the UV reference spectrum for the calix[4]arene (Table 1) which came from Aldrich. The instrument was controlled via UV WinLab software. A matched set of 1 cm quartz cuvettes was used for the blank (ACN) and sample (dissolved in ACN). A spectral range of 190–350 nm was selected for scanning, with a slit width of 2 nm. The scan speed was 750 nm min⁻¹ with a data interval of 1 nm.

2.7 Synthetic procedures

Table 1 details the structures, names and molecular weights of the compounds that could be formed during these esterification reactions, and Table 3 summarises the reactions A to F that were carried out. The first four reactions (A to D) were run at the same time on the same scale in a parallel synthesiser system (Radleys Carousel Reaction Station, Shire Hill, Saffron Walden, Essex,

CB11 3AZ, UK), using DMF as solvent, Na₂CO₃ as base, and varying only the stoichiometry between the two principle reactants. For reactions A to D, to a suspension of calix[4]arene (150 mg scale for all reactions) in anhydrous DMF, was added base followed by the dropwise addition of EtBrOAc. The mixture was then heated to 70 °C for the specified reaction time (see Table 3). The reaction mixture was then cooled to room temperature, poured onto ice and subsequently extracted with four aliquots of ethyl acetate (4 \times 25 ml). The ethyl acetate extracts were combined and then washed with four aliquots of water (4 \times 25 ml) and brine solution (4 \times 25 ml). The organic extract was then dried over anhydrous MgSO₄ and the solvent removed under reduced pressure. Reaction E was carried out according to the previously reported method for making the diester substituted calix[4]arene [45], with the ratio of EtBrOAc:Calix[4]arene set at 2:1, acetone as the solvent and K₂CO₃ as the base. Reaction F was the same as reaction E, except that Na₂CO₃ was used as the base.

The tetraester (Table 1) was prepared in-house using well-known synthetic procedures [46]. A pure sample of the 1,3 diester was obtained by flash column chromatography using 10% ethylacetate/hexane as eluent. ¹H NMR (400 Hz) (CDCl₃): 6.95 (4H, s), 6.74 (4H, s), 4.64 (4H, s), 4.38 (4H, d), 4.21 (4H, q), 3.26 (4H, d), 1.27 (6H, t), 1.19 (18H, s), 0.91 (18H, s).

3 Results and discussion

3.1 LC method development

3.1.1 Column selection

A number of reversed-phase LC columns were evaluated (e.g. phenyl, cyano and C8), but C18 was found to be superior in terms of resolving power. Two types of C18 columns were required for this work—a Supelco C18, 250 \times 2.1 mm, 5 μ m (also a 250 \times 4.6 mm, 5 μ m version for the LC-DAD) and a Zorbax RX-C18, 150 \times 2.1 mm, 5 μ m. All but one of the LC methods detailed in Table 2 used a reversed phase system, and most employed a C18 column or equivalent. According

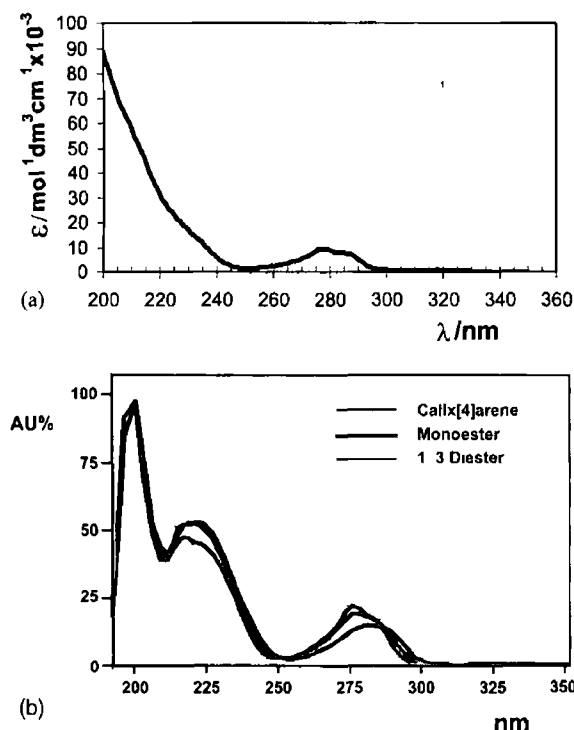


Fig 1 (a) UV Spectrum of the calix[4]arene starting material (see Table 1 for structure) Conditions Sample prepared directly to a concentration of 0.02 mg ml^{-1} in ACN and analysed on a Perkin Elmer UV VIS NIR Spectrophotometer Absorbances converted to molar extinction coefficients (b) On Line UV Spectra obtained using the Varian LC DAD system, of the calix[4]arene starting material the monoester and the 1,3 diester showing only slight differences in the region 270–300 nm and around 225 nm Absorbances normalised to maximum value for comparison Conditions LC Method 2 was performed on Varian LC DAD System The method used a scaled up version of LC Method 2 employing a Supelco C18 $250 \times 4.6 \text{ mm}$ $5 \mu\text{m}$ column with a mobile phase of 92/8/0.25 ACN/water/formic acid at a flowrate of 1.5 ml min^{-1} and an injection volume of $20 \mu\text{l}$ Chromatograms were equivalent to those obtained with the LC MS system using LC method 2

to previous work [39,41], the retention of calixarenes on a C18 or equivalent phase is determined mainly via hydrophobic interactions (CH- π) between the *t*-butyl groups on the upper rim and the sorbent surface, and other non-specific dispersion forces, hence these compounds are discriminated from each other on the basis of their hydrophobicity and their size Their hydrophobicity is determined mainly by the presence of the *t*-butyl groups on upper rim (which are non-polar) and to

a lesser extent, the lower rim substituents (which have varying polarity)

3.1.2 Choice of UV wavelength

During the course of this research, it became apparent that the MS results varied widely in sensitivity with respect to the various esters, and quantitative extrapolations were therefore very misleading (see Section 3.3.1 for details) Therefore, in order to obtain yield information, UV detection was important As the UV spectra for the partially substituted calix[4]arenes (see Table 1 for structures) had not previously been published, it was important to identify spectral regions where the extinction coefficients were high and similar in value

The spectrum for the starting material calix[4]arene in ACN shows a maximum at 277.5 nm (ϵ ca 9500) with a shoulder at 286 nm (see Fig 1a) Obviously, maximum sensitivity would be obtained at wavelengths down towards 200 nm, which further restricts the choice of mobile phase and reaction matrix In Table 2, ethyl acetate was employed in two methods [40,41] but due to its high background absorbance, required the use of the less sensitive wavelength of 288 nm Higher wavelengths also had to be employed in methods based on solvents such as dichloromethane [36] and toluene [37,38] The lowest wavelength used in the methods shown in Table 2 was 228 nm, in Dodi's normal phase system [44]

Spectra obtained on-line using the Varian LC-DAD, for peaks identified as the calix[4]arene, the monoester and 1,3 diester have UV maxima at approximately 200, 220–225 and 270–285 nm, with spectral minima at 215 and 254 nm (see Fig 1b) Comparison with the reference spectrum of the calix[4]arene (see Fig 1a) with its spectrum obtained on-line using the Varian LC-DAD shows close agreement, particularly from 225 to 300 nm The differences in the region 200–225 nm may be due to solvent effects, as the mobile phase contained 8% water and 0.25% formic acid, whereas the reference spectrum was obtained using ACN as the solvent The monoester and 1,3 diester spectra in the region of 275 nm show a slight red-shift (the 1,3 diester to a greater extent

than the monoester) and adoption of a more regular shape compared to calix[4]arene. This effect is due to the effect of substituting the ester groups onto the phenyl chromophore, creating ether linkages. An important conclusion from this work is that the molar extinction coefficients of the calix[4]arene, the monoester and 1,3 diester (Table 1) are very similar over the regions 200–215 and 230–250 nm. Furthermore, the molar extinction coefficient of the tetraester is also similar in these regions (data not shown), so it is reasonable to presume that in these regions, absorbance could be used to estimate concentration. The wavelength of 210 nm was selected for the LC-MS work, as this was a reasonable compromise between sensitivity and similarity. Hence LC-UV chromatograms obtained at this wavelength would be sensitive and could be used to estimate relative yields of each product.

3.1.3 Mobile phase selection

High proportions of organic solvent were required in the mobile phase in order to elute the calix[4]arene compounds from the columns, a feature common to most of the analytical methods in Table 2. THF was tried, but was found to result in split peaks with poor overall shape. The use of methanol caused some undesirable effects such as peak tailing (a feature noticed by Graham et al. [41]) and unpredictable retention times. Rodriguez et al. found that peak shapes improved as the percentage of methanol in the mobile phase was reduced [35]. Hence, ACN was chosen since it could solubilise the components for sample preparation, was compatible with ESI, and had a low UV cutoff at 190 nm. High proportions of this solvent had previously worked well for Vocanson et al. [36], Kalchenko et al. [39] and Thibodeaux et al. [42] (see Table 2). Water was added at a level of 8% to the mobile phase for LC Method 2 (which used the Supelco C18 column), to achieve better separation between the mono- and diester substituted derivatives.

In previous work, acetic acid [36,41], trifluoroacetic acid [40] or phosphoric acid [42] have been successfully employed to keep the pH low. This has the effect of improving resolution and controlling peak tailing by reducing surface

silanol effects [40]. However, only volatile acids can be used in conjunction with the mass spectrometer and so formic acid was employed for both the LC-MS and the LC-DAD systems at a concentration of 0.25%.

In principle, esterification can give rise to the five substituted products listed in Table 1. Hence, the LC method(s) should be able to discriminate between these products and the starting material calix[4]arene in the shortest possible time. Due to the extreme hydrophobicity of the tetraester relative to the other compounds, it would only elute in a reasonable timeframe with the shorter column and 100% ACN (LC Method 1). However, under these conditions, the monoester and the diester isomers (1,3 diester and 1,2 diester) eluted very closely together and in fact, the monoester and 1,2 diester merged into a single peak (see Fig. 2a). This is difficult to prevent, since very high proportions of ACN are required to elute any of these calix[4]arene compounds from the HPLC column at all (90–100% ACN), so use of a gradient is not feasible. A longer C18 column (250 mm instead of 150 mm) and reduction of the proportion of ACN (and increasing the proportion of water accordingly)—LC Method 2—did improve separation but at the expense of elongating the runtime, and losing the peak for the tetraester in the baseline (see Fig. 2b). The order of elution—1,3 diester, monoester and 1,2 diester—can probably be explained on the basis of shape alone. The 1,3 diester is a symmetrical molecule and the ligands may even curl up into the cavity to some extent, making it spherical in shape. The monoester is basically a small calix[4]arene with a single ligand dragging along the sorbent phase which would slow it down relative to the 1,3 diester. The 1,2 diester has two of these ligands (both on the same side of the molecule, making it unsymmetrical) which would slow it down to a greater extent while moving along the C18 column.

3.2 MS method development

Direct infusion of samples at low flow rates facilitated on-line optimisation of the MS condi-

tions. Various parameters were changed until the cleanest spectra with the highest intensity peaks were obtained. Inputting the target mass into the Bruker software (or the median target mass in the case of a range of analytes) automatically set certain parameters, although some of these settings, e.g. octopole voltage, were changed and checked manually in order to further optimise the MS method. At all times, due consideration was taken of the fact that the LC methods developed

would have to be compatible with the mass spectrometer.

3.3 Analytical results

3.3.1 LC and MS results

Fig. 4 shows both direct infusion results and LC results for the 2, 5 and 24 h samples from Reaction C. Mass spectra from direct infusion of samples of the reaction mixtures (described in

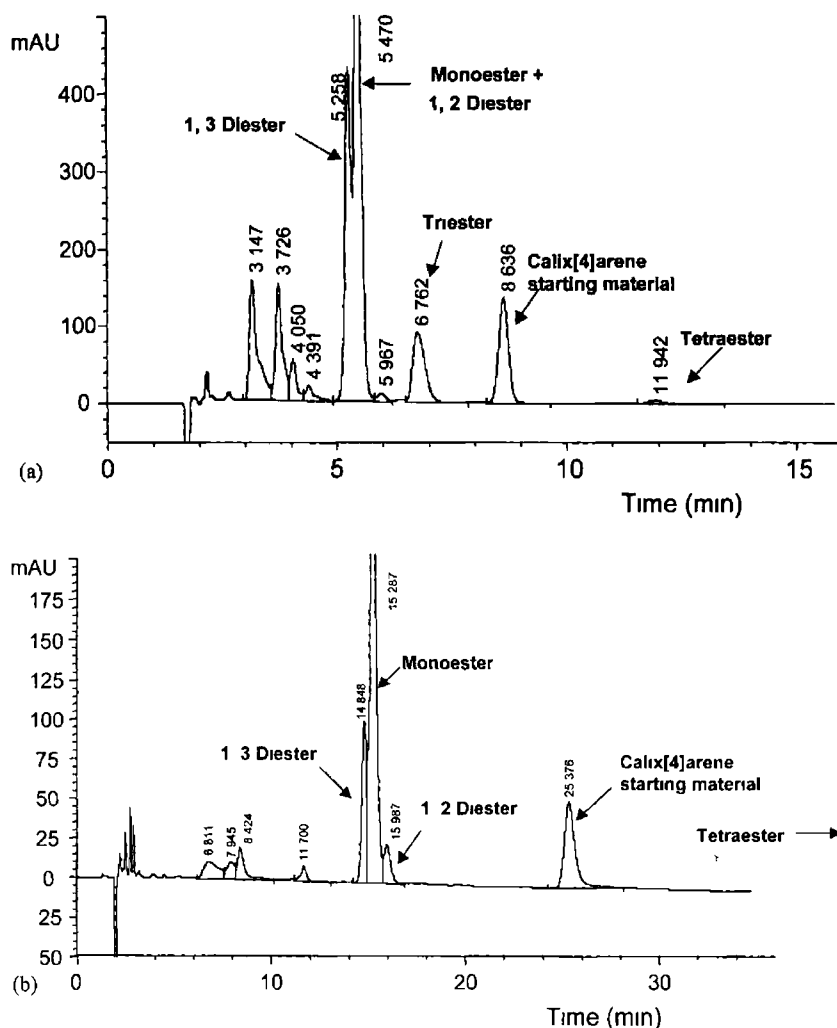


Fig. 2 (a) Chromatogram of a 15 h sample from Reaction E (spiked with diester) using LC Method 1. Conditions: LC Method 1 used with the LC MS system employing a Zorbax RX C18, 150 × 2.1 mm, 5 μm column with a mobile phase of 100/0.25 ACN/formic acid at a flowrate of 0.2 ml min⁻¹. The monitoring wavelength was 210 nm and an injection volume of 4 μl was used. (b) Chromatogram of a 24 h sample from Reaction A using LC Method 2. Conditions: LC Method 2 used with the LC MS system employing a Supelco C18, 150 × 2.1 mm, 5 μm column with a mobile phase of 92/8/0.25 ACN/water/formic acid at a flowrate of 0.3 ml min⁻¹. The monitoring wavelength was 210 nm and the injection volume was 4 μl.

Table 4

LC Results of 24 h samples taken from Reactions A to D (Solvent DMF base Na₂CO₃, all samples taken after 24 h)

Reaction no	Ratio of EtBrOAc Calix[4]arene	Relative area percent results				
		Calix[4]arene%	Monoester%	1,3 Diester%	1,2 Diester%	Sum of diesters%
A	1:4	16.8	63.2	14.5	5.5	20.0
B	1:2	11.9	46.8	32.8	8.5	41.3
C	1:1	0.0	16.7	72.8	10.5	83.3
D	2:1	3.5	24.9	60.4	11.2	71.6

Table 3) prepared in ACN, all showed a base peak of 843.5 Da (820 + Na), indicating the presence of the diester substituted calix[4]arene product. In these MS traces, smaller peaks for the monoester + Na (peak at 757.5 Da), triester + Na (929.5 Da) and tetraester + Na (1015.5 Da) were also evident in some of the samples. The results suggested that all samples were composed mainly of diester. The fact that the peaks obtained for the five substituted products listed in Table 1 and the starting calix[4]arene material were mainly sodiated, with a small proportion potassiated, agrees with previous MS work carried out on selected nitrogen-free calixarenes by laser desorption ionisation MS [47].

Careful examination of the LC-UV chromatograms and mass spectra in Fig. 3 raise a number of issues. The 2-h sample chromatogram implies that there is one main product at 15.03 min with a minor impurity which precedes the main peak. The mass spectrum of the same sample shows a large signal for the diester (843.5 Da) and a minor signal for the monoester (757.5 Da) for this mixture. Initially, we interpreted this as meaning the product was mainly diester, in agreement with the MS results. However, on continuing the reaction for longer times (5 h, 24 h), it became clear that the 15.03 min peak was gradually disappearing, and the fore-peak was growing—see Fig. 3. Comparison of the mass spectra proves that the declining signal is due to the monoester. Hence, the MS is clearly much more sensitive to the diester relative to the monoester. We attribute this difference in sensitivity to different affinities to sodium ions. The 1,3 diester is more predisposed to com-

plexing the cation than the monoester, due to the symmetrical arrangement of two ligating groups at the lower rim that can envelop the sodium ion, in a manner similar to the tetraester, which is known to be an excellent sodium complexing agent. In contrast, the monoester possesses only a single ligating carbonyl group and can be therefore much less efficient at sodium complexation than the 1,3 diester. Hence, as the samples pass through the MS instrument, a much higher proportion of the diester will be populated with sodium ions, which will lead to a more sensitive signal compared to the monoester.

3.3.2 Reaction stoichiometry

Samples from each of the first four reactions A to D were taken at 2, 5 and 24 h and worked up to give a solid. LC analysis showed that all of the samples from these reactions were in fact mixtures containing at least monoester, diester and calix[4]arene. In general, the starting material could be seen to decrease with time while the mono- and diesters were seen to increase with time (see Fig. 3 for an example of this phenomenon). Depending on the stoichiometry of calix[4]arene to EtBrOAc used in the reaction, an increase in the formation of diester over time corresponded to a decrease of monoester, and vice-versa.

The results of these experiments therefore showed that as the ratio of EtBrOAc to calix[4]arene increases, the ratio of diester to monoester increases also. A stoichiometry somewhere between 1:1 and 2:1 appears to be optimal (reactions C and D, see Tables 3 and 4). The 24-h

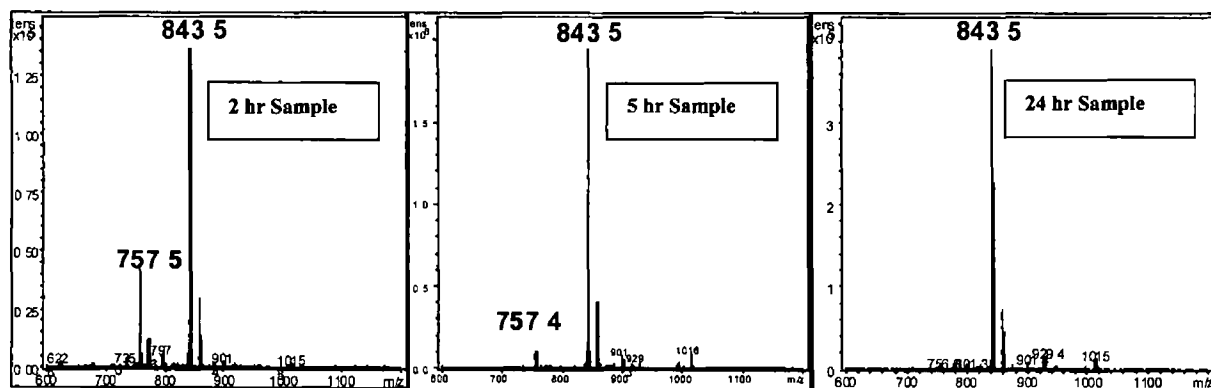
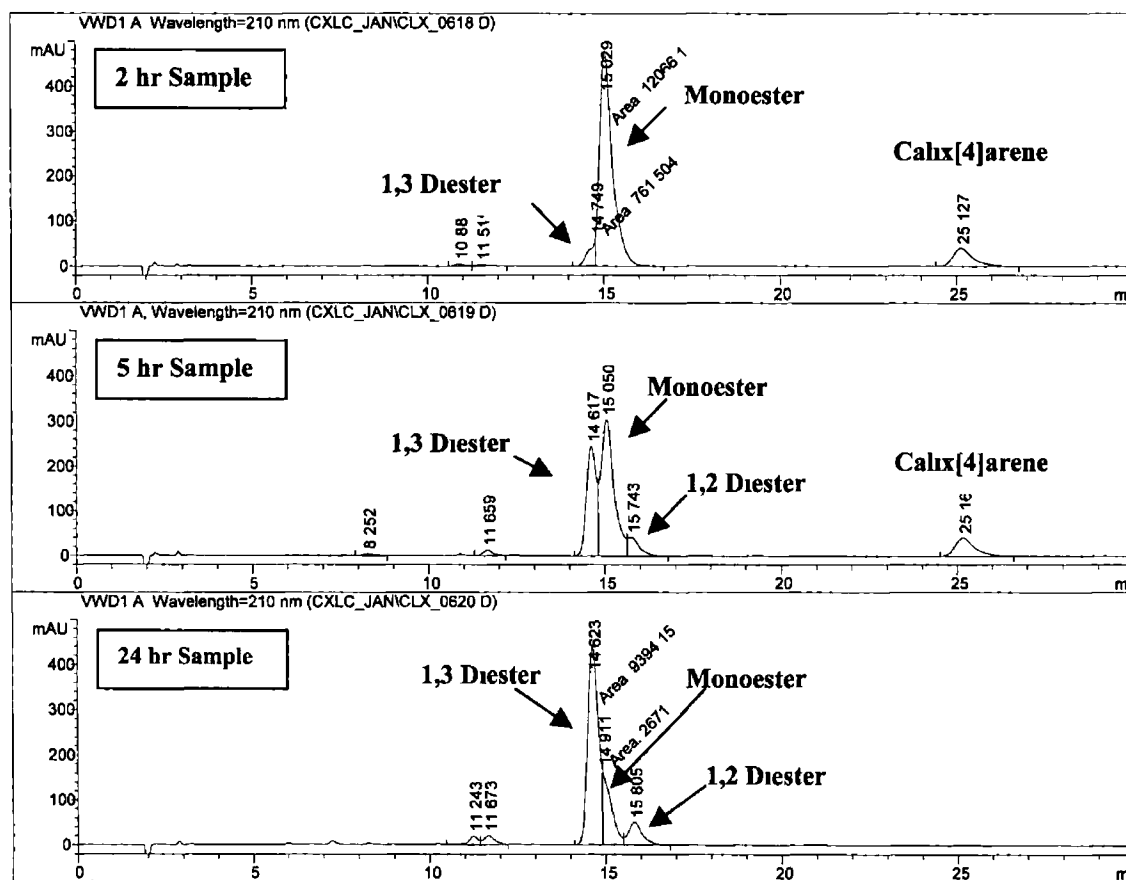


Fig 3 LC chromatograms and direct infusion mass spectra for 2, 5 and 24 h Samples from Reaction C, showing that the MS results are not quantitative. Conditions: Sample was infused into the ESI source (positive mode) at a rate of $4 \mu\text{l min}^{-1}$. The nebulisation gas and drying gas were set to 15 psi and 4 l min^{-1} , respectively. The temperature of the source was maintained at 250°C . LC settings as for Fig. 2b.

samples from these reactions were almost orange in colour, while other samples from this series of experiments were pale yellow products

3.3.3 Isomers of the diester

A further conclusion of this research is that two forms of the diester substituted calix[4]arene are obtained, probably positional isomers of each other (1,3 and 1,2 diesters, Table 1). Fig. 4 shows an expanded view of the UV and TIC chromatograms, over the range 12–18 min, obtained for a sample of reaction A taken after 24 h. Three peaks are evident in the region 13.5–15.5 min. From the UV trace, the second peak is the most significant product, and this is identified from the mass spectrum as the monoester. The satellite peaks before and after the monoester both give identical mass spectra, corresponding to the mass

of the diester derivative. By spiking samples with pure 1,3 diester, we were able to assign the first of the diester peaks as the 1,3 diester since it increased in area. The ante-peak is identified as the 1,2 diester since there was no change in its area upon spiking.

3.3.4 Reaction reagents and conditions

Samples from reactions E and F (see Table 3) were taken at 15 h—which is the length of time recommended in the literature [45]—and worked up to give a solid. LC-MS results suggest that neither reaction produced much diester. Reaction E (pale green solid) produced a mixture of mainly mono-, tri- and tetraester, while reaction F (pale yellow solid) produced only tetraester. Fig. 2a shows a chromatogram of the product of reaction E after 15 h (spiked with additional diester to confirm its absence). Clearly, a variety of products is obtained, but mainly the monoester with some triester. Controlling this reaction proved difficult, as it is very sensitive to the granular form of the base, and the presence of trace quantities of water [48]. The only difference between these reactions was the base used (K_2CO_3 in reaction E, Na_2CO_3 in reaction F). However, switching to DMF as the solvent (as in reactions A to D) improved matters. Table 4 shows that the yield of the 1,3 diester from reaction C is over 70% after 24 h, and yields of this magnitude are relatively easy to reproduce. We therefore recommend the following final reaction conditions: DMF to be used as the solvent, Na_2CO_3 to be used as the base and a reaction time of at least 24 h (see Fig. 3).

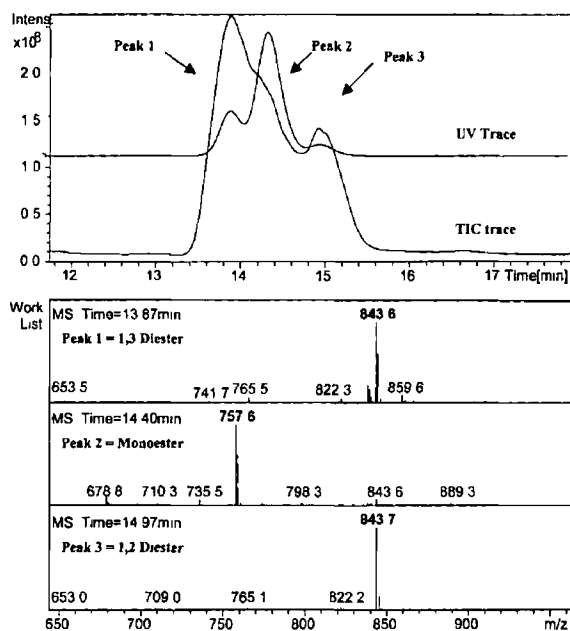


Fig. 4. UV chromatogram superimposed onto the total ion current along with the relevant mass spectra for each of the three peaks, for the 24 h sample from Reaction A. Conditions: LC Method 2 used a Supelco C18 150 × 2.1 mm 5 μ m column with a mobile phase of 92/8/0.25 ACN/water/formic acid at a flowrate of 0.3 ml min⁻¹. The monitoring wavelength was 210 nm and an injection volume of 4 μ l was used. The ESI source was in the positive mode. The nebulisation gas and drying gas were set to 35 psi and 9 l min⁻¹, respectively. The temperature of the source was maintained at 300 °C.

4 Conclusions

It is evident from this work that the monitoring of the formation of the 1,3 diester substituted product of calix[4]arene is not as straightforward as previously thought. For these calix[4]arene compounds, direct injection MS results can be misleading due to large differences in the relative sensitivity to the mono- and diesters. LC alone only gives an indication of the composition of the samples investigated, and this initially appeared to back up the direct infusion MS results. However,

when these techniques were used together as LC-UV-MS, unambiguous identification of the reaction products was made possible. The LC method was also able to distinguish between the 1,3 and 1,2 isomers of the diester. The results obtained in this work (from LC-UV-MS and LC-DAD) made possible the determination of relative amounts of each ester-substituted calix[4]arene. Overall, LC-UV-MS has proven to be very powerful for identifying and analysing the products obtained in these reactions, and extremely valuable in allowing optimisation of the reaction conditions.

Acknowledgements

Financial support from the Higher Education Authority of Ireland under the PRTL I initiative (GMCM), Enterprise Ireland (Basic Research Grant SC99/131, KN) and The School of Chemical Sciences, Dublin City University (RW) is gratefully acknowledged.

References

- [1] C D Gutsche, Calixarenes Revisited, Monographs in Supramolecular Chemistry, Royal Society of Chemistry, Cambridge UK 1998.
- [2] D Diamond, M A McKervey, *Chem Soc Rev*, (1996) 15–24.
- [3] A Ikeda, S Shinkai, *Chem Rev* 97 (1997) 1713–1734.
- [4] Y K Agrawal, S Kunji, S K Menon, *Rev Anal Chem* 17 (2) (1998) 69–139.
- [5] R Ludwig, *Fies J Anal Chem* 367 (2) (2000) 103–128.
- [6] D Diamond, K Nolan, *Anal Chem* 73 (2001) 22A–29A.
- [7] R J Forster, D Diamond, *Anal Chem* 64 (15) (1992) 1721–1728.
- [8] K Cunningham, G Svehla, S J Harris, M A McKervey, *Analyst* 118 (4) (1993) 341–345.
- [9] T Grady, A Cadogan, T McKittrick, S J Harris, D Diamond, M A McKervey, *Anal Chim Acta* 336 (1–3) (1996) 1–12.
- [10] T McKittrick, D Diamond, D J Marrs, P O'Hagan, M A McKervey, *Talanta* 43 (7) (1996) 1145–1148.
- [11] P Kane, D Fayne, D Diamond, M A McKervey, *J Mol Mod* 6 (2000) 272.
- [12] K M O'Connor, G Svehla, S J Harris, M A McKervey, *Talanta* 39 (11) (1992) 1545–1554.
- [13] X Zeng, L Weng, L Chen, X Leng, Z Zhang, X He, *Tet Letts* 41 (25) (2000) 4917–4921.
- [14] L Chen, X Zeng, H Ju, X He, Z Zhang, *Microchem J* 65 (2) (2000) 129–135.
- [15] C Perez Jimenez, L Escriche, J Casabo, *Anal Chim Acta* 371 (2–3) (1998) 155–162.
- [16] H J Cho, J Y Kim, S K Chang, *Chem Letts* 6 (1999) 493–494.
- [17] P A Gale, Z Chen, M G B Drew, J A Heath, P D Beer, *Polyhedron* 17 (4) (1998) 405–412.
- [18] W H Chan, X J Wu, *Analyst* 123 (12) (1998) 2851–2856.
- [19] T Grady, T Butler, B D MacCraith, D Diamond, M A McKervey, *Analyst* 122 (8) (1997) 803–806.
- [20] M Loughran, D Diamond, *Food Chem* 69 (1) (2000) 97–103.
- [21] M Kubinyi, I Mohammed, Ziegler, A Grofcsik, I Bitter, W Jeremy Jones, *J Mol Struct* 408 9 (1997) 543–546.
- [22] T Grady, T Joyce, M R Smyth, S J Harris, D Diamond, *Anal Comm* 35 (4) (1998) 123–125.
- [23] Y Kubo, S Maeda, S Tokita, M Kubo, *Nature* 382 (1996) 522.
- [24] Y Okada, Y Kasai, J Nishimura, *Tet Letts* 36 (4) (1995) 555–558.
- [25] H Otsuka, S Shinkai, *Supramol Sci* 3 (4) (1996) 189–205.
- [26] S Friebe, S Gebauer, G J Krauss, G Goermer, J Krueger, *J Chromatogr Sci* 33 (6) (1995) 281–284.
- [27] S Gebauer, S Friebe, G Gubitz, G J Krauss, *J Chromatogr Sci* 36 (8) (1998) 383–387.
- [28] S Gebauer, S Friebe, G Scherer, G Gubitz, G J Krauss, *J Chromatogr Sci* 36 (8) (1998) 388–394.
- [29] T Sokolchik, U Menyess, U Roth, T Jira, *J Chromatogr A* 898 (1) (2000) 35–52.
- [30] C D Gutsche, B Dhawan, K H No, R Muthukrishnan, *J Am Chem Soc* 103 (1981) 3782.
- [31] F J Ludwig, A G Bailie Jr, *Anal Chem* 56 (1984) 2081–2085.
- [32] F J Ludwig, A G Bailie Jr, *Anal Chem* 58 (1986) 2069–2072.
- [33] Y Zhang, I M Warner, *J Chromatogr A* 688 (1–2) (1994) 293–300.
- [34] M Sanchez Pena, Y Zhang, I M Warner, *Anal Chem* 69 (16) (1997) 3239–3242.
- [35] I Rodriguez, H K Lee, S F Y Li, *Talanta* 45 (4) (1998) 683–691.
- [36] F Vocanson, R Lamartine, D Duchamp, J B Regnouf de Vains, *Chromatographia* 41 (3–4) (1995) 204–206.
- [37] Y Saito, H Ohta, H Terasaki, Y Katoh, H Nagashima, K Jinno, K Itoh, R D Trengove, J Harrowfield, S F Y Li, *J High Resolut Chromatogr* 19 (8) (1996) 475–477.
- [38] K Jinno, K Tanabe, Y Saito, H Nagashima, R D Trengove, *Anal Commun* 34 (6) (1997) 175–177.
- [39] O I Kalchenko, J Lipkowski, R Nowakowski, V I Kalchenko, M A Visotsky, L N Markovsky, *J Chromatogr Sci* 35 (2) (1997) 49–52.
- [40] I Rodriguez, S F Y Li, B F Graham, R D Trengove, *J Liq Chromatogr Relat Technol* 20 (8) (1997) 1197–1209.

- [41] B F Graham J M Harrowfield R D Trengove, I Rodriguez S F Y Li J Chromatogr Sci 35 (5) (1997) 232–236
- [42] S J Thibodeaux, M Sanchez Pena Y Zhang S H Shamsi I M Warner, Chromatographia 49 (3–4) (1999) 142–146
- [43] Y Q Feng, Y L Hu, J S Li, Y Liu, S L Da, Y Y Chen Fenxi Ceshi Xuebao 19 (2) (2000) 1–4
- [44] A Dodi, Analisis 28 (1) (2000) 93–96
- [45] E M Collins, M A McKervey, S J Harris, J Chem Soc Perkin Trans I (1989) 372–374
- [46] M A McKervey E M Seward G Ferguson B Ruhl S J Harris J Chem Soc Chem Comm, (1985) 388
- [47] K Linnemayr G Allmaier Eur Mass Spectrom 3 (1997) 141–149
- [48] Personal communication from Professor M A McKervey Queen s University Belfast

Cation Binding Selectivity of Partially Substituted Calix[4]arene Esters

Aogan Lynch,^a Kathrin Eckhard,^{a,b} Gilhan McMahon,^a Rachel Wall,^a Paddy Kane,^a Kieran Nolan,^a Wolfgang Schuhmann^b
Dermot Diamond^{a*}

^a National Centre for Sensor Research, Dublin City University, Dublin 9, Ireland, e-mail: dermot.diamond@dcu.ie

^b Chemistry Department, University of Bochum, Universitätsstr 150, Bochum, 44870, Germany

Received December 28, 2001

Final version April 3, 2002

Abstract

Partially substituted calix[4]arene ethyl ester derivatives were synthesized as important precursors for new series of non symmetrical ion and molecule receptors by reacting *p*-*t* butyl calix[4]arene and ethyl bromoacetate. Characteristics of PVC membrane ion-selective electrodes based on the mono- and di-ester derivatives were compared to those of the well known calix[4]arene tetraester cationophore. Sodium selectivity is only manifested with the tetraester derivative, whereas the diester complexes potassium and caesium, as well as sodium. Energy minimized structures for the complexes show the ester groups are involved in sodium complexation for the tetraester and diester derivatives, whereas for the monoester, the aryl macrocycle is more important. This provides an excellent example of the critical importance of preorganization on host guest selectivity which in turn defines the selectivity of chemical sensors based on such receptors. The influence of this selective ion binding behavior on the characterization of these derivatives using mass spectroscopy is discussed.

Keywords: Calixarenes, Ion receptors, PVC membrane, Cationophore, Potentiometric detection, Liquid chromatography, Mass spectrometry

Dedicated to Professor Gary Christian on the Occasion of His 65th Birthday

1 Introduction

Calixarene ester derivatives have well-known ion-binding characteristics which make them attractive agents for use in potentiometric ion sensors [1–4]. In particular calix[4]arene tetraesters have excellent selectivity for sodium ions, and are available commercially for making sodium selective electrodes [5]. In these, and most other calixarene derivatives, the groups attached to the phenoxy oxygen atoms of the so-called ‘lower-rim’ (see Table 1) are of the same type, and the binding sites are therefore more-or-less evenly distributed in space. More recently, we have become interested in calix[4]arene derivatives in which the pendent groups are not the same. For example, receptors with the same binding sites attached by different spacer groups at the opposite 1,3 and 2,4 positions would result in a tetrahedral spatial distribution of sites, with different selectivity than the conventional tetraesters. However, the isolation of the 1,3-disubstituted precursor has been more difficult than predicted. To identify the optimum conditions for generation of this diester, a series of derivatization reactions between *p*-*t*-butyl calix[4]arene and ethyl bromoacetate was carried out [6].

Careful attention to characterization of the reaction products, and optimization of the separation conditions enabled pure samples of the monoester, the 1,3-diester and the tetraester to be obtained. In this article, we demonstrate

that the sodium selectivity of calix[4]arenes in ion-selective electrodes is only manifested in the tetraester. The diester exhibits Nernstian responses to a number of ions, whereas the monoester does not produce functioning electrodes. These electrochemical results along with energy minimized 3-d models of the sodium complexes explain why mass spectral (MS) data obtained by direct infusion of reaction products give rise to misleading results. Combined with the energy minimized structures, this study is an excellent example of the importance of molecular preorganization in defining the ion-binding selectivity of these receptors, which in turn provides an insight into the molecular basis for observed selectivity obtained with the corresponding chemical sensors.

2 Experimental

2.1 Materials and Apparatus

All membrane components with the exception of the calixarene compounds were, Selectophore grade obtained from Fluka Chemicals. Metal nitrates were also obtained from Fluka and were of the ‘puriss. p. a.’ standard or higher. Ultra Pure water from a Barnstead EASYpure water purification system was used throughout. A double junction calomel electrode was used as the reference electrode,

with the outer junction containing saturated KNO_3 and the inner reference containing saturated KCl . All measurements were carried out at $25 \pm 0.5^\circ\text{C}$. Voltages were captured using an MIO-16 National Instruments data acquisition card, using an in-house developed virtual instrument (LabVIEW version 4.0, National Instruments, Austin, Texas) after impedance conversion.

2.2 Preparation of Electrodes

All PVC membranes used were fabricated using the method of Diamond et al. [7]. The ionophore (10 mg) and potassium tetrakis(4-chlorophenyl)borate (KTPClPB) ion exchanger (2 mg) were dissolved in 1 g plasticizer (*o*-nitrophenyl octyl ether, *o*-NPOE). To this solution 500 mg high molecular weight PVC was added and stirred to give a thick slurry. Tetrahydrofuran (THF) was then added to the slurry slowly, with stirring until a clear solution was obtained. This solution was stirred for one hour to ensure thorough mixing. The membranes were then cast in glass rings (28 mm i.d.) fixed on a glass plate and allowed to set overnight, loosely covered to allow for slow evaporation of the THF. From this master membrane, small discs were cut using a cork borer. Electrodes were prepared by clipping these discs into conventional ISE bodies containing Ag/AgCl wires as the internal reference.

Four electrodes were prepared with 0.1 M NaCl internal filling solution: one with the monoester, one with the 1,3-diester, one with the tetraester, and one blank membrane with no ligand in the membrane (all other membrane components including KTPClPB were present in the amounts mentioned above). Sodium calibrations were carried out for all four electrodes with no interfering background to begin with, and then fixed interference studies were carried out in 10^{-1} M LiCl, KCl, CsCl, CaCl_2 and MgCl_2 .

2.3 Synthetic Conditions

The reactions for this work were carried out in a parallel synthesizer system (Radleys Carousel Reaction Station, Shire Hill, Saffron Walden, Essex, CB11 3AZ, UK), using DMF as solvent and Na_2CO_3 as base. To a suspension of calix[4]arene (150 mg scale) in anhydrous DMF, was added base followed by the dropwise addition of EtBrOAc. The mixture was then heated to 70°C for the specified reaction time. The reaction mixture was then cooled to room temperature, poured onto ice and subsequently extracted with four aliquots of ethyl acetate (4×25 mL). The ethyl acetate extracts were combined and then washed with four aliquots of water (4×25 mL) and brine solution (4×25 mL). The organic extract was then dried over anhydrous MgSO_4 and the solvent removed under reduced pressure.

A pure sample of the 1,3-diester was obtained by flash column chromatography using 10% ethylacetate/hexane as

eluent. ^1H NMR (400 Hz) (CDCl_3): 6.95 (4H, s), 6.74 (4H, s), 4.64 (4H, s), 4.38 (4H, d), 4.21 (4H, q), 3.26 (4H, d), 1.27 (6H, t), 1.19 (18H, s), 0.91 (18H, s).

2.4 LC-MS and MS Characterization

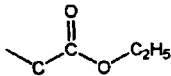
A Hewlett-Packard (HP) Esquire Liquid chromatography (LC) system was used in combination with a HP UV-vis variable wavelength detector and a Bruker mass spectrometer (MS) which could be used in both direct infusion or LC modes. The LC was a HP1100 liquid chromatograph, with a low-volume pump, an in-line degasser and an autosampler, controlled via HP ChemStation software. The LC method had the following parameters: Zorbax RX-C18 column, 150×2.1 mm, $5 \mu\text{m}$ column with a mobile phase of 100/0.25 v/v acetonitrile/formic acid at a flowrate of 0.2 mL/min. The monitoring wavelength was 210 nm and an injection volume of $4 \mu\text{L}$ was used. The MS module of the instrument comprised the ionization chamber (electrospray), the ion-trap to collect the ions and then to release them according to mass, and the ion detector to generate the mass spectrum. The nebulization gas and drying gas were set to 35 psi and 9 L/min, respectively. The temperature of the source was maintained at 300°C . The octopole voltage was 2.83 V, the skimmer 1 voltage was 50 ± 5 V and the trap drive voltage was 57 ± 2 V (depending on the chosen target mass). Mass spectral data was generally collected in the scan range 400–1200 m/z . When automated fragmentation information was required, the software was set up to subject the most abundant ion to MS-MS analysis, using an isolation width of 4 Da and a collision amplitude of 1.80.

For direct infusion samples, using the syringe injector of the mass spectrometer, samples were infused into the ESI source (positive mode) at a rate of $5 \mu\text{L}/\text{min}$. The nebulization gas pressure (15 psi), drying gas flowrate (4 L/min) and temperature (250°C) were reduced in comparison to the LC-MS parameters as when the MS is connected in series with the LC, the incoming LC eluent must be successfully converted into the gas phase. The octopole voltage, the skimmer 1 voltage, the trap drive voltage and the scan range were as for LC mode. When on-line MS-MS was being carried out, an isolation width of 4 Da and a collision amplitude of 1.60 to 2.10 were used depending on the ion being fragmented.

2.5 Molecular Modelling

All molecular modelling calculations were carried using Spartan software [8], SGI version 5.0.1 running on a Silicon Graphics workstation with a MIPS R10000 Rev 2.7, 195-MHz CPU, an IRIX operating system (release 6.3) and 128 MB of RAM. Geometry optimizations were carried out with the Merck Molecular Force Field (MMFF) [9] until the terminating gradient of 1×10^{-5} kcal mol $^{-1}$ Å $^{-1}$ was reached. Partial charge surface maps based on extended Huckel calculations were generated using Chem-3d Pro (Cam-

Table 1 Names and Structures of the calix[4]arene derivatives discussed in this research

Chemical Name	Name used in this article	Mass (a. m. u.)	Substituent Groups at Lower Rim H	
				
p t butyl calix[4]arene	Calix[4]arene	648	R ₁ , R ₂ , R ₃ , R ₄	none
Mono-ethyl calix[4]arene ester	Monoester	734	R ₂ , R ₃ , R ₄	R ₁
1,3 Di ethyl calix[4]arene ester	1,3 Diester	820	R ₂ , R ₄	R ₁ , R ₃
1, 2 Di ethyl calix[4]arene ester	1,2-Diester	820	R ₃ , R ₄	R ₁ , R ₂
Tri-ethyl calix[4]arene ester	Triester	906	R ₄	R ₁ , R ₂ , R ₃
Tetra-ethyl calix[4]arene ester	Tetraester	992	none	R ₁ , R ₂ R ₃ R ₄

bridgesoft, Cambridge, MA, USA) after importing the energy minimized molecular coordinates

3. Results and Discussion

Table 1 details the structures, names and molecular weights of the compounds that could be formed during these

esterification reactions Isolation of the pure 1,3-diester is difficult for a number of reasons. Firstly, as Table 1 shows, a number of reaction pathways may occur, and it is therefore vital that the optimum conditions for maximising the yield of the 1,3-diester are identified However, in order to achieve this, it must be possible to separate and unambiguously identify the reaction products. Separation is difficult, due to the structural similarity of the various products, and

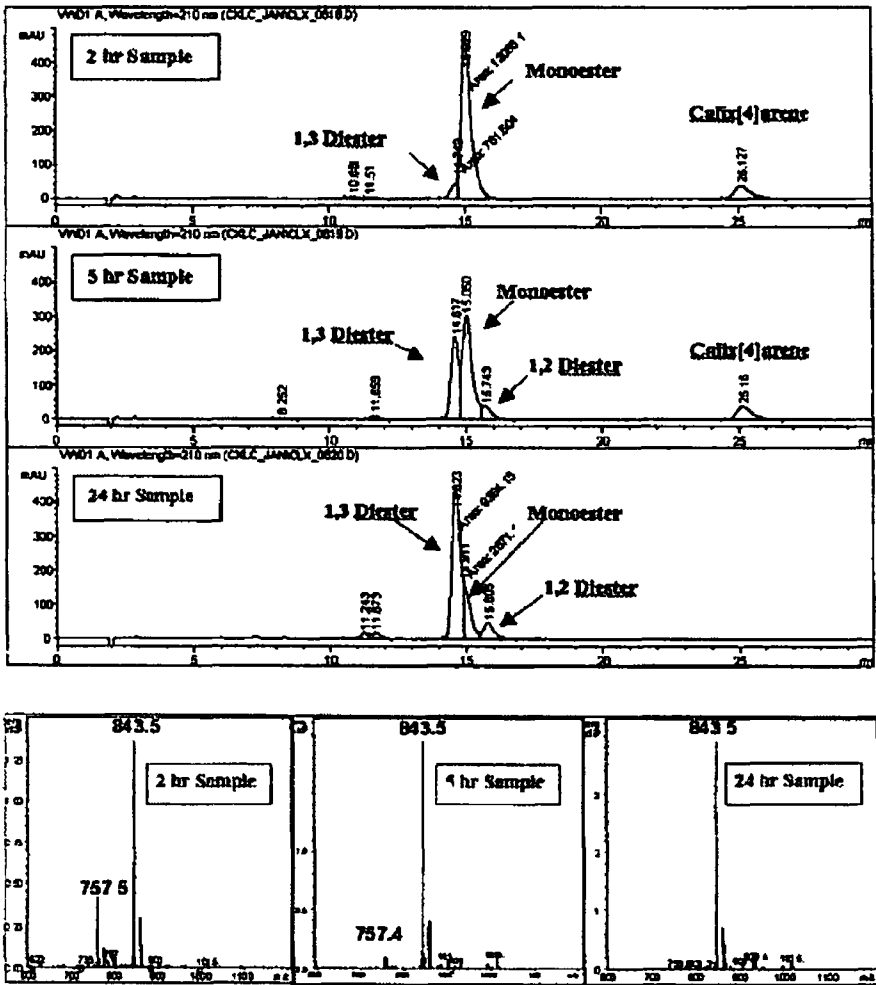


Fig 1 LC-UV (210 nm) Chromatograms (top) and Direct Infusion Mass Spectra (bottom) for samples taken at 2, 5 and 24 hours after reaction initiation

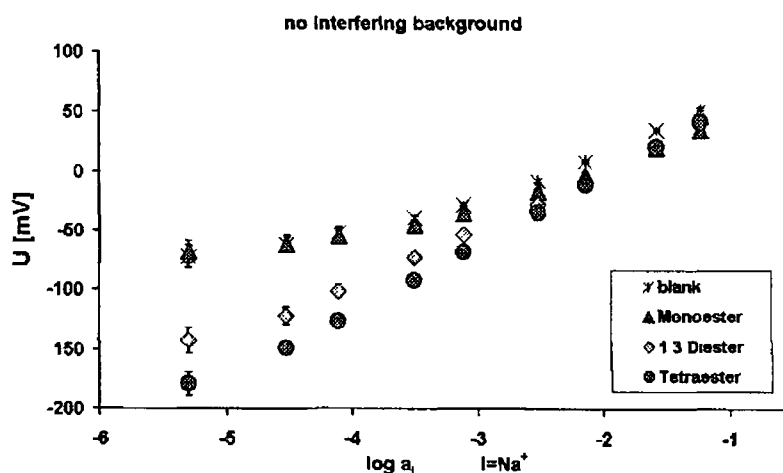


Fig 2 Response to sodium in the absence of any possible interferents (Tetraester slope 58.3 mV, $R^2 = 0.9998$) Points are average of three replicates standard deviation bar masked by point symbol

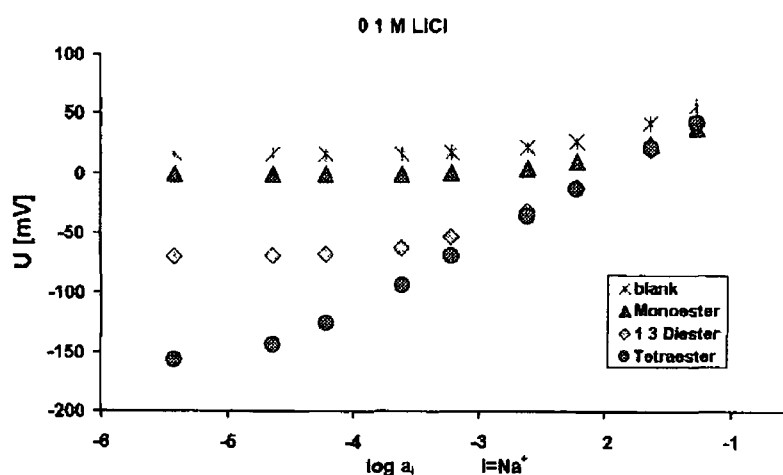


Fig 3 Response to sodium in the presence of 0.1 M LiCl (tetraester slope of 56.22 mV)

characterization using direct infusion can be misleading due to the different ion-complexation behavior of the products

Figure 1 shows both direct infusion results and LC results for the 2, 5 and 24 hour samples taken from the reaction. Mass spectra from direct infusion of samples of the reaction mixtures prepared in acetonitrile, all showed a base peak of 843.5 Da ($820 + \text{Na}^+$), indicating the presence of the diester substituted calix[4]arene product. In these MS traces, a less sensitive response for the monoester + Na^+ (peak at 757.5 Da), triester + Na^+ (929.5 Da) and tetraester + Na^+ (1015.5 Da) were also evident in some of the samples. As sodium ions tend to be ubiquitous, it appeared that the ligands were complexing trace quantities of sodium prior to MS analysis. The fact that the data obtained for the five derivatives listed in Table 1 were mainly equivalent to the sodium complex, with a small proportion equivalent to the potassium complex, agrees with previous MS work carried out on selected nitrogen-free calixarenes by laser desorption/ionization MS [10].

Careful examination of the UV chromatograms and mass spectra in Figure 1 raises a number of issues. The 2 hour sample chromatogram implies there is one main product at 15.03 min with a minor impurity which precedes the main peak. The mass spectrum of the same sample shows a large signal for the diester + Na^+ (843.5 Da) and a minor signal for the monoester + Na^+ (757.5 Da) for this mixture (bottom left). Initially this was interpreted as meaning the product was mainly diester in agreement with the MS results. However on continuing the reaction for longer times (5 hr, 24 hr), it became clear that the 15.03 min peak was gradually disappearing, and the fore-peak was growing (Figure 1). Comparison of the mass spectra proves that the declining signal is due to the monoester, as the peak at 757.5 Da disappears. The explanation of this is as follows.

In the UV-vis chromatograms (Figure 1), the detector sensitivity is approximately equal for the mono-, di-, and tetraester derivatives, as the absorbance at 210 nm arises from the aryl moieties that are common to all three. Hence

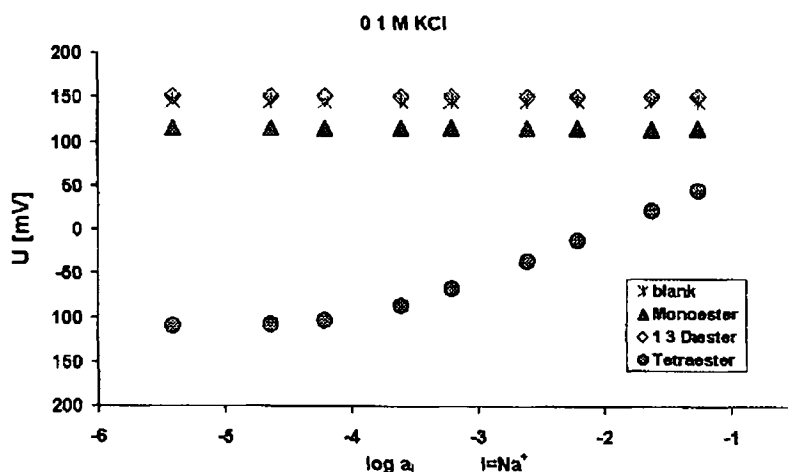


Fig 4 Response to sodium in the presence of 0.1 M KCl

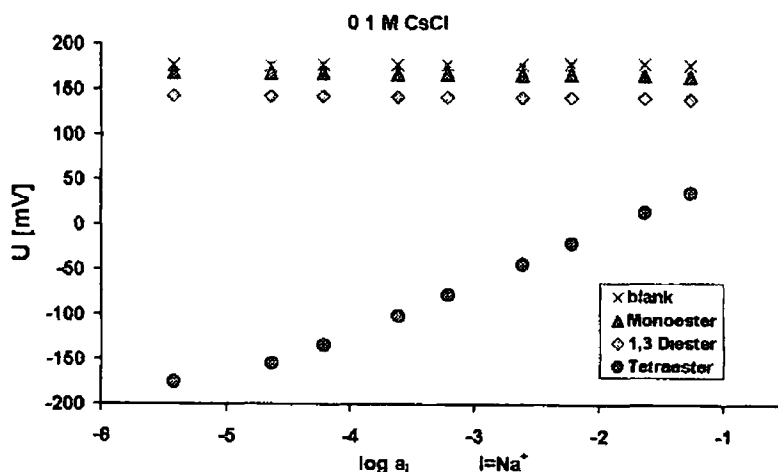


Fig 5 Response to sodium in the presence of 0.1 M CsCl

the LC-UV peaks are reflections of the relative abundance of each derivative in the reaction mixture. Identification of the main product after two hours by direct infusion MS suggests it is the diester, but this not correct. In fact the main product after two hours is the monoester, but the diester predominates in the mass spectrum due to its much higher uptake of sodium ions. In other words, the monoester is almost 'invisible' in the mass spectrum due to low ionization efficiency under the conditions employed.

To confirm this, the cation complexation behavior of these ligands were investigated directly, by incorporating them into PVC membrane electrodes. The tetraester has been used very successfully in this manner for the potentiometric determination of sodium for many years [11–14] and has been incorporated successfully into commercial blood analyzers [15]. Figure 2 shows the response of all four electrodes to NaCl calibration solutions. The tetraester responded as expected with a Nernstian slope of 58.3 mV per decade, whereas the response of the monoester is almost identical to that of the blank electrode, which does not

contain an ionophore. The diester response profile is more like that of the tetraester, with a slightly reduced slope.

To investigate size-based selectivity, a series of fixed interference experiments were carried out using Li^+ , K^+ and Cs^+ as the interfering ion. Figure 3 shows the response of the three ligands, and a blank electrode, to the same sodium calibration sequence as Figure 2, but in a constant background of 10^{-1} M LiCl. The tetraester has sufficient selectivity for sodium ions to remain almost unaffected, while the diester responds to Na^+ from about 10^{-3} M upwards, implying around 100-fold Na^+ selectivity. In the case of the monoester, the response is again almost identical to the blank, suggesting the ligand has no influence on the response characteristics of the membrane. In the presence of 10^{-1} M KCl (Figure 4) the superior selectivity of the tetraester is once again evident. However, with the partially substituted ligands, the response to sodium is completely suppressed. This lack of sodium discrimination in the presence of larger group I cations is further illustrated in the case of caesium (Figure 5).

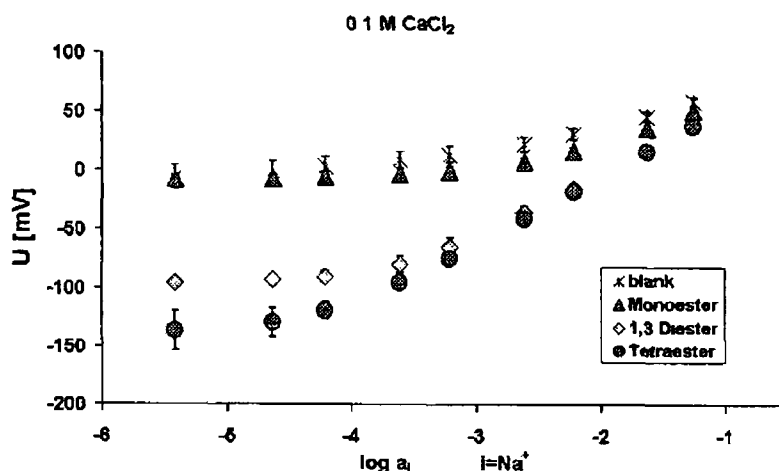


Fig 6 Response to sodium in the presence of CaCl_2 . Points are average of three replicates, standard deviation bar masked by point symbol

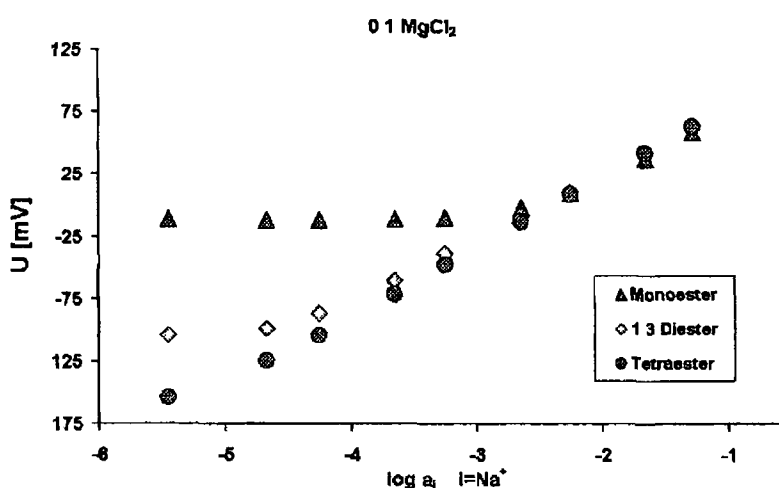


Fig 7 Response to sodium in the presence of MgCl_2

Figures 6 and 7 demonstrate the excellent selectivity for the tetraester against the group II ions, Mg^{2+} and Ca^{2+} . Once again, the monoester is incapable of influencing the response characteristics relative to the blank membrane, whereas the diester-based membrane exhibits reasonably good selectivity for Na^+ against these group II cations.

These results suggest that for the monoester-based membranes, the response characteristics are dominated by the ion-exchanger, and the ligand is therefore only a weak ion-complexing agent. In contrast, the diester can effectively complex Na^+ ions, and is selective against Mg^{2+} , Ca^{2+} and Li^+ , but appears to accommodate the larger group I cations K^+ and Cs^+ .

Figure 8 shows the energy minimized structures of the Na^+ complexes of the tetraester (a), the diester (c) and the mono-ester (d). We have previously studied the 3-d structure of calixarene complexes in this way [16, 17], and have validated our approach carefully using X-Ray structures as reference data sets [18]. We are therefore confident

that these structures are a reasonable approximation of the true geometry of the complexes. In the tetraester- Na^+ complex (a), the macrocycle adopts a beautiful symmetry, and the Na^+ ion is held in the center of an octahedral cavity defined by the four phenoxy oxygen atoms at the calix[4]arene lower rim, and the four carbonyl oxygen atoms of the pendent ester groups. For the diester- Na^+ complex (c), a much more open structure is evident, with the Na^+ ion associating closely with the phenoxy oxygen atoms. The open, flexible nature of the diester enables it to easily accommodate the larger K^+ ion also (Figure 8b) and in this case, the carbonyl oxygens appear to be more involved. For the monoester- Na^+ complex (Figure 8d) the ion appears to associate more with the negative charge density of the aryl groups than the phenoxy oxygens, which is an indication of the relative weakness of the interaction compared to that of the diester and tetraester Na^+ complexes.

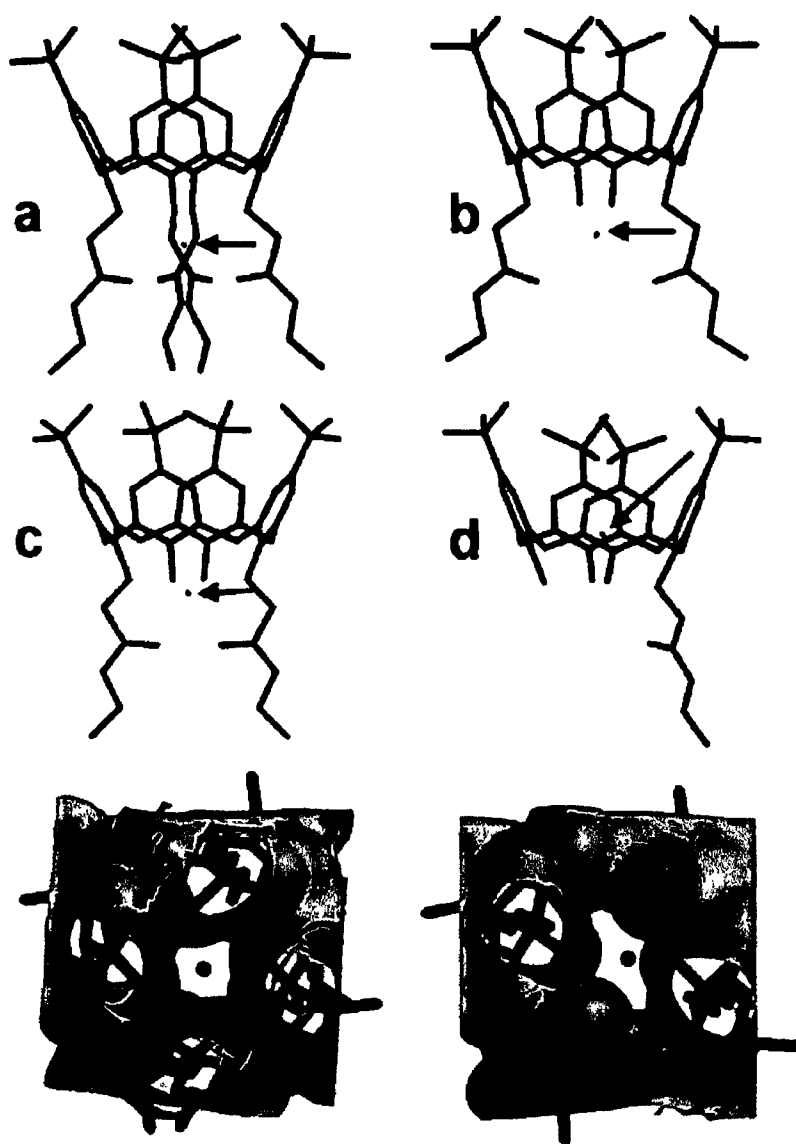


Fig 8 Energy minimized structures for the tetraester Na⁺ complex (a), the diester-K⁺ complex (b), the diester-Na⁺ complex (c) and the monoester-Na⁺ complex (d) Position of cation indicated by arrow Comparison of partial charge surface maps for the tetraester-Na⁺ (e) and diester Na⁺ complexes (f) Negative density regions are displayed in blue and positive regions in red

Surface maps of the partial charge density distribution for the tetraester and diester sodium complexes are shown in Figure 8e and f, respectively, looking upwards through the cavity from the lower rim. These show the sodium ion sitting in the middle of a well-defined region of very negative charge density in the case of the tetraester, whereas for the diester, this region is much more open, leading to lower binding energies in general, and a less selective interaction with the sodium ion. The combination of molecular modelling and potentiometric measurements provides an insight into the molecular basis for observed behavior of chemical sensors, and can help the rational design of future receptors for electrochemical devices. The electrochemical selectivity data can also help with the interpretation of data obtained with other analytical techniques used to character-

ize of synthetic products generated in the search for new receptors, such as the mass spectral data illustrated in this study. Recent breakthroughs in the theory of potentiometric ion-sensing devices offers a route to new sensors with extremely low limits of detection, opening the way to many new areas of application and a renaissance in research in potentiometry [19]. However, the key to future success will lie in the availability of ion-receptors for key analytes that offer much greater selectivity than currently available. Understanding the molecular basis of selective ion-binding will be a crucial factor in realising this vision. Alternatively, for certain applications (e.g., ion-sensors as detectors for ion-chromatography), it is preferable to have ionophores that complex a broad range of ions. In that case, the 1,3-disubstituted calix[4]arenes would be a preferable platform to explore.

4 Conclusions

Partially substituted calixarene esters have been synthesized and their selectivity for Group I and Group II ions assessed using ion-selective electrodes relative to the equivalent tetraester. The electrode selectivity data has been used to explain the relative sensitivity of mass spectroscopy to these ligands. The basis for the observed selective ion-binding behavior has been illustrated through molecular modelling calculations. The 1,3 diester has been isolated in pure form and its electroanalytical behavior characterized. This ligand will provide a route to a new series of ion-receptors with different binding groups at the 1,3 and 2,4 positions. We intend to use this to produce receptors with different spatial arrangements of binding sites (e.g. tetrahedral) compared to the conventional tetra-substituted calix[4]arenes. This preorganization of the binding sites may lead to preferential complexation with tetrahedrally shaped guest-ions that have complementary charge distribution, leading to new patterns of selectivity for the corresponding ion-sensors. The 1,3-diester calix[4]arene ionophore produces sensors that exhibit Nernstian behavior with a number of ions. Such devices may find applications as detectors for separation systems.

5 Acknowledgements

We would like to acknowledge support for the NCSR under the National PRTL programme, and grant aid from Enterprise Ireland (Basic Research Grant No SC/99/131, Research Innovation Grant No RIF/2001/062), the School of Chemical Sciences, DCU (RW) and the German Government Exchange Programme (KE).

6 References

- [1] R. Forster, F. Regan, D. Diamond, *Sens. Actuators B* **1991**, *4*, 325.
- [2] D. Diamond, K. Nolan, *Anal. Chem.* **2001**, *73*, 22A–29A.
- [3] D. Diamond, M. A. McKervey, *Chem. Soc. Rev.* **1996**, 15.
- [4] F. Cadogan, K. Nolan, D. Diamond, in *Calixarenes 2001* (Eds Z. Asfari, V. Bohmer, J. Harrowfield, J. Vicens), Kluwer Academic Press, Dordrecht, The Netherlands **2001**, ch. 34, pp. 627–641.
- [5] See for example the calix[4]arene tetraethyl ester described as sodium ionophore X, available from Fluka Product Number 71747, CAS 97600-39-0, MDL Number MFCD00145373.
- [6] G. McMahon, R. Wall, K. Nolan, D. Diamond, *Talanta* **2002**, in press.
- [7] J. Lu, Q. Chen, J. Wang, D. Diamond, *Analyst* **1993**, *118*, 1131.
- [8] Wavefunction Inc., 18401 Von Karman Avenue, Suite 370, Irvine, CA 92612 USA. <http://www.wavefun.com>
- [9] T. Halgren, *J. Am. Chem. Soc.* **1992**, *114*, 7827.
- [10] K. Linnemayr, G. Allmaier, *Eur. Mass Spectrom.* **1997**, *3*, 141.
- [11] D. Diamond, G. Svehla, *TrAC* **1987**, *6*, 2, 46.
- [12] D. Diamond, G. Svehla, E. Seward, M. A. McKervey, *Anal. Chim. Acta* **1988**, *204*, 223.
- [13] A. Cadogan, D. Diamond, M. R. Smyth, M. Deasy, M. A. McKervey, S. J. Harris, *Analyst* **1989**, *114*, 1551.
- [14] R. Forster, D. Diamond, *Anal. Chem.* **1992**, *64*, 1721.
- [15] A. Lynch, D. Diamond, M. Leader, *Analyst* **2000**, *125*, 2264.
- [16] S. E. J. Bell, A. M. McKervey, D. Fayne, P. Kane, D. Diamond, *J. Mol. Model.* **1998**, *4*, 44.
- [17] P. Kane, D. Fayne, D. Diamond, A. M. McKervey, *J. Mol. Model.* **2000**, *6*, 272.
- [18] D. Fayne, P. Kane, D. Diamond, S. E. J. Bell, A. M. McKervey, *J. Mol. Model.* **1998**, *4*, 259.
- [19] A. Ceresa, E. Bakker, B. Hattendorf, D. Gunther, E. Pretsch, *Anal. Chem.* **2001**, *73*, 343.